Developing physiologically relevant *in vitro* tissue engineered models of the vaginal mucosa for applications in vaginal tissue research

By:

Sarah Shafaat
190205342

A thesis submitted in partial fulfilment of the requirements for the degree of Doctor of Philosophy

Faculty of Engineering
Department of Materials Science and Engineering
The University of Sheffield

August'2022

Abstract

Pelvic floor disorders such as pelvic organ prolapse (POP) and stress urinary incontinence (SUI) affect 50% postmenopausal women worldwide with 11% are at a lifetime risk of surgery. There is currently a treatment gap for patients requiring surgical intervention following the ban on using polypropylene (PPL) mesh in the urogynecological reconstructive procedures in 2019 by the FDA. There is an urgent need to design better biomaterials to support the female pelvic floor and to develop suitable preclinical testing systems for these new biomaterials.

This project aimed at developing physiologically relevant *in vitro* tissue engineered (TE) models of the vaginal mucosa to enable laboratory-based preclinical testing of existing and new biomaterials and to study the cellular response to these biomaterials in an *in vitro* modelling system.

Tissue engineered (TE) vaginal models were developed by culturing primary sheep vaginal epithelial cells and fibroblasts on decellularised sheep vaginal tissues at an air-liquid interface (ALI) for three weeks and tested for their estradiol -17β [E_2] responsiveness. Then wounded vaginal models were developed to study the process of vaginal wound healing and for implantation of biomaterials developed for the pelvic floor to investigate the cellular and tissue response towards these materials in the absence and presence of E_2.

TE vaginal models recapitulated the histological features of the native vaginal tissue and formed stratified squamous epithelia on decellularised vaginal matrices over three weeks at an ALI culture. Cellular metabolic activity and proliferation remained high and the models showed a dose-dependent response to E_2. I was able to study the time course of vaginal wound healing and the wounded models implanted with biomaterials were able to discriminate between biomaterials that were likely to cause a fibrotic tissue response (PPL) from those that caused tissue remodelling (PU Z3) *in vitro*. In summary, these models showed promising results as preclinical testing models and can contribute towards the development and testing of novel biomaterials designed for the female pelvic floor repair.

Publications

1. **S. Shafaat,** S. Roman, C. Chapple, S. MacNeil, and V. Hearnden, "Estradiol-17β [E_2] stimulates wound healing in a 3D *in vitro* tissue engineered vaginal wound model. Submitted to the Journal of Tissue Engineering on 02-Nov-2022 (status: accepted on 15th December' 2022).
2. **S. Shafaat,** N. Mangir, C. Chapple, S. MacNeil, and V. Hearnden, "A physiologically relevant, estradiol-17β [E_2] -responsive *in vitro* tissue-engineered model of the vaginal epithelium for vaginal tissue research," *Neurourol. Urodyn.*, 2022. https://doi.org/10.1002/nau.24908.
3. **S. Shafaat,** N. Mangir, S. R. Regureos, C. R. Chapple, and S. MacNeil, "Demonstration of improved tissue integration and angiogenesis with an elastic, estradiol releasing polyurethane material designed for use in pelvic floor repair," *Neurourol. Urodyn.*, vol. 37, no. 2, 2018. https://doi.org/10.1002/nau.23510.
4. M. Akram, **S. Shafaat,** D. Abbas Bukhari, and A. Rehman. "Characterization of a Thermostable Alkaline Protease from Staphylococcus aureus S-2 Isolated from Chicken Waste", *Pakistan journal of zoology*, vol. 46, no. 4, 2014, pp. 1125-1132. 8p.
5. M. Javed, S. Zahoor, **S. Shafaat,** I. Mehmooda, A. Gul, H. Rasheed, A. Imran Bukhari, N. Aftab, and I. Haq. "Wheat bran as a brown gold: Nutritious value and its biotechnological applications." *African Journal of* Microbiology *Research*, vol. 6, no. 4, 2012, pp. 724–733. ISSN 1996-0808.
6. **S. Shafaat,** M. Akram and A. Rehman. "Isolation and characterization of a thermostable alpha-amylase from *Bacillus subtilis*." *African Journal of Microbiology Research*, vol. 5, no. 20, 2011, pp. 3334-3338. ISSN 1996-0808.

Publications (in preparation)

1. **S. Shafaat** *et al.,* Developing novel tissue-engineered wound vaginal models for preclinical study of vaginal tissue response towards implanted biomaterials designed for the female pelvic floor repair. In preparation.
2. **S. Shafaat** *et al.,* Tissue engineered *in vitro* vaginal models: Current status and future implications in vaginal tissue research. A review. In preparation.

Oral Presentations

1. Developing physiologically relevant tissue engineered models of the vaginal epithelium for applications in vaginal tissue research. **BioSheffield22': 21st June'22.** Organised by the Department of Materials Science and Engineering, The University of Sheffield, Diamond Building, UK. **2022.**

   Winner of Best Oral presentation Award
2. Developing an estradiol-17β [E_2]- responsive tissue engineered (TE) sheep vaginal model for *in vitro* studies on vaginal pathogenesis and preclinical testing of biomaterials to be used in the female pelvic floor repair. **BioMedEng21': 6-7 Sep21.** The University of Sheffield, UK. **2021**.
3. Developing an estradiol-17β [E_2]- responsive tissue engineered (TE) model for applications in vaginal tissue research. **Tissue and Cell Engineering Society TCES21'** Virtual Conference: The University of Edinburgh, UK, 6-7 July21'. **2021.**
4. Designing tissue engineered female genital model for evaluating biomaterials to be used in the female pelvic floor repair. **Advanced Biomaterials Seminar ABS: 19 April 21'**. Department of Materials Science and Engineering, Kroto research institute, The University of Sheffield, UK. **2021.**
5. Demonstration of improved tissue integration and angiogenesis with an elastic, estradiol releasing polyurethane material designed to support pelvic floor. **Advanced Biomaterials and Tissue Engineering**, Organized by Pulsus (October 17-18,2018), Rome, Italy. **2018.**
6. Demonstration of improved tissue integration and angiogenesis with an elastic, estradiol releasing polyurethane material designed to support pelvic floor. **6Th International Symposium on Biomedical materials (ISBM)** (14-16 December 2017), Organized by IRCBM, COMSATS Institute of Information technology, Lahore Campus. **2017.**

Acknowledgements

This PhD thesis represents a major transformation for me both on a personal as well as on an academic level. I am truly grateful to the University of Sheffield for awarding me the Faculty of Engineering postgraduate research committee (UPGRC) scholarship to undertake my PhD without which this research could not have taken place.

Firstly, I would like to express my sincere gratitude to my PhD supervisors; Dr. Vanessa Hearnden and Prof. Sheila MacNeil for giving me this opportunity to work on this project and for their continuous support, enthusiasm and guidance throughout my journey. Despite all odds including the Covid19 pandemic, it was because of my wonderful supervisors that I was able to accomplish the goals of this PhD project within the intended time period. A very special thanks to Prof. Christopher Chapple for providing me funds to publish my research.

I would like to thank Dr. Anthony Bullock, Dr. Sabiniano Roman, Dr. Naside Mangir and Dr. Sanad Saad for their help and guidance whenever i needed it the most. I am also grateful to all my friends and colleagues at the Kroto research institute for their continuous support and assistance that made my PhD journey memorable and exciting.

I would also like to thank my mom, sister and my daughter without whom I would never be able to pursue my PhD. Thank you all for your support.

Abbreviations

α-SMA	alpha-smooth muscle actin
λ_{em}	emission wavelength
λ_{ex}	excitation wavelength
µg	microgram
µg/mL	micrograms per millilitre
µL	microlitres
µL/min	microlitres per minute
µm	micron metre
%	percentage
°C	degree celsius
2D	two dimensional
3D	three dimensional
A°	angstrom
a.u.	fluorescence intensity unit
AA	ascorbic acid
ADMSCs/ADSCs	Adipose derived mesenchymal stem cells
AI	anal incontinence
ALI	air-liquid interface
AMS	American medical systems
ANOVA	analysis of variance
ATCC	American tissue culture collection
AUGS	American urogynecological society
BMI	body mass index
BMSC	bone marrow-derived mesenchymal stem cells
$CaCl_2$	calcium chloride
CAM	chick chorioallantoic membrane
CAS	Cambridge Antibiotic Solution
CaSki	cervical cell line
cm	centimeter
cm^2	centimeter square
cyt 10	cytokeratin 10

cyt 19	cytokeratin 19
DAPI	4',6-diamidino-2- phenylindole
DC	direct current
DCM	dichloromethane
de-ECM	decellularised extracellular matrix
de-SVT	decellularised sheep vaginal tissue
DED	de-epidermised dermis
DMEM	Dulbecco's modified Eagle's Medium
DMF	*N, N*-Dimethyl formamide
DMSO	dimethyl sulfoxide
DNA	deoxyribonucleic acid
DPX	Dibutyl phthalate, Polystyrene, Xylene
ds-DNA	double stranded DNA
DT	Difco-trypsin
E/ YM	Young's modulus
E_2	estradiol-17β
ECE	ectocervical epithelial cells
ECM	extracellular matrix
EDTA	ethylenediaminetetraacetic acid
eMSCs	endometrial mesenchymal stem cells
End1/ E6E7	endocervical cell line
ER	estrogen receptor
ER-α	estrogen receptor-alpha
ER-β	estrogen receptor-beta
F/A	force per unit area
FBS	foetal bovine serum
Fi	fecal incontinence
FRAME	Funds for the replacement of animals in medical experiments
FT	Full thickness
g	gram
g/cm^3	grams per cubic centimetre
GAG	Glycosaminoglycans
H & E	haematoxylin and eosin

hADM	human acellular dermal matrices
hADMSC	human adipose derived mesenchymal cells
Ham's F12	Nutrient mixture F-12 Ham
HCl	hydrochloric acid
hECE	human ectocervical epithelial cells
hEGF	human epidermal growth factor
HIV-1	Human immunodeficiency virus 1
HNVEC	human normal vaginal epithelial cells
HSV-2	Herpes Simplex Virus-2
HT	hormonal therapy
HVE	human vaginal epithelium
i3T3s	irradiated 3T3 murine fibroblasts
IAP	intraabdominal pressure
ICS	International continence society
IHF	immunohistofluorescence
IL	interleukin
IMS	industrial methylated spirit
IU/mL	infectious units per millilitre
KDa	kilo Daltons
kg/m^2	kilogram per square meter
kV	kilo volt
LET	Local oestrogen therapy
LP	lamina propria
M	molar
M1	macrophage type 1
M2	macrophage type 2
MAUDE	Manufacturer and User Facility Device Experience
mg	milligrams
mg/L	milligram per litre
mg/mL	milligrams per millilitre
mL	millilitres
mm	millimetre
mM	millimolar
mm/s	millimetres per second

mm^3	cubic millimeter
MMP	matrix metalloproteinases
MPa	mega Pascals
MRI	magnetic resonance imaging
MRKHS	Mayer-von-Rokitansky-K€uster-Hauser syndrome
mRNA	messenger ribonucleic acid
MSCs	mesenchymal stem cells
MTT	3-(4,5-dimethylthiazol-2-yl)-2,5-diphenyl-2H-tetrazolium bromide
Mw	molecular weight
N	Newton
N-9	Nonoxynol-9
N/mm^2	Newton per millimetres square
NaCl	sodium chloride
NaOH	sodium hydroxide
NDRI	US National Disease Research Interchange
NICE	National Institute for Health and Care Excellence
nm	nanometre
OAB	overactive bladder
OF	oral fibroblasts
P/S	penicillin/streptomycin
PA	Polyamide
PBS	phosphate buffer saline
PCL	Polycaprolactone
PDGF	platelet derived growth factor
PFDs	Pelvic floor dysfunctions
pg/mL	picograms per millilitre
pH	power of hydrogen ion concentration
PLA	Polylactic acid
PLGA	Polylactic-co-glycolic acid
POP	Pelvic organ prolapse
POP-Q	Pelvic organ prolapse quantification system
Post-M	postmenopausal
PPL	Polypropylene
Pre-M	premenopausal

PT	partial thickness
PU	Polyurethane
PVDF	Polyvinylidene fluoride
R&D	research and development
REV/min	revolutions per minute
rpm	revolutions per minute
RVI	Rabbit vaginal irritation
RWV	rotating wall vessel
SD	standard deviation
SDS	sodium dodecyl sulfate
SEM	scanning electron microscopy
SGS	Society of gynecological surgeons
SIS	small intestinal submucosa
SMCs	smooth muscle cells
SMI	Slug mucosal irritation
STLV	Slow turning lateral vessel
SUI	Stress urinary incontinence
SVT	sheep vaginal tissues
T_3	3, 3', 5- Triiodothyronine/ apo-Transferrin
TE	Tissue engineered
TE	Tris-EDTA
TEER	transepithelial electrical resistance
TERM	Tissue engineered repair material
TGFβ	transforming growth factor β
THF	tetrahydrofuran
Triton X100	toctyl phenoxy polyethoxy ethanol
TVT	tension-free vaginal tape
UBM	urinary bladder matrix
UI	Urinary incontinence
US FDA	United States Food and Drug Administration
UTS	ultimate tensile strength
v/v	volume by volume
VEC	vaginal ecto-cervical

Vk2/E6E7	vaginal keratinocytes line
WD	working distance
wt/v	weight by volume
µm	micrometre

Table of Contents

List of Figures

List of Tables

Chapter 1:
INTRODUCTION

1.1 Introduction:

In the field of women's health, pelvic organ prolapse (POP) and stress urinary incontinence (SUI) are related urogynecological disorders that affect a large number of postmenopausal women globally. Common symptoms include prolapse of rectum, bladder or urethra through the vagina due to weakening of the pelvic floor muscles responsible for providing intact foundation and support to these organs. These are serious health concerns affecting approximately 40-50% postmenopausal women and have a debilitating impact on their mental health and social life [1].

The pathophysiology of these disorders is complex and multifactorial. There are several treatment options available for the management of POP and SUI depending on the type, extent and staging of prolapse. Symptomatic POP can be treated by pelvic floor muscle exercises, use of pessary or local application of estrogen cream [2]. However, in the progressive stages of POP, treatment with oestrogen therapy [3] and eventually pelvic floor reconstructive procedures become inevitable.

Surgical reconstructive procedures for POP and SUI mainly involve placement of a graft material to support the prolapsed organs in a hammock-like manner. The primary choice for a graft material is autologous graft from either fascia lata or rectus fascia [4] with advantages of decreased rejection and erosion rates. However, in prolapsed patients, autologous fascia is not sufficiently durable due to its already weakened tissue properties and there are also potential risks of herniation at the harvest site, increased operation time and morbidity [5].

Synthetic mesh grafts *e.g.,* polypropylene (PPL) mesh have advantages of increased durability and tensile strength with less chances of disease transmission compared to biological grafts [6]. Although originally designed for hernia repair, these meshes gained considerable popularity in pelvic floor reconstructive procedures from the beginning of 1980's. Ignoring the obvious anatomical differences between abdominal and vaginal wall, the first commercial polypropylene-based mesh (Gynemesh®) for pelvic floor reconstruction was approved by the US FDA in 2002 [7]. Although, a higher anatomical success rate was achieved by using mesh grafts compared to placebo but there were about 10-30% cases who presented with severe post-operative mesh complications associated with its use [8].

The US Food and Drug administration (FDA) issued the first concerned warning regarding mesh-related complications in transvaginal surgeries in 2008 and later in 2016 reclassified polypropylene mesh from class I to class III (high risk) devices [9]. Following this, in April 2019, the FDA ordered all surgical mesh manufacturers to stop selling and distributing their products [10]. Currently, there is a real need to develop and test new biomaterials for use in pelvic floor reconstruction that can provide essential mechanical support and biocompatibility with reduced risk of tissue erosion and complications.

To ensure biosafety and biocompatibility of newly developed biomaterials for pelvic floor repair, testing of these materials has mainly relied on animal models [11]. Owing to the growing concerns on reliability of data from animal experiments and violation of animal rights, continuous efforts are in place to develop alternative preclinical testing models. In this context, tissue engineered (TE) models can serve as better alternatives in providing an appropriate 3D environment to recapitulate human body physiology for testing of biomaterials [12]. *In vitro* tissue engineered pre-clinical models can provide us with a better understanding of numerous pathological conditions and cellular mechanisms in a controlled environment.

Several studies have been reported on attempts to design *in vitro* TE vaginal models with the main aim for transplantation and reconstruction purposes to repair or augment native vaginal tissue [13]. Another major application of these models was to study pathogenesis and drug development strategies for diseases such as HIV-1 infection [14], HSV-2 infection [15] and cervical cancer. Drug permeation studies through vaginal route [16] and vaginal irritation models [17] are a few examples of TE vaginal models with a real impact on the pharmacological industry.

An appropriate TE construct should replicate the architecture and mechanical properties of the native tissue which can be attained by selecting the most suitable scaffold [18]. The choice of scaffold is the key element in model design as it directs the cellular behavior and functions. A wide variety of materials are available as 3D cell growth supports ranging from natural materials to synthetic polymers. Among them, decellularised extracellular matrices (de-ECM) have significant advantages including retention of 3D matrix framework and biochemical cues for directing cell adhesion, proliferation and migration to match the native tissue. Current available *in vitro* vaginal models such as EpiVaginal™ from MatTek Life sciences are expensive and lack the lamina propria component in their constructs as the primary human cells are cultured on polycarbonate membranes or collagen substitutes.

In addition to this, three-dimensional (3D) *in vitro* wound tissue models are valuable preclinical models to understand the process of wound healing and to develop effective treatment strategies. Over the past decade, TE wound models have been used in the area of skin [19], cornea [20] and bone [21] tissue engineering. However, developing TE wound vaginal models have not previously been reported and are successfully reported in this project for the first time. In this PhD project, cost effective, accessible, reproducible, ethically sound and physiologically relevant tissue engineered (TE) models of the vaginal mucosa were developed using sheep vaginal tissues to study the oestradiol-responsiveness and biocompatibility of potential biomaterials developed for pelvic floor repair. For this purpose, decellularisation of sheep vaginal tissue was carried out using a combination of physical and detergent methods to serve as 3D matrix support for primary sheep vaginal fibroblasts and epithelial cells. This concept was based upon my understanding of TE skin [22], [23] and oral mucosa models [24]. Biomaterials implantation within the TE model along with conditions of mechanical injury (wound models) under estradiol -17β [E_2] administration enabled us to replicate the *in vivo* conditions that materials experience post-implantation. To date, this approach is the first of its kind to study the paravaginal tissue response towards implanted biomaterials *in vitro* under conditions resembling the clinical state.

1.2 The human female pelvic floor:

The human female pelvic floor is a dome-shaped, complex functional unit that is mainly composed of striated muscles and encloses the organs of the pelvis *i.e.,* bladder, vagina and rectum. None of these have any inherent shape or strength. While the role of fascia is to strengthen and support the organs, the role of ligaments is to suspend the organs and act as anchoring points for the muscles [25]. Muscle forces stretch the organs to contribute to their shape, form and strength.

The female pelvis is divided into three regions: anterior, middle and posterior which is separated by the vaginal walls attached to the pelvic sidewalls. The middle compartment only exists in the female pelvic floor and contains the female genital organs such as the ovaries, uterus, cervix and the vagina [25]. The anterior region is composed of the urethra and the bladder whereas the posterior region contains the rectum and anus. The normal function of the pelvic organs is dependent upon the integrity and support of the pelvic floor maintained by the synergistic action of muscles, fascia, ligaments and the bony architecture provided with a rich network of nerve supply. The bladder and urethra and the vagina and uterus are attached to the

pelvic walls by a system of connective tissue called as the endopelvic fascia. The endopelvic fascia and associated ligaments form a mesh-like group of collagen fibres interlaced with elastin, smooth muscle cells, fibroblasts and vascular structure. The endopelvic fascia is a continuous unit with variable thickenings and provides a capsule containing pelvic organs and allows displacements and changes in volume.

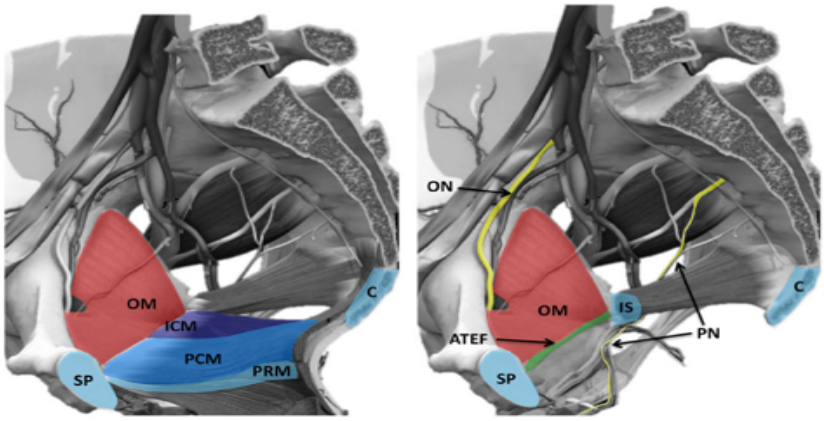

Figure 1.1: Anatomy of the female pelvic floor muscles and nerves. SP: symphysis pubis, C: coccix, IS: ischiatic spine, ATEF: arcus tendineus of the endopelvic fascia, OM: obturator muscle, ICM: ileo-coccygeus muscle, PCM: pubo-coccygeus muscle, PRM: pubo-rectalis muscle, ON: obturator nerve, PN: pudendus nerve. Reproduced with permission from [26].

1.3 Components of the pelvic floor:

The bony pelvis:

The human pelvis is a bowl-shaped bony structure which protects the abdominal and pelvic organs and also provides support to the spinal column [27]. It is composed of the ilium, ischium, pubis, sacrum and the coccyx and also provides the attachment site for muscles, ligaments and fascial layers to support the respective pelvic organs in place. The female pelvis is shorter, wider and more circular compared to the male. Various parts of the bony pelvis can be used as clinical landmarks in pelvic reconstructive surgery by the gynecologists.

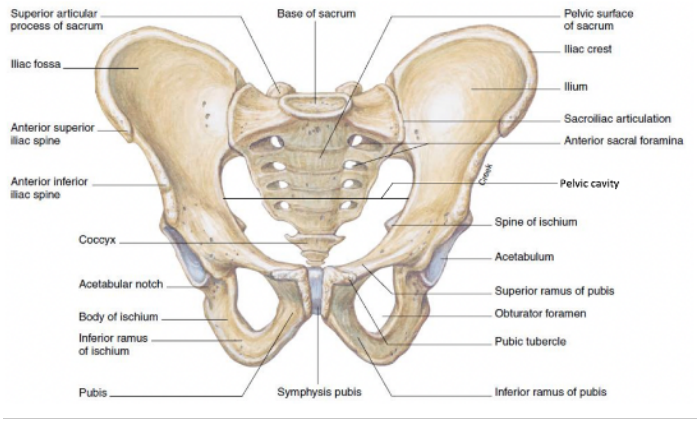

Figure 1.2: Anterior view of the pelvis. Adapted from [28].

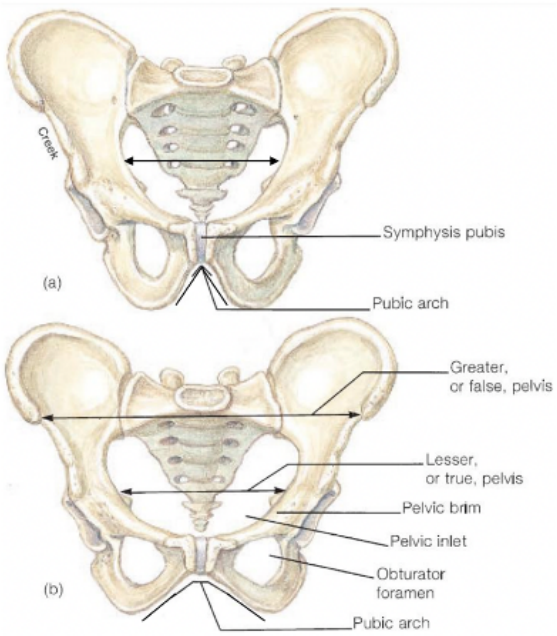

Figure 1.3: Anatomical variations between the (a) male and the (b) female pelvis. Adapted from [28].

The pelvic floor connective tissue:

The pelvic floor connective tissue is mainly composed of striated muscles, smooth muscles, collagen and elastin. These components act in concert, reinforcing each other but are different in terms of their specificity in functions. The striated muscles which include the pelvic diaphragm have a resting tone and can be modified both voluntarily and involuntarily during birth [29]. The fascia and tendons of these muscles play an important role in supporting the pelvic organs. On the contrary, the smooth muscle fibres are in active tone maintaining a

rhythmic contractility which is mediated by the autonomic nervous system. The elastic tissue is composed of an irregular network of elastin fibres consisting of amorphous elastin and microfibrils [30]. These fibres responds to stress by coordinated stretching without losing their elasticity as these have a natural tendency to bounce back to their original state. Any changes in these elastic fibres are responsible for the connective tissue biomechanical changes that lead to the development of the vaginal wall prolapse [31]. The collagen component is composed of interlacing meshwork of collagen fibres (predominantly collagen type III) that provides flexibility to the tissues but have relatively less stretchability compared to the elastic tissue fibres [32]. Both the elastin and collagen components of the pelvic floor connective tissue are continuously remodelled during the lifespan of an individual including childbirth, pregnancy, BMI, menopause and ageing.

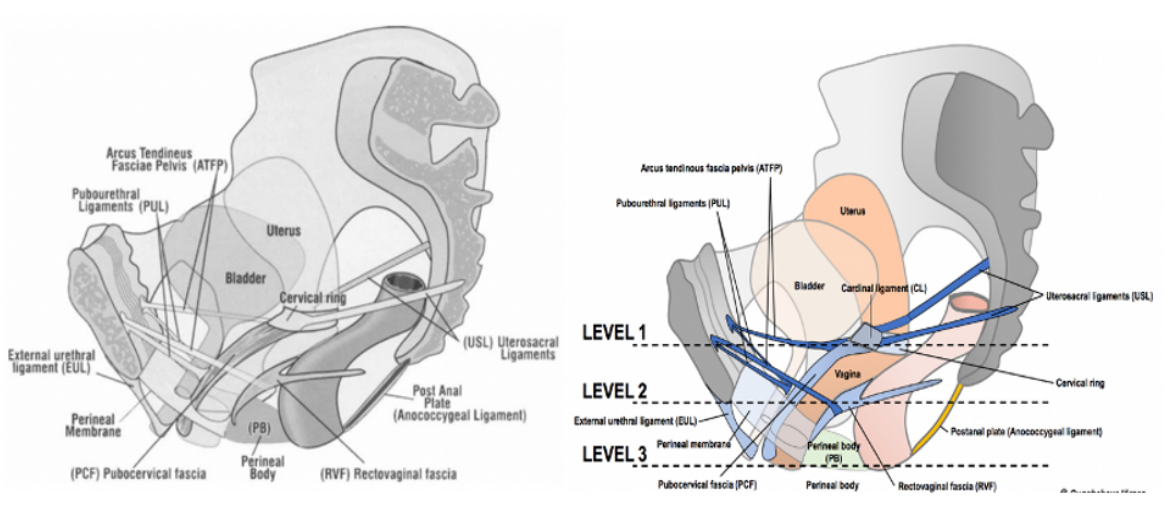

Figure 1.4: (A) A schematic 3D sagittal section of the main connective tissue structures of the pelvis depicting their attachments to the organs of the pelvic floor and pelvic bones and (B) associated levels of support. Reproduced with permissions from [33], [34].

The pelvic diaphragm:

The pelvic viscera occupies most of the pelvic floor and is embedded in the connective tissue layers forming the endopelvic fascia. The pelvic diaphragm is a 2-6 mm thin sheet of muscles that provides an intact tension-free foundation for the suspension of pelvic organs in the form of a hammock-like support at the bottom of the abdomino-pelvic cavity [35].

Along with the bony pelvis, the levator ani and coccygeus muscles form the floor of the pelvis and play an important role in protecting the endopelvic fascia from excess stretching and

straining by providing a lifting support at different levels (Figure 1.4B). The levator ani muscles along with its superior and inferior fascial coverings constitutes the pelvic diaphragm and consists of three subdivisions, named according to its origin of insertion: pubococcygeus, iliococcygeus and puborectalis [36].

The medial and anterior pubococcygeus, originating on the face of the pubis, is a V- or U-shaped sling that extends about 1.5 cm on both sides and stretches downwards and posteriorly. These muscles are thicker (1-2 cm) along the median margin and provide support and protection to the urethra, vagina, rectum and the upper portion of the perineal body. From a gynaecologist's viewpoint, these muscles are the most clinically significant region of the levator ani as they provide attachment site to the connective tissue and protect both external and internal genitalia.

The intermediate iliococcygeus, originating from the surface of the obturator internus fascia, is a dome shaped thinner muscle that measures around 0.5 - 1 cm in thickness. These muscles provide support to the coccyx and the lower sacrum. The puborectalis shares a common origin with the pubococcygeus that forms the deep layers of the triangular ligament. It passes downwards and backwards, continue with the deep external anal sphincter and provide muscular support for the anorectal junction.

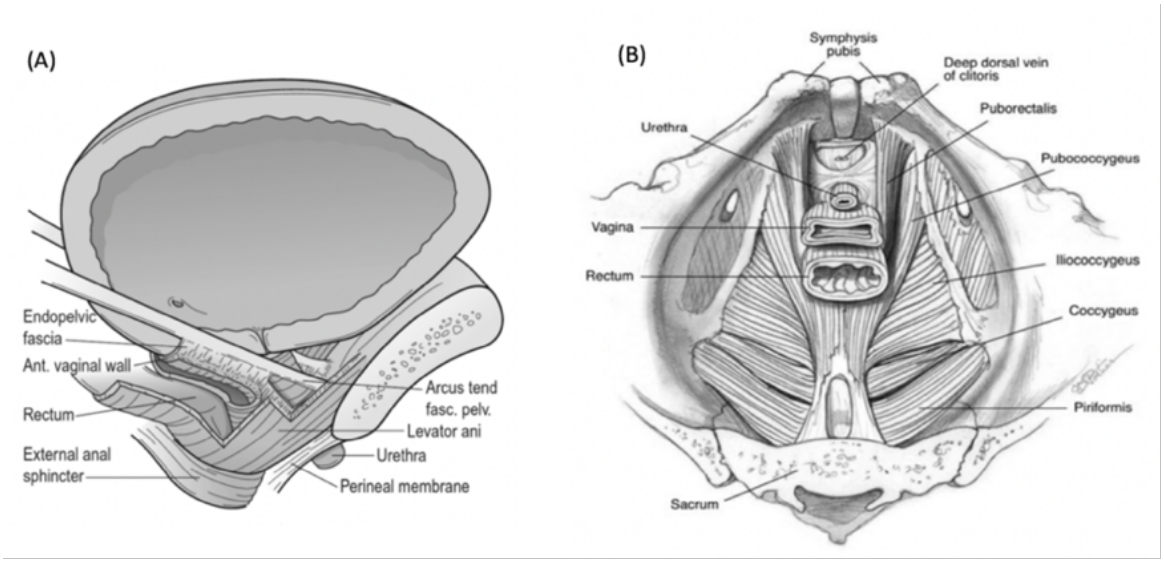

Figure 1.5: (A) Lateral view of the components of the urethral support system. The levator ani muscle serves multiple supportive role for the rectum, vagina and urethrovesical neck along with the endopelvic fascia. Reproduced with permission from [37]. *(B)Pelvic view of the levator*

ani demonstrating its four main supporting components: puborectalis, pubococcygeus, iliococcygeus and coccygeus. Reproduced with permission from [38].

The levator ani muscles contract to hold the pelvic organs enclosed at rest position and during activity they sustain the pressure dynamics developed in the intraabdominal walls. The levator ani is a highly specialized voluntary muscle that have connections with the external anal sphincter and act in concert [39]. These muscles are in a constant state of tone imparted by the presence of neuromuscular pressure receptors allowing to mediate the control of rectal incontinence [39]. The urethra is supported against the dynamic intraabdominal pressure (IAP) with a layer of the anterior vaginal wall and the connective tissue that attaches it to the pelvic bones through the pubovaginal section of the levator ani muscle. These supportive structures together maintain the sphincter closure of the urethra and prevents stress urinary incontinence (SUI). The vascular network also plays an important role in preventing urinary incontinence. The urethra is surrounded by large venous vessels that appear to be disproportionate for the adequate blood supply forming a spongy body. However, the intravascular pressure within these vessels ensures a mechanical force on the urethra and is responsible for prevention of urinary leakage.

1.4 Biomechanics of the pelvic floor:

Pelvic floor muscles are neuronally controlled and supported by the connective tissue arranged in a 3D arrangement. The support mechanism of the pelvic floor is provided by the combination of muscles, fascia and ligaments and weakening of these supportive structures can lead to the development of pelvic floor disorders (PFD) such as pelvic organ prolapse (POP) and stress urinary incontinence (SUI). These disorders pose a major public health concern and affect millions of women around the world. Based on a US encounter database, the estimated lifetime risk of surgery for either POP or SUI in women is as high as 20% with a substantial recurrence rate resulting in reoperation (29.2% of cases). Both POP and SUI are clinically challenging disorders due to their unclear pathophysiology, inadequate treatment and mishandling of cases. The pelvic floor is a dynamic environment with a combination of muscles, fascia and ligaments working together to keep the pelvic organs in place. Understanding of the biomechanics of the pelvic floor supportive tissues is key to understanding the onset of pelvic floor disorders. The biomechanics of tissues can be categorised as active or passive behavior and can be studied by using either *ex vivo* methods or *in vivo* methods [40]. The *ex vivo* methods include uniaxial or

biaxial tensile testing while the *in vivo* testing involves examining muscle stretching using ultrasound or electromyography.

The loading environment of the pelvic floor:

There are several anatomical components that contribute towards the support of the pelvic floor. Smooth muscles such as levator ani and the vaginal wall contributes towards the active biomechanical properties of the pelvic floor and able to generate force through muscle contractions [41]. Passive biomechanical properties of the pelvic floor allow tissues to respond to pressure changes by transmitting load without generation of external forces [42] and these can be divided into structural and mechanical properties. These properties can be measured by a conventional uniaxial tensile test as shown in Figure 1.6.

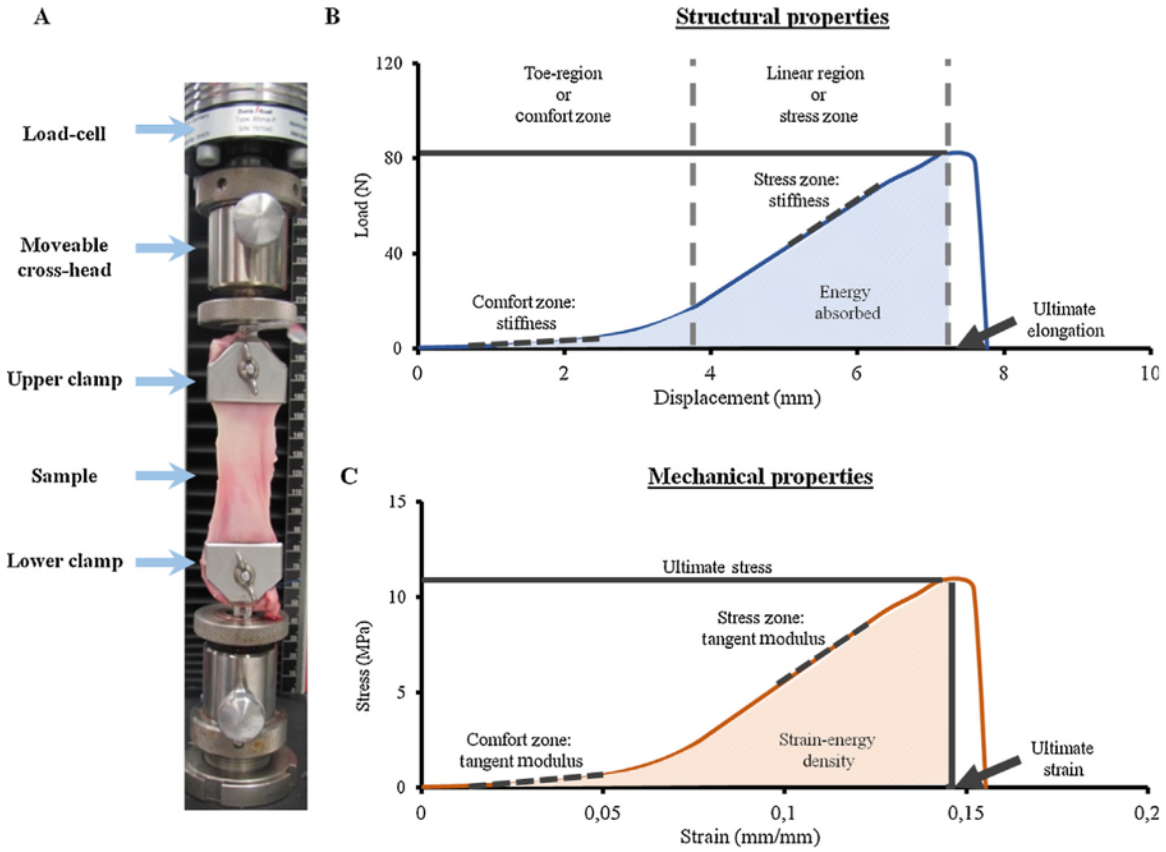

Figure 1.6: Representative in vitro measurement of structural and mechanical properties of a tissue sample by uniaxial tensile testing. (A) An example of tissue sample clamped in a tensiometer for tensile testing. (B) Illustration of different regions of the load-displacement curve. (C) A stress-strain curve from a uniaxial tensile test. Reproduced with permission from [43].

Studies on the biomechanics of human pelvic floor muscles have reported mainly passive properties which means that the muscles and fascia of the human pelvic floor can resist deformation and transmit load without generating any external forces [43]. These properties are crucial as the pelvic floor muscles are constantly being loaded by intra-abdominal pressure and various activities such as walking, jumping, coughing, sneezing, obesity *etc.* [44] The female pelvic floor muscles and tissues experience drastic pressure changes during conditions such as pregnancy, childbirth or prolonged labor. A combination of IAP and these elevated loads presents a higher risk for injury to the pelvic floor muscles and increased chances of developing pelvic floor disorders such as POP, SUI or fecal incontinence.

During the lifetime of an individual, different pelvic floor tissues have different degrees of stiffness and respond to strain differently [44]. Studies have suggested that in younger women, the uterosacral ligaments and the vagina responds similarly to everyday small displacements but as women get older, the ligaments become more rigid and there is a mismatch in the biomechanical properties of the ligaments and the vaginal tissue [45]. In elderly women, as the ligaments became stiffer and less extensible compared to the vaginal tissue there is a non-uniform transfer of load between these tissues and such individuals are vulnerable to developing pelvic floor dysfunctions [46].

1.5 Pelvic floor dysfunctions (PFDs):

Pelvic floor dysfunctions (PFDs) embrace a wide variety of clinical conditions that involve functional abnormalities of the pelvic floor leading to impaired urinary and sexual functions and rectal voiding [47]. These conditions include pelvic organ prolapse (POP), urinary incontinence (UI/SUI), anal incontinence (AI), sexual dysfunctions, fecal incontinence (Fi), overactive bladder (OAB) symptoms and several chronic pain syndromes [48]. PFDs affect millions of women worldwide and have a significant impact on the quality of life and can be particularly distressing and bothersome.

Prevalence of PFDs:

Globally, it has been estimated that 11- 35.5% of women suffer from PFD's [49] while in developed countries 46% of women experience at least one form of PFDs [50]. The proportion of women suffering from one or more PFD increases significantly with age and accounts for 53% of the elderly population [51]. An estimated one in every five women will undergo surgical intervention for treating PFDs in their lifetime. Evidence from several countries have

identified common risk factors for PFDs such as advancing age, parity, obesity, vaginal birth and trauma to the lower genitourinary tract. In many developing countries women are hesitant in reporting their reproductive health problems due to the social stigma involved and lack of availability of special reproductive care and hence, the magnitude of the problem remains largely unknown.

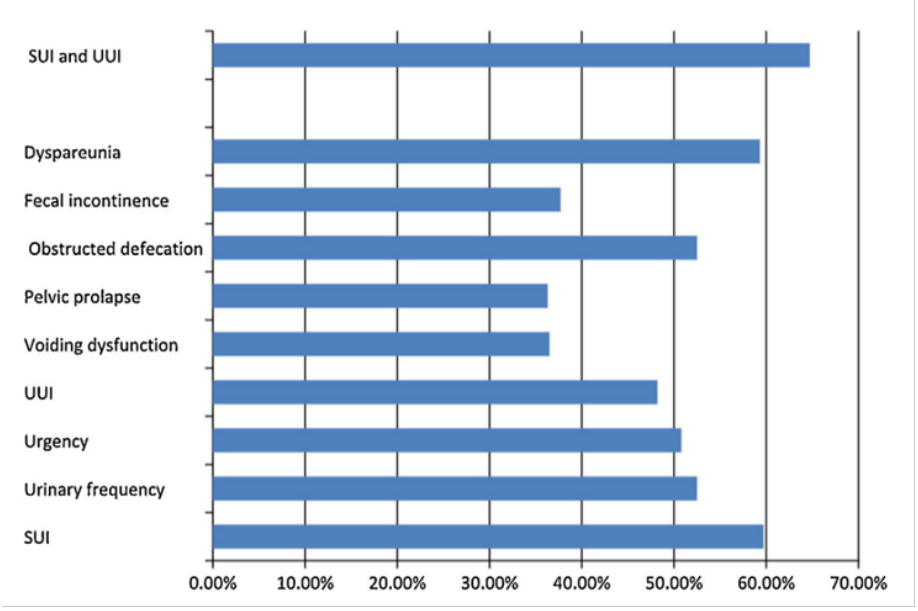

Figure 1.7: Prevalence of pelvic floor disorder symptoms. Reproduced with permission from [52].

It has been estimated that stress urinary incontinence affects around 30-60% of adult woman whereas 11-15% are affected by the pelvic organ prolapse (POP) [50] and many women present with a combination of these conditions. Both pelvic organ prolapse (POP) and stress urinary incontinence (SUI) are common conditions and their prevalence increases with age.

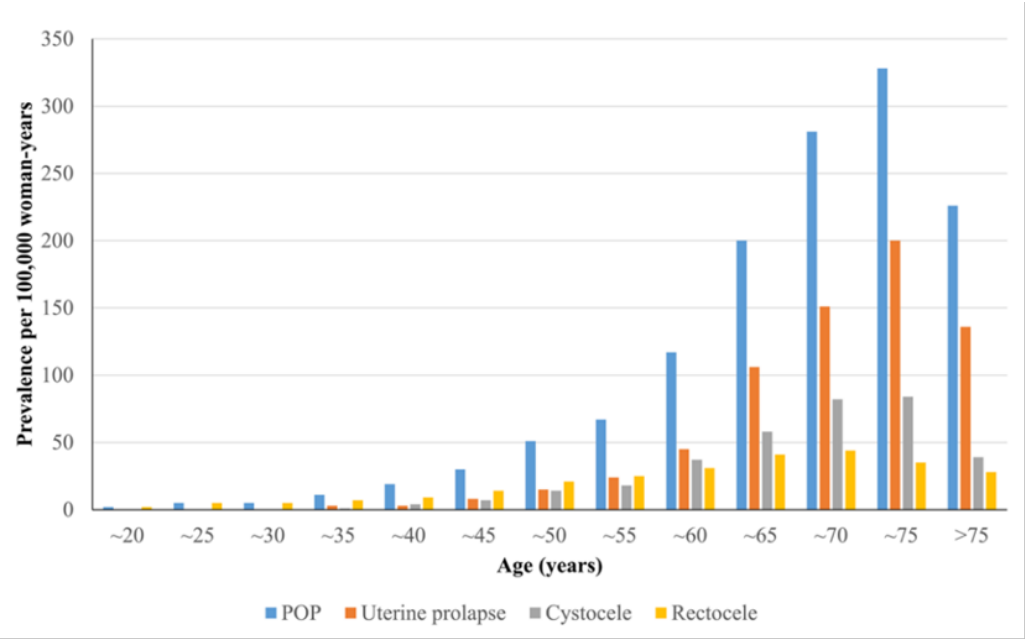

Figure 1.8: An increase in prevalence of POP and SUI with age. Reproduced with permission from [53].

Economic and healthcare burden of PFDs:

The economic and healthcare burden of pelvic organ prolapse (POP) and stress urinary incontinence (SUI) is enormous as POP is one of the major indication of gynecological surgery including hysterectomy (>55 years old) in women worldwide. In 1997, more than 225,000 surgical procedures were undertaken for treating POP in the USA [54] that accounted for an estimated cost of more than US$1 billion [55]. In the UK, 20% of women suffering from any form of prolapse are on the waiting list for a major gynecological procedure [56]. Based on the data from a regional study, 15-18% of all women will undergo surgical intervention for some type of prolapse in their lifetime worldwide and 30% of these women undergo recurrent surgical procedure [57].

1.6 Pelvic organ prolapse (POP) and stress urinary incontinence (SUI):

Pelvic organ prolapse (POP) is a disorder exclusive to women in which organs of the pelvic floor, which is normally supported by the pelvic floor muscles, such as bladder, bowel and uterus herniate or protrude into the vagina [58]. POP is also referred to as the urogenital prolapse which is the downward descent of a single or a combination of pelvic organs. Most patients with POP are asymptomatic however, depending on the type and stage of prolapse the

symptoms can be bothersome which eventually require surgical intervention. There are different types of prolapse depending upon the type of organ bulging through the vaginal wall including: cystocele or anterior wall prolapse characterised by the displacement of the bladder from its normal position while rectocele refers to the prolapse of the rectum. Another prolapse type is the drop of the uterus into the vagina called the uterine prolapse.

As defined by the International Continence Society "Urinary incontinence (UI) is a condition in which involuntary loss of urine that causes a social or hygienic problem and is objectively demonstrable" [59]. The most prevalent type of UI is the stress urinary incontinence (SUI) which is the involuntary loss of urine or urine leakage during coughing, sneezing or any other physical activity including running or weightlifting that can happen due to increase in intraabdominal pressure (IAP) [60]. Although SUI is not a life-threatening disease, it is socially and mentally debilitating for women and may result in reduced quality of life.

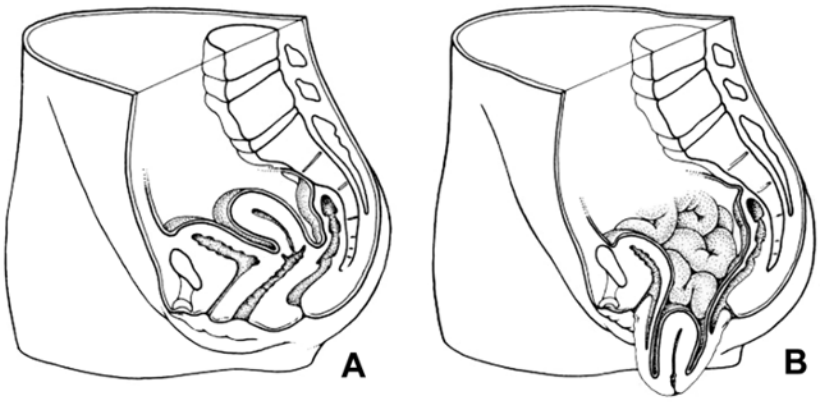

Figure 1.9: Mechanism of pelvic organ prolapse (A) normal anatomical position (B) total pelvic organ prolapse. Reproduced with permission from [61].

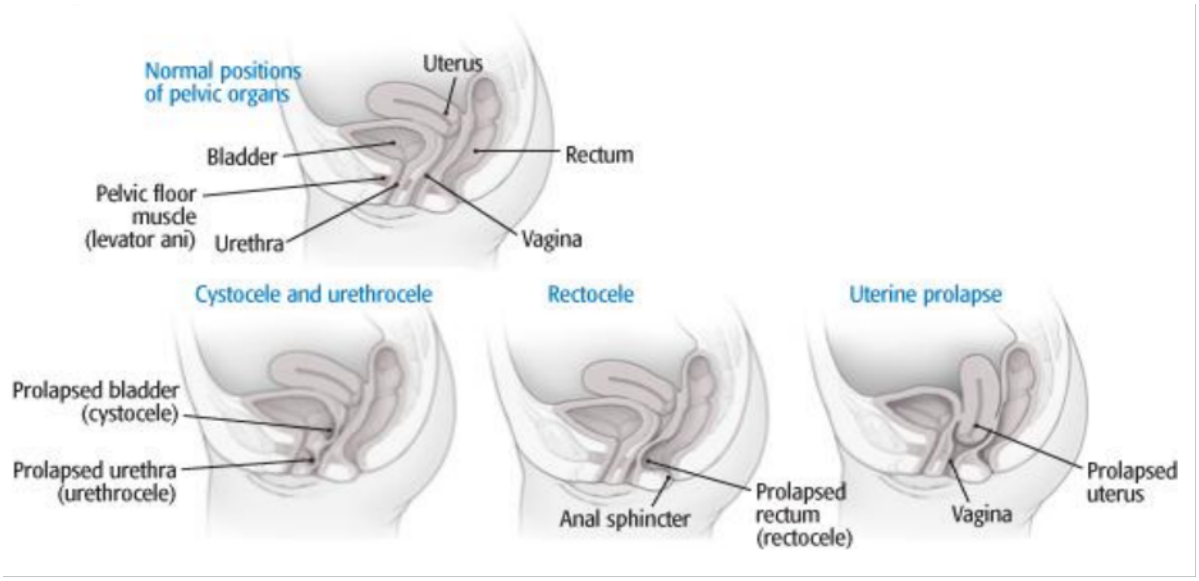

Figure 1.10: Sagittal representation of POP involving different injury sites and prolapsed respective pelvic viscera through the vagina. Adapted from [62].

Mechanism of pelvic organ prolapse:

In the human female pelvic floor, the levator ani muscle is the most predominant supporting muscle for both pelvic and the abdominal organs. These muscles act synergistically with the striated muscles of the anterior vaginal wall to endure changes in the intraabdominal pressure and distribute the mechanical load and pressure changes equally on the associated muscles and fascia. Any disease or trauma that causes weakening of these muscles will result in an unequal distribution of load on any one of the pelvic floor organs that may cause it to prolapse. The muscle components of the levator ani complex are tonically contracted at rest that keep the genital hiatus closed and provide a stable foundation for the pelvic viscera [63]. Muscle trauma or denervation of the levator ani causes a decline in the muscle tone that results in an open urogenital hiatus, weakening of the levator plate and a bowl-like configuration. Such anatomical derangements were commonly observed in patients suffering from different grades of pelvic organ prolapse using 3D magnetic resonance imaging (MRI) assessment [64].

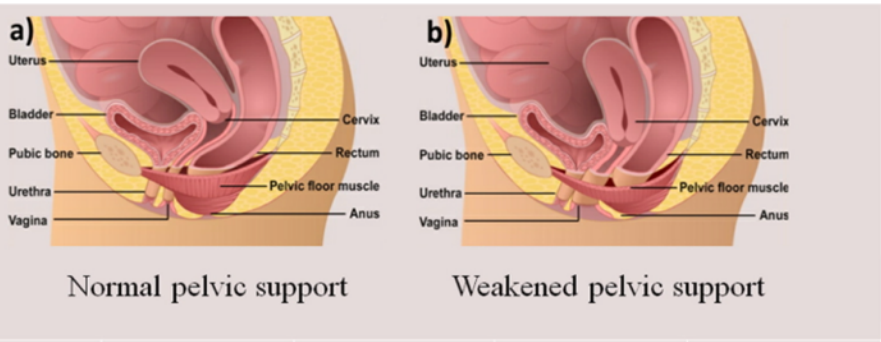

	Pre-menopause	Post-menopause	Pre-menopause	Post-menopause
Elastic modulus / MPa	6.65 ± 1.48	10.26 ± 1.10	9.45 ± 0.70	12.10 ± 1.10
Ultimate tensile strength / MPa	0.79 ± 0.05	0.42 ± 0.03	0.60 ± 0.02	0.27 ± 0.03
Ultimate strain	0.68	0.37	0.50	0.14

Figure 1.11: Anatomical structure and biomechanical properties of the pelvic floor support system (a) healthy pelvic floor and (b) weakened pelvic floor. Reproduced with permission from [65].

Staging of POP:

In routine gynecological care, examination of the pelvic floor can reveal the earlier signs of prolapse with 43-76% patients presenting with symptoms of loss of vaginal or uterine support [66]. Women who develop pelvic organ prolapse often present with symptoms of vaginal bulging or pelvic pressure or have complaints of recurrent feelings of urgency and pelvic discomfort. There is no clear consensus on what level of prolapse represents a deviation from the normal uterovaginal support, however, most clinicians would agree that prolapse of any pelvic organ beyond the hymen is a clinically significant symptom. In 1996, a new method for quantifying pelvic organ prolapse (POP-Q) was published by an international committee [67] that was later reviewed and adopted by the International continence society (ICS), American Urogynecological Society (AUGS) and the Society of Gynecological Surgeons (SGS). The POP-Q system is now accepted as the gold standard system for reporting the different stages of the prolapse in patients [68].

Stage 0: No prolapse demonstrated

Stage I: The most distal portion of the prolapse is more than 1cm above the level of the hymen

Stage II: The most distal portion of the prolapse is 1 cm or less proximal to or distal to the plane of the hymen

Stage III: The most distal portion of the prolapse is more than 1 cm below the plane of the hymen

Stage IV: Complete prolapse of the total length of the lower genital tract is demonstrated

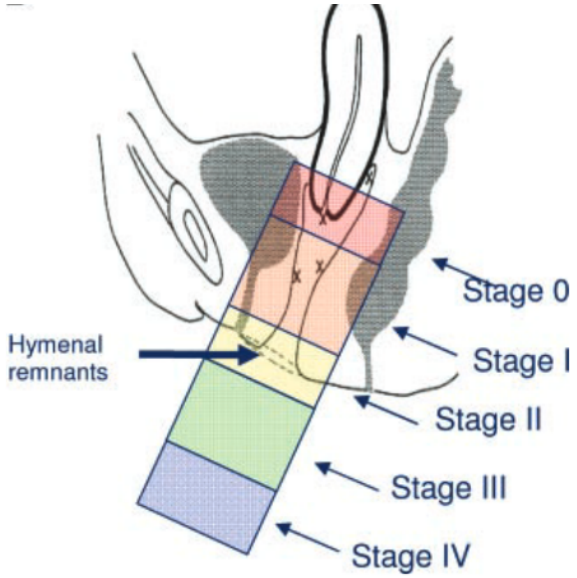

Figure 1.12: Prolapse staging- 0, I, II, III and IV (uterine- by the position of the leading edge of the cervix). Reproduced with permission from [69].

1.7 Risk factors for POP and SUI:

Pelvic organ prolapse and stress urinary incontinence can coexist in women and the cause of these disorders is likely to be multifactorial. Pregnancy, vaginal delivery, prolonged second stage of labor, increased BMI, age, menopause and hereditary factors are the most prevalent risk factors identified.

Pregnancy and vaginal delivery:

Several systematic studies have proposed multiple vaginal deliveries and parity as a significant risk associated with the development of POP and SUI. According to an Oxford Family Planning study, an increase in the vaginal parity was the strongest risk factor for developing POP in younger women compared to the nulliparous [70]. Similar reports by Pelvic Organ Support Study showed that there is a direct correlation between increased risk of developing POP with increasing parity [66]. The attributable risk of vaginal delivery for the development of POP was studied by the California health maintenance organization. Their findings showed that women with the medical history of one or more vaginal deliveries are at a higher risk of

developing symptomatic POP compared to those that had a caesarean section [71]. DeLancey *et al.,* [72] imaged the levator ani muscles from nulliparous women and compared it with those in women after vaginal birth using magnetic resonance imaging (MRI). They documented that about 20% of women who have given birth vaginally were presented with visible defects in the levator ani muscles compared to the nulliparous women. This study provided the first scientific proof that supports the evidence of injury to the levator ani muscles in women due to vaginal delivery which is a major risk of developing POP.

Menopause:

The menopause is defined as the onset of amenorrhoea (permanent cessation of menstruation) that marks the end of a women's reproductive capability [73]. Both oestrogen and progesterone receptors located throughout the urogenital tract are sensitive towards the hormonal changes which a woman experiences during menopause [74]. The decline in oestrogen level during the menopause is sensed by the oestrogen receptors present in the vaginal wall which causes changes in the vaginal area. These changes include reduced elasticity of the vaginal wall, changes in the vaginal wall connective tissue, vaginal epithelium thinning and reduced vascularity of the vagina [75]. All these changes can lead to urogenital symptomatology as both the female genital and lower urinary tract are closely related. Approximately 50% of postmenopausal women complain about dyspareunia, dysuria, urgency and recurrent bladder infections which can lead to urinary incontinence or vaginal prolapse and can have adverse effects on the quality of life [76].

Oestrogen depletion:

The sex steroid oestrogen plays a crucial role in maintaining a healthy female pelvic floor. Oestrogens play their role by interacting with their high-affinity intracellular oestrogen receptor (ER) present in the pelvic floor organs and structures such as the bladder, urethra, vaginal wall, levator ani muscles and utero-sacral ligaments [77]. Oestrogen is responsible for increasing the cell maturation index and collagen turnover in the epithelial tissues of genito-urinary tract [78] and also increase the amount of muscle fibres in the urethral muscle layers [79].

There are two subtypes of ER: ER-α and ER-β, both extensively found in the vaginal wall. Studies have shown a significant difference in the expression of ER-α and ER-β receptors in the vaginal wall of premenopausal and postmenopausal women and the expression of ER-β was markedly reduced in postmenopausal women [77]. Reports have suggested that the ER receptors in the vaginal wall are the key targets for oestrogen action and changes in the expression of ER receptors in the anterior vaginal wall of postmenopausal women are the leading cause of SUI [74], [80].

Connective tissue disorders:

Connective tissue disorders resulting in architectural changes in the collagen crosslinking are suggested to contribute towards the prevalence of POP and SUI. Ehlers-Danlos and Marfan syndrome are two heterogenous group of connective tissue disorders involving collagen and fibrillin 1 gene defects respectively [81], [82]. Cohort studies investigating patients with these connective tissue disorders revealed a high incidence (33 - 50%) of POP and SUI among these patients [83]. The authors concluded the etiological role of connective tissue disorders is a major contributing factor in the pathogenesis of pelvic floor dysfunctions.

Molecular Basis:

Investigations on the molecular mechanisms may further aid in the identification of women at a higher risk of developing POP and SUI. Connell *et al.,* [84] studied the correlation between HOXA11 gene expression levels and the possible onset of POP and SUI in HOXA11-Knockout mice . HOXA11 is a transcription regulator in development of the urogenital tract in early developmental stage. The authors reported absence of uterosacral ligaments in HOXA11-neagative mice. Further studies revealed a decline in the levels of collagen I, III and HOXA11 gene expression in uterosacral ligaments of patients with POP associating HOXA11 as a contributing factor.

In another study by Kushner *et al.,* [85] collagenolytic activity in women suffering from stress urinary incontinence was significantly higher compared to the continent control group. Using a competitive enzyme immunoassay, the authors reported an increased level of urinary helical peptide α1 620-622 secretion associated with un-crosslinked collagen in women with SUI. Chen *et al.,* [86] reported similar findings by examining the anterior vaginal wall biopsies from patients with SUI and stage II-POP. A higher (80%, $p = 0.05$) quantitative mRNA expression

of matrix metalloproteinases (MMP-1, MMP-2 and MMP-9) was reported that is consistent with increased collagen degradation compared to control group.

Other risk factors:

Obesity is another identified factor for the development of POP and SUI. Swift *et al.,* [66] carried out a multicenter observational study on patients visiting outpatient gynecology clinics. Their multivariate analysis revealed age, increased body mass index (BMI), pregnancy, Hispanic race and increasing weight of a vaginally delivered infant as contributing risk factors for the development of POP and SUI.

Collagen changes in the vaginal wall from prolapse patients:

The onset of POP and SUI is multifactorial and various investigations have reported mechanical, neurological as well as connective tissue factors. Collagen is the main component of pelvic floor connective tissue and play a crucial role in resisting the tensile forces. In 1996, Jackson formulated his theory of pathogenesis of POP by stating that POP patients have a reduced collagen content and an increased metalloproteinase activity (MMPs) compared to non-POP patients [87]. He postulated that in young patients with POP there is ahigh turnover of collagen that resulted in an increased production of immature cross-linked collagen fibres in the vaginal wall. This hypothesis still appears to be valid in later investigations.
Evidence has suggested that patients with POP have altered collagen metabolism that resulted in an increase in collagen type III and a decline in collagen type I that caused stiffness in the uterosacral ligament and anterior vaginal wall of these patients [88]. The switch from type I to type III collagen resulted in greater distensibility as type III collagen consists of thin and fragile fibres but also contributes towards fragility of the vaginal wall as these fibres are unable to support the mechanical loading of the pelvic organs in daily routine [89]. Moalli *et al.,* [90] histologically analysed human vaginal tissue biopsies and revealed significant changes in the arrangement of collagen fibres in POP women compared to control.

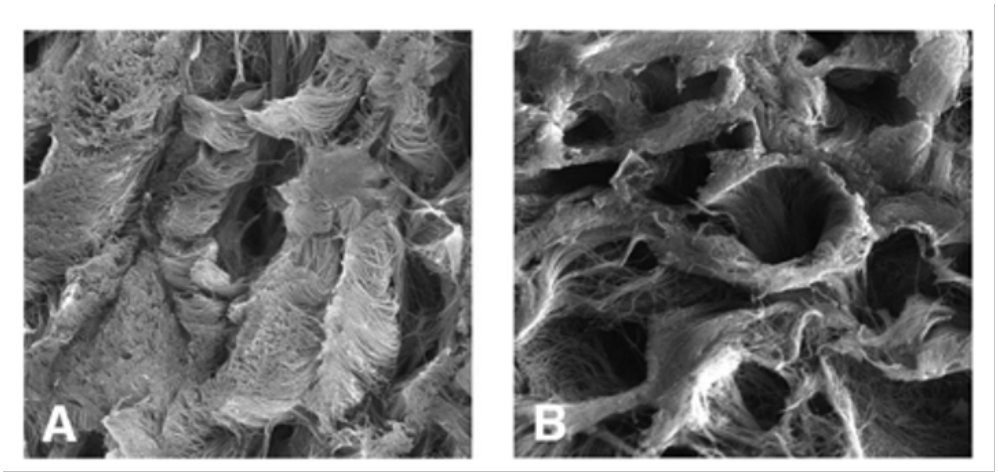

Figure 1.13: Representative scanning electron micrographs of the vaginal subepithelium showing arrangement of collagen fibres in (A) a control and (B) a premenopausal patient with prolapse. Reproduced with permission from [90].

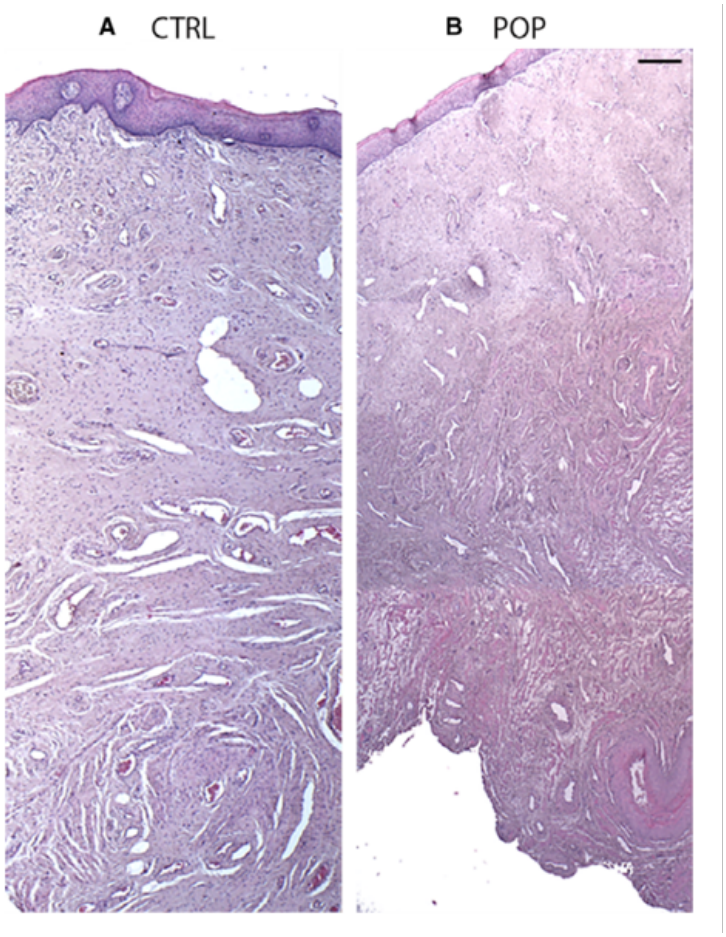

Figure 1.14: Haematoxylin and Eosin (H&E) staining of anterior vaginal wall of (A) control and (B) POP samples. Visible histological differences could be seen in the organisation of the muscle fibres in the lamina propria of the vaginal tissue from POP patients. Reproduced with permission from [91].

Changes in the muscularis propria in POP patients:

A hallmark of POP is the disorganised architecture of the muscularis propria containing disrupted arrangement of muscle fibres in tissue biopsies of prolapsed patients. More recently, Sferra *et al.,* studied the altered remodelling of the muscularis propria in the anterior vaginal wall of POP patients due to a reduction in the presence of concentrated elastic fibres and imbalanced extracellular matrix turnover as a result of overexpression of matrix metalloproteinases (MMPs). At the cellular level, it has been demonstrated that the smooth muscle cells in the muscularis undergo an aberrant trans-differentiation into myofibroblasts that could be the underlying cause of structural modifications and collagen synthesis of the anterior vaginal wall of POP patients [92]. Ruiz-Zapata *et al.,* [93] isolated vaginal fibroblasts from human biopsies of normal and prolapsed anterior vaginal wall tissues and expanded in cell culture medium. The cultured vaginal fibroblasts from postmenopausal prolapsed tissues showed lower contractile capacities, altered mechano-responses and produced altered matrices *in vitro* compared to the control.

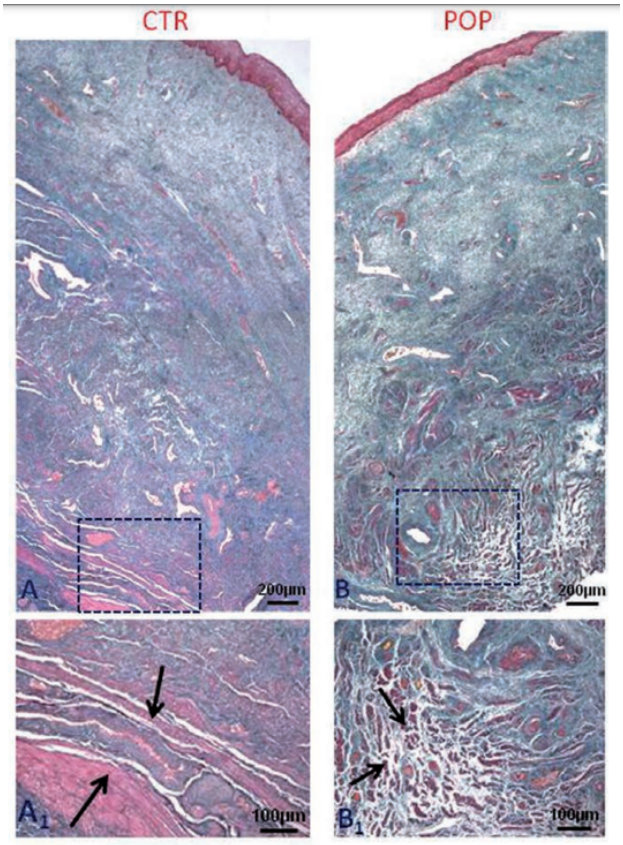

Figure 1.15: Histological features from the anterior vaginal wall of control and POP patients. Masson's trichrome staining showing (A&A1) typical muscularis architecture with SMCs well organized in fibres (B&B1) muscularis in POP patients showing poorly organized SMCs with a distorted muscular architecture. Reproduced with permission from [92].

1.8 Management of pelvic floor dysfunctions:

Depending on the severity of the problem and its origin *i.e.,* either a congenital defect or an acquired, several non-surgical and surgical treatment options are available to the patients. The main goal of the conservative management is to improve symptoms, delay progression and to avoid surgery for POP as much as possible.

Non-surgical treatments:

The world-wide epidemiology of pelvic floor dysfunctions (PFDs) is currently unknown as patients may be reluctant to discuss their symptoms due to embarrassment and associated social stigma. There is a need to increase awareness and understanding of these conditions in the healthcare community to provide support to these patients. According to the National Institute for Health and Care Excellence (NICE) guidelines, women with a BMI greater than 30 kg/m^2 should be advised on weight loss as a preventive measure for PFDs [94].

Pelvic floor muscle exercises:

Pelvic floor muscle training involves exercises to improve pelvic floor muscle strength, tone, endurance to recover the muscle support to the pelvic organs. It has been reported that there is a 17% higher chance of improvement of symptoms by one stage of POP after pelvic floor muscle exercises compared to the control group [95].

Intravaginal devices:

Vaginal pessaries have long been used in clinical practice as a viable option for women with pelvic organ prolapse and stress urinary incontinence as an alternative to surgical intervention [96]. These are often offered as a first line of management of POP in elderly women with significant comorbidities that makes them poor surgical candidates [97]. Pessaries are mechanical supportive devices that are placed intravaginally to restore the prolapsed organ back to their normal anatomical position. They came in a variety of shapes and sizes and are made up of medical-grade silicone or latex rubber that provides the advantages of durability, longer shelf-life, non-allergenic and are easily sterilised *via* autoclaving [98]. However, this noninvasive conservative treatment is used for short-term symptomatic relief with an associated risk of developing infection or inflammatory responses in the patients.

Figure 1.16: Commercially available pessaries with a wide range of sizes and designs. From Milex Products Inc.

Hormonal administration:

Evidence has suggested that a decline in oestrogen levels of postmenopausal women affects the periurethral tissues and develop pelvic laxity which contributes to POP and SUI. Local hormonal therapy (HT) in the form of topical vaginal creams, tablets or suppositories has proved to be an effective strategy by improving the symptoms of incontinence, thinning of vaginal epithelium, dysuria and recurrent infections [99]. Tyagi *et al.,* [100] investigated the effects of local oestrogen therapy (LET) in 52 postmenopausal women suffering from severe prolapse. They concluded that LET significantly increased the protein and gene expression levels of matrix extracellular proteins (collagen and elastin) and reduced undesirable ECM degradation that strengthened the vaginal ECM in tissue biopsies compared to control.

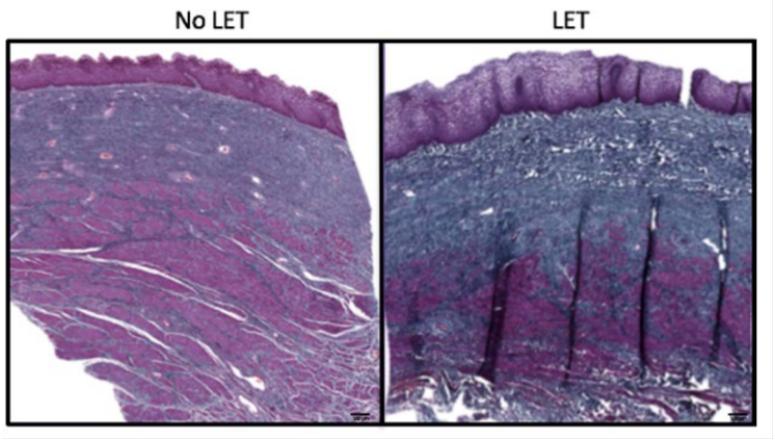

Figure 1.17: Modified Masson's Trichrome staining for visualization of total collagen (blue) and elastin (black) in tissue biopsies from control (no LET) and treated (LET) women. Scale bar 500 µm. Reproduced with permission from [100].

Surgical treatments:

Surgical intervention is inevitable in women for the treatment of symptomatic POP where conventional treatments fail to improve symptoms. Broadly, two surgical approaches are used in clinical practice: abdominal and transvaginal with different forms of biological or synthetic graft materials. The initial surgical technique for SUI performed by Von Giordano using gracilis muscle flap dates back to 1907 [101] with later developments of the surgical techniques by Burch in 1961 [102] referred to as the Burch colposuspension, recalled as the gold standard primary surgery for SUI. However, the success rate of laparoscopic Burch colposuspension relays on the surgeon's experience and skills. In 1998, Ulmsten *et al.,* [103] introduced the tension-free vaginal tape (TVT) procedure by using the synthetic mesh sling. The TVT mesh slings were originally evolved from the surgical mesh used for abdominal hernia repair in 1950s. Since the late 1990s, there was a tangential increase in the development of synthetic mesh products by the manufacturers in line with the increasing acceptance of minimally invasive mesh procedures for POP and SUI by the surgeons as well as patient community.

1.9 The pelvic mesh:

In 1996, the US Food and Drug Administration (FDA) first approved the use of synthetic PPL (Marlex®) [104] for SUI and later in 2002 for POP patients (Gynemesh®) [105]. Later on, surgical mesh products were evolved into "Mesh Kits" that include guided trocars and associated tools to help with insertion and placement of graft material around the prolapsed organs to provide them lifting support. The first "Mesh Kits" were approved in 2004 by the FDA under the names of Apogee and Perigee manufactured by the American Medical Systems (San Jose, CA, USA) [106]. By the end of 2010, an estimated 75,000 women had received mesh implants for POP and 200,00 for SUI in the United States alone [107].

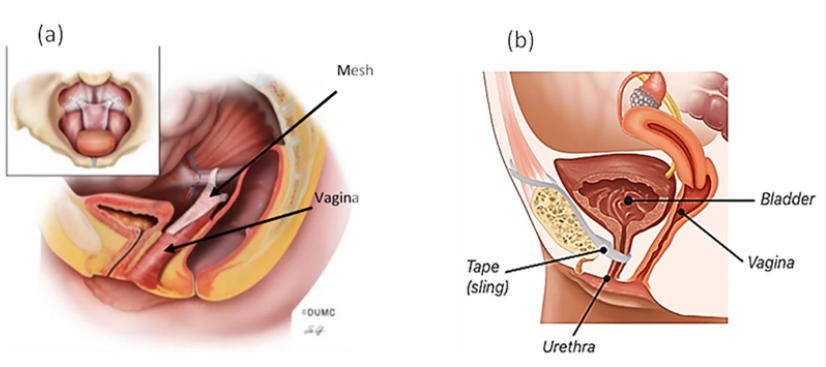

Figure 1.18: Examples of (a) a mesh type used for POP. Reproduced with permission from [108] *and (b) a sling used for SUI. Reproduced with permission from* [109].

In the late 1980s the polypropylene mesh had been used as the gold standard synthetic graft material in gynecology to treat women experiencing vaginal prolapse and urinary incontinence. Polypropylene (PPL) is a permanent material made out of synthetic filaments that is neither absorbable nor degraded [110]. These PPL meshes differ in their composition (monofilament vs multifilament), architecture (woven vs knitted), porosity, weight and biomechanical properties (flexibility and stiffness). An ideal graft for POP and SUI repair should be non-inflammatory, inert, non-toxic, mechanically compatible with the host tissue, non-carcinogenic, convenient to use by surgeons and affordable.

Classification:

According to Amid [111], biomaterials for POP repair are classified into 4 categories:
Type I: Macroporous- the mesh pore size is > 75 μm, which is desirable for infiltration by the fibroblasts, macrophages, neo-collagen and newly formed vasculature (angiogenesis).
Type II: Microporous- the mesh pore size is < 10 μm which presents a barrier to neo-tissue formation.
Type III: Hybrid (macroporous/microporous) contains multifilament components.
Type IV: submicron pores.
The pore size is crucial in designing synthetic implants as it determines the infiltration of macrophages and leucocytes into the implant site in order to prevent infections. A larger pore size (> 75μm) is also required for fibroblasts migration and blood vessels ingrowth to allow for proper implant integration with the native fascia [112]. The mechanical properties of the mesh such as strength and flexibility are also dependent upon the knitting pattern, fibre architecture and pore size. Microporous (< 10μm) mesh are stiffer that restrict the infiltration of fibroblasts and macrophages but allow entry of most bacteria (< 1μm in diameter) and are prone to infections [113]. The micropores result in a colonization of immune cells on the periphery of implanted material that results in encapsulation and graft rejection. In addition, microporous meshes are more elastic, light weight and are less prone to infection and tissue erosion [113]. Thus, monofilament microporous Type I meshes of low weight were the preferred choice for prolapse surgery. Some examples of synthetic mesh in urogynecology surgery are given in Table 1.1.

Table 1.1: Types of synthetic mesh for POP and SUI treatment. (Information included from manufacturers sites and brochures for product information).

AMS – American Medical Systems, Inc., Minnetonka, MN, USA. Ehicon – Johnson & Johnson Medical, Somerville, NJ, USA. Gynacare – Ethicon Women's Health & Urology, Somerville, NJ, USA. AMA – American Medical Associaton (Distributed by Boston Scientific).

Devices (Brand)	Mesh type	Advantages
IntePro™ (AMS)	Lightweight polypropylene (50 g/m^2) and considerable porosity (> 10 μm)	Formulation commonly used in other meshes. High flexibility.
Intemesh™ (AMS)	Silicone-coated polyester. InhibiZone (rifampin and minocycline) impregnated in silicone	High support for soft tissues and great regenerative capacity
Apogee™ (AMS)	Type 1 polypropylene mesh	Minimally invasive
Anterior, Apical and Posterior Elevate® (AMS)	IntePro® Lite: Ultra-lightweight polypropylene (< 50 g/cm^2)	Low density allows extreme anatomic comfort and adequate vaginal mobility. Minimal invasive insertion kit and approach. Effective in cystocele and enterocele repair
Perigee® (AMS)	IntePro® or IntePro® Lite	Tension-free mesh
Prolene™ (Ethicon)	Type 1 polypropylene mesh	Well formulated used in other meshes
Vycril™ (Ethicon)	Absorbable mesh of polyglactin 910 (90% glycolide and 10% lactide)	Non-antigenic and nonpyrogenic. Great polymeric absorption during tissue ingrowth

Vypro™ (Ethicon)	Lightweight polyglactin 910	Bigger pores and better biomechanical behaviour than Prolene™
Vypro™ II (Ethicon)	Lightweight multifilament mesh composed Prolene™ 50% and VicrylTM 50%.	Long-term tissue integration. Effective formation of tissue connective scar
Prolite™ (Atrium)	Macroporous polypropylene mesh. Monofilaments aligned parallel	Monofilaments wellspaced angles allow optimal material 2D flexibility
Prolite Ultra™ (Atrium)	Lightweight (50 g/cm^2) Litemesh™ with microfilaments and 25% less material than Prolite™	Softer and comfortable. Tensile strength reinforcement that is 83% stronger than the normal abdominal wall tissue
Gynemesh™ PS (Gynacare)	Prolene™ Soft Mesh	70% more flexible than Prolene™. Lower density reduces the mesh wear
Prolift® (Gynacare)	Gynemesh™ PS	High strength retention during surgical insertion

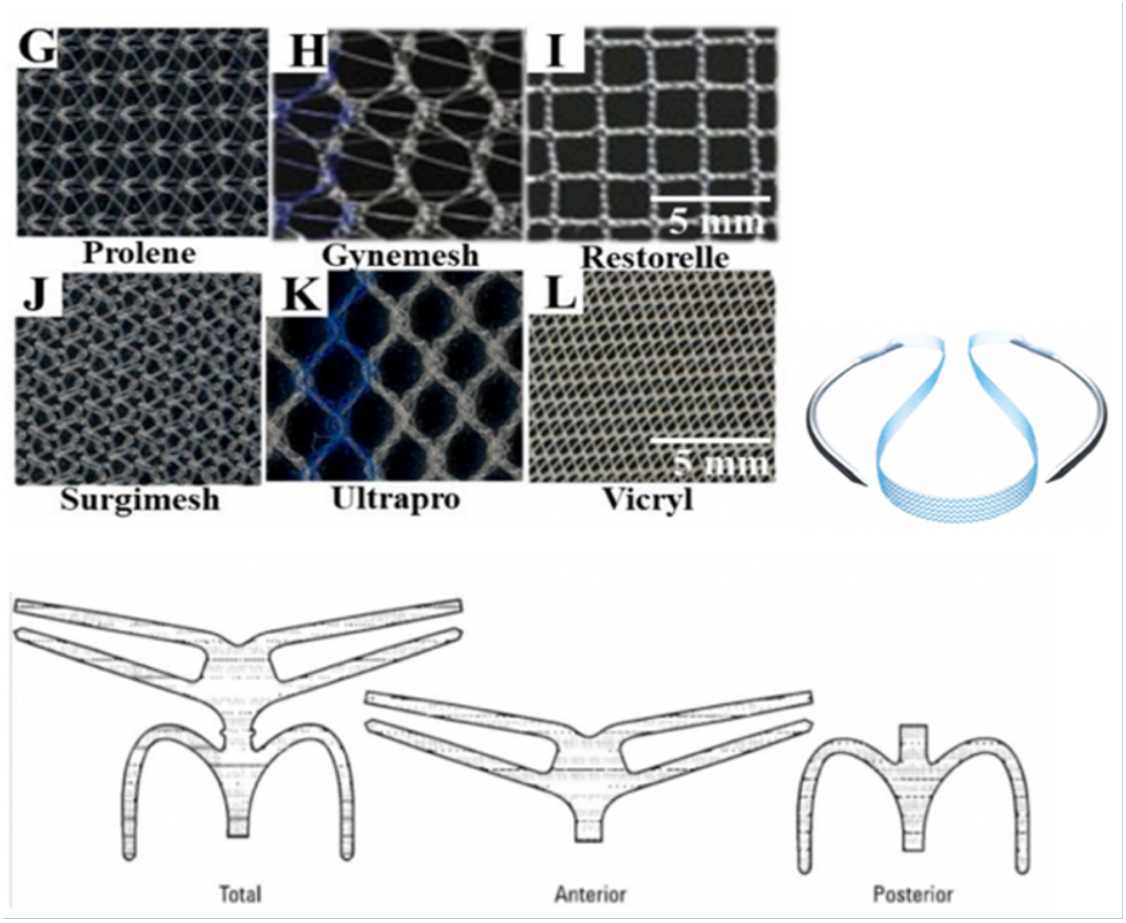

Figure 1.19: Types of mesh used in the POP surgery. Reproduced with permission from [114].*TVT (tension-free vaginal tape) with Trocars for bladder incontinence (from Ethicon; product description). The Prolift® Total, Anterior and Posterior mesh implants (from Instructions for Use).*

The mesh scandal:

Despite initial encouraging data, the FDA raised its first concern regarding mesh implants in 2008 when it received more than 1,000 reports of mesh complications in patients receiving these implants where the majority were unable to be corrected surgically [115]. This was followed by two reports of warnings regarding mesh implants complications in 2008 and in 2011 by the FDA. They received 1,503 reports of mesh associated complications between 2008-2010 and deemed transvaginal PPL mesh for POP repair as a high-risk procedure. The most common complications reported were mesh infection, chronic pelvic pain, vaginal erosion, dyspareunia, vaginal scarring with mesh shrinkage and recurrent prolapse [105].

The follow-up of these reports indicated that the number of adverse events reported were underestimated leading to a ban on these mesh products in the UK, Australia and New Zealand

in 2018 [116]. In 2019, the FDA's Manufacturer and User Facility Device Experience (MAUDE) reviewed more than 100,000 cases of mesh complications and concluded that the benefits of mesh surgery outweighed the risks and ordered manufacturers to stop selling PPL mesh for transvaginal repair of POP [117]. This “Mesh Scandal” has now been acknowledged as an important issue in healthcare where surgeons and manufacturers are now facing billion dollars lawsuits against them.

Current NICE guidelines for the management of Urinary incontinence and Pelvic organ Prolapse in women:

NICE guidelines [NG123] published on 02 April 2019 included detailed recommendations on the surgical and non-surgical management of POP and SUI. According to these guidelines, patients suffering from SUI and if the non-surgical management has failed, the following surgical options can be recommended (provided that the NICE patient decision aid be used):

a) Colposuspension
b) An autologous rectus fascial sling

The option of a retropubic mid-urethral mesh sling can only be included with high caution provided with the following advice to patients (NICE guidelines section 15.7-15.9):

1. The patient should be informed that the mid-urethral mesh sling is a permanent implant, and that complete removal might not be possible.
2. The patient should be given written information about the implant, including its name, manufacturer, date of insertion and the implanting surgeon’s name and contact details.
3. If planning a retropubic mid-urethral mesh sling procedure, surgeons should use a device from type1 macroporous polypropylene mesh sling, preferably colored for high visibility during mesh insertion and revision.

There is a public concern about the use of mesh procedures for women suffering from pelvic organ prolapse and the current NICE guidelines do not recommend the use of synthetic polypropylene mesh insertion for anterior vaginal wall prolapse. However, for other prolapse repair such as uterine or vault prolapse, if patients do opt for polypropylene mesh insertion,

they need to be informed that the details of the procedure and its subsequent short- and long-term outcomes must be collected in a national registry.

Current regulations concerning transvaginal mesh implants in pelvic organ prolapse (POP) surgery:

The controversy surrounding the transvaginal mesh implants for POP is currently being extensively debated among the urogynecology experts and the general public. In the past decade, about 61 different types of mesh implants could be found in the US market mainly because of the FDA's Premarket notification Approval [510(k)] process. According to this, only substantial equivalence to a precursor product was necessary for a new medical device to be approved and sold in the American medical device market. Prior success of polypropylene mesh in the correction of incisional hernias and latter successful use of polypropylene mid-urethral slings for urinary stress incontinence paved its way to be used in transvaginal POP surgical repair without sufficient preclinical safety testing.

After reports of severe post-operative mesh complications, in January 2016, the FDA increased the risk class for transvaginal meshes and reclassified them from risk class II to class III and demanded a thorough follow-up safety data. This was followed by a prompt disallow of the sales of anterior transvaginal mesh implants by the FDA in 2019 that caused a worldwide stir among the urogynecological experts.

In the UK, the regulatory situation concerning the use of transvaginal mesh implants remained dynamic over the past couple of years. In 2017, the NICE (National institute for Care and Health Excellence) recommended that polypropylene mesh augmented POP repair should only be used in clinical studies [118]. In 2018, the independent Medicines and Medical devices safety regulators demanded a halt in the use of transvaginal meshes and the only possibility of using it was when no alternative options were available. In 2019, the NICE updated its stand on the mesh implants with retropubic slings being offered as a treatment option for stress urinary incontinence while transvaginal mesh for POP remained prohibited. According to a recent statement by the House of Commons, the use of transvaginal mesh is still on hold. In the US, the UK, Canada, Australia, New Zealand and France transvaginal mesh implants have been removed from market however, in most mainland European countries, Asia and South America they are still available as surgical option for POP.

Reclassification of Urogynecological surgical mesh and mesh-related Instrumentation:

On January 6, 2017, the FDA issued an order to reclassify surgical instrumentation for use with urogynecological surgical mesh under the amended Federal Food, Drug and Cosmetic Act (the FD&C Act) following FDA's comprehensive adverse event analysis [119]. The FDA's findings concluded that general controls were insufficient to provide a reasonable assurance of safety and effectiveness for urogynecological surgical mesh instrumentation and that there was sufficient evidence to establish special controls to provide such assurance.

According to the final order:

1. The surgical instrumentation for use with urogynecological mesh were reclassified from class I (general controls) exempt from premarket notification to class II (special controls) and subject to premarket notification and identified as "specialised surgical instrumentation for use with urogynecological surgical mesh".

2. The surgical mesh for transvaginal pelvic organ prolapse (POP) repair was reclassified from class II (special controls) to class III (premarket approval) category of devices.

To ensure a reasonable level of safety and effectiveness of the device, all new surgical mesh developments are now required to fill premarket approval application (PMA) or notice of completion of a product development protocol for surgical mesh for transvaginal POP repair. Manufacturers of urogynecological surgical mesh instrumentation that have not been legally marketed prior to January 6, 2017, must obtain 510 (k) clearance and demonstrate compliance with the special controls included in the final order before marketing the device.

1.10 Types of grafts for pelvic floor reconstructive procedures:

Biological grafts:

Amidst the rising rates of complications associated with the use of synthetic PPL mesh, alternative biological grafts have gained attention due to their biocompatibility, lower infection rates and adequate foreign body reaction as possible materials for pelvic floor reconstructive surgeries. Abed *et al.,* carried out a systematic review of incidences of graft complications including graft erosion and wound granulation in patients following vaginal prolapse repair

and concluded a lower erosion rate (approximately 10%) for biological grafts in comparison with the synthetic implants [8]. However, biological grafts present certain limitation in terms of cost, inadequate tissue strength and unavailability of long-term follow-up data. Biological grafts can be divided into three categories; autologous graft (from patient's own body), allografts (tissues harvested from human donors or cadavers) and xenografts (tissues harvested from animals). In the 1990s, allografts and xenografts were initially used for SUI and later in 2001, the FDA approved the use of these biological grafts for POP surgery [120].

Autologous grafts

Traditionally, the patient's own native tissue such as rectus fascia, fascia lata, vaginal epithelial tissue, buccal mucosa have been used for reconstructive surgeries of pelvic floor or any congenital deformity of the vaginal tissue [121]. Main disadvantages are the donor site morbidity, inadequate quantity and quality of available tissue and unpredictable durability of the graft to provide reinforcement of the prolapsed tissue. In addition, weak mechanical properties of the connective tissue may compromise the desired physical support that resulted in a higher recurrence rate after native tissue repairs [122].

Allografts:

In clinical practice, tissues harvested from the cadaveric donor fascia lata have been used for reconstruction of pelvic floor for more than 3 decades. These cadaveric grafts have advantages of similar histomorphology of the native fascia without causing the usual complications and donor site morbidity associated with the use of autologous fascia. Concerns regarding the risk of transmission of HIV from the donor tissues, adequate decellularisation and sterility and unpredictable absorption and integration of allografts into host tissues are a few drawbacks. Variability in data on success rate of allografts for POP repair exists in literature owing to the variation in donor fascia architecture in terms of tensile strength and collagen fibre orientation [123].

Xenografts:

Animal derived matrices such as processed porcine tissues, small intestinal submucosa (SIS) (Stratasis®, Surgisis®), bovine pericardium (Veritas) and dermis (Pelvisoft®, Pelvicol®, InteXen®) are popular sling materials for SUI repair. Similar to allografts, xenografts pose a

theoretical risk of infection and are strictly regulated by the FDA guidelines. The host response towards xenografts depends on the porosity and crosslinking of collagen. Chemical crosslinking is introduced to the acellular matrix to improve its strength, however, the added crosslinking resulted in poor cellular infiltration and an adverse foreign body reaction leading to graft encapsulation [124]. There are associated concerns on the loss of mechanical strength and early degradation at the repair site during tissue remodelling while using xenografts for POP repair.

*Table 1.2: Biological grafts used in POP and SUI surgery. * Device not mentioned since graft is harvested from patients. Adapted from* [124].

Catagory	Composition	Brand-Device
Autologous grafts	Fascia lata	*
	Rectus fascia	*
	Vaginal mucosa	*
	Buccal mucosa	*
Allografts	Cadaveric dermis	AlloDerm® (LifeCell Corporation, Branchburg, N.J.) Repliform® (Boston Scientific, Natick, Mass.) Bard Dermal Allograft (CR Bard, Murray Hill, N.J.) Axis Tutoplast Processed Dermis (Mentor, Santa Barbara, Calif.) Duraderm® (CR Bard)
	Cadaveric fascia lata	Suspend Tutoplast (Mentor) FasLata® (CR Bard, Covnington, Ga.) ReadiGraft® (LifeNet, Virginia Beach, Va.)
Xenografts	Porcine dermis	Pelvicol® Acellular Collagen Matrix (CR Bard), PelviSoft® BioMesh (CR Bard), PelviLace® Biourethral Support System (CR Bard) InteXen (American Medical Systems, Minnetonka, Minn.) Zenoderm® (Ethicon Ltd., Scotland)

	Porcine small intestinal submucosa	Symphasis® Smart Remodeling Matrix (Cook Urological, Inc., Bloomington, Ind.) Surgisis® Soft-Tissue Graft (Cook Urological) Stratasis® TF Tension-Free Urethral Sling (Cook Urological) FortaGen® (Organogenesis, Canton, Mass.
	Bovine dermis	Xenform® Soft-Tissue Repair Matrix (Boston Scientific) Cytrix® (TEI Biosciences, Boston, Mass.)
	Bovine pericardium	Veritas® (Synovis Surgical Innovation, St Paul, Minn.)

1.11 Tissue engineering of the genitourinary tract:

In recent years, multidisciplinary studies involving urogynecology and biomedical engineering have focused on designing new biomaterials and developing existing surgical techniques and designing graft materials with trocars for insertion of mesh into the pelvic floor. The success of prolapse surgery is usually compromised as the urogenital and lower abdominal tract is a dynamic environment as it sustains intraabdominal pressure (IAP) changes. Thus, it has become more important to understand the biomechanical and cellular behavior of implanted biomaterials into the pelvic floor.

The rationale behind using the PPL mesh for pelvic floor reconstruction is to provide desired support to the prolapsed organs and help regenerate the damaged tissue. Although synthetic meshes are mechanically strong but their non-degradability and poor histocompatibility have caused serious post-operative complications such as mesh erosion, infection, exposure and chronic pain [125]. On the other hand, biological grafts have better biocompatibility, but their poor mechanical properties and faster degradation rate limit their clinical promotion and application. The ongoing scrutiny regarding the safety, efficacy and tolerability of PPL mesh for the treatment of POP and SUI remains controversial. There is a substantial clinical need to develop therapies and technologies to bridge the gap to provide patient-care therapies that have been created by the ban on using mesh implants for POP and SUI.

Tissue engineering is a branch of regenerative medicine that uses a combined approach of cells, biomaterials and growth factors to develop biomaterials that can be implanted into an area of

tissue damage to promote native tissue repair and regeneration. The addition of cellular component into the synthetic polymer scaffold have resulted in accelerated tissue repair compared to scaffolds without cells when implanted in abdominal walls female sprague-dawley rat model [126].

1.12 Biomaterials for the pelvic floor repair:

Increasingly, tissue engineering approaches are being used in medical research to improve tissue regeneration and long-term outcomes of surgical interventions. In the area of pelvic floor research, several different primary cells, cell lines and stem cells have been explored by culturing these onto different biomaterials to improve the host tissue response towards these materials. Mesenchymal stem cells (MSCs) are pluripotent cells that can be differentiated into different lineages such as smooth muscles, bone, adipose cells, tendons and ligaments driven by their microenvironment. MSCs have low immunogenicity and can be employed using both autologous and allogeneic applications without subsequent immunosuppression. In urogynecology research bone marrow-derived mesenchymal stem cells (BMSC) and adipose derived mesenchymal stem cells (ADMSCs/ADSC) have been used to repair urethral sphincters and improve the symptoms of SUI in rat models [127], [128].

In response to the complications associated with synthetic PPL meshes, Hachim *et al.,* [129] developed IL-4 coated PPL mesh to mitigate the host inflammatory response towards an M2 remodelling phenotype. Their results showed that the modified PPL mesh was capable of shifting the early-stage macrophage polarisation from M1 to M2 response that can improve the biomaterial integration downstream. Several studies have investigated other biological, non-biological, degradable and nondegradable polymers to use within the context of pelvic floor repair. Among these polylactic acid (PLA) is a commonly used polymer for bioengineering. Electrospun and functionalised PLA have been developed by Mangir *et al.,* [130] that showed good biocompatibility and increased extracellular production by cultured cells in in vitro studies. Other potential polymeric materials include polylactic-co-glycolic acid (PLGA), polyamide (PA), polyurethane (PU), polyvinylidene fluoride (PVDF) and polycaprolactone (PCL).

A promising alternative to synthetic polymers in pelvic floor repair surgery are biodegradable acellular matrices derived from xenogenic extracellular matrices (ECMs) [131]. ECMs are decellularised matrices commonly obtained from porcine and examples include porcine urinary bladder matrix (UBM) and small intestinal submucosa (SIS). These biological grafts have been

investigated to improve graft integration into the host tissue that can lead to constructive remodelling around the implant site as the implanted material degrades over a time period.

Table 1.3: Selected examples of potential biomaterials used for pelvic floor regeneration. Adapted from [132].

polytetrafluoroethylene (ePTFE), polypropylene (PP), polyester (PE), polyvinylidene fluoride (PVDF), platelet rich plasma (PRP), small intestine submucosa (SIS), urinary bladder matrix (UBM), fibroblast growth factor (FGF), poly(L-lactide)-tri-methylene carbonate-glycolide (PLTG), interleukin-4 (IL-4).

Biomaterials	Examples	Advantages	Limitations
Synthetic materials	PPL, ePTFE, PE, PVDF	Nondegradable, high mechanical strength, variety of designs	Chronic infection and inflammation, mesh erosion and exposure, urinary dysfunctions, implant encapsulation and infection, absence of host tissue integration, mesh shrinkage
Cell-seeded synthetic materials	PPL+ transduced human foreskin fibroblasts (KiF5)	Enhanced biocompatibility, good mechanical strength and stability	Potential chronic infection and inflammatory host tissue response
Enhanced synthetic materials	PPL + PRP, PPL+ IL-4	Increased fibroblasts adhesion, decreased inflammatory cell infiltration, increased collagen production. Ability to shift host tissue response towards M2 macrophage response	Potential chronic infection and inflammatory host tissue response
ECMs	SIS, bovine dermis, cadaveric human dermis	Biodegradable, increased infiltration of M2 macrophages,	Poor mechanical properties, potential immunological response,

		constructive tissue remodelling	potential risk of infection, poor biocompatibility, microporosity can cause chronic inflammatory response in host tissue
Cell-seeded ECMs	SIS, bovine dermis, cadaveric human dermis+ Myoblasts/fibroblasts	Biodegradable, increased cellular infiltration and collagen production, enhanced biomechanical properties, neovascularisation	Potential risk of adverse immunological response, microporosity can cause chronic inflammatory response in host tissue
Modified ECMs	UBM + Sca-1 antibody + bFGF	Biodegradable, improved biocompatibility, host cell infiltration and differentiation to smooth muscle cells in vivo.	Potential risk of adverse immunological response, microporosity can cause chronic inflammatory response in host tissue
17-β-estradiol releasing electrospun materials	PLTG, PLA/PLA+ADSC, PU/PU +ADSC	Improved mechanical properties, increased in ECM deposition, elastic behavior in case of PU, mimicking native tissue architecture, good material porosity and enhanced angiogenesis.	Hydrophobic nature, Further *in vivo* studies required to test efficacy

Table 1.4: Summary of in vitro and in vivo evaluation of electrospun matrices. Adapted from [133].

Biomaterial	Aim	*In vitro* findings	*In vivo* findings
Poly (lactic-acid) PLA	Urogynecological implant Ascorbic acid releasing scaffold	Biocompatible, Increased cellular metabolic activity and ECM production, increased collagen production,	Cellular infiltration into the implant, implant remodelling, neo-tissue formation and angiogenesis
Poly-(caprolactone) (PCL)	Skin TE, Modified by culturing MSCs for hernia repair	High tensile strength, cell viability and proliferation	Extensive cellular migration into the implant, formation of neo-dermal tissue
Poly (lactic-coglycolic acid) (PLGA)	Bladder TE Urethral reconstructive material	Matrix deposition by cultured cells Reduced tensile strength after sterilization Scaffold contraction	Implant integration into tissue Neo-tissue formation
Poly (Urethane) (PU)	Soft TE Vascular grafts ECM mimic to improve UBM performance in subcutaneous rat model	Good mechanical properties, High tensile strength and cellular proliferation	Cellular infiltration into the implant, Implant integration and neo-tissue formation No signs of herniation
Silk	Urethral reconstruction, vascular tissue conjugates	Endothelial and smooth muscle cell attachment and proliferation	Cellular infiltration, tissue ingrowth, No inflammation, Degradation *in vivo*

Polymer blends **PLGA/PCL** **PLA/PCL** **PCL/collagen**	Scaffolds for urological and pelvic floor reconstruction	Increased biomechanical properties, Greater cell adhesion and proliferation, Increased matrix production	Neo-tissue and matrix formation, Increased implant survival time, microvascularisation and tissue ingrowth, bladder tissue regeneration

1.13 Biomaterials developed by the pelvic floor research group in the Kroto research institute:

Over the past 10 years, our pelvic floor research group in the Kroto research institute have been working on developing better biomaterials for the female pelvic floor repair. A range of polymeric and natural biomaterials have been investigated including AlloDerm®, cadaveric dermis, synthetic polypropylene mesh, porcine small intestine submucosa (SIS), porcine dermis, electrospun poly-L-lactic acid (PLA) and polyurethane (PU) with and without cultured fibroblasts and ADSCs.

Mangera *et al.,* [134] investigated the biocompatibility and biomechanical properties of seven potential candidate materials by culturing oral mucosal fibroblasts on these scaffolds. *In vitro* studies on collagen production by cells on these scaffolds revealed that SIS and PLA are better candidates for pelvic floor repair compared to the synthetic PPL. Sabiniano *et al.,* [135] studied the potential of two autologous cell sources *i.e.,* human oral fibroblasts (OF) and human adipose derived stem cells (ADSC) cultured on electrospun and thermo-annealed PLA scaffolds. They concluded that under strained conditions both cell types showed good proliferation and attachment, extracellular matrix production and biomechanical *properties in vitro.* Hence, OF and ADSC are both beneficial in constructing a tissue engineered repair material (TERM) for POP and SUI.

Nadir *et al.,* [136] used a different approach by culturing oral fibroblasts (OF) on static and mechanically stimulated (using fluid shear force) electrospun PLA scaffolds and monitored the effect of different media supplements (ascorbic acid-2-phosphate, glycolic acid and 17-b-oestradiol) on cellular viability, collagen production and mechanical properties of these scaffolds. They concluded that under mechanical stimulation, the cultured OF produced

significantly increased amount of collagen and mechanically strong matrices in the presence of ascorbic acid in the culture medium.

These studies led to the idea of incorporating additional growth stimulators and hormones such as ascorbic acid (AA) and 17-β-estradiol into the electrospun PLA and polyurethane (PU) matrices which were further investigated by Mangir *et al.,* [130], [137] and Shafaat *et al.,* [138]. These studies demonstrated the potential of AA-releasing PLA scaffolds and 17-β-estradiol releasing PLA and PU scaffolds in terms of collagen production and improved biomechanical properties of these scaffolds designed for pelvic floor repair. In addition, *ex-ovo* chick chorioallantoic membrane (CAM) assays revealed that 17-β-estradiol releasing PLA and PU scaffolds can stimulate angiogenesis and improved cellular infiltration and tissue integration. Both electrospun PLA and PU matrices were also implanted in a rabbit abdominal wall defect model to study the *in vivo* tissue response towards these materials in comparison with the commercial PPL and polyvinylidene fluoride (PVFD) meshes [139]. After 90 days of implantation, histopathological analysis of the explanted tissues revealed better host tissue integration by PLA and PU scaffolds compared to the synthetic meshes. Furthermore, immunohistochemical analysis showed that both PLA and PU exhibited an M2 dominant profile compared to PPL and PVFD where M1 was the dominant one leading to a constructive tissue remodelling around the area of implantation of PLA and PU.

The next challenge was to develop better *in vitro* preclinical tissue engineered (TE) models that can examine the cellular response towards these potential biomaterials and have the ability to discriminate between a “good” and a “bad” vaginal tissue response. These preclinical studies will then lead to the next stage in the biomaterials development in which animal models could be used to examine the host response towards these TERM and also changes in the biomechanical properties and material degradation over time in long-term material implantation.

1.14 Models for studying POP and SUI:

The human female pelvic floor is a complex unit of interdependent network of pelvic bones, connective tissues and muscles that can sustain simultaneous dynamic intraabdominal pressure, counteract gravitational forces while keeping all the pelvic organs in place. Recent advances in computational modelling have developed better models such as Magnetic resonance imaging (MRI)-derived computational modeling of the female pelvis to understand and quantify the

biomechanics of the pelvic floor [140]. However, it should be kept in mind that most computational models used to date are patient specific with specific symptoms and causes of prolapse so the interpretations of the findings when applied to the broader population is always questionable.

Increasingly, animal models have been employed to better quantify the biomechanical properties of the pelvic floor and also as host for biomaterials implantation for pelvic floor repair. These animal models are thought to provide us with better *in vivo* predictability of biocompatibility and mechanical performance of developed materials as they can mimic the native human body physiology in terms of complexity and dynamics.

1.15 Animal models for POP:

Due to the relative complexity of the pelvic floor and the dynamics of the associated tissue and fascia, it is inevitable to study the associated biomechanics and functioning of potential biomaterials developed for pelvic floor repair in complex representative experimental models. Animal models afford the opportunity to test pelvic floor biomechanics and biomaterials more rigorously in a controlled environment. Of course, there is no ideal animal model substitute for the human pelvic floor and the choice of these models is highly dependent upon the proposed experimental hypothesis to be tested. For example, where testing biocompatibility and safety of biomaterials is desired small animal models such as rodents and rats' abdominal defects and vaginal implantation serves as suitable models. On the other hand, where testing of biomechanics of the pelvic floor and mechanical stability of implanted materials is desired, larger animal models such as rabbits, non-human primates, sheep and dogs are considered to be better experimental models.

Rodents:

Rodents are the most commonly used animal models for gynecological research because of their small size, ease to work with and a large availability in numbers. Both rats and mice have a shorter oestrous cycle and hence allow for quick investigations of processes that may take a longer time in other species. Moalli *et al.,* [141] studied the rat vagina as the model to investigate the structural support of the vagina and mechanism of prolapse. Ulrich *et al.,* [142] studied the mechanical changes in commercial synthetic mesh used for POP and SUI repair post implantation in a rat model. They tested four clinical meshes Gynemesh PS™, Polyform

Lite™, Restorelle™ and UltraPro™ in abdominal walls of Sprague Dawley rats and reported *in vivo* changes in their mechanical properties 90 days post-implantation. This study provided evidence regarding post implantation increased stiffness and significant mechanical changes in the commercial meshes in rat models however, one major limitation is the selected site of implantation. Although the rat abdominal hernia model is commonly an acceptable experimental model to evaluate the tissue and mechanical response of meshes *in vivo* however, the abdominal wall does not mimic the native vaginal milieu. In addition to this, the small fetus size in rodents and their different posture renders the rodent model not suitable to study conditions that can lead to the development of prolapse.

Rabbits:

In urogenital research, the rabbit model is the gold standard preclinical model for testing of newly developed microbicide irritancy potential as recommended by the FDA which is discussed in later sections. The rabbit model has the added advantage over the rat model in terms of larger tissue area, but the vaginal anatomy of the rabbit is very different to that of humans which limits its applications in pelvic floor research. Nevertheless, several studies have tested biomaterials designed for pelvic floor repair in rabbit models with the aims of testing the histological and biomechanical outcomes. Pero *et al.,* [143] tested the commercial PPL mesh and human acellular dermal matrices (hADM) graft by implantation in the abdominal wall and vaginal submucosa of rabbits. After 180 days post-implantation they observed abnormal findings and clinical complications in the PPL group compared to the hADM in explanted tissues and concluded the rabbit is a good model to evaluate the biological and biomechanical performance of materials for pelvic reconstructive surgery. However, the main limitation is the translatability of these results from an animal model to human scenario due to interspecies differences.

Non-human primates:

The pelvic floor anatomy of the non-human primates closely resembles with that of humans that make them valuable models for studies on POP. Similar to humans, the Rhesus macaques develop permanent pelvic soft tissue changes as a result of vaginal birth and the normal support of the pelvic organs is provided by the continuous remodeling of the pelvic floor fascia. Otto *et al.,* [144] have also detected the expression of 17β-estradiol receptor (ERα) by vaginal

fibroblasts in vaginal submucosa of rhesus macaque tissue explants, a feature exclusive to human vaginal fibroblasts. These features have made rhesus macaque an excellent model for POP. Shaffer *et al.,* [145] investigated the impact of commercial Gynemesh PS™ and MatriStem™ extracellular matrix bioscaffold on the vaginal smooth muscle cells of rhesus macaque. Immunohistochemical analysis of the explanted tissues revealed that the Gynemesh PS™ implantation had a negative impact on the contractility of the vaginal smooth muscle cells which was apparent by the macro- and microscopic muscle morphology compared to the extracellular matrix bioscaffold (MatriStem™).

Sheep (Ovine model):

In terms of vaginal tissue histomorphology, the sheep are the closest animals to humans. Sheep are an established reproductive models for humans as they have prolonged labors and can develop spontaneous uterovaginal prolapse related to vaginal birth [146]. Additionally, sheep have also been used to investigate the biocompatibility and mechanical performance of grafts used for pelvic reconstructive surgery. Emmerson *et al.,* [147] developed a functionalised polyamide (PA) mesh dip-coated in gelatin to deliver endometrial mesenchymal stem cells (eMSC) to improve the biocompatibility of the synthetic mesh in an ovine model of pelvic organ prolapse. More recently, Hympanova *et al.,* [148] compared the native tissue biological and inflammatory response towards implanted commercial light weight PPL mesh with electrospun polyurethane (PU) in sheep model. Their results showed that the electrospun PU was integrated well into the native tissue and showed an M2 macrophage response at early stages of implantation which is an indication of constructive remodeling.

Summary of animal models in pelvic floor research:

Animal models allow for controlled studies which are useful to understand the risk factors that contribute to the development of POP and SUI in humans. In addition, they are useful preclinical models in determining the biological and mechanical behavior of newly developed biomaterials for pelvic floor repair. However, the cost and ethical concerns involved with animal testing is challenging in terms of acquiring sufficient data to support the safety and biocompatibility of biomaterials. In addition, the interspecies differences in the vaginal tissue anatomy and histomorphology present a limitation in translatability of these results into clinical relevance to women.

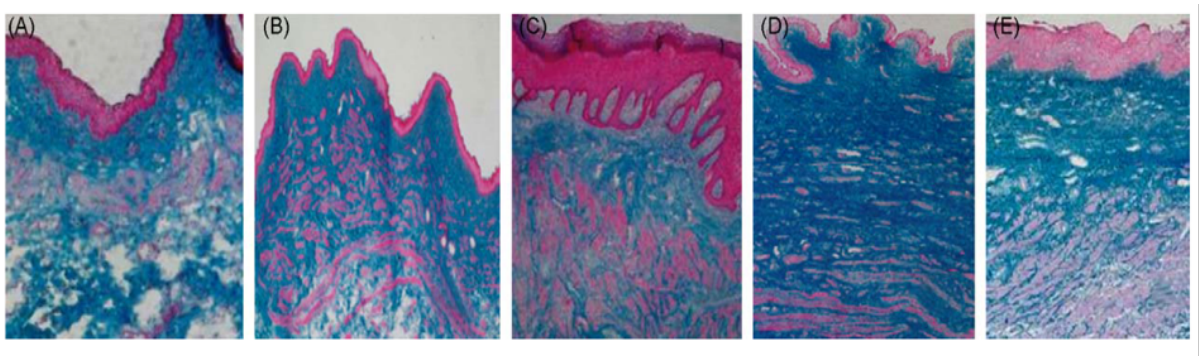

Figure 1.20: Histological images of trichrome staining of the vaginal epithelium of different animal models (A) rat, (B) rabbit, (C) primate, (D) sheep with respect to humans. Reproduced with permission from [149].

Other in vivo models:

Ex ovo CAM assay:

Current animal models for testing biomaterials for the female pelvic floor repair are expensive, time consuming, labor intensive and require surgical expertise for biomaterial implantation/removal and rigorous ethical approval. Valdes *et al.,* [150] first reported the chick chorioallantoic membrane assay (CAM) as an *in vivo* alternative assay to test biomaterials in living developing chick embryos. After fertilisation, the allantois of the developing chick embryo evaginates after 3 days of incubation and fuses with the adjacent mesodermal layer of the chorion and forms a highly vascularised network known as the chorioallantoic membrane (CAM). The CAM assay has been established as an experimental system for implantation of decellularised matrices and scaffolds to study cellular proliferation, tissue integration and angiogenesis without the risk of implant rejection as the CAM is inherently immunodeficient [151]. Moreover, the CAM assay has been used as a test system to study tumor invasion and metastasis and macro and microvasculature changes around tumors and neoplastic implants [152].

The pelvic floor tissue engineering group in the Kroto research institute modified the *in ovo* CAM assay by cultivating the CAM outside of eggshells in petri dishes to improve visualisation of the implanted material and surrounding area. This became known as the *ex ovo* CAM assay. Mangir *et al.,* [137] studied the electrospun oestradiol -releasing poly-l-lactic acid (PLA) mesh with cultured human adipose derived mesenchymal cells (hADMSC) developed as a potential biomaterial for POP using this *ex ovo* CAM assay. Their results showed that the implanted material could stimulate neoangiogenesis in CAM and is a promising material to be further

investigated for pelvic floor repair. Shafaat *et al.,* [138] reported improved tissue integration and neoangiogenesis by implantation of 17-β-estradiol releasing polyurethane (PU) scaffold on the CAM assay.

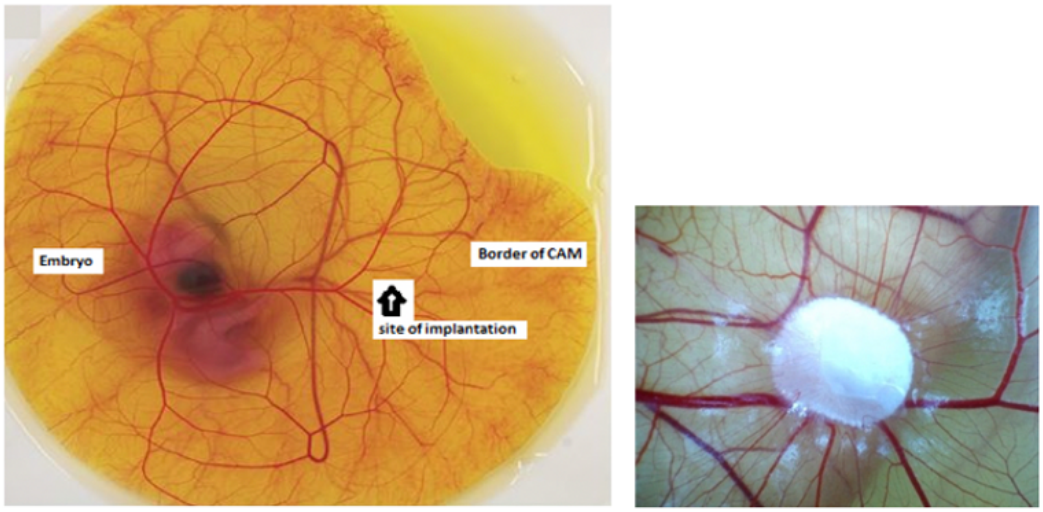

Figure 1.21: The ex-ovo CAM assay. Macroscopic view of the developing chick in a dish and area of implantation of biomaterial is marked on the CAM vasculature. Biomaterial implantation on CAM observed at day 14 of incubation. (Images originally captured by self).

The CAM assay is a relatively simple, low-cost, quick method for evaluating tissues and cellular response towards biomaterials and does not involve rigorous ethical approval from the ethics committee compared to other animal testing. However, several limitations such as lack of a developed immune system, high sensitivity towards environmental factors pH, oxygen tension and difficulty in interpretation of real neovascularization compared to falsely increased vasculature due to rearrangement of existing vessels provides challenges in broader applicability of CAM assay for biomaterials testing. In addition, the lack of available antibodies that can cross react with avian cytokines and antigens is a serious limitation while studying molecular response of cells towards biomaterials.

Table 1.5: Comparison between chick chorioallantoic membrane (CAM) assay and other animal models.

Chick chorioallantoic membrane (CAM) assay	**Mammalian models**
Low cost	Moderate to high cost (Rats, rodents, rabbit---moderate; dogs, rhesus macaque, sheep--- high)
Very simple procedure for implant placement	More complex surgery for implant placement. Additional requirements of expertise and facility such as operating room, anesthesia facilities *etc.*
Allows direct and continuous visualisation of implant site throughout the experiment	Does not allow visualisation of implant site throughout the experiment
Implantation time about two weeks	Implantation time about few months to years
Easy acquisition of tissue samples post-implantation	More invasive surgical excision is required to acquire tissue samples post-implantation
Cost-effective model in terms of analysing data	Cost-ineffective model in terms of analysing data

1.16 The female genitourinary tissue:

The Vagina:

The vagina is the female sexual organ by definition and described as an elastic fibromuscular tube that extends about 7-15 cm from the cervix to the vulva in length, greater than 4 cm in width and approximately 150 – 200 μm in thickness [153]. In the central region, the vagina appears as H-shaped as the side walls are suspended by being attached to the paravaginal lateral connective tissue [153]. The posterior vaginal wall is longer than the anterior one which is why the cervix is positioned asymmetrical at the vaginal vault [154].

The vagina is attached laterally to the sidewalls of pelvis with the help of connective tissue and smooth muscles adherent to the adventitia of the vaginal wall blood supply. This arrangement tends to fix it in position sidewise whereas the adjoined muscularis imparts tone and permits it to adapt to pressure changes. The normal support of the vagina and uterus is provided mainly by the pelvic floor muscles along with the fibromuscular connective tissue "the endopelvic fascia" [153]. In a healthy female, the vaginal axis is in a horizontal plane in an upright body position which is achieved at three different levels of vaginal support as described by DeLancey [155].

Level 1: Upper vagina and the uterine cervix is supported by the uterosacral-cardinal ligament

Level 2: Attachment of vaginal sidewalls to the pelvis is supported by the paravaginal fascia

Level 3: Distal vaginal fusion to the perineum is supported by the perineal membrane and levator ani.

The vaginal wall is composed of various cell layers: the vaginal mucosa, an intermediate lamina propria, muscularis and the adventitia which provides the structural support to the vagina [156]. The vaginal mucosa is lined by a nonkeratinised, stratified squamous epithelium that forms rugal folds and provides distensibility [157]. Beneath the epithelium, there is lamina propria that consists of fibroblasts, collagen fibres, blood vessels and nerves and other cell types such as polymorphonuclear leukocytes [17]. Within the lamina propria are thin layers of elastic fibres underlined by a well-developed fibromuscular layer. The vaginal lubrication is provided by the transudates from the blood vessels as the vaginal lamina propria lacks any glands. The vaginal mucosa is coated by fluid that contains endometrial and cervical secretions and vaginal wall transudates [158]. This composition of vaginal fluid varies according to an individual's health status, age, menstrual cycle and parity [159]. In a healthy woman, the vaginal pH is acidic (3.5 - 4.5) during the reproductive age, but it can vary along the different stages of the menstrual cycle or due to any pathological condition of the vagina. This acidic pH is maintained by the presence of lactic acid bacteria that metabolize the glycogen into lactic acid in the vaginal epithelial cells [160]. This is an important feature of the vaginal epithelium as it provides a barrier to the entry of vaginal pathogens through the vaginal epithelium.

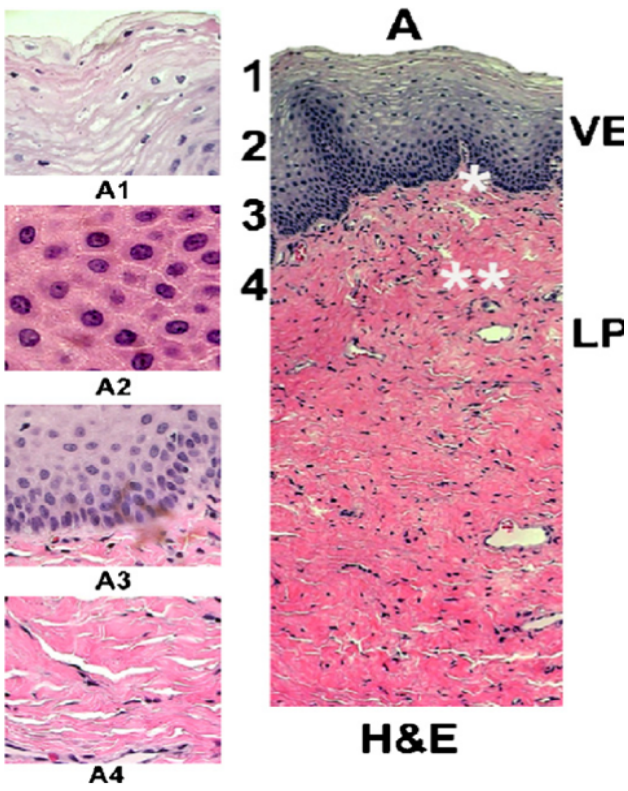

Figure 1.22: Stratified squamous epithelium of the human vagina and the supporting lamina propria stained by haematoxylin and eosin. (A) 20X, the vaginal epithelium (VE) showing stratified epithelial layers. The lamina propria (LP) 40X has two parts: papillary (*) and reticular (**). Reproduced with permission from [161].

The vaginal epithelium:

The human vaginal epithelium is a non-keratinised, stratified squamous epithelium with an average thickness of 150 – 200 μm in premenopausal women [162]. This type of epithelium has different thicknesses at different sites and has a differentiated surface layer adapted to fulfill the demands of that particular tissue in terms of protection against any physical, chemical or biological insult to the underlying tissues. It has a typical organisation of epithelial cells arranged in a basal layer, suprabasal layers, several glycogen-rich middle layers and an apical or superficial layer. As the epithelial cells migrate and differentiate apically, only the suprabasal and superficial layers of cells contain glycogen. It is estimated that in a week's time 10-15 layers of the vaginal epithelium is replaced due to the epithelial cell turnover [16]. The vaginal epithelial cells are identifiable by showing differential expression of different keratins such as cytokeratin 10 and 13 [163]. There are numerous folds called "rugae" present in the

epithelium that increases the surface area of the vaginal epithelium considerably and also provide distensibility.

The vaginal epithelium is non-keratinised as opposed to the keratinised dermal epithelium and hence, has a more flexible, less differentiated surface. The vaginal mucosa is moist due to the secretions from the glands of the cervix as it lacks glandular structures within the vaginal mucosa. The underlying lamina propria is composed of connective tissue consists of collagen matrix along with vascular and neural elements plays an important role in the maintenance and integrity of the epithelium. The major cell types in the lamina propria are the fibroblasts and a varied number of migratory inflammatory cells.

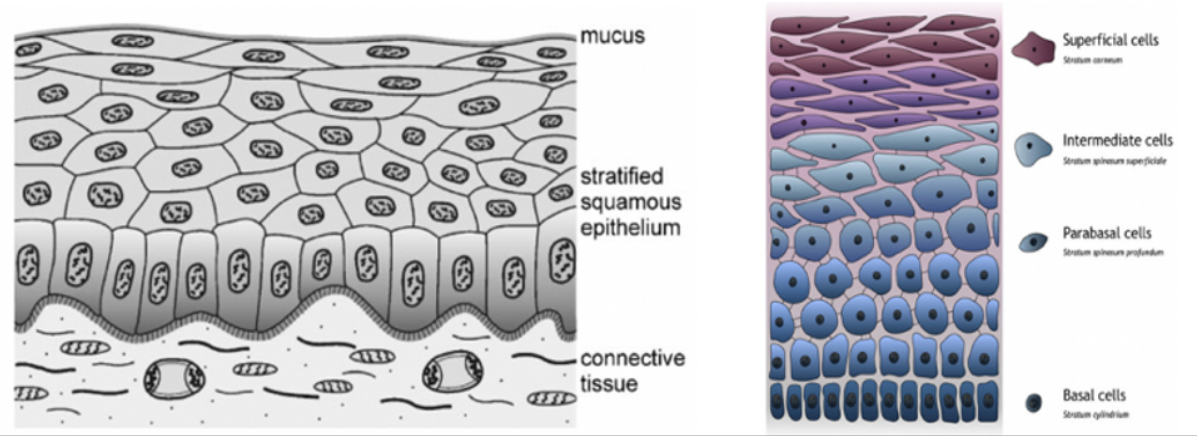

Figure 1.23: Representative drawing of non-keratinised stratified squamous mucosa found on the tissue linings of oral mucosa and the vagina. Reproduced with permission from [162]. *Schematic of non-keratinised stratified squamous vaginal tissue. Reproduced with permission from* [16].

Role of Oestrogens:

The thickness of the vaginal epithelium changes considerably throughout a woman's life and is subjected to environmental and hormonal fluctuations. Oestrogens play a significant role in maintaining the thickness, integrity and glycogen content of the vaginal epithelium. In younger women, before the onset of puberty, the vaginal epithelium is thinner consisting of only basal and a few suprabasal layers. Following puberty, the vaginal epithelium thickens and consists of an average 24 - 28 layers of epithelial cells [164]. In postmenopausal women, decline in oestrogen concentration causes vaginal epithelium atrophy and a decrease in the glycogen content of the epithelial cells causes the superficial layers to keratinise [165].

1.17 The stratified squamous epithelium permeability barrier:

The vaginal epithelium is a natural protective barrier against the entry of pathogens through the vaginal wall. Any changes in the integrity of this barrier due to factors such as hormonal changes, inflammation or infection has been linked to increased risk of vaginally transmitted diseases such as human immunodeficiency virus (HIV) and herpes simplex virus type 2 (HSV-2) infection [166]. Worldwide sexually transmitted diseases are epidemic and have severe health, social and economic consequences. Globally, it has been estimated that there are 3 million cases of HIV and 23.6 million cases of HSV-2 have been reported yearly by the World Health Organisation [167]. The epithelium barrier function is mainly due to the presence of intercellular junctions between epithelial cells. There are three main types of intercellular structural adhesions present in the vaginal epithelium: tight junctions, adherins and desmosomes [168]. All these junctions together form a tissue permeability barrier within a specialized mucosal epithelium such as the vagina. In stratified squamous epithelia, the permeability barrier is also dependent upon the composition of lipids within the superficial epithelial layers. In addition, the colonisation of the vaginal epithelium by the lactobacilli that maintains the acidic microenvironment by producing lactic acid from glycogen also serves to prevent invasion of vaginally transmitted pathogens [169].

In recent years, considerable progress has been made to develop drugs that can be administered through the vaginal route. For years, the concept of vaginal administration of drugs remained unclear, however, with the development of new drug delivery mechanisms including intravaginal rings that have caused a dramatic increase in interest in this particular area of drug delivery [170]. Current vaginally administered treatments include topical microbicides, hormone replacement, infertility treatments and contraception [171], [172]. Moreover, the vagina has also been explored as a route for vaccine delivery [173]. As the development of vaginally administered drugs is increasing, it is now crucial to understand the vaginal physiology and microstructure that has a profound effect on the efficacy and permeability of these treatments.

The barrier function and drug delivery in the vagina is dependent upon a variety of factors including vaginal pH, vaginal fluid and epithelium thickness as well as the drug properties. The vaginal epithelium thickness plays a key role in the acquisition of sexually transmitted diseases and is affected by the local administration of drugs and hormones [174].On the other hand, vaginal formulations and drugs for local or systemic therapy intended to vaginal administration

must be formulated to ensure penetration of this mucosal barrier. Thus, in order to develop any model system to test the effects of therapeutic agents or to study pathogenesis of vaginally transmitted diseases, this vaginal epithelium barrier must be carefully recapitulated.

1.18 Pathologies of the female genitourinary tissue:

There are several pathologies that can affect the proper functioning and the structure of the vagina which can be congenital, acquired or cancer. Congenital malformations include bladder or cloacal exstrophy in which the anatomical structures of the pelvis fail to fuse in the midline during the developmental stages of the fetus.

Congenital anatomical defects of the vagina can be corrected by reconstructive surgery where outside donor tissue sources are often required. Patients suffering from cervical, vagina, bladder, uterus or rectal cancers often require partial or total vaginal resection to treat the cancer followed by scar tissue formation. This can lead to anatomical and functional compromises to the vagina and can have severe mental and social effects on patients. Moreover, transient or long-term damage to the vagina and its supporting structures due to any injury, childbirth, parity or hormonal changes have been widely documented in women of every age globally. Pelvic floor dysfunctions including POP and SUI are among the major areas of concern regarding female sexual and urogenital health.

1.19 Model systems for studying vaginal mucosa:

Worldwide millions of women suffer from a number of potential gynecological problems over their lifespan that can affect their mental and sexual health. Women can develop several vaginal problems including bacterial vaginosis [175], vulvovaginal candidiasis [176], vaginal atrophy [177] and pelvic organ prolapse [178]. Other instances like congenital conditions such as Mayer-Rokitansky Küster-Hauser syndrome or androgen insensitivity syndrome result in vaginal agenesis and cervical or colorectal cancer may cause abnormal vaginal function. Despite advancements in the gynecological health research, it is imperative to model both healthy and pathological vaginal tissues to facilitate innovation and novel treatments for reconstructive procedures of the female genitourinary tract.

Access to human tissue and cells is a serious limitation for researchers in the field of pharmaceuticals, drug toxicity testing, therapeutics development and regenerative medicine. There are several ethical and practical constraints regarding the use of human organs, tissues

and cells in gynecological research to investigate vaginal formulations efficacy, safety and permeation through the vagina. The technical complexity, ethical issues and high cost for the use of human tissue and cells in vaginal research has limited researchers to develop high throughput data on newly developed vaginal pharmaceuticals and treatments. Over the years, researchers have realised the inevitable need to develop preclinical models and test systems that are complimentary to the use of human tissues so that the number and cost of using human tissues in vaginal research can be reduced.

1.20 *In vivo* models:

The human vaginal mucosa is constantly being exposed to bacteria and viruses and the vaginal epithelium acts as a natural barrier to infections. Several pharmaceutical or personal care products formulated for application through the vaginal route can occasionally cause undesirable local or systemic side effects that need to be assessed during the preclinical phase. The current US FDA approved gold standard preclinical test for determining the irritation potential of these microbicides and formulations is the *in vivo* rabbit vaginal irritation (RVI) model [179]. However, the RVI model is not appropriate to be used for screening of other types of products for intimate use such as incontinence products and cosmetics [17].

Traditionally animal testing has been done for the testing of newly developed vaginal formulations and involves both macroscopic observations such as development of erythema or ulceration around the animal tissues and histological examination of the tissues collected after exposure of the experimental animal to the test compounds [180]. Currently there is no standardised tissue or animal model that can truly mimic the anatomical and physiological complexity of the human vagina. Nevertheless, in addition to the ethical and regulatory concerns regarding the use of animal models for the testing of human products, the large number of potential drug candidates developed by the pharmaceutical industries all over the world require large number of animal models for the preclinical screening that ultimately makes the whole process of microbicide development highly costly.

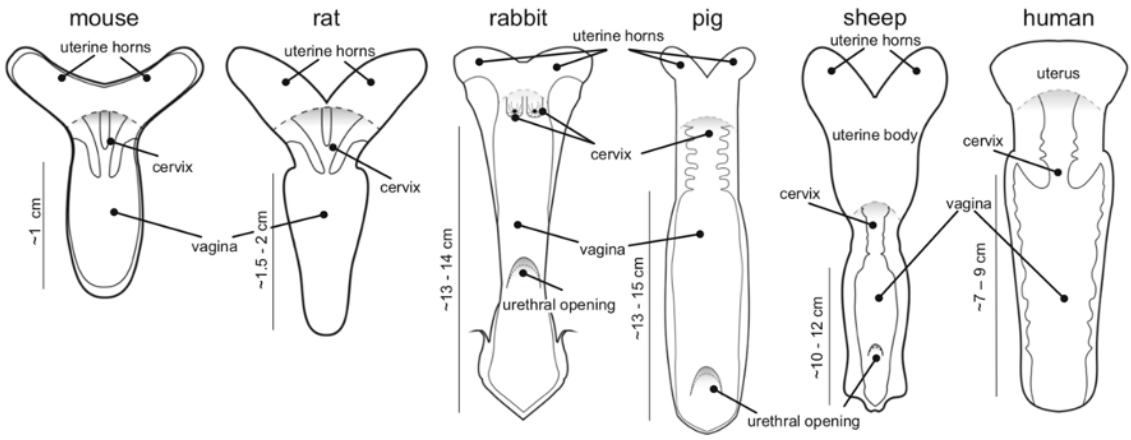

Figure 1.24: Schematized anatomical variations of the vagina in relation to their relative size across different species. Reproduced with direct permission from the authors [181].

Selection criteria for animal models in vaginal tissue research:

While choosing an animal model for vaginal research, there are certain criteria to be considered including: cost, ethical regulations, anatomical and physiological relevance with human tissue, risk of transmission of infections and available expertise. The mouse and rat models are popular choices due to their low cost, availability and ease in handling. However, there are subtle differences in the vaginal tissue architecture compared to humans. The vaginal epithelium of rats and mouse is keratinised that limits the permeability of tested compounds and tissue damage and hence, these are not reliable in testing the efficacy of microbicides and vaginally applied drugs. On the other hand, the rabbit vaginal epithelium is more susceptible to irritation and has high permeability as it is composed of simple columnar epithelial cells. These factors warrant careful consideration when analysing data sets obtained from the RVI assay. The pig and sheep are large animal models that are suitable for predictive interpretations in designing size-matched medical devices for human implantation and developing surgical techniques for pelvic floor repair. However, significant drawbacks include cost, ethical regulations, holding facility requirements, veterinary surgical expertise and potential risk of transmission of infections. Nevertheless, none of the available animal models are ideal in recapitulating the human vaginal microenvironment for gynecological research and ongoing conscious efforts are being made to develop alternatives to animal testing in vaginal research.

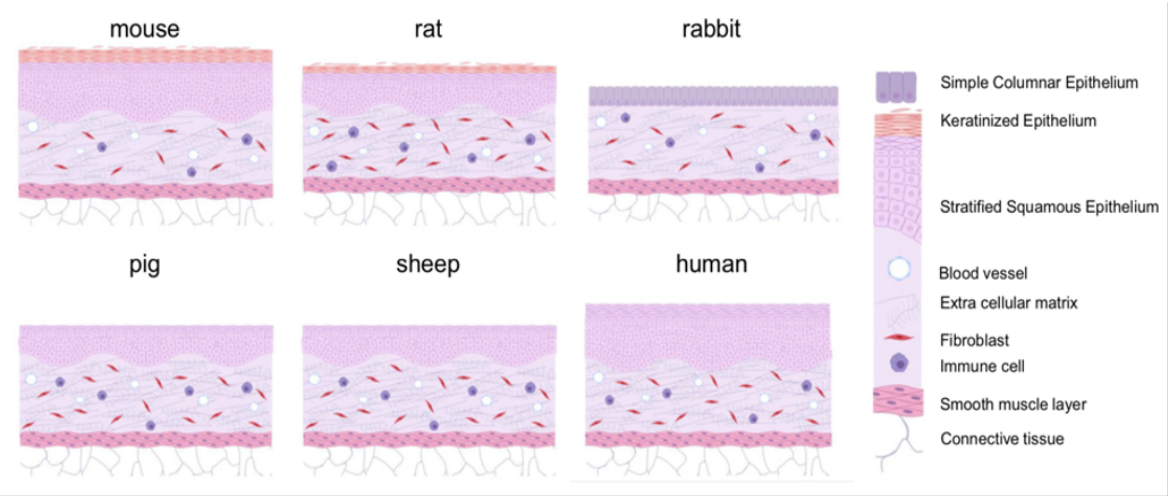

Figure 1.25: Schematic of the histological features of vaginal epithelium among different species. Reproduced with direct permission from the authors [181].

The Mouse model:

The mouse model has several advantages such as it is inexpensive compared to other animal models, prolific breeding and well established biological and genetic studies. Catalone *et al.,* [182] carried out toxicity testing of candidate topical microbicides in the Swiss Webster mouse model and evaluated the cervicovaginal tissue toxicity and inflammation at the cellular level. Their results for N-9 and PEHMB microbicides were correlated with the human colposcopic findings which support the use of this model for preclinical evaluation of potential microbicides. The mouse model has another advantage as the entire mouse genital tract can be harvested to analyse specific regions for evaluation of tissue epithelial disruption and inflammation which is critically important to develop effective microbicides candidates because HIV can infect any region of the female reproductive tract. Several studies have utilised the murine model for preclinical assessment of safety and efficacy of microbicides and spermicide formulations [183] and established that this model is an effective and inexpensive method that can bridge between the *in vitro* cytotoxicity assays and clinical trials for determining the safety and efficacy of microbicides. Regardless, the keratinised murine vaginal epithelium which differs from the human vaginal epithelium should be considered while utilizing this model as the best testing strategy because the keratinised epithelium is less permeable and more resistant to damage by the potential human microbicides.

The Rat Model:

Similar to the mouse model, the rat model is a potential vaginal model to investigate the preclinical efficacy and permeability of microbicides because of their low cost, ease of access and similarities with the human reproductive cycle. Many studies on female rat models (including Wistar and Sprague Dawley) have been carried out by different research groups to understand the structural properties of the vagina-supporting tissue complex [141] and the differential effects of oestrogens on the vaginal wall [184].

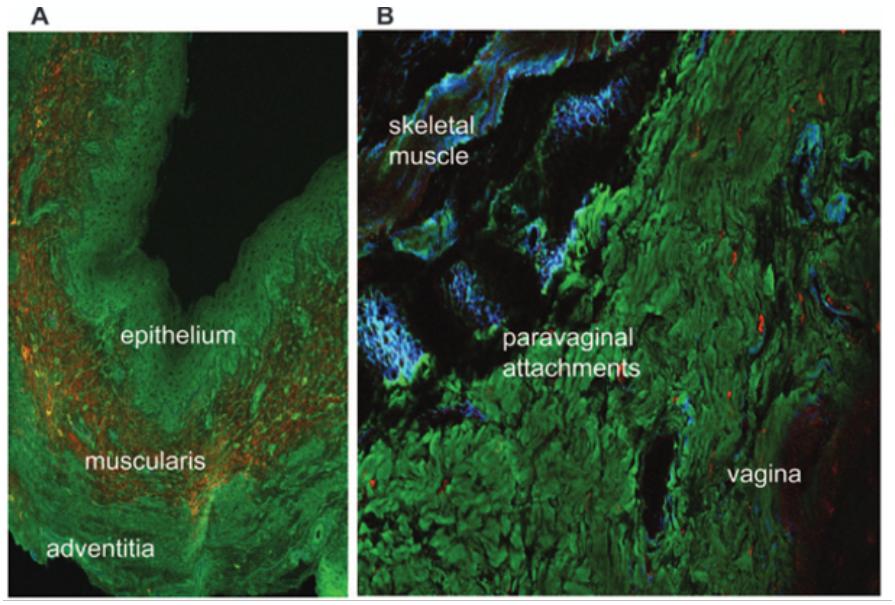

Figure 1.26: Fluorescence imaging of the rat pelvis labelled with antibodies to collagens I (red), III (green) and V (blue). (A) cross section of rat vagina demonstrating the three layers (epithelium, muscularis and adventitia) typically seen in humans. (B) Magnified view showing the paravaginal attachments at level II support. Reproduced with permission from [141].

The rat vagina also serves as a useful model to demonstrate the cyclic changes observed during the different estrous stages which are closely associated with the hormonal fluctuations similar to the human reproductive cycle. Montoya *et al.,* [185] studied the effects of vaginally administered oestradiol in ovariectomised rat models on collagen assembly and biomechanical properties of the vaginal wall. Clinically, local oestrogen therapy is given to postmenopausal women for the treatment of vaginal atrophy, dyspareunia and stress urinary incontinence that have shown improvements in the vaginal epithelium thickness and promotes neovascularisation [186]. Whereas systemic oestrogen therapy in postmenopausal women resulted in increased expression of collagen I and III in the vaginal wall connective tissue [187].

Studies in rat models demonstrated similar effects of oestrogen therapy on the rat vaginal epithelium thickness and increase in vaginal wall distensibility. The structural similarities of the rat vaginal wall with the human vaginal wall has allowed investigators to extrapolate their studies in rat models to that of humans. Regardless, as with other species, the key regional differences in embryonic origin of the rat vagina and its microflora should be taken into consideration.

The Rabbit Model:

Since long, the *in vivo* rabbit vaginal irritation (RVI) model is the preferred choice to test for vaginal microbicide irritancy potential and toxicity [188]. The RVI test is performed by injecting the test compound into the vagina of mature rabbits and after specific time points the rabbits are euthanized and the vaginal tissues are resected. Histological examination of vaginal tissue sections is then carried out to check for epithelial ulceration, oedema or leukocyte infiltration. There are several limitations in using rabbit models due to anatomical dissimilarities of the rabbit vaginal epithelium with that of the human. About two thirds of the rabbit vaginal epithelium is lined with a columnar epithelium which is entirely different from the human stratified squamous epithelium [17]. This structural feature cause rabbit vaginal epithelium highly sensitive towards vaginal irritants compared to its human counterpart that may lead to false positive results in testing compounds used in vaginal formulations.

Moreover, unlike the human vaginal epithelium the rabbit vaginal epithelium lacks the presence of *Lactobacilli* and acidic microenvironment, absence of reproductive cyclic stages and cervical mucus production and also human-specific markers of inflammation. Despite these major dissimilarities between the rabbit and human vaginal tissue, the rabbit model serves as the gold standard for FDA mandated preclinical testing of irritancy potential of microbicides candidates.

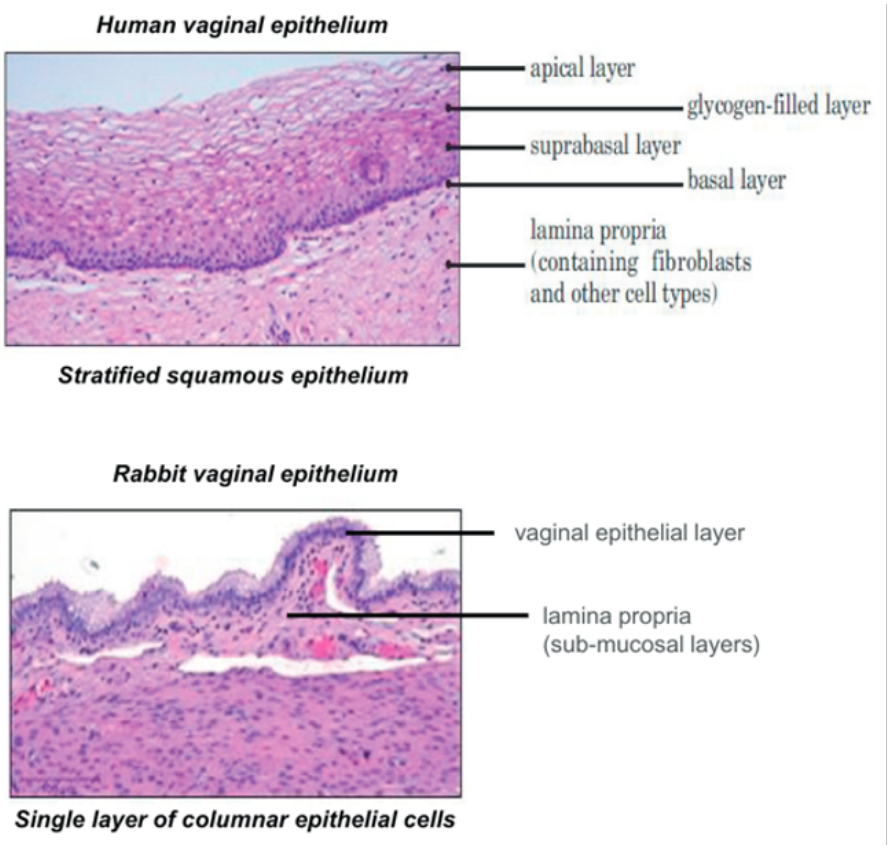

Figure 1.27: Comparison between H&E stained tissue sections of human and rabbit vaginal epithelium. Reproduced with permission from [179].

The Monkey model:

Rhesus monkeys have also been used to test the irritancy potential of vaginal microbicides and microbicide loaded vaginal rings [189], [190]. Vaginal application of the test compound is carried out by administration through a catheter into the test animals and after a defined time period, vaginal biopsies are taken and evaluated. Although the monkey's vaginal mucosa has structural and functional properties which are more similar to human native tissue than the rabbits, these animal models are very expensive in terms of maintenance. These animals require special facilities for keeping them, surgical expertise, rigorous ethical approval, expertise in handling and also carry the risk of transmissible infections and viruses.

The Porcine model:

The pig model provides another potential animal model for studying human vaginal pathologies, wound healing and microbicide efficacy. The pig and human vagina share similarities in anatomy, pH, vaginal and cervicovaginal secretions, vaginal mucus production

and inflammatory response towards microbicides [162]. D'Cruz *et al.,* [191] carried out potential microbicide irritancy and toxicity testing using in vivo pig model and correlated the levels of key cervicovaginal inflammatory cytokines (IL-1β and IL-8) with histological changes to determine the degree of vaginal inflammation. However, permeability studies by Eyk and Bijl [192] concluded that there were considerable differences between the porcine and the human vaginal mucosa towards different permeants and hence, these differences should be taken into consideration while using porcine as an animal model for vaginally applied drugs.

The Sheep model:

In terms of similarities with the human urogenital tract, sheep are the most closely related animal and has been extensively explored for gynecological research. Accordingly, sheep have become the animal model of choice for reproductive research due to the similarities with human in anatomy of the pelvic floor, fetus to pelvic ratio, response towards reproductive hormones and spontaneous development of pelvic organ prolapse [181]. Moreover, histologically the sheep vaginal epithelium also resembles human vaginal tissue the most as it is a non-keratinised stratified squamous epithelium with an underlying submucosa enriched with vasculature unlike other animal models of vaginal tissue research. These properties have made sheep an attractive model for microbicide permeability and toxicity testing. Vincent *et al.,* [193] have demonstrated similar effects of benzalkonium chloride on sheep vaginal epithelium thinning in a dose-dependent manner reported in humans. These features have recognized sheep as the most physiologically relevant predictive toxicology screening model for human microbicides. In recent years, a few groups have shifted their focus on utilizing sheep as an alternative model to RVI assay for more relevant preclinical testing of contraceptives [194] and vaginal microbicides for human use [195].

The sheep pelvic floor offers many similarities with the human on a biomechanical and molecular level. Hympanova *et al.,* [196] studied the functional changes in the sheep vaginal wall associated with the different stages in the reproductive cycle and correlated their findings with those reported in humans. Similar to humans, the sheep vaginal walls were reported to be stiffer in their mechanical properties attributed to higher collagen content in low serum oestrogen levels. Additionally, sheep have the capacity to develop spontaneous pelvic organ prolapse and hence can provide a parallel model environment in terms of human reproductive research [149].

The Slug Model:

Preclinical toxicity testing of vaginal microbicides and formulations using vertebrate animals has been severely criticised due to ethical and financial considerations. Adriaens and Remon [197] developed an alternative test using the terrestrial slug, *Arion lusitanicus*, the only invertebrate test organism for irritancy potential of vaginal microbicides. The Slug Mucosal Irritation assay (SMI) was developed at the Laboratory of Pharmaceutical Technology of the University of Ghent, Belgium and has been used as a comparable test to the RVI assay to evaluate the mild and moderate irritating substances by many groups [198]. Briefly the rationale for using the SMI assay is that the slugs when in contact with the test substance will produce mucus, reduce body weight and release enzymes (LDH and ALP) associated with the irritancy potential.

Dhondt *et al.,* utilized the SMI assay for evaluation of local tolerance of vaginal formulations and their results showed good correlation with the *in vivo* data using animal models (mouse and macaque) and also with the clinical data for some of the tested compounds [198]. Later, the same group showed comparable results from SMI assay with that of the RVI on local tolerance of vaginal gels [199]. Several studies have suggested the use of SMI assay in the early phases of pharmaceutical development to evaluate their local irritancy tolerance without using vertebrates to minimise ethical concerns regarding animal testing in the R&D [200], [201]. However, one major drawback of the SMI model is that only test compounds in the form of solids, semi-solids or liquids could be tested which limits the use of this model to evaluate irritancy potential of newly developed vaginal rings, films or tablets.

Table 1.6: Advantages and disadvantages of using whole animal test systems for vaginal tissue research.

Species	Advantages	Disadvantages
Rat **Mouse** **Rabbit** **Monkey** **Pig** **Sheep** **Slug**	**General:** Whole organism reaction Complex system provides a dynamic response All related systemic components are involved Testing of full strength and concentration of the test compounds can be used.	**General:** Concerns for animal rights and welfare Legal and ethical approval required Expensive in most cases Non-human tissues Technical and labor extensive
	Specific: **Rat and Mouse**: inexpensive, easy maintenance and prolific breeding **Rabbit**: FDA approved animal model, inexpensive, easy maintenance **Monkey and Porcine**: share similarities with the human vaginal tissue both anatomically and physiologically **Sheep**: closest to human in terms of similarities in the vaginal mucosa, similar biomechanical and physiological properties with humans	**Specific:** **Rat and Mouse**: Keratinised epithelia and structurally different from human vaginal mucosa, permeability data of compounds vary from human studies, keratinised epithelia more resistant to damage by potential vaginal formulations **Rabbit:** Reproductive anatomy is very different from human; vaginal epithelium is largely columnar which is non representative of the human counterpart **Monkey and Porcine**: Expensive models, require technical expertise, difficult to handle, increased risk of transfer of infections and viruses

	Slug: inexpensive, easy to handle, similar response towards compounds causing itching and burning in human vaginal mucosa.	**Sheep**: Expensive model, surgical expertise required, differences in vaginal microflora **Slug**: Can only be used to predict irritancy potential of solids, semi-solids or liquid vaginal formulations, very preliminary model in R&D.

Limitations of using animal models:

Many animal species have been used as *in vivo* models for preclinical testing of mucosal toxicity such as monkeys, dogs, rabbits, rats and mice. Due to the interspecies differences in genital tract anatomy, physiology and histology, these animal models are unable to mimic the vaginal tissue response towards tested compounds as seen clinically in humans. The variability of genital tract infectivity and the oestrous cycle of experimental animals are key variables to consider while planning the experiments as these affect the data collection. Moreover, the toxicological endpoints differ for different experimental animal species because of the differential sensitivity towards topically applied drug candidates. There is now an urgent need to develop sensitive, reliable, reproducible and physiologically relevant non-animal based *in vitro* vaginal models for preclinical testing of potential biomaterials and drug candidates for human vaginal tissue.

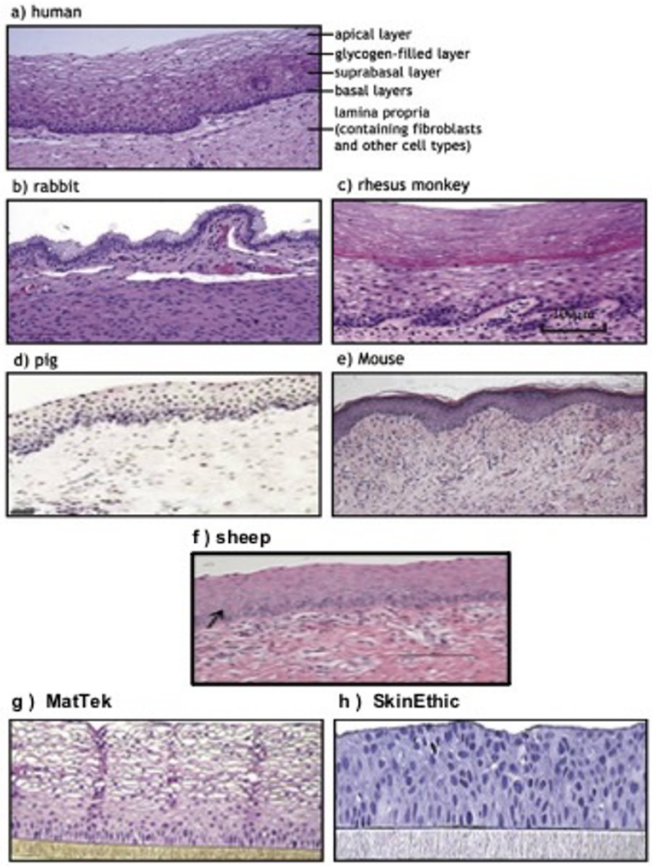

Figure 1.28: Comparison between H&E stained vaginal epithelium of: (a) human, (b) rabbit, (c) rhesus monkey, (d) pig, (e) mouse, (f) sheep, (g) EpiVaginal from MatTek Corporation (Ashland, MA, USA) and (h) HVE- Human vaginal Epithelium from SkinEthic (Nice, France) adapted from [16]*. Reproduced with permission from FRAME.*

1.21 *In vitro* models:

Design and development of *in vitro* models have become increasingly popular among the research community as these models can avoid many ethical and regulatory issues that apply when working with humans and animals. Although animal models and clinical trials offer more complex and complete experimental conditions involving all the influencing factors, *in vitro* experiments have the advantages of low cost, flexibility, convenience and fast results.

The three Rs principle:

Traditionally animals have been used in the field of medical research due to their complex physiology, biology and pharmacology which have led researchers to important discoveries and advancements in the field of biomedical sciences. For years, animal research was unavoidable to study vaginal pathogenesis, cervical cancer pathology, identification of

therapeutic targets in the vagina, understanding the onset and progression of pelvic floor dysfunctions and also develop pharmaceuticals that can be administered through the vaginal route. The human vaginal mucosa is a non-keratinised stratified squamous epithelium up to the ectocervix that shifts its architecture to a simple columnar layer at the endocervix. Currently, several therapeutic and prophylactic applications through the vaginal route has been considered in clinical practice especially hormonal compounds that relies upon efficient absorption through the vaginal mucosa. In the preclinical phase, potential vaginal drug candidates are characterised in terms of their permeability through the vagina, pharmacokinetics, toxicological effects, therapeutic efficacy and potential metabolites production in the body. This information often requires the use of animals in the vaginal tissue research. Most commonly used animal models are rats and mice whereas biomechanical studies on the pelvic floor support require complex animal models such as rabbits, dogs, pigs or monkeys. Despite the benefits associated with the use of animals in scientific research, concerns from animal rights activists led to reforms and regulations of the use of animals in research. Therefore, in 1959, two researchers Russell and Burch proposed alternatives to animal research by defining their 3Rs principles in the book "The principles of humane experimental technique" [202].

The first R is for Replacement and involves strategies and approaches to replace the use of animal in preclinical testing by developing alternative methods. In recent years, there has been more focus on developing *in vitro* and *in silico* model systems for preclinical assessment of physicochemical parameters of potential drug candidates. These include toxicity, permeability and pharmacokinetic behavior of molecules being testing in *in vitro* models that can recapitulate *in vivo* physiology closely.

The second R is for Reduction of the number of animals used in the scientific research without having an impact on the nature and quality of data obtained from a particular experimental design. In recent years the sample size is critically evaluated to design a quality study. In addition, development of novel non-invasive imaging and monitoring techniques have allowed researchers to achieve qualitative data along with a significant reduction in the number of experimental animals.

The third R is for refinement of the experimental procedures involving animals by building enriched environments for the welfare of experimental animals. The law requires special consideration is to be given to the living conditions of the animal during the course of experimentation and ensuring the most painless and least aggressive techniques for animal testing.

The concept of 3Rs has led researchers to develop alternative methods to animal testing such as those based upon *in vitro* testing models. In recent years, the focus of vaginal research has shifted towards developing alternative methods for testing vaginal microbicides irritancy and permeability in *in vitro* models that are more predictive of human native tissue response, less time-consuming, less ethical details and more cost effective. Studies on vaginal *ex vivo* cultures, *in vitro* models, organoid cultures, various cell lines and reconstructed tissue models have potential applications in pre-clinical testing for personal, cosmetic care and contraceptive products safety and screening.

Cell culture systems:

Cell culture systems have consistently been used as alternatives for the *in vitro* toxicity screening of cosmetic and personal care compounds, in light of consumer concerns regarding animal testing and as a shift towards cruelty free testing. Research in the field of dermal and ocular irritants have broadly utilised cell culture systems for screening and validation of different toxicological endpoints, however, their use has been limited in the assessment of vaginal irritants. It is crucial that the key players in this area of research should consider these culture systems as their future objectives of regulatory process.

Sobel vaginal epithelial cultures:

In 1979, Sobel *et al.,* [203] reported the development of human vaginal epithelial cultures from healthy adults. The explanted vaginal tissues on glass slides started to form enlarged colonies of epithelial cells after two weeks in culture that stratify as a multilayer (3-5 cells thick) epithelium from the outgrowths at 21 days that resembled vaginal epithelial cells *in vivo*. Their epithelial cells culture remained proliferative upto two weeks and later formed keratinisation of the superficial layers. Although the group achieved stratified epithelium, but they were unable to establish a continuous line of vaginal epithelial cells *in vitro* and there was considerable variability among the different explanted tissues.

More recent study by Krebs *et al.,* [204] used primary human vaginal epithelial cells isolated from vaginal walls of patients undergoing reconstructive surgeries for potential toxicity testing of vaginal microbicides. The group demonstrated high sensitivity of primary vaginal epithelial cells towards vaginal topical microbicides and hence, these investigations represent initial

stages of *in vitro* modelling of the vaginal microenvironment. Although these investigations have served to advance our understanding of microbicidal toxicity, their epithelial cell culture lacked the complex architecture of the vaginal epithelium and needs to be complimented with further studies in multifaceted systems for validation of their results.

The Gorodeski Model:

In late 80s, Gorodeski *et al.,* [205] successfully isolated human ectocervical epithelial cells (ECE) from the ectocervical tissues collected from patients aged 22-49 years undergoing hysterectomy. They isolated and expanded the primary human ECE on feeder layers and characterised the cultured cells in terms of morphology, expression of cytokeratins and their ectocervical origin as the cells expressed their typical epithelial cell morphology, undergo stratification and displayed unique keratin expression pattern in culture similar to *in vivo* conditions [205].

They also determined the keratin expression profiles from cultured ECE that resembled in vivo ectocervical cells especially keratin 19. Keratin 19 is characteristically expressed by non-keratinised stratified epithelia such as the ectocervix and endocervix whereas it is absent in the epidermis [206]. Their model is useful for studying the hormonal regulation of ECE cell differentiation as their model depicted estradiol responsiveness reciprocating *in vivo* modulation of cellular response towards sex steroids. Their 2D ECE cell culture model responds to estradiol by formation of mature envelop forms while progesterone exposure inhibited envelop maturation and stratification of the cultured cells. These observations are in concordance with the *in vivo* physiological environment as estradiol promotes cellular differentiation in ectocervical cells. Although this model is useful for studies on the effects of sex steroids, their model lacked the native ectocervical epithelial stratification and is of human origin that limits the scope for a broader research audience as human tissue samples are costly and require complex ethical approvals from research commodities.

The modified Gorodeski model for permeation studies:

Later, the Gorodeski model was modified to develop stratified epithelial cell layers to investigate permeability of different vaginal formulations. Human ectocervical epithelial cells (hECE) were grown on collagen coated ceramic based filters and on plastic and compared to the cervical cell line (CaSki) in terms of stratification and expression of keratin profiles [207].

Both cell types, when cultured on filters, were differentiated and stratified to form 5-12 layers of squamous epithelium resembling the *in vivo* biological characteristics of human cervical-vaginal epithelium.

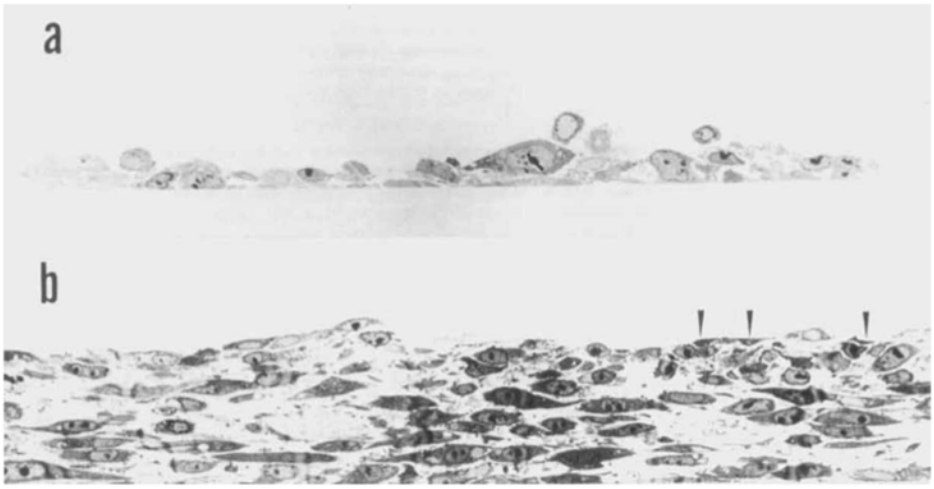

Figure 1.29: Effect of permeable support on the stratification of Human ectocervical epithelial cells (hECE) in vitro. Cultures 12 days post confluency on (a) solid and (b) filter support. Reproduced with permission from [207].

This study reported the established culture conditions for hECE cells but when these cells were compared to the cervical cell line (CaSki), the latter ones were better differentiated on the filter membranes. The filter membrane supported improved proliferation and differentiation of CaSki cells however, the cell lines do not represent the real cell behavior. Apart from easy maintenance and quick growth rate, the cell lines cultures are immortalised cells that are not true representatives of the *in vivo* cellular behavior.

Monolayer cultures of cell lines:

In recent years, monolayer cultures of immortalized and transformed cell lines have gained popularity to assess the microbicide toxicity testing and to study the pathophysiology of vaginally transmitted diseases. Rajan *et al.,* [208] utilized an immortalised cell line derived from normal primary vaginal cells obtained from human biopsies to study the mechanism of pathogenesis of microbicides. They studied the interaction of *Escherichia coli* with the vaginal cell line to understand key stages involved in the progression of urinary tract infections (UTIs) in women. Although this particular cell line presented a promising model to investigate bacterial adherence to the vaginal epithelial cells and pathogenesis of bacterial infections of the

lower urinary tract, however, this cell line has not been investigated to screen microbicide irritation potential. This limits its applications in microbicide profiling.

The CaSki cell line models:

Over the years, different cellular models were developed and compared in terms of their applicability in vaginal research. The human ectocervical epithelial cells (hECE) were established as a model for the ectocervical epithelium and considered in permeability studies of microbicides. ECE16-1 and CaSki, both immortalised cell lines depicted characteristic profiles of metaplastic and endocervical epithelium respectively [209]. In later studies, the CaSki endocervical cell line was reported to form monolayer cultures which can be modified to form stratified cultures depending upon the cell seeding densities. These stratified cultures are valuable preclinical models for studying transport mechanisms and permeability of drugs through the vaginal epithelium [210]. Studies involving cell line cultures resulted in substantial basic knowledge for the vaginal permeability barrier and hence paved ways in developing drugs and therapies that can be administered through the vaginal route.

Commercially available immortalised cell lines:

There are several immortalised cell lines that are commercially available from the American Tissue Culture Collection (ATCC) for comparative studies on cytotoxicity and permeability testing of vaginal microbicides as shown in Table 1.7.

N-9 cytotoxicity testing:

Nonoxynol-9 (N-9) is one of the first compounds to be used as a topical microbicide effective against HIV-1 that was evaluated using different animal models. Experiments conducted to study the sensitivity of the vaginal mucosa towards N-9 in albino rabbits [211][212] and rats indicated an intense inflammatory response towards N9 with significant degenerative cervicovaginal epithelial changes. Catalone *et al.,* [182] studied the cytotoxicity of N-9 towards endocervical cell line (End1/ E6E7) and vaginal keratinocytes line (Vk2/E6E7) and their results correlated with the *in vivo* data from the mouse models. These cell lines were also used for testing mucosal toxicities of different vaginal microbicides by measuring their cytokine release profiles *in vitro*. Although useful *in vitro* testing models, these cell lines often differ in their sensitivities to the same agent [213]. In addition, their gene expression profile and lack of

stratification differ from the native vaginal epithelium and thus limit their use in the microbicide permeability and toxicity testing.

1.22 Explant models:

In recent years, surgical explants from human and animal models have been increasingly used as a primary *in vitro* method for microbicide evaluation which more closely mimic the physiological features of the human reproductive tract tissue. These explanted or *ex vivo* models are not only used for drug permeability assays but also enable histological evaluation of vaginal tissue before and after drug application. While some reports may classify the *ex vivo* models as *in vitro*, these two concepts are entirely different based upon the origin of the models. The *ex vivo* or explant models require surgical tissue excision from animals or humans whereas the *in vitro* tissue models are grown or reconstructed in an artificial milieu in a laboratory setup.

Human explanted cervico-vaginal tissues:

Human explanted tissues are usually obtained from women undergoing planned hysterectomies. High throughput screening involving explanted tissues requires initial assessment of tissue quality and morphology but most importantly the viability of the explanted tissues usually assessed by the MTT assay [214]. There are several companies and tissues repositories that offer explants of human tissues including Asterand (Detroit, MI, USA) and US National Disease Research Interchange (NDRI; Philadelphia, PA, USA) that provide fresh explanted tissues from patients upon request for use in the research programs [17]. However, it remains unlikely that sufficient tissue becomes available for high throughput toxicity screening. Concerns regarding the acquisition and maintenance of human explanted tissue in the laboratory has enabled researchers to look into alternatives such as the use of frozen tissues or animal explanted tissues.

Fink *et al.,* [215] first developed the *in vitro* human cervico-vaginal explant culture to study the epithelium metaplasia. They cultured large tissue explants on stainless steel grids in agarose-gelled medium to study the early events in the infection of HSV_1 and HSV-2. Later O'Brien adapted their protocol to study glycoprotein production from normal and malignant cervico-vaginal explants by using smaller sized (5 mm^3) explants in immersion and in ALI cultures. They concluded that the ALI technique was superior to the immersion culture as it maintains the explants in an *in vivo*-like conditions that helped in retaining the native histological characteristics of the explanted tissues [216]. One major limitation of this study

was that only a limited number of explanted tissues was used and only two samples from fetal cervical tissues were used.

Studies have utilised human cervical tissue explants for research into understanding the early mechanism of transmission of HIV infection [217] that later bridges the gap between the preclinical and early clinical trials of potential HIV microbicides [218]. Merbah *et al.,* [14] reviewed the applications of cervico-vaginal explanted tissue models to study HIV-transmission and considered future directions of these studies.

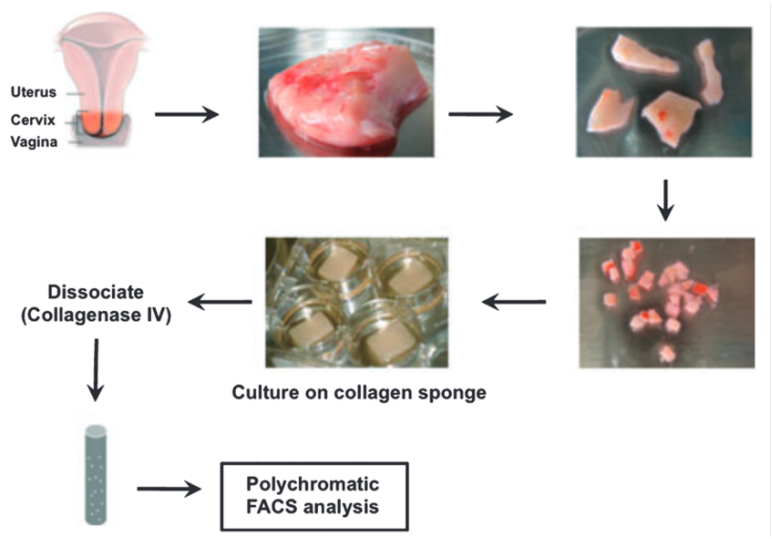

Figure 1.30: Characterisation of human cervico-vaginal tissue. Explants of human cervico-vaginal tissue is dissected into small blocks and cultured on top of collagen rafts at an air-medium interface. This method is useful in the study of productive infection of HIV. Reproduced with permission from [14].

Gupta *et al.,* [219] reported the use of previously frozen explanted cervical tissue to test the efficacy of microbicides and showed that the frozen-thawed cervical explants can offer an alternative model to the freshly explanted tissues. However, it is highly doubtful that these frozen-thawed tissues could retain their intrinsic permeability features and viability to be used in permeability studies of microbicides or in longer experiments [220].

Anderson *et al.,* [221] reviewed the issues confining the data interpretation from experiments utilizing human cervical explanted tissues for microbicide screening such as unknown clinical history and hormonal status of patients. One serious technical limitation is that, in general, human explanted tissue needs to be used within 12 hours of surgical removal which otherwise can affect the permeability and responsiveness of the tissues towards the tested materials. These

explanted models have several caveats such as limited life span in culture, limited donor tissue availability, progressive deterioration of the tissue architecture, variability among donor tissues and requirement of ethical approval [213].

Animal explant models:

Vaginal tissues obtained from different animal species such as rabbits, rodents, monkeys, pigs and sheep have been used for irritability and permeability studies of vaginal microbicides for many years [222]–[224]. However, due to anatomical and histological differences in the vaginal epithelia of different species, results from animal studies differ from those in human explanted tissues. Berginc *et al.,* [224] developed an *in vitro* bovine vaginal model to characterise the biopharmaceutical properties of drugs coated on liposomes for vaginal delivery. It was concluded that their model's ability to discriminate between high and low permeability compounds through the explanted bovine vaginal tissue cultured on transwells was very low and could not be correlated with the clinical data. Also, bovine epithelium histology differs significantly from the human vaginal epithelium that consequently effects the permeability of compounds through the epithelium.

Human and porcine vaginal tissue share similarities in the architecture of the vaginal epithelium as both have stratified squamous epithelium supported on a connective tissue component [162]. In addition, the ultrastructure of the vaginal epithelium such as the organization of the granules and intercellular lipid lamellae are common in humans and in pigs [225]. There are also less ethical concerns regarding the use of animal tissue and most laboratories can procure animal explanted tissues from the local abattoirs or from the companies that provide fresh explanted porcine tissue such as Sioux-Preme Pork Products (Sioux Center, IA, USA). Hence, porcine vaginal mucosa could be a useful in vitro alternative to human explanted tissue for testing the safety of cosmetic and personal-care products. However, Eyk and Bijl [192] reported significant differences in results from testing of molecules permeability through the vaginal explants from human and porcine. The use of porcine vaginal explants has now become questionable for screening of products designed for human use due to their inability to accurately model human vaginal absorbability. In addition, as with human explants, the shorter viability time period also implies to the porcine explanted tissues. In recent years, more focus has been given to animal-free and cruelty-free testing of cosmetics and skin-care products due to the consumer demand.

Table 1.7: Comparison of different model systems for human vaginal mucosa studies.

Model system	Characteristics	Advantages	Disadvantages
Cell culture	Single layers of cells having different morphological features depending upon the tissue source and type	Relatively inexpensive and easy to grow in culture medium	Absence of barrier function, no physiological resemblance with the native tissue
Organ culture	Formation of a differentiated and stratified non-keratinised epithelium under appropriate culture conditions	Organotypic morphology is relatively easier to achieve and is inexpensive	Not easily reproducible, can't mimic the functional characteristics of tissue *in vivo*, Barrier tends to be more permeable towards compounds compared to *in vivo*
Rodent	Vaginal mucosa with keratinized epithelium	Complex physiological model, inexpensive, easy maintenance, easy to handle	Keratinised epithelium is not representative of the human vaginal epithelium, Epithelium will tend to be less permeable and more resistant to damage by the tested compounds
Rabbit	Vaginal mucosa with variable morphology, largely columnar epithelium	Complex physiological model, inexpensive, easy maintenance, easy to handle	Not a good model for human vaginal tissue as most of the vaginal epithelium is columnar

			epithelium, unable to recapitulate human vaginal physiology
Monkey	Vaginal mucosa with non-keratinised epithelium	Structural resemblance with human tissue	Very expensive to purchase and maintain, difficult to handle, risk of transmission of infections
Porcine	Vaginal mucosa with non-keratinised epithelium	Structural and functional resemblance with human tissue	Expensive, larger animals difficult to handle, require surgical expertise
Porcine- ***ex vivo***	Vaginal mucosa with non-keratinised epithelium on a collagen-like support	Inexpensive, easy to maintain in culture, No regulatory concerns	Absence of vasculature limits their applicability
Human- ***ex vivo***	Vaginal mucosa with non-keratinised epithelium on a collagen-like support	Viability for at least 12 hours after surgical removal, structurally and physiologically accurate	Limited availability, ethical concerns, limited viability, potential transfer of infectious agents

1.23 From 2D cell culture to 3D vaginal tissue models:

The transition from using 2D cell monolayers to 3D organ culture and reconstructed tissue models was motivated by the need to study cellular behavior in models that can mimic the native tissue morphology and architecture. 3D tissue and organ models can recapitulate the natural 3D environment of living tissues and therefore, have been used in R&D and preclinical safety and toxicological testing of potential drug candidates. Traditional 2D cultures have several drawbacks including genetic aberrations, downregulation of signal transduction network in prolonged culture conditions and possible transformation of oncogenes. In addition, the 2D cell cultures are deprived of the extracellular matrix and cell lines are not able to

remodel in a uniform nutrient-rich environment and these monolayer cultures are unable to recapitulate *in vivo* physiology.

Organoid models:

The recent shift from the use of 2D cell cultures towards organotypic 3D cell culture systems is logical, given that the organs and tissues are 3D structures. Indeed, 2D cultures have provided researchers with understanding of pathophysiology of vaginally transmitted diseases as well as effectiveness of microbicides however, it is now increasingly evident this approach is not predictive of in vivo tissue responses. One major reason is the loss of cellular physiology and differentiation in prolonged 2D culture conditions which in turn results in the loss of cellular response and hence, physiological relevance of these 2D culture systems.

The vaginal epithelial cells provide the first line of defense against sexually transmitted diseases in women and play a critical role in the immunological response towards invading pathogens. Hjelm *et al.,* [226] developed a 3D vaginal epithelial model for toxicity testing of potential microbicides effective against sexually transmitted diseases such as AIDS. Their model was developed using a rotating wall vessel bioreactor (RWV) technology to create 3D organotypic vaginal epithelial cells that exhibited the physiologically relevant features *in vivo*. The rotating wall vessel technology can produce organoid models in a physiological low fluid shear environment that was employed to study vaginal viral and bacterial pathogenesis.

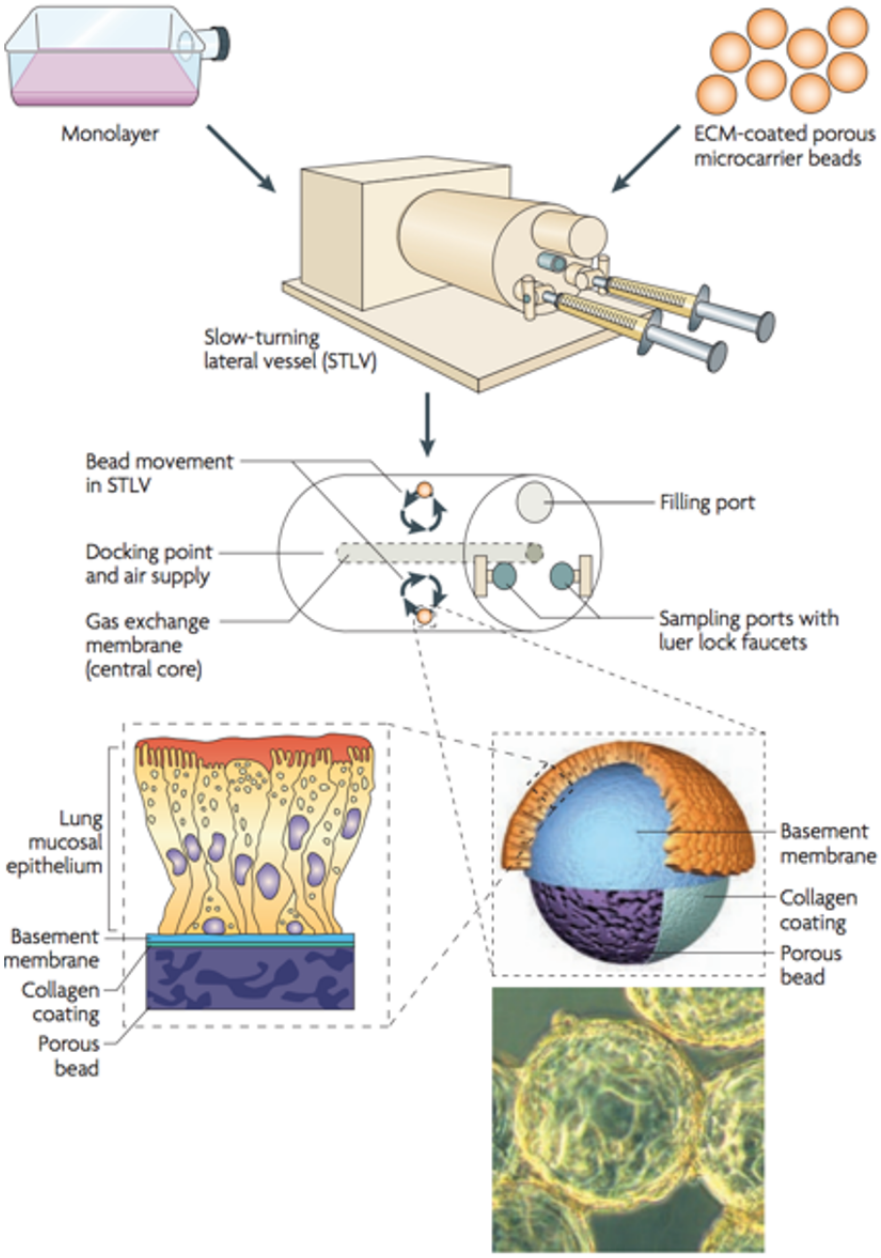

Figure 1.31: Rotating wall vessel technology (RWV). Confluent monolayer cultures are trypsinised and introduced into the slow-turning lateral vessel (STLV) along with the porous microbeads coated with the extracellular matrix. Rotation of the vessel along a horizontal axis caused sedimentation of the cells on the beads resulting in the formation of 3D organoids. Reproduced with permission from [227].

Their vaginal epithelial cell model was developed by growing the cells on porous, collagen-coated microbeads in the RWV system to produce aggregates of differentiated and stratified 3D organoids of the epithelial cells over a time period of 3 weeks in culture as shown in the Figure 1.32. The 3D vaginal epithelial cell model showed remarkable resemblance to the *in*

vivo tissue with features including microvilli, tight junctions, microfolds and mucus. This model has been utilised in screening and toxicological studies of vaginal microbicides and pathophysiology of sexually transmitted viruses. One major limitation of this model is that in their preliminary investigations, their 3D vaginal cells were not responsive towards 17β-estradiol. Although the vaginal organoids were producing mucin *in vitro* and were positive for the expression of differentiation markers, their estradiol-unresponsiveness is a major limitation of these organoid models to be used in studies where hormone-responsive characteristics are desired.

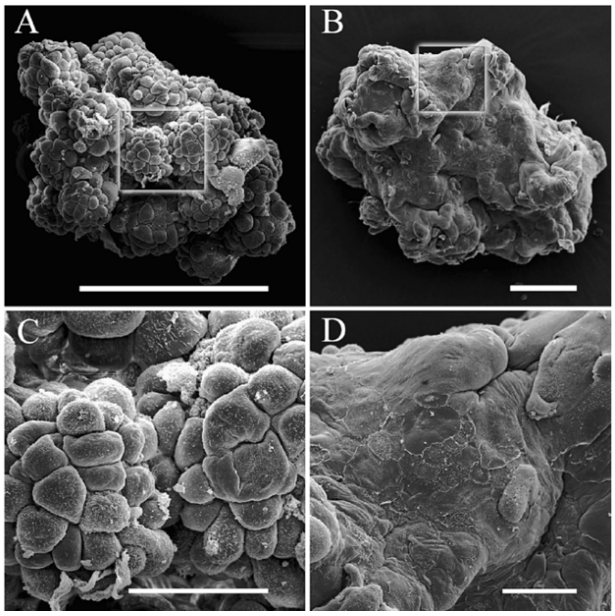

Figure 1.32: Scanning electron microscopy images of early and late development of 3D organoids of vaginal epithelium in low (A and B, scale bar=200μm) and high (C and D, scale bar=50μm) magnification. Reproduced with permission from [226].

1.24 Reconstructed tissue models:

The simplicity of *in vitro* cell culture, explanted tissues and organoids models in vaginal research can lead to limitations in terms of *in vitro* to *in vivo* data correlation and translation of microbicides into clinics.

EpiVaginal™ model:

The EpiVaginal™ tissue model series was developed by MatTek Corporation (Ashland, MA, USA) to provide 3D *in vitro* culture systems for toxicological and permeability testing of vaginal microbicides, irritancy potential of feminine hygiene products including contraceptives

and modelling of vaginally transmitted diseases such as HIV-1 (MatTek Corporation). These models were developed using human derived vaginal-ectocervical epithelial cells isolated from biopsies collected from healthy individuals undergoing hysterectomy for benign indications. Four different types of EpiVaginal™ models are commercially available from MatTek [228]:
VEC-100- An epithelial model containing vaginal epithelial cells (VEC)
VLC-100- An epithelial model containing vaginal epithelial and immunocompetent dendritic cells
VEC-100-FT- the tissues are similar to VEC-100 but include a collagen gel matrix containing fibroblasts to mimic the lamina propria
VLC-100-FT- the tissues are similar to VEC-100-FT but dendritic cells are also incorporated.

In the case of VEC-100 and VLC-100, the ectocervical vaginal epithelial cells were seeded in plain inserts and cultured for 4 days in submerged conditions. The models were later raised at an air-liquid interface to allow for tissue differentiation and formation of a stratified, epithelial-like, multilayered vaginal ectocervical cell lining (10-16 layers). In the case of VEC-100-FT and VLC-100-FT, fibroblasts were isolated from human ectocervical tissues and mixed with a collagen-solution before seeding into the polycarbonate microporous inserts to mimic the lamina propria like structure. This is followed by seeding of the vaginal ectocervical epithelial cells on top and maintenance in culture conditions described above [229]. The dendritic cells were obtained from cord blood CD34+ hematopoietic progenitor cells to include in the VLC models series.

The EpiVaginal™ tissues were composed of highly stratified vaginal epithelium similar to the native *in vivo* tissue such as the basal, parabasal, glycogenated and superficial layers supported on membrane filters. Immunofluorescence staining of the models revealed formation of tight junctions. The vaginal tissue models have consistent thickness of the epithelium, are highly reproducible and are intended to be cultured at an air-liquid interface to better resemble the native vaginal mucosa (MatTek Corporation). These models were originally developed to test the toxicity potential of various drugs and vaginally applied formulations but later on reports suggested the value of these models for vaginal drug permeability testing and selected examples are given below in Table 1.8:

Table 1.8: Selected examples of permeability studies performed using EpiVaginal™ tissues. Adapted from [230].

Tissues	Test drugs/molecules	Dosage form	Comments
VEC-100-FT	UC781	Gel	Tissue-associated drugs level were tested
VEC-100-FT	Biotin-labelled human IgG	-	IgG was selectively and bidirectionally transported via neonatal Fc receptor
VLC-100 and VLC-100-FT	RC-101 peptide	-	Experiments conducted over 6 days after preliminary tissue infection with HIV-1 for 3 days
VEC-100-FT	IQP-0528 and tenofovir	Gel	Tested over 3 days with daily gel application

One major limitation of these models is that they are recommended to be used within a few days from purchase as longer culture conditions (beyond one week) resulted in loss of normal morphology of these models (MatTek Corporation). Hence, these models are impractical for use in longer experiments. Another limitation of these models is that the EpiVaginal™ tissues are commercially available with a tissue surface area of 0.5 cm^2 that offers a smaller surface area to carry out drug permeability studies. Most pharmaceutical industries prefer tissue models of larger surface area around 2-4 cm^2 to increase the volume of total amount of drugs that can be tested and eluted to determine permeability potential of drug candidates. In addition, there is now more interest in the determination of membrane-associated drugs to test their local effects on the vaginal mucosa. For this intention, these EpiVaginal™ tissues models are not desirable due to the lack of lamina propria-epithelium junctions in the models that are representative of the native vaginal mucosa.

Ayehunie *et al.,* [231] first examined the utility of *in vitro* EpiVaginal vaginal ecto-cervical (VEC) tissue models to test various feminine-care products safety by applying the test substances topically on the models for different exposure times. They concluded that the EpiVaginal VEC tissue model was a promising tool for assessment of preclinical testing of

vaginal care products. Later, they studied the pathophysiology and early events in the HIV-1 infection using VLC-100 tissue models by incorporation of dendritic cells derived from human umbilical cord blood into the VEC-100 tissue models [232]. Their results showed that these models were useful, non-animal *in vitro* models to screen new compounds and therapeutic agents directed for use for women's health.

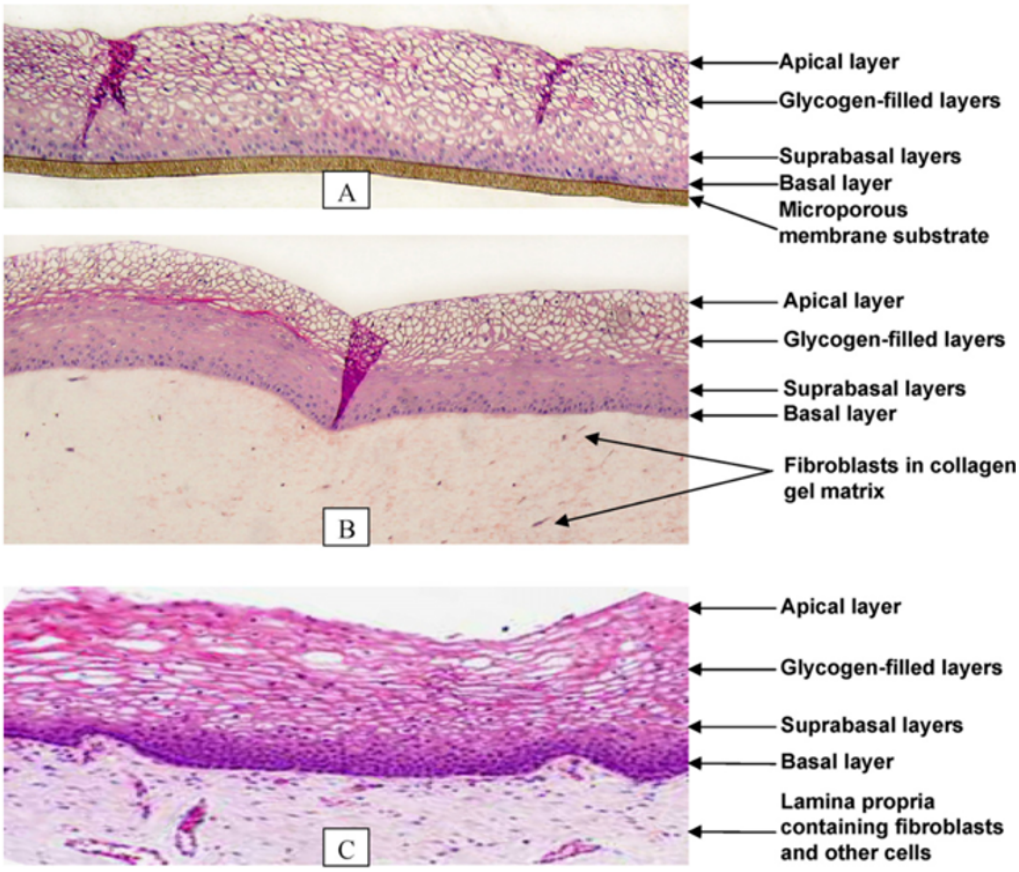

Figure 1.33: H & E stained cross sections of: (A) EpiVaginal™ VEC-100 tissue, (B) EpiVaginal™ VEC-100-FT tissue with epithelial and lamina propria layers, and (C) native human explant vaginal tissue. Reproduced with permission from [229].

Ayehunie *et al.,* [229] tested various compounds commonly found in the vaginal products to predict their irritancy potentials by utilising EpiVaginal™ tissues and compared their results with the traditional animal model of rabbit vaginal irritation (RVI) assay. The conventional FDA approved RVI assay has several limitations such as histological differences in the cervicovaginal tissues of rabbits and humans, lack of cyclic reproductive stages unlike humans and unresponsiveness to many human genital pathogens [233]. These species related differences make RVI unpredictive of human irritants and toxicity of vaginal compounds. The

results of EpiVaginal™ tissues were more promising than RVI assays in terms of their *in vitro* end points and relatability to human applications.

Table 1.9: Comparison between in vitro EpiVaginal™ model and rabbit vaginal irritation assay. Adapted from [229].

	***In vitro* EpiVaginal™ method**	**Rabbit vaginal irritation assay (RVI)**
Histology	Epithelium is non-keratinised, Resembles native human vaginal tissue.	Epithelium is keratinised
Reproducibility	Highly reproducible	variable
Study turnaround time	3-4 days	15-30 days or even more
Animal alternative model	Yes	No
Relevance to humans	High	moderate

1.25 Model to study HSV-2 infection:

Herpes Simplex Virus type 2 (HSV-2) is among the most common and prevalent sexually transmitted disease that primarily targets the genital tract mucosal epithelium and the virus replicates within the vaginal epithelial cells. Globally, it has been estimated in 2012 that over 417 million people suffer from existing HSV-2 infection [234] that damages the genital tract mucosa and causes ulceration through which opportunist pathogens and viruses can invade the human body. Currently there is no effective treatment or prophylactic or therapeutic vaccine available in clinics for genital HSV-2 infection. In addition, the potential anti-HSV-2 vaccines developed and initially tested on animal models were not able to make into clinics as they were rendered not suitable for humans. One of the main reasons is the lack of *in vitro* virus infection models which can closely mimic the *in vivo* human vaginal physiology.

Zhu *et al.,* [15] developed a 3D HSV-2 infection model to establish a human cell-based microphysiological system to study the mechanism of virus biology and susceptibility of primary human vaginal epithelial cells to HSV-2. They isolated the human normal vaginal

epithelial cells (HNVEC) from human vaginal biopsies and cultured in Matrigel to provide a basement membrane matrix. The Matrigel 3D cultures were maintained at an air-liquid interface to achieve stratification of the epithelium as shown in Figure 1.34.

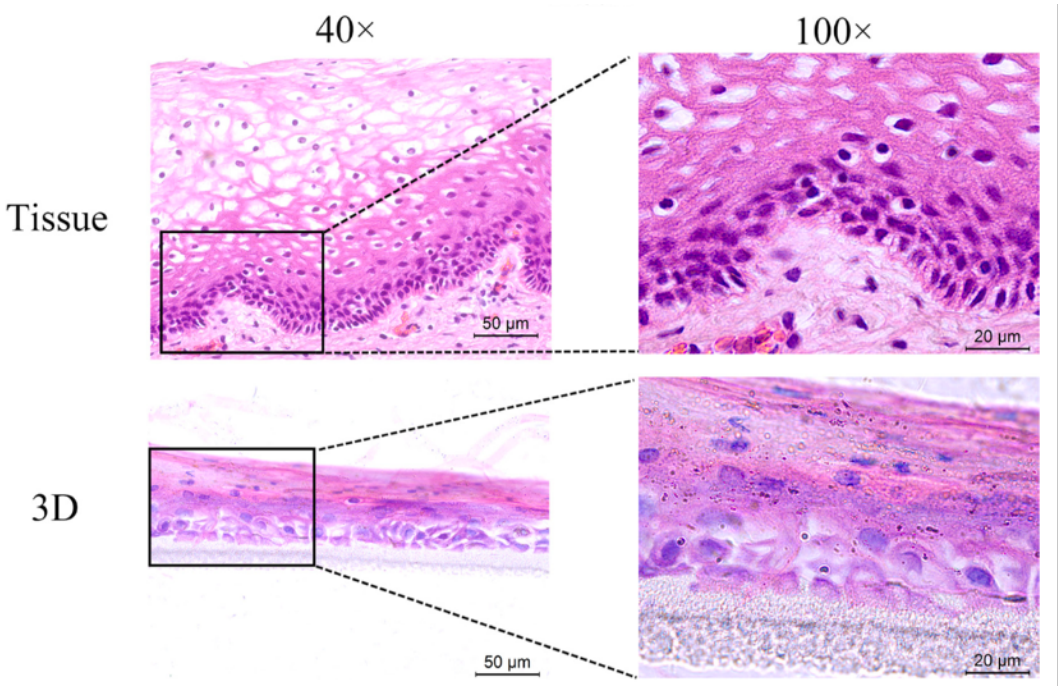

Figure 1.34: H&E stained sections of native vaginal tissue and 3D Matrigel containing HNVEC. The stratified epithelium polarity was achieved by culturing the 3D models at an air-liquid interface (ALI) for 14 days before fixed. Reproduced with permission from [15].

This study investigated the pathological changes in their 3D model after HSV-2 entry and concluded that the integrity of the vaginal epithelia of their models was gradually destroyed from the apical surface towards the basal layers over the HSV-2 infection time. Hence, this model could be a valuable tool for human genital viral biology research and anti-viral drug discovery. However, there are several concerns regarding the use of Matrigel in cell culture applications and drug discovery owing to its complex and variable composition [235]. High variability in biochemical and mechanical properties among a single batch of Matrigel have led to uncertainty of cellular behavior and reproducibility of data.

1.26 Models to study vaginal drug permeation:

In recent years, the vaginal route has been considered of great interest for local and systemic drug delivery due to its larger surface area and efficient permeability. Due to the ethical and practical constraints regarding the use of human tissue and organs, research has now shifted to develop alternative methods and models to predict drug permeability through the vaginal mucosa. These include cell culture systems, explants and reconstructed models that provide a simple, economical, reproducible and ethically accepted methods in the early stages of the development of vaginal formulations. Some selected examples of *in vitro* models to study the drug permeation through the vaginal wall is given in Table 1.10.

Table 1.10: In vitro models available for preclinical testing of drug permeability through the vaginal barrier. TEER (transepithelial electrical resistance).

	***In vitro* model**	**Source**	**Features studied**	**References**
Cell- based models	HEC-1A-cell line	Human endometrial carcinoma	Drug permeation and solubility TEER	[236]
	hECE- human ectocervical epithelial cells	Normal cells isolated from human biopsies	TEER	[205], [209], [237]
	CaSki- human cervical epithelium cells- cell line	Human epidermoid carcinoma	Transepithelial electrical conductance	[210]
	C-33A- cervix cancer cell lines	Human cervical retinoblastoma	TEER	[238]
	Primary vaginal epithelial cell culture	Human biopsy from healthy women	Drug permeability	[239]
Reconstructed tissues	VEC-vaginal ectocervical	Normal, human derived	Sodium fluorescein leakage.	[240]

	tissue model (EpiVaginal™)	vaginal ectocervical epithelial and dendritic cells-MatTek Corporation	Inflammatory cytokine release. Potential use for screening and assessment of the irritation, penetration metabolism, or efficacy of active ingredients or final formulations for vaginal application	
	HVE®-Human vaginal epithelium	A431 cells derived from a vulval epidermoid carcinoma grown on a polycarbonate filter-SkinEthic	Screening and assessment of the irritation, penetration, metabolism, or efficacy of active ingredients or final formulations for vaginal application	[241]

1.27 Commercially available 3D models of the vaginal mucosa:

Models of the vaginal mucosa are used for testing pathogen transmission, vaginal infections and screening of potential drug candidates to administer through the vaginal route. EpiVaginal™ was utilised for testing of new anti-HIV formulation [242], a biodegradable intravaginal polyurethane ring for dapivirine delivery [243], vaginal gel containing microbicide [240], vaginal tablets [244] and to test the transport of bovine insulin through the vaginal mucosa [245]. Alves *et al.,* [246] investigated the co-infection mechanism of *Candida albicans* and *Candida glabrata* by utilising the reconstituted human vaginal epithelium (HVE) *in vitro*. Their study showed that the HVE model coupled with specific analysis tools is a valuable tool to understand the pathophysiology of vaginal candidiasis, colonisation and tissue damage by measuring the expression of specific virulence genes by these pathogens.

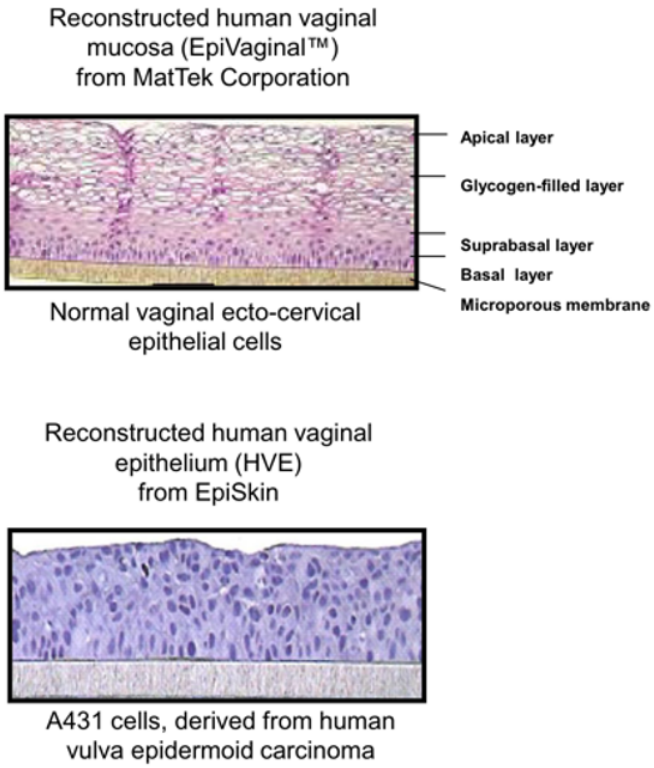

Figure 1.35: Comparison between H&E stained vaginal epithelium of: reconstituted human vaginal mucosa (MatTek corporation) and EpiSkin. Reproduced with permission from [179].

Table 1.11: Characteristics of commercially available vaginal mucosa tissue models.

Tissue model	Company	Description
EpiVaginal™	MatTek	Derived from basal, parabasal, glycogenated intermediate and superficial cell layers originates from normal, adult female vaginal epithelial and dendric cells, exhibiting histological, ultrastructural, protein and cytokeratin expressions characteristic of the native vaginal tissue.
Human Vaginal Epithelium (HVE)- SkinEthic™	EpiSkin	Basing on A431 cell line (from vulval epidermoid carcinoma)
Reconstructed Human Vaginal Epithelium RHV	ATERA	Consisting of human epithelial cells, generated of human epithelial cell line A431

Table 1.12: Advantages and disadvantages of different models applied for vaginal research.

	In vitro **Cell culture models Reconstructed tissue models**	***Ex vivo*** **Tissue explants**	***In vivo*** **Laboratory animals**
Advantages	Cultures are relatively inexpensive, easy to grow, reproducible	Entire cell structure, better tolerance to formulations, parallel efficacy testing	Data is produced in complex system with all physiological and anatomical representation
Disadvantages	Absence of systemic component, Organotypic cultures tend to be more permeable than *in vivo* conditions, Absence of vascular components.	Limited number available, Expensive, Shorter life span in culture, Ethical approval required, High variability among different batches Technically demanding	Time and cost expensive, Regulatory and ethical concerns Interspecies differences cause difficulty in correlating the data to humans, Technically challenging

1.28 3D tissue engineered vaginal tissues grafts for vaginal reconstructive procedures:

Tissue engineering of the vaginal tissues is required not only for tissue modelling but also for surgical reconstruction in patients with vaginal abnormalities. There are many diseases that necessitate the substitution or restoration of the native human vaginal tissue. Vaginal anomalies include congenital vaginal deformities such as vaginal agenesis, MRKH (Mayer-von-Rokitansky-K€uster-Hauser) syndrome or they can arise due to trauma to the genital tract.
Reconstructive surgical procedures to restore the structure and function of the vaginal tissue rely upon availability of donor tissue and tissue engineered vaginal substitutes. Although

currently there are many surgical techniques and grafts are available for vaginal reconstruction, none of the therapies available are without complications. There are two main approaches for vaginal reconstruction:

1) Resection of the existing malfunctioned vaginal tissue to create the future neovaginal space and subsequently lining with a graft material [247].
2) Replacement with a vascularised tissue such as the myocutaneous flaps [121] or intestinal segments [248] where the gap is much bigger.

There are several graft materials that have been used in clinics to line the surgically created cavity including, vaginal epithelial tissues, buccal mucosa decellularized matrices, amniotic membrane, full-thickness and split-thickness dermal grafts [249]. Nonetheless, these graft materials are associated with post-operational contracture or stenosis that may require long-term dilation. In case of buccal mucosa vaginoplasties, associated donor-site morbidities are clinically challenging as large tissue volumes need to be harvested to create the neovagina [250]. Many problems are associated with the use of intestinal segments such as extensive surgery, excessive mucous production and possible malignancy [251]. Tissue engineering using autologous cells has provided researchers with a therapeutic venue for patients requiring vaginal reconstructive surgeries that can avoid many of the complications of the above-mentioned procedures.

Raya-Rivera *et al.,* [252] developed tissue engineered autologous vaginal organs for implantation into patients with MRKHS. They obtained consented autologous vulvar tissue biopsies from patients and isolated the epithelial and muscle cells and then cocultured on decellularised porcine intestinal submucosa to reconstruct the vaginal organs *in vitro*. The engineered tissues were implanted into the four patients and long-term clinical outcomes were investigated by taking yearly tissue biopsies. This was the first attempt where vaginal organs were engineered and implanted into patients with successful outcomes that provided a viable option for vaginal reconstruction. However, this four patients pilot study has inherent limitations due to the limited number of patient's involved. In addition, the use of decellularised xenogenic scaffold has the drawbacks of a possible immunological reaction and risk of transmitting infection that may lead to inflammation and fibrosis around the vaginal grafts.

1.29 3D tissue engineered vaginal tissues by self-assembly technique:

The current vaginal reconstructed graft materials and diagnostic models are not ideal as these rely upon exogenous scaffolds or synthetic membranes that can trigger immunological response in the patients leading to post-operative complications. To avoid these possible disadvantages, Orabi *et al.,* [253] developed a fully autologous scaffold -free vaginal graft using primary vaginal epithelial cells and stromal cells isolated from tissue biopsies of patients. The vaginal epithelial cells sheets were developed using a self-assembly technique, then superimposed on Whatman paper followed by culturing of epithelial cells at an air-liquid interface culture *in vitro*. These vaginal equivalents were then implanted subcutaneously in 6 nude mice to test the integration and survival into the host tissue.

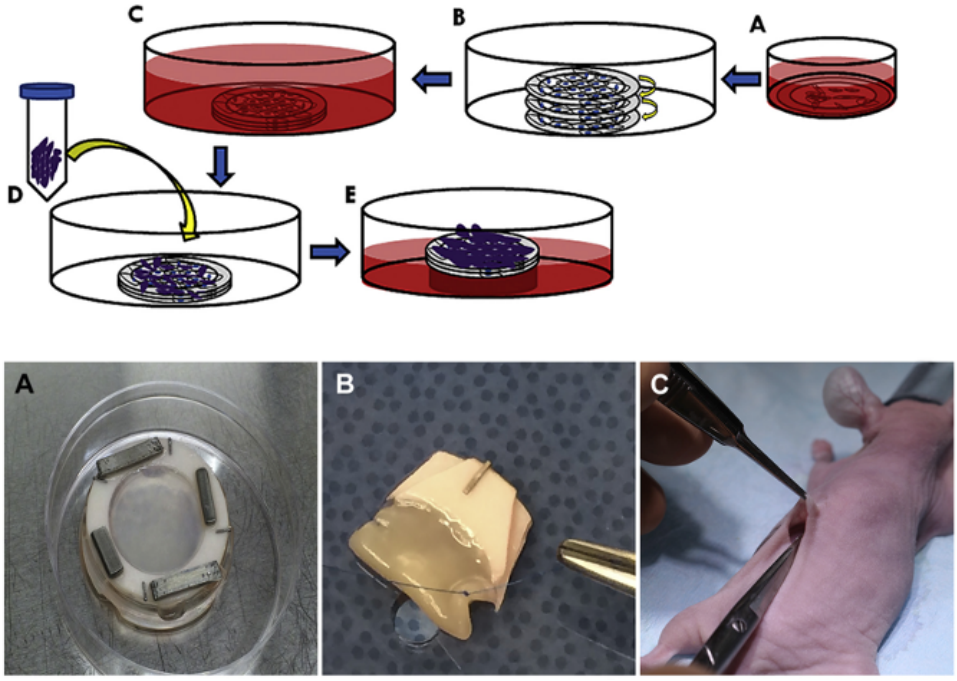

Figure 1.36: Preparation of vaginal construct in vitro and animal implantation. The upper panel shows the steps involved in in vitro formation of vaginal equivalents (A to E). Vaginal stromal cells cultivated for 21 days followed by superimposition of cells sheets. Vaginal epithelial cells were seeded on top of the sheets and were cultured at an ALI for 21 days to allow for stratification. The lower panel represents the in vivo subcutaneous implantation of the human vaginal equivalents into the nude mice (A to C). The macroscopic appearance of vaginal constructs pre-implantation where the Whatman paper holds the cellular sheets. The equivalents were folded, sutured on the sides and implanted in the subcutaneous space on the back of nude mice. Reproduced with permission from [253].

These biomimetic *in vitro* vaginal equivalents formed well-differentiated epithelium and survived *in vivo* for two weeks. Limitations of the study include insufficient biomechanical properties of the grafts compared to the native vaginal tissues as the connective tissue of the equivalents were mainly formed by the secretions of the cultured stromal cells. This is a major drawback of this study as the grafts couldn't be handled appropriately during the surgical implantation into mice and are unable to provide any kind of structural support to the native tissue. Other limitations include the possible unavailability of the native tissue from patients in case of cancer, absence of smooth muscle cells, longer time needed for graft preparation (21 days for stromal cells cultivation followed by 21 days in ALI for stratification), smaller study design with only six animals for implantation that needs further optimisation. For most tissue substitutes produced via self-assembly technique requires around 60 days for the production of constructs with appropriate cellular differentiation [156]. All these limitations need to be addressed before designing further experiments using self-assembly techniques for vaginal equivalents into future studies.

Table 1.13: In vitro models used for vaginal tissue research (adapted from [17]*).*

	Description	**Cell source**	**Reported/potential use**	**End points**
Cell culture systems	Human vaginal epithelial cells	Human biopsy	Study of the effects of different exogenous factors on the growth and differentiation of vaginal epithelial cells	Cell viability Measurement of release of chemokines (IL8) and cytokines (IL-1, IL-6, TNFα) Inflammatory mediators (PGs, VEGF), Transcription factors (NF-κB, AP-1)
	CRL-2614 (Ect1/E6E7) — immortalised epithelial cell line CRL-2615 (End1/E6E7) — immortalised epithelial cell	ATCC	Studies on cervico-vaginal physiology Testing of pharmacological agents for intravaginal applications	

	CRL-2616 (Vk2/E6E7) — immortalised epithelial cell line from human vagina		Preclinical evaluation of topical vaginal microbicides	
	Immortalised human vaginal epithelial cell line	Human biopsy	Studies on the mechanisms of bacterial adherence to the vaginal epithelial cells	
Explants	Human vaginal tissue	Human biopsy	Safety evaluation and risk assessment of ingredients and finished products.	Tissue viability Cytokine release Inflammatory mediators Signs of infection
	Porcine vaginal epithelium	Porcine excised tissue		
Reconstructed tissues	CellEstrous Species: rat The system models the vaginal epithelium during the estrous cycle Commercially available	CellnTEC	Studies on the oestrous cycle	Tissue viability Cytokine release (IL-1, IL-6, IL-8)
	VEC-100 Species: human Epithelial vaginal-ectocervical cells	MatTek	Potential use for screening and assessment of irritation potential, permeability,	

	Commercially available		metabolism, or efficacy of compounds or final formulations for vaginal application	
	VLC-100 Species: human Epithelial tissue containing epithelial VEC and immunocompetent dendritic cells Commercially available, patented	MatTek	Toxicity studies of feminine hygiene, vaginal care and microbicide products	
	VEC-100-FT Species: human Full thickness version of VEC-100 which includes epithelial cells and a fibroblast-containing lamina propria Commercially available	MatTek	Study of HIV-1 and other sexually transmitted infections	
	VLC-100-FT Species: human Immunocompetent version of VEC-100-FT which includes dendritic cells Commercially available, patented	MatTek	Study of HIV-1 and other sexually transmitted infections	

	RHVE Species: human Human vaginal epithelium reconstructed by using A431 derived from a vulval epidermoid carcinoma Commercially available	SkinEthic	Potential use for screening and assessment of the irritation, penetration, metabolism, or efficacy of active ingredients or final formulations for vaginal application.	

Take home message:

Models of vaginal tissues are useful for *in vitro* studies on microbicide irritancy potential, permeability of vaginally applied drugs, hormonal and infectious studies and pathophysiology of vaginally transmitted viruses such as HIV and HSV. Reconstructed vaginal models are also required for reconstructive surgery of the vaginal tissues due to deformity of the vagina caused by either disease or trauma.

These models include 2D culture systems, tissue explants, organoids and 3D models. *In vitro* 2D models lack the complex 3D tissue architecture, cell types, cellular differentiation and epithelial stratification. Tissue explants have the shortcomings of insufficient viability for longer experiments, ethical concerns, limited tissue availability for large-scale experiments and risk of potential transfer of viruses or diseases.

Many thousands of animals are experimented on and euthanized for use in the scientific research each year. Animal models cannot accurately model the *in vivo* human physiological conditions due to interspecies anatomical and histological differences, are associated with the need for rigorous ethical approvals, require technical expertise for surgical procedures, are costly and can lead to misinterpretation of results. The available 3D reconstructed tissues incorporate exogenous membranes or collagen component that does not truly represent the lamina propria of the native vaginal tissue. These models also lack specific cell types, have

poorly differentiated vaginal epithelium, are non-responsive to oestradiol, are very costly and not really accessible for many researchers due to the requirement to access and incorporate human cells and tissues.

The idea of using tissue engineering strategies for pelvic floor repair is relatively new. In light of the current ban on polypropylene pelvic mesh, the need for developing new materials and treatment methods is acute. So far, evidence from the most closely relevant reconstructive hernia surgery is able to provide some proof of concept in animal models but the pelvic floor is an entirely different entity from the abdominal region. PPL mesh failure in pelvic floor reconstruction has further highlighted these significant anatomical and physiological differences between hernia repair and pelvic floor repair. The success rate of PPL mesh in hernia repair is far better than in the pelvic floor repair and hence, it is fundamental to design biomaterials specific for a particular anatomical region. Most importantly, the mesh scandal has raised the undeniable impact of preclinical safety and efficacy testing of potential biomaterial before their use in clinics.

Unfortunately, a perfect POP animal model does not exist nor does a perfect match of scaffold, cell and growth factors for implantation into the human pelvic floor. The vagina of commonly used laboratory animals such as rats, rodents and rabbits react differently to mesh implantation to that of humans. The use of larger animals such as the rhesus macaque or the squirrel monkey and sheep are limited by the ethical concerns and cost involved. Hence, clinically relevant, safe, and cost-effective approaches arereally needed. This leads to the development of 3D *in vitro* preclinical models for early evaluation of safety and biocompatibility of potential biomaterials for pelvic floor repair and hence, the main aim behind this PhD project.

AIMS AND OBJECTIVES

The aim of this project was to develop cost effective, physiologically relevant *in vitro* 3D tissue engineered (TE) models of the vaginal mucosa as preclinical models to test novel biomaterials designed for applications in the female pelvic floor repair.

The specific objectives to accomplish in this thesis were:

1) To develop and characterise an *in vitro* tissue engineered model of the vaginal epithelium and underlying lamina propria by using decellularised sheep vaginal tissues as a scaffold.

2) To study the effect of the female sex hormone 17-β-estradiol [E_2] on the development of the TE model to seek to recapitulate the effect of this hormone on *in vivo* vaginal physiology.

3) To develop an *in vitro* tissue engineered wound vaginal model in which to study early events in wound healing.

4) To investigate the effect of physiological concentrations of 17-β-estradiol on wound healing in the 3D tissue engineered vaginal model.

5) To use TE wound vaginal models as preclinical testing models for implantation of potential biomaterials designed for the female pelvic floor repair. The aim is to develop these models to detect early tissue and cellular response towards existing and candidate materials to help distinguish between a “good” and “bad” material responses *in vitro*.

Chapter 2:

Developing physiologically relevant tissue engineered models of the vaginal mucosa

2.1 Aim:

To develop and characterise tissue engineered (TE) models of the vaginal mucosa using decellularised sheep vaginal tissue and cultured primary sheep vaginal epithelial cells and fibroblasts.

The specific objectives to achieve were:

- To analyse different stages of the development of tissue engineered vaginal models over time.
- To compare the histology and viability of cultured models under static and dynamic culture conditions over time.
- To determine the effect of different concentrations of female sex steroid estradiol-17β on the TE vaginal models.
- To determine the effect of different concentrations of 17-β-estradiol on the expression of key regulatory markers and cytokeratin expression in the TE vaginal models.

2.2 Introduction:

Tissue engineering is an emerging field of regenerative medicine that can be used to develop biological scaffolds to repair and promote functional rehabilitation of the compromised pelvic floor and help to regenerate the native tissue. In addition, tissue engineered *in vitro* vaginal models may be valuable preclinical models to study mechanisms of vaginal tissue repair and cellular response towards hormones, injury and bioscaffolds designed for the pelvic floor repair. Tissue engineered models have three primary components: scaffolds, cultured cell types and additional growth factors and hormones.

The choice of scaffold is the key factor in designing TE models as it can redirect cellular growth and differentiation which can stimulate tissue regeneration [65]. Ideally, the scaffold should have good biocompatibility and be able to recapitulate the *in vivo* microenvironment of the native tissue to provide an *in vitro* environment recognised by cells as physiologically relevant. In this regard, decellularised extracellular matrix (ECM) has emerged as a promising scaffold

material derived from whole native tissues that have their cellular components removed leaving behind only the architectural and ECM protein components [254].

Decellularised ECM- a gold standard scaffold:

Among naturally derived biomaterials, decellularised scaffolds are of particular interest in tissue engineering applications due to their closest proximity with natural tissue-specific architecture. Decellularisation is the process of elimination of cellular components of natural tissues by using physical, chemical or biochemical processes while retaining the native extracellular matrix (ECM) architecture [255], [256]. In order to translate decellularised ECM (de-ECM) as scaffolds in clinical setup for grafting, the removal of cellular components greatly reduces the risk of immunological and inflammatory responses that may ultimately lead to graft rejection [257]. Whereas, the use of de-ECM to construct *in vitro* preclinical models does not always require complete elimination of cellular components as these remnants provide an optimal level of antigens that contributes towards regulation of cellular behaviour and recapitulate tissue regeneration *in vitro* [254]. Several studies have suggested that upon decellularisation of different tissues, many key bioactive components such as glycosaminoglycans, collagen types and growth factors (transforming growth factor-β and vascular endothelial growth factor) are retained within the de-ECM that are beneficial in triggering the appropriate cellular response [258], [259].

A brief history of decellularised extracellular matrices:

Badylak and colleagues first proposed the decellularisation technique for porcine small intestinal submucosa (SIS) by detergent method in 1955 [260], [261] and since then, a marked increase in decellularisation studies have been reported in literature. Another milestone was achieved by Ott and colleagues in 2008 [262] who successfully decellularised whole organs scaffolds by a perfusion method. They published their findings of whole rat heart decellularisation while preserving the vascular architecture followed by studies on recellularisation of the structure by seeding with endothelial and cardiac cells and their potential applications in cardiovascular regenerative medicine [263]. Nevertheless, the functional complexity of different organs poses a major challenge in clinical translation but has a major role in construction of *in vitro* tissue engineered (TE) models.

In recent years, the focus has shifted more towards decellularised tissue products as they require less time and treatment with decellularisation solutions, hence allowing for their wider

applications in regenerative medicine. Many decellularised tissue types have been reported in literature such as dermis [264], [265], small intestinal submucosa (SIS) layer [257], bladder wall [266], neural tissue [267], adipose tissue [268], pericardium [269], ligaments and tendons [270]. Table 2.1 enlists some of the commercially available decellularised matrices and their clinical applications in plastic and reconstructive surgery.

Table 2.1: A few examples of clinical applications of decellularised matrices in plastic and reconstructive surgery [271].

Product/company	Tissue/ECM source	Applications
AlloDerm® (LifeCell Corp., USA)	Human dermis	Wound, hernia, pelvic and breast reconstruction
FlexHD® (Ethicon/Johnson & Johnson, USA)	Human dermis	Wound, hernia and breast reconstruction
MatriStem® (Acell Inc., USA)	Porcine UBM	Wound and surgical soft tissue repair
Oasis® (Cook Biotech Inc., USA)	Porcine SIS	Wound and surgical soft tissue repair
Surgisis® (Cook Biotech Inc., USA)	Porcine SIS	Pelvic and hernia reconstruction
AlloMax™ (Davol Inc., USA)	Human dermis	Hernia, chest wall and post-mastectomy breast reconstruction
Meso BioMatrix™ (Kensey Nash Corp., DSM, The Netherlands)	Porcine mesothelium	Congenital, surgical or oncologic soft tissue defects repair
Matriderm® (Dr. Suwelack Skin&Health Care, Germany)	Bovine dermis	Full- and split-thickness skin regeneration
Endoform™ (Aroa Biosurgery, New Zealand)	Ovine forestomach submucosa	Acute and chronic wounds repair
Zimmer Collagen™ (Zimmer Inc., USA)	Porcine dermis	Wound and surgical soft tissue repair
Collamend™ (Davol Inc., USA)	Porcine dermis	Hernia/abdominal wall repair
Permacol™ (Medtronic, Inc. & Covidien, USA)	Porcine dermis	Hernia/abdominal wall and breast reconstruction
XenMatriX™ (Davol Inc., USA)	Porcine dermis	Hernia/abdominal wall repair
SurgiMend™-SurgiMend PRS (TEI Biosciences, USA)	Fetal/neonatal bovine dermis	Various soft tissue repair and reconstruction (hernia, breast)
Tutopatch® (RTI Surgical, Inc., USA)	Bovine pericardium	Duraplasty, oral-maxillofacial surgery, hernia and pelvic repair
Veritas® (Synovis Surgical Innovations, USA)	Bovine pericardium	Pelvic floor, pelvic /rectal prolapse, and hernia repair
Axis™ (Coloplast Corp., USA)	Human dermis	Pelvic floor repair and urethral sling implantation
Repliform® (Boston Scientific, USA)	Human dermis	Enteroceles, rectoceles, cystoceles and pelvic floor repair
Suspend® (Coloplast Corp., USA)	Human fascia lata	Pelvic floor repair and urethral sling implantation
FasLata® Allograft (C.R. Bard, USA)	Human fascia lata	Pelvic floor and pelvic organ prolapse reconstruction
Strattice™ (LifeCell Corp., USA)	Porcine dermis	Hernias/body wall repair and breast reconstruction
InteXen™ (American Medical Systems, USA)	Porcine dermis	Pelvic organ prolapse repair
Xenform™ (Boston Scientific, USA)	Bovine dermis	Pelvic floor defect and soft tissue repair
Epiflex® (Hannover Medical School, Germany)	Human dermis	Burns/scars treatment and breast reconstruction
DermaMatrix® (Synthes CMF, USA)	Human dermis	Replacement, repair or reinforcement of soft tissues

Decellularisation protocols:

In literature, there are several methods to produce decellularised matrices from tissues and organs, but the main goal of any decellularisation protocol is to efficiently remove cellular and nuclear components while minimising the damage to the composition and mechanical integrity of the ECM framework [256]. The most robust and effective decellularisation protocols include a combination of physical, chemical and/or enzymatic treatment to minimise the time period for decellularisation while effectively removing the cellular remnants.

Physical treatments involve agitation, centrifugation, sonication, repeated cycles of freezing and thawing, mechanical massaging or applying pressure changes. All these techniques disrupt the cell membranes and opens up the ECM crosslinking to facilitate cell contents removal with subsequent treatments. Chemical treatments involve use of ionic solutions, detergents and chaotropic agents that can destroy the ionic and covalent bonds responsible for intracellular and extracellular connections. Enzymatic treatment involves the use of trypsin and proteases that can effectively remove cellular content but can also disrupt collagen crosslinking in the ECM. Details of some decellularising agents and their mode of action is given in Table 2.2.

Table 2.2: Commonly used decellularisation agents and their potential mode of action [256].

Method	Mode of action	Effects on ECM
Physical		
Snap freezing	Intracellular ice crystals disrupt cell membrane	ECM can be disrupted or fractured during rapid freezing
Mechanical force	Pressure can burst cells and tissue removal eliminates cells	Mechanical force can cause damage to ECM
Mechanical agitation	Can cause cell lysis, but more commonly used to facilitate chemical exposure and cellular material removal	Aggressive agitation or sonication can disrupt ECM as the cellular material is removed
Chemical		
Alkaline; acid	Solubilizes cytoplasmic components of cells; disrupts nucleic acids	Removes GAGs
Non-ionic detergents		
Triton X-100	Disrupts lipid–lipid and lipid–protein interactions, while leaving protein–protein interactions intact	Mixed results; efficiency dependent on tissue, removes GAGs
Ionic detergents		
Sodium dodecyl sulfate (SDS)	Solubilize cytoplasmic and nuclear cellular membranes; tend to denature proteins	Removes nuclear remnants and cytoplasmic proteins; tends to disrupt native tissue structure, remove GAGs and damage collagen
Sodium deoxycholate		More disruptive to tissue structure than SDS
Triton X-200		Yielded efficient cell removal when used with zwitterionic detergents
Zwitterionic detergents		
CHAPS	Exhibit properties of non-ionic and ionic detergents	Efficient cell removal with ECM disruption similar to that of Triton X-100
Sulfobetaine-10 and -16 (SB-10, SB-16)		Yielded cell removal and mild ECM disruption with Triton X-200
Tri(*n*-butyl)phosphate	Organic solvent that disrupts protein–protein interactions	Variable cell removal; loss of collagen content, although effect on mechanical properties was minimal
Hypotonic and hypertonic solutions	Cell lysis by osmotic shock	Efficient for cell lysis, but does not effectively remove the cellular remnants
EDTA, EGTA	Chelating agents that bind divalent metallic ions, thereby disrupting cell adhesion to ECM	No isolated exposure, typically used with enzymatic methods (e.g., trypsin)
Enzymatic		
Trypsin	Cleaves peptide bonds on the C-side of Arg and Lys	Prolonged exposure can disrupt ECM structure, removes laminin, fibronectin, elastin, and GAGs
Endonucleases	Catalyze the hydrolysis of the interior bonds of ribonucleotide and deoxyribonucleotide chains	Difficult to remove from the tissue and could invoke an immune response
Exonucleases	Catalyze the hydrolysis of the terminal bonds of ribonucleotide and deoxyribonucleotide chains	

Methods to achieve efficient tissue decellularisation and cell removal:

The presence of remaining cellular components in the decellularised ECM can contribute towards cytocompatibility problems when used as scaffolds for *in vitro* models and trigger adverse immune response when implanted *in vivo* [272], [273]. Although it is quite impossible to remove hundred percent of cells from a decellularised ECM, but it is possible to quantitively

measure any remaining cellular remnants such as double-stranded DNA (dsDNA), membrane associated proteins or by staining nuclei of cells. The minimum acceptable criteria for using decellularised ECM for the purpose of *in vivo* constructive remodelling is listed as follows [274].

• <50 ng dsDNA per mg ECM (dry weight)

• <200 bp DNA fragment length

• Lack of visible nuclear material in fixed tissue samples when stained with 4',6-diamidino-2-phenylindole (DAPI) or H&E.

There are several methods to determine whether all the cellular components have been effectively removed from the decellularised ECM. Histological analysis of the tissues by standard haematoxylin and eosin (H&E) staining can provide one with initial data of the presence or absence of cellular materials accompanied by detection of cytoplasmic components using Masson's Trichome staining. Immunohistochemical analysis can also be carried out to detect particular tissue specific markers such as collagen IV, actin, cytokeratins and vimentin [275]. The presence of DNA can be detected by staining the tissue sections with DAPI (a fluorophore that binds with the AT clusters in the minor groove of DNA helix) [276]. In addition, mechanical testing of the decellularised ECM provides an insight into the integrity and presence of structural components after the treatment.

Removal of residual decellularisation solution within the ECM:

Treatment with decellularising agents can have a profound effect on the mechanical and biochemical properties of the remaining ECM. Reports on detergent method decellularisation have suggested that in certain tissues these chemicals disrupt the collagen crosslinking and thereby decreased the mechanical strength of the scaffold [270], [277]. It has also been reported in literature that most detergents like sodium dodecyl sulfate (SDS) and toctyl phenoxy polyethoxy ethanol (Triton X-100) are capable of removing GAG molecules from the ECM which directly effects the viscoelastic behaviour of the decellularised scaffolds [278]. In addition, these detergents are also known to be cytotoxic if they remain within the tissues at a higher concentration which directly affects the seeding density of a particular cell type in *in vitro* tissue models [256]. The duration of exposure to the decellularisation agents also has an impact on the overall mechanical properties of the ECM.

Challenges of using decellularised ECM (de-ECM):

Finding an ideal sterilisation protocol for de-ECM is challenging but crucial to construct *in vitro* models. Prolonged treatment with acids or solvents like ethanol, changes the mechanical properties of the scaffold and can cause significant cytotoxicity that can be minimised by using slightly acidic electrolysed water [279]. Other sterilisation treatments such as ethylene oxide or gamma radiations are also reported to cause structural damage to ECM and alters the mechanical properties of the scaffolds [280]. *In vitro* tissue constructs require a particular environment such as a closed culture system or bioreactor to keep the cultured cells alive and functioning. Biochemical cues along with the physiological and environmental conditions significantly affect the functionality of the construct and should be closely monitored [281].

In this chapter, TE vaginal models were developed using native sheep vaginal matrices that were decellularised using low concentrations of ionic and non-ionic detergents in a way so that the unique native-tissue specific architecture remained unchanged. The choice of sheep as the vaginal tissue donor was made as sheep is the animal which most closely resembles humans in terms of reproductive anatomy, connective tissue levels of support for the genitourinary tract. In addition, the sheep are the only animals that may develop antepartum cervico-vaginal prolapse similar to humans [282]. The vaginal tissue architecture is also similar in both humans and sheep in terms of length and diameter [283]. The native sheep vaginal tissue was used as the source of isolation of primary sheep vaginal epithelial cells and fibroblasts and the TE vaginal models were cultured for 3-4 weeks under static and dynamic culture conditions. The TE vaginal models were then characterised to determine their physiological relevance for applications in vaginal tissue research.

2.3 Materials and Methods:

2.3.1 Cell culture facility:

All cell culture work was carried out aseptically in Class II laminar flow hoods (Walker Safety Cabinets, Glossop, Derbyshire, UK). Prior to conducting any cell culture, it was ensured that the laminar flow hood and the laboratory equipment used within them were sterile using 70 % v/v industrial methylated spirits (IMS) (Fisher Scientific UK Ltd, Loughborough, UK) spray or by autoclaving the supplies. All laboratory plastic wear was purchased from Costar, High Wycombe, Buckinghamshire, UK and Greiner Bio-one, Gloucestershire, UK. All cell types used in this PhD project were cultured and maintained at 37 °C in humidified incubators containing 5% CO_2.

2.3.2 Cell culture chemicals and media:

Tissue culture flasks (T25 and T75) were purchased from NuncTM (Nalgene, UK). Tissue culture basal media was from Sigma-Aldrich, UK. Foetal Bovine serum (FBS) was purchased from Biowest Biosera (UK). Cambridge Antibiotic Solution (CAS) (Product code: 04-301) was purchased from Source Bioscience Healthcare UK Ltd.

Dulbecco's modified Eagle's Medium (DMEM)
DMEM (D0819) was purchased from Sigma-Aldrich, UK (AQmedia™) with 4500 mg/L glucose, L-alanyl-glutamine and sodium bicarbonate.

Nutrient mixture F-12 Ham
Ham's F12 (N4888) was purchased from Sigma-Aldrich, UK with sodium bicarbonate.

Foetal bovine serum
FBS (heat inactivated) was purchased from Advanced Protein Products, Brierley Hill, UK and was stored frozen at -81 °C.

Penicillin/Streptomycin
P0781 was purchased from Sigma-Aldrich, UK

Amphotericin B

Amphotericin B solution (A2942) was purchased from Sigma-Aldrich, UK and stored in dark conditions protected from light.

Adenine

Adenine (A2786) was purchased from Sigma-Aldrich, UK. It was prepared by mixing 0.5 g of the product in 50 mL distilled water. 1M hydrochloric acid (HCl) was added gradually during mixing until the powder was dissolved completely. The solution was filter sterile and then the total volume was made up to 80 mL with distilled water to get a final concentration of 6.25 μg/mL.

Insulin

Bovine insulin (I6634) was purchased from Sigma-Aldrich, UK. It was prepared by adding 10 mg of the product in 1 mL 0.01 M HCl and dissolved. Then 9 mL of distilled water was added to the solution to get a final concentration of 1 mg/mL.

Hydrocortisone

Hydrocortisone (H0888) was purchased from Sigma-Aldrich, UK. It was prepared by adding 25 mg of the powder in 1 mL distilled water and dissolved. The final volume was made up to 10 mL by adding PBS.

Cholera toxin

Cholera toxin A (C8180) was purchased from Sigma-Aldrich, UK. First, a stock solution was prepared by adding 1.9 mL distilled water to 1 mg aliquot, dissolved and stored at 4 °C. The working solution was prepared by dissolving 100 μL of stock solution with 10 mL of media supplemented with serum.

3, 3', 5- Triiodothyronine/apo-Transferrin

3, 3', 5- Triiodothyronine (T_3) IRMM469 and apo-Transferrin (T1428) was from Sigma-Aldrich, UK. Two separate solutions were prepared. 13.6 mg of T_3 was dissolved in 1 mL 0.02 M sodium hydroxide (NaOH) and then the final volume was made up to 100 mL with distilled water. 250 mg of apo-Transferrin was dissolved in 30 mL PBS. The final solution was made

by adding 0.5 mL of the T_3 solution in 30 mL of the apo-Transferrin solution and the final volume was made up to 50 mL with PBS.

Epidermal growth factor (hEGF)

Epidermal growth factor (11376454001) was purchased from Sigma-Aldrich, UK. The solution was prepared by dissolving 100 μg of the powder in 1 mL of distilled water.

Cambridge Antibiotic Solution

Cambridge Antibiotic Solution (CAS) (Product code: 04-301) was purchased from Source Bioscience Healthcare UK Ltd. The solution was used neat from the bottle whenever required.

2.3.3 Preparation of cell culture media

Green's medium:

Vaginal epithelial cells isolated from sheep vaginal tissue were cultured in Green's medium. Green's medium was prepared 500 mL at a time and stored at 4 °C and used for upto one month. To ensure sterility of the medium prepared, 10 mL medium was incubated at 37 °C for 24 hours prior to use. The composition of Green's medium is given in Table 2.3:

Complete DMEM medium:

Vaginal fibroblasts isolated from sheep vaginal tissue were cultured in complete DMEM medium. Media was prepared 500 mL at a time and stored at 4 °C and used for upto one month. To ensure sterility of the medium prepared, 10 mL medium was incubated at 37 °C for 24 hours prior to use. The composition of complete DMEM medium is given in Table 2.4:

Table 2.3: Composition of Green's medium. All products were from Sigma-Aldrich, UK unless otherwise stated.

Component and supplier	Volume and stock solution	Final concentration	Storage
Dulbecco's Modified Eagle's Medium (DMEM)	330 mL	66 % v/v	4 °C
Nutrient Mixture F12 (Ham's F12)	108 mL	21.6 % v/v	4 °C
Foetal bovine serum (FBS) (Advanced Protein Products, Brierley Hill, UK)	50 mL	10 % v/v	-20 °C
Penicillin/Streptomycin	5 mL of 10,000 IU/mL penicillin and 10,000 µg/mL streptomycin	100 IU/mL penicillin 100 µg/mL streptomycin	-20 °C
Amphotericin B	1.25 mL of 250 µg/mL	0.625 µg/mL	-20 °C
Adenine	2 mL of 6.25 µg/mL	0.025 µg/mL	-20 °C
Insulin	2.5 mL of 1mg/mL	5 µg/mL	4 °C
3,3,5- Tri-iodothyronine/ Apo-Transferrin	0.5 mL of 1.36 µg/mL T_3 and 5 mg/mL apo-transferrin	1.36 ng/mL T_3 and 5 µg/mL apo-transferrin	-20 °C
Hydrocortisone	80 µL of 2.5 mg/mL	4 µg/mL	4 °C
Epidermal growth factor (EGF)	25 µL of 100 µg/mL	5 ng/mL	-20 °C
Cholera Toxin	500 µL of 8.47 µg/mL	8.47 ng/mL	4 °C

Table 2.4: Composition of complete DMEM medium. All products were from Sigma-Aldrich, UK unless otherwise stated.

Component and supplier	Volume and stock solution	Final concentration	Storage
Dulbecco's Modified Eagle's Medium (DMEM)	445 mL	89 % v/v	4 °C
Foetal bovine serum (FBS) **(Advanced Protein Products, Brierley Hill, UK)**	50 mL	10 % v/v	-20 °C
Penicillin/Streptomycin	5 mL of 10,000 IU/mL penicillin and 10,000 µg/mL streptomycin	100 IU/mL penicillin 100 µg/mL streptomycin	-20 °C

2.3.4 Cells storage, maintenance and passaging

All cell types were stored in liquid nitrogen dewar at a temperature of -196 °C.

Materials

Phosphate buffer saline (PBS):
PBS tablets were purchased from Oxoid Ltd, Basingstoke, Hampshire, UK. At a time 500 mL of 100 mM PBS was prepared by adding 5 tablets of PBS in 500 mL distilled water and dissolved. PBS was autoclaved prior to use for cell culture.

Trypsin-EDTA:
Trypsin-EDTA (T3924) was purchased from Sigma-Aldrich, UK and stored at -20 °C. Before using in cell culture, the bottle was thawed in a water bath at 40 °C.

Cryopreservation media:

Cryopreservation media was prepared by adding 90% v/v FBS (Advanced Protein Products, Brierley Hill, UK) in 10% v/v dimethyl sulfoxide (DMSO) (D1435) purchased from Sigma-Aldrich, UK. For each use, the media was prepared fresh as necessary.

Passaging of cells:

Cultured cells at 37 °C in incubators when reached at 80% confluency were passaged to ensure continuation of cellular proliferation. For this purpose, cell culture media was removed from the cell culture flasks and cells were washed with 5 mL PBS to remove any cell debris or residual serum proteins. Then 5 mL of trypsin-EDTA solution was added to the flasks and incubated for 5 min at 37 °C. The flasks were then observed under a light microscope to ensure that all cells get detached from the tissue culture plastic. Then 5 mL of supplemented cell culture media was added to neutralise the trypsin-EDTA and contents were transferred into 20 mL centrifuge vials. Cells were then centrifuged at 1000 revolutions per minute (rpm) using a benchtop centrifuge. After centrifugation, the supernatant was discarded, and the pellet was resuspended in the desired volume of cell culture medium.

Cell counting:

Cell counting was performed using a modified Neubauer haemocytometer (Weber Scientific International, Middlesex, UK). Ten μL of cell suspension was loaded on the haemocytometer and a glass coverslip was carefully placed over the loaded region. The haemocytometer was then carefully placed on the stage of the light microscope (Motic, BA210 series) and the counting grid was focused. The cells were counted in at least three alternate $1mm^2$ squares (volume 1×10^{-4} mL) of the haemocytometer and their average was calculated. The cell number was calculated by using the following formula:

$$\text{Total cells/mL} = \frac{\text{Average number of cells counted per } 1mm^2 \text{ square} \times \text{dilution factor}}{\text{Volume counted } (1 \times 10^{-4} \text{ mL})}$$

e.g., Average cell count of 100 cells x1 (dilution factor) x volume counted ($1x\ 10^{-4}$) = 1 million cells per mL.

Cryo-preservation of cells:

For cryo-preservation of cells, the protocol for passaging cells described in the above section was performed up to centrifugation. After centrifugation, the supernatant was discarded, and the pellet was resuspended in the cryopreservation media. The volume of media was added so that there was a total of 1-3x 10^6 cells/mL of cryo-preservation media. The cell suspension was then transferred 1mL into each cryovial (Cellstar cryovials purchased from Greiner bio-one, Gloustershire, UK) labelled accordingly (cell type, batch no., passage no. and date). The cryovials were then transferred into Nalgene™ Cryo 1°C freezing container (Nalgene Co., New York, USA) and stored at -80 °C. This freezing container allowed a controlled rate of cooling for cells at 1°C per minute -80 °C. After 24 hours, the vials were then transferred to the liquid nitrogen dewar (-196 °C).

Thawing and culturing of cells:

When required, the cryovials were removed from the liquid nitrogen (using the appropriate safety measures) and thawed in 37 °C water bath. Once thawed, the appropriate cell culture media (prior warmed at 37 °C in water bath) was added to the cryovials, then transferred to centrifuge vials to centrifuge at 1000 rpm for 5 mins. After centrifugation, the supernatant was discarded, and the pellet was resuspended in culture medium.

All cells were cultured in T75 cell culture flasks in humidified incubators at 37 °C containing 5% CO_2. The cell culture medium was changed twice a week with fresh medium to maintain cellular proliferation and viability. Once, the cells reached 80% confluency, they were either passaged or cryopreserved for further use depending on the experimental plan. All primary sheep vaginal cells were used up to passage 3-4. All new batches of cells were tested for mycoplasma infection before using in experiments.

2.3.5 Sheep vaginal tissue:

Materials

All scalpel blades, scalpel holders, scissors and forceps were purchased from Swann-Morton, Hillsborough, Sheffield, UK. The instruments for tissue dissection were sterile using autoclaving prior to use.

Difco-Trypsin

Trypsin (T4799) was purchased from Sigma-Aldrich, UK. Difco trypsin (DT) solution was prepared by adding 0.5 g trypsin in 100 mL PBS and dissolved. Then 0.5 g of D-glucose was added to the solution and pH adjusted to 7.4 with 2M NaOH and then the final volume of the solution was made up to 500 mL with PBS. The concentration of DT solution was 0.1% wt/v. The solution was then filter sterile using 0.22 µm pore size filter and supplemented with 1% v/v P/S (100 IU/mL Penicillin, 100 µg/mL Streptomycin) and 0.625 µg/mL amphotericin B. The solution was divided into 10 mL aliquots and stored at -20 °C.

Collagenase A

Collagenase A (from *Clostridium histolyticum* COLLA-RO) was purchased from Sigma-Aldrich, UK. The solution was prepared 0.5% wt/v by dissolving 0.05 g collagenase A in 10 mL supplemented Dulbecco‟s Modified Eagle‟s Medium (DMEM) and stored at -20 °C.

Collection and transportation of sheep vaginal tissue:

Sheep urogenital tract (intact) was obtained from R.B Elliott & Son Ltd. Stud Farm Abattoir, Calow, Chesterfield (S44 5UN) and transported in airtight container sealed within a Tissue collector plastic bucket. The label on the bucket was filled (by stating the type of sample, the date of collection, amount of tissue and their weight) and signed. Prior to sealing, the tissue samples were collectively weighed and ensured they were from healthy sheep by confirmation with the abattoir manager.

The tissue samples were driven back to the Kroto Research Institute (KRI), University of Sheffield in an electric vehicle provided by the University of Sheffield transportation services.

Dissection:

Tissue samples brought into the lab were washed twice with PBS (supplemented with 1% v/v P/S (100 IU/mL Penicillin, 100 µg/mL Streptomycin) 20 minutes each. The samples were then processed in Class II Biosafety cabinet for animal tissue processing under sterile conditions. The intact urogenital tract of each tissue sample was first placed on a sterile cutting board and with the help of scalpel blade, forceps and scissors (surface sterilised with 70% v/v IMS) sheep vaginal tissue was dissected from the urogenital tract as shown in Figure 2.1 and tissue sections used for analysis as shown in Figure 2.2. Extreme care was taken while dissecting the sheep vaginal tissues from the intact urogenital tracts. All instruments used for the dissection were autoclaved prior to use. Individual urogenital tract with associated organs (including ovaries, bladder, cervix, vagina and urethra) was first laid flat on the sterile cutting board (surface sterilised with 70% IMS). With the help of a sterile scalpel blade, an inclined incision was made in the anterior region of the vaginal canal near to the cervix, Next, with the help of a sharp, sterile surgical scissors the vaginal canal was cut open lengthwise (8-9cm) along the entire length of the canal until the posterior region just above the urethra. Caution was taken to prevent rupturing of the bladder during this whole process so that to prevent urine leakage that would cause contamination and infection problems. Once, the vaginal canal was flat open, with the help of a scalpel blade, the associated fascia, fat and tissue debris was gently scrapped off from the posterior region of the vaginal canal. Lastly, the vaginal tissue was completely removed from the urogenital tract and placed in a sterile Petri dish containing PBS. This process was repeated for each tissue sample and vaginal tissues collected after dissection were washed thrice with sterile PBS supplemented with P/S before further processing. The remaining urogenital tissues were disposed off following the protocol of animal tissue waste disposal in the Kroto S20 laboratory.

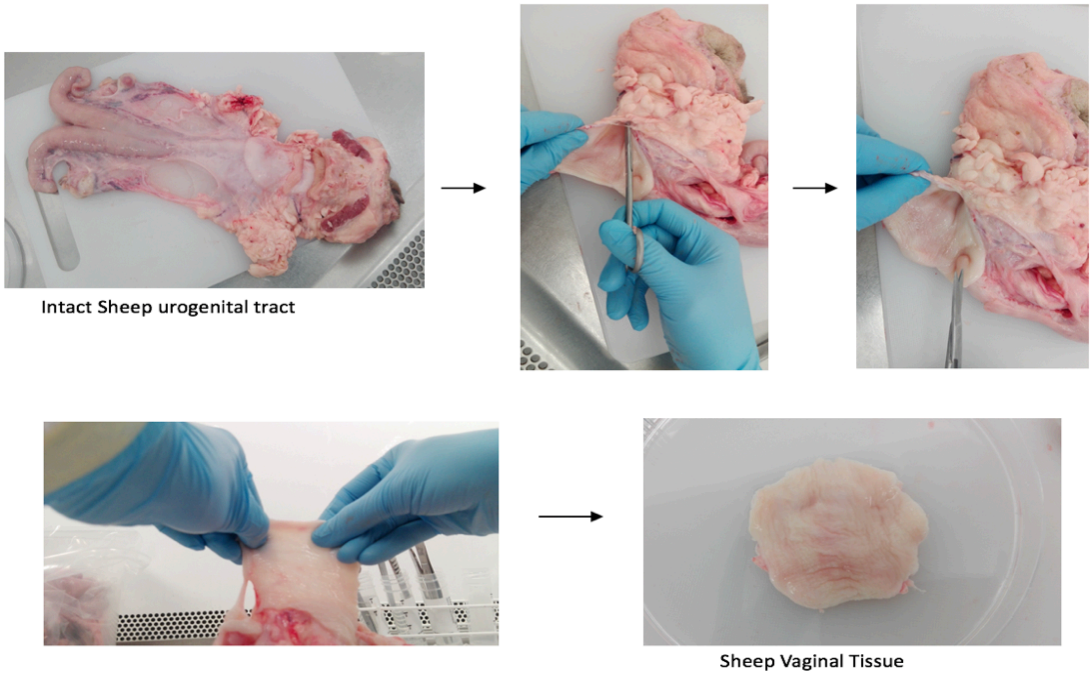

Figure 2.1: Steps for the dissection of sheep vaginal tissue (SVT). Intact urogenital tract was obtained from the abattoir and dissected across the length of vaginal tissue starting below the cervix all the way until vulva at the posterior end.

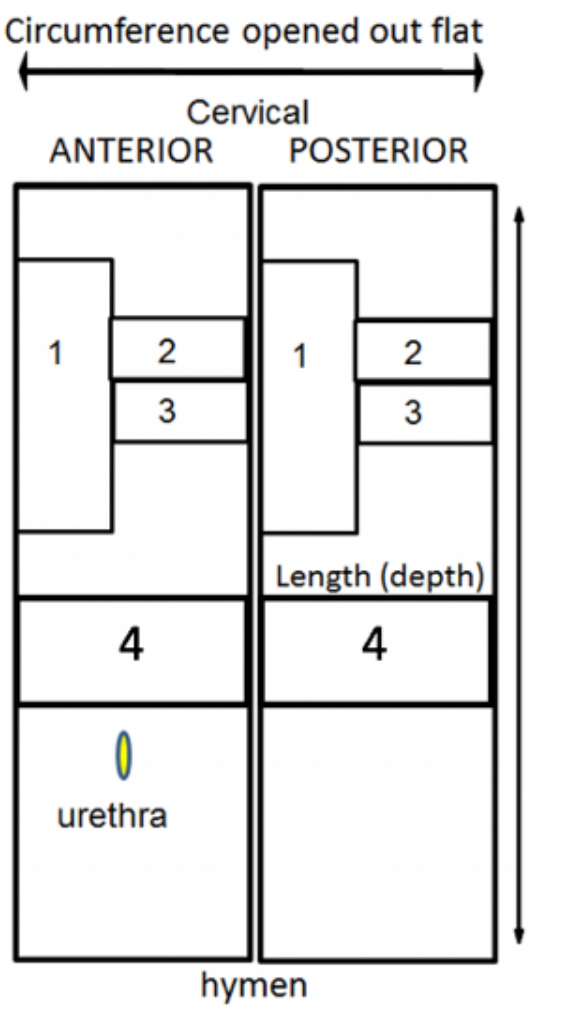

Figure 2.2: Schematic showing dissection of sheep vaginal tissue (SVT). Regions marked as 1, 2 and 3 were used for the decellularization procedure. Region 4 was used for the isolation of the primary vaginal epithelial cells and fibroblasts.

Preparation of feeder layer for epithelial cell culture:

Irradiated 3T3 murine fibroblasts were used as a feeder layer for culturing vaginal epithelial cells isolated from the sheep vaginal tissue. Murine 3T3 fibroblasts (XCELLentis, Gent, Belgium) were expanded in regular T75 culture flasks followed by culturing in CellSTACK® (Corning Life Sciences Inc, New York). Cellular growth and proliferation were monitored daily. Once 80 % confluent, the cells were centrifuged and resuspended in sterile 25mL universals in fresh medium. The cells were then irradiated using a cobalt-60 source irradiator and exposed to 60 Grays (6000 Rad) of radiation to arrest cell growth. The irradiated murine 3T3 (i3T3) cells were then cryopreserved until use as described in section 2.3.4.

Isolation of primary vaginal epithelial cells from SVT:

Sheep vaginal epithelial cells were isolated and cultured from sheep vaginal tissue (SVT) as described by Asencio *et al.,* [284] following the technique of Rheinwald and Green [285].

SVT stored at 4°C was taken out and washed twice with PBS (supplemented with 1% v/v P/S (100 IU/mL Penicillin, 100 µg/mL Streptomycin) before using. SVT was placed in a sterile petri dish and was cut into 0.5 cm^2 tissue sections using sterile scalpel blade and forceps. Tissue sections were incubated overnight with 10 mL of 0.1% wt/v Difco trypsin in a universal tube at 4°C. After incubation, the contents of the universal tube were taken out in a petri dish and 3 mL Green's media was added to neutralise the trypsin. Epithelial layer was carefully separated from the underlying lamina propria with the help of sterile forceps. The underside of the epithelium and the upper surface of lamina propria were gently scrapped with scalpel blade to remove basal epithelial cells. Freshly- isolated vaginal epithelial cells were collected in Green's media in a sterile universal tube and centrifuged at 1000 rpm for 5 min. After centrifugation, supernatant was discarded, and the pellet was resuspended in 10 mL of Green's media and placed in a sterile T75 tissue culture flask with a feeder layer of irradiated murine 3T3 (i3T3) fibroblasts. Culture flask was incubated at 37 °C in a humidified incubator (Thermofischer Scientific) with 5% CO_2.

Isolated epithelial cells cultures were maintained and passaged at 80% confluency into subcultures with feeder layer of irradiated murine 3T3 (i3T3) fibroblasts. Residual i3T3 were removed by adding 0.02% v/v EDTA into the culture flasks before the epithelial cells were detached using trypsin. For construction of TE vaginal models, epithelial cells were used from passage 2-3.

Isolation of primary vaginal fibroblasts from SVT:

Sheep vaginal fibroblasts were isolated and cultured from sheep vaginal tissue (SVT) as described by Skala *et al.,* [286].
During isolation of primary epithelial cells, the lamina propria of vaginal tissue was separated in a sterile petri dish. Mincing was done by rolling a surgical scalpel blade over the tissue and then incubated overnight in 10 mL 0.5% wt/v Collagenase A solution (supplemented with 1%

v/v P/S (100 IU/mL Penicillin, 100 µg/mL Streptomycin) in a sterile universal tube at 37°C in a humidified incubator (Thermofischer Scientific) with 5% CO_2.
After incubation, the tubes were then centrifuged at 2000 rpm for 10 min. The supernatant was carefully discarded, and the pellet was resuspended in complete DMEM medium. The cell suspension was cultured in sterile T25 tissue culture flasks with vented lids and incubated at 37 °C in a humidified incubator (Thermofischer Scientific) with 5% CO_2. Isolated primary vaginal fibroblasts culture was maintained and passaged at 80% confluency and cells from passage 3-4 were used for construction of TE vaginal models.

Preparation of decellularised sheep vaginal tissues (de-SVT):

This involved dissection, sterilisation, de-epithelialisation and dellularisation of sheep vaginal tissue.
Dissection of sheep vaginal tissues was carried out as stated in section 2.3.5. Tissue sections measuring 4 cm^2 were placed separately in two primary decellularisation solutions.

- Solution A (0.25% wt/v sodium deoxycholate, 0.25% v/v Triton X100 in PBS supplemented with 1% CAS)
- Solution B (1M NaCl solution in PBS)

Both solutions A and B containing the tissue sections were placed on a Stuart® Platform Rocker STR6 at 40 REV/min overnight. Two different methods of decellularisation were used: 1) detergent method decellularisation and 2) Hypertonic + detergent method decellularisation. Different steps involved in the decellularisation processes are outlined in Table 2.5.

De-epithelialisation of SVT was performed aseptically inside Class II Biosafety cabinet for animal tissue processing. Vaginal tissue samples were removed from the decellularisation solutions A and B after 24 hrs and placed in sterile petri plates. With the help of a sterile forceps, epithelium was gently removed from the underlying lamina propria and tissue samples were washed with sterile PBS. Tissue sections were then placed in the secondary decellularisation solution (0.25% wt/v sodium deoxycholate, 0.5% v/v Triton X100 in PBS (supplemented with 1% CAS) on a Stuart® Platform Rocker STR6 at 40 REV/min for four days. After incubation, decellularised sheep vaginal tissues were washed twice with sterile PBS (to remove any traces of Triton X100) and stored at 4°C in sterile PBS until use.

Table 2.5: Methods used for the decellularisation of SVT. CAS = Cambridge antibiotic solution, PBS = Phosphate buffered saline, P/S = 100 IU/mL penicillin, 100 µg/mL streptomycin.

Steps	Detergent Method	Hypertonic + Detergent method	Duration of treatment
1)Primary decellularisation solution	0.25% wt/v sodium deoxycholate + 0.25% v/v Triton X100 in PBS supplemented with 1% v/v CAS	1M NaCl in PBS supplemented with 1% v/v CAS	Incubated for overnight on a Platform Rocker STR6 at 40 REV/min
2) Epithelium removal	Gentle scraping with sterile forceps	Gentle scraping with sterile forceps	-
3) Washing (twice)	Sterile PBS	Sterile PBS	30 mins each
4)Secondary decellularisation solution	0.25% wt/v sodium deoxycholate + 0.5 % v/v Triton X100 in 100 mL PBS supplemented with 1% v/v CAS	0.25% wt/v sodium deoxycholate + 0.5 % v/v Triton X100 in 100 mL PBS supplemented with 1% v/v CAS	Incubated for 4 days on a Platform Rocker STR6 at 40 REV/min
5) Washing (twice)	Sterile PBS	Sterile PBS	30 mins each
6)Storage of decellularised matrices	At 4°C in sterile PBS supplemented with 1% v/v P/S	At 4°C in sterile PBS supplemented with 1% v/v P/S	Up to 1 month

Preparation of De-epidermised dermis (DED):

DED was obtained from Dr. Vanessa Hearnden Research Group (collected under NHS research ethics approval YH/15/0177) and was stored at 4 °C. The tissue was then treated in 1M sodium chloride solution for 24 hours at 37 °C The tissue was then taken out in a sterile petri dish and

the epithelium was gently removed by peeling off with the help of sterilised pair of surgical forceps. Washing was done 3 times with PBS. The processed DED was then stored at 4°C in Green's media until use.

2.3.6 Developing and culturing tissue engineered (TE) vaginal models:

A schematic of key stages involved in the development of TE vaginal models is shown in Figure 2.4.

De-epithelialised, decellularised sheep vaginal tissues (de-SVT) were sterilised as stated in section 2.3.5. Tissue sections were cut (1.5x 1.5 cm^2) aseptically with the help of sterilised surgical scalpel blades and placed in a 6-well culture plate with the basement membrane side facing upwards.

For each experiment performed, the decellularised sheep vaginal tissues were cultured with allogeneic primary vaginal epithelial cells and fibroblasts. This is due to the fact that in the beginning of this PhD project, primary sheep vaginal epithelial cells and fibroblasts were isolated from each sample collected from the abattoir according to the protocols described in the above section. But, as soon as the cultures were established for both primary cell types, cell banks were established, and cells were stored in liquid nitrogen. For the purpose of developing tissue engineered vaginal models, the decellularised vaginal tissues were collected from different sheep and used in a single experiment in order to meet the requirements of sample repeats (*n*), as from a single sheep urogenital tract only 6-7 tissue engineered models could be developed. The vaginal models were cultured with allogeneic vaginal epithelial cells and fibroblasts expanded in culture and used between passage 2-3.

Sterilised chamfered surgical stainless-steel rings containing an internal diameter of 8mm were placed on top of each de-SVT in such a way such to ensure a tight seal around the edges of the rings. Each ring was seeded with a 500 µL co-culture cell suspension of primary vaginal fibroblasts and epithelial cells (between passage 2-3) in Green's media at a seeding density of 3 x 10^5/model and 6 x 10^5/model respectively. While 4 mL Green's media was added to the outside of rings to stop leakage of the cell solution from within the rings. The cultures were incubated at 37 °C with 5% CO_2 overnight.

After 24 hrs, the rings were removed with the help of sterile forceps and culture plates re-incubated in same conditions overnight. After 3 days, sterile stainless-steel grids were placed in new 6-well culture plates and TE vaginal models were carefully transferred to the grids using a set of sterile forceps with the cell seeded side facing upwards. The wells were then topped up

with Green's media to overflow the grids but not the model in order to maintain an air-liquid interface (ALI). The models were cultured in Green's media for 3 days under submerged conditions and then for an additional three weeks at an air-liquid interface (ALI) at 37 °C with 5% CO_2 and media changed twice every week. Blanks and controls were run alongside using cell free de-SVT and native SVT. Models were fixed at different time points (days 5, 9 and 15) in 3.7% v/v formaldehyde to trace the progress of reepithelialisation. An illustration of the two key stages of submerged culture and air-liquid interface (ALI) is given in Figure 2.3.

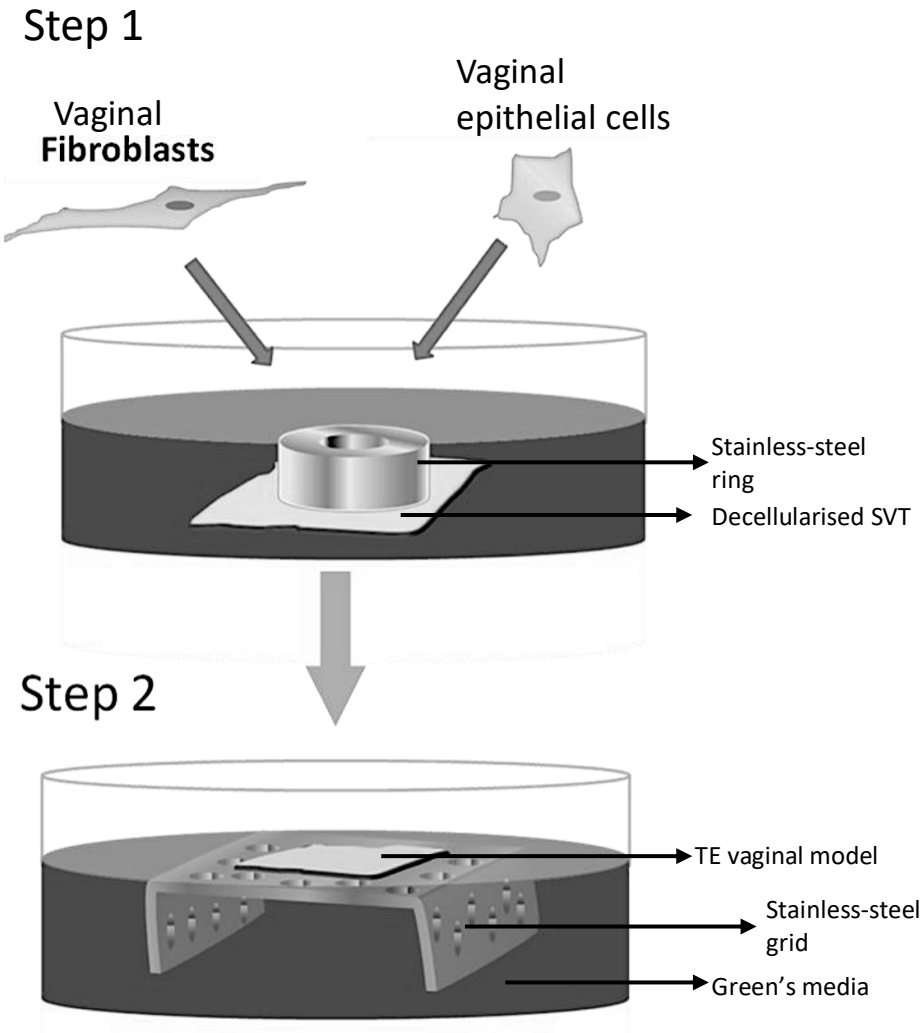

Figure 2.3: Illustration of transferring TE vaginal models to air-liquid interface (ALI).

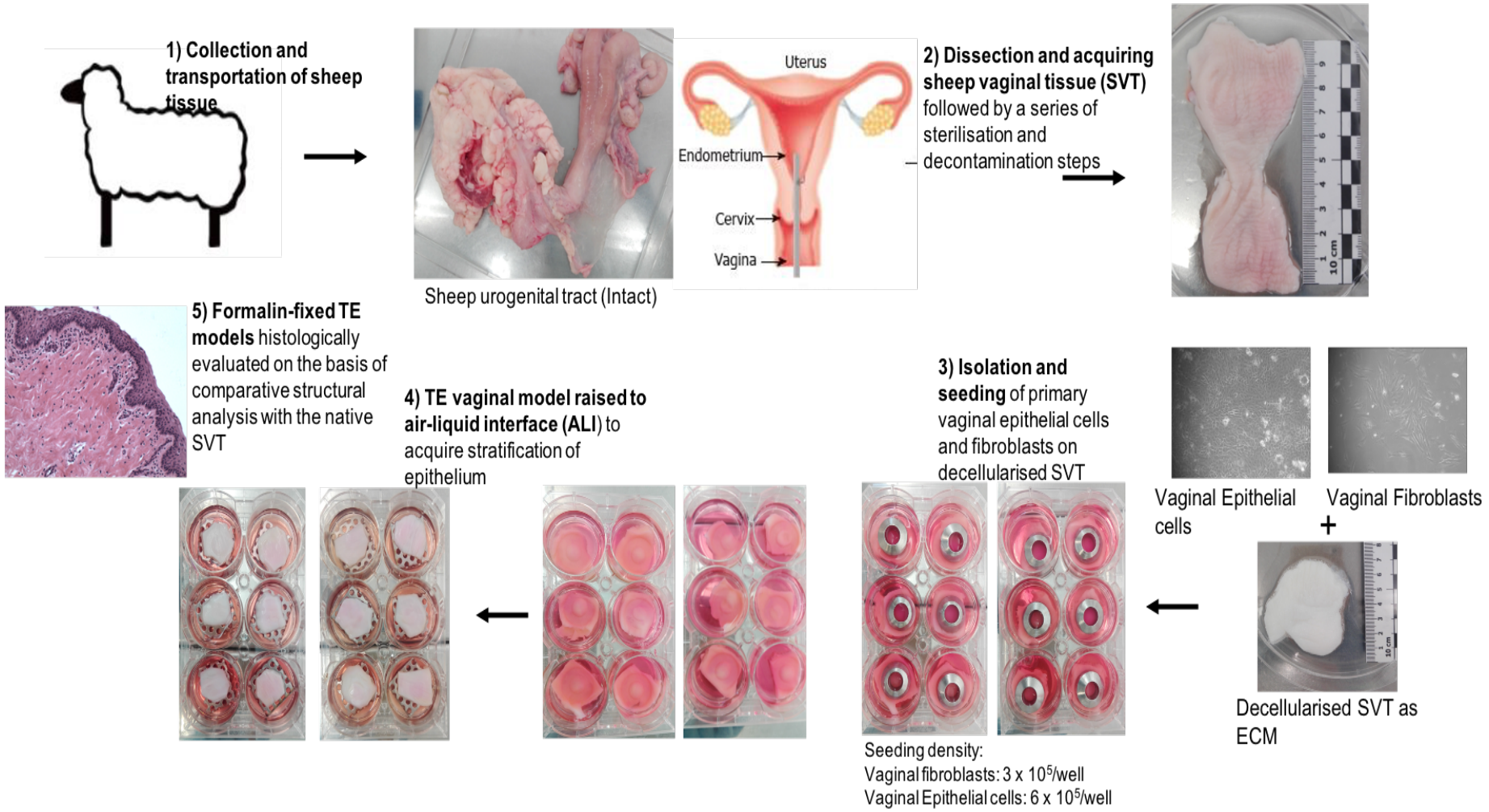

Figure 2.4: A schematic showing key stages involved in the in vitro construction of Tissue engineered (TE) sheep vaginal models.

2.3.7 Culturing TE vaginal models under static and dynamic culture conditions:

TE vaginal models developed as discussed in section 2.3.6 were cultured under both dynamic and static conditions. Under static conditions, the models were raised to ALI by transferring the tissue sections to stainless-steel grids in a 6-well tissue culture plate and incubated in 37 °C with 5% CO_2 in humidified incubators in an upright position and remained undisturbed through three weeks incubation time period.

Under dynamic conditions, the vaginal models were seeded and transferred to stainless steel grids as described in section 2.3.6. The 6-well culture plates were then transferred to a Stuart® Platform Rocker STR6 at 40 REV/min for three weeks to provide a fluid flow-induced shear stress to the cultured TE models. The models were incubated in 37 °C with 5% CO_2 in humidified incubators and media changed twice a week.

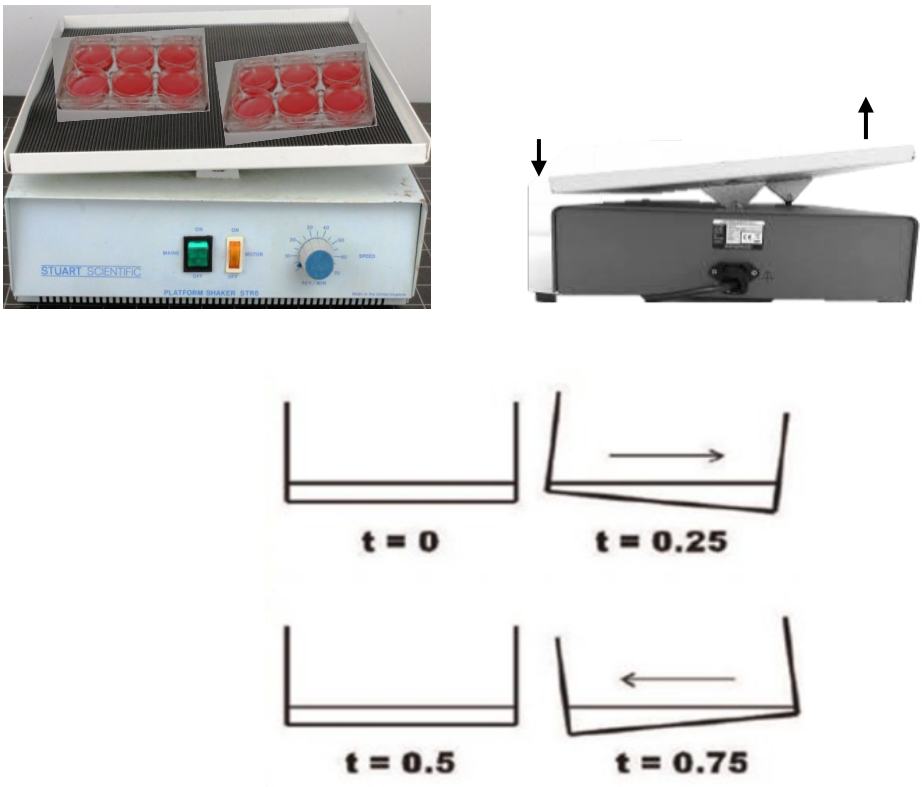

Figure 2.5: Experimental setup for dynamic culture conditions and illustration of the direction of movement of Platform rocker. Schematic of fluid movement in a well plate during different time points (t) in one cycle.

2.3.8 Fixation of TE vaginal models:

Materials

3.7% formaldehyde:

Paraformaldehyde (8.18715) was purchased from Sigma-Aldrich, UK. A 3.7% v/v solution was prepared by dissolving 37 mL of the product in 100 mL PBS to make the solution.

TE vaginal models were washed at different experimental end points with PBS and placed into 3.7% v/v formaldehyde overnight or for at least 24 hours at room temperature prior to tissue processing for histological analysis.

2.3.9 Viability testing of cultured cells on de-SVT and DED:

Materials:

Resazurin sodium salt solution (R7017) was purchased from Sigma-Aldrich, UK. The product was stored in a cool dry place and protected from light.

Resazurin® assay was performed to determine the metabolic activity of cultured cells on de-SVT and DED. A stock solution of resazurin sodium salt was prepared by dissolving 0.124 g of product in 100 mL PBS in an aluminum foil covered container that could be stored at 4 °C for a month. A working solution of 1:20 dilution (1mL stock solution of resazurin in 20mL PBS) was prepared freshly to use for the assay. At different experimental end points, the media present in the TE models culture plates was aspirated and 250 µL of resazurin working solution was added aseptically into each well. The culture plates were wrapped with aluminum foil to protect from light exposure and incubated at 37 °C, 5% CO_2 for an hour and a half. After incubation, 100 µL of the solution was taken out from each well and transferred in triplicates into 96-well plate. The absorbance at λ570 nm was then measured in a colorimetric plate reader (Bio-TEK, NorthStar Scientific Ltd, Leeds, UK). Blanks and controls were run alongside using cell free de-SVT and DED. Metabolic activity of cultured cells was quantified at days 3, 7 and 14 and samples were fixed with 3.7% formaldehyde afterwards.

2.3.10 Histological analysis of decellularised SVT and TE vaginal models:

Tissue processing:

Formaldehyde-fixed tissue samples were placed in individual cassettes (Leica Biosystems IP Biopsy Cassettes III) and loaded into a "dip and dunk" Leica TP1020 benchtop tissue processor (Leica microsystems, Milton Keynes, UK) that involves a series of steps including dehydration, clearing, infiltration and blocking out. The samples were processed through a series of dehydration and wax treatment for about 16-18 hours as described in Table 2.6.

Table 2.6: Series of events for processing of tissue samples.

Solution	Time exposed
10% neutral buffered formalin	1 hour
70% alcohol	1 hour
70% alcohol	1 hour
90% alcohol	1 hour
90% alcohol	1 hour
Absolute alcohol	1 hour
Absolute alcohol	1 hour
Absolute alcohol	1 hour
Xylene	1 hour 30 mins
Xylene	1 hour 30 mins
Paraffin Wax	2 hours
Paraffin Wax	2 hours

Wax embedding:

Tissue samples after processing were embedded in paraffin using HistoCore Arcadia, Leica Biosystems (Leica microsystems, Milton Keynes, UK) Embedder. Each TE vaginal model was embedded separately in a perpendicular orientation in stainless steel moulds in hot wax using HistoCore Arcadia H heated Paraffin Embedding Station and then cooled to -6 °C on HistoCore Arcadia cold plate. Once frozen, the wax blocks were transferred to freezer for 24 hours prior to sectioning.

Tissue sectioning:

Tissue sections were cut using a HistoCore AUTOCUT, Leica Biosystems (Leica microsystems, Milton Keynes, UK) microtome. Wax blocks were first trimmed until the region of interest and then 5µm thick tissue sections were cut and transferred to a water bath set at 41 °C. The tissue sections were then carefully transferred and mounted on Polysine™ adhesion microscopic slides (Epredia™, Germany). The slides were air dried for 24 hours before commencing any staining procedures.

2.3.11 Haematoxylin and Eosin (H&E) staining:

Haematoxylin and Eosin (H&E) staining on the slides was performed according to the protocol described by Feldman *et al.,* [287]. The slides were treated with different solutions for different time periods and the details are given in Table 2.7. After staining, the slides were mounted with DPX (Dibutyl phthalate, Polystyrene, Xylene) and coverslips were placed carefully on the top of the stained samples in such a way so as to avoid entrapment of air bubbles.

Table 2.7: Series of events during H&E staining.

Solution	Time exposed	Purpose
Xylene	3 mins	To remove the wax from the slides
Xylene	3 mins	
Absolute alcohol	1 min	To gradually rehydrate tissue sections
70% v/v alcohol	30 seconds	
Distilled water	1 min	To remove any debris from the slides
Weigert's hematoxylin	1min 30 seconds	To stain the cell nuclei purple or blue
Running tap water	4 mins	To remove excess stain
Eosin Y	5 mins	To stain the extracellular matrix (ECM) pink
Tap water	dunk	To remove excess stain
Tap water	dunk	
70% v/v alcohol	dunk	To gradually dehydrate tissue sections

Absolute alcohol	30 seconds	
Xylene	10 seconds	To dehydrate tissue samples and remove any residual stains or impurities
Xylene	dunk	

H&E staining protocol described here worked well on slides containing tissue sections of TE vaginal models and partial-thickness wound vaginal models. However, when slides containing tissue sections of partial-thickness wound models with biomaterials implantation were treated with xylene in the initial step, it was observed that the biomaterials (both PU and PPL) got detached from the surface of glass slide when in contact with xylene. However, the H&E images taken afterwards showed region of implantation on the TE wound models. To further aid in the understanding of H&E images of TE wound models with biomaterials implanted, light microscopy images of tissue sections before and after staining is included in "chapter 4 results" section of this thesis.

2.3.12 Picrosirius red staining:

Materials

Weigert's iron hematoxylin solution:
Weigert's iron hematoxylin solution (HT1079) was purchased from Sigma-Aldrich, UK. The solution was filter using a 11μm pore size to remove any undissolved particles prior to use.

Picrosirius red stain:
Direct Red 80 (365548) was purchased from Sigma-Aldrich, UK. Picrosirius red stain was prepared by dissolving 0.1g of the product in 100 mL saturated aqueous solution of Picric acid (1.3% v/v in H_2O) available from Sigma-Aldrich (P6744-1GA) .

Acidified water:
Acidified water was prepared by adding 5 mL acetic acid (glacial) to 1 litre of deionised water.

Picrosirius red staining was performed on 5µm thick tissue sections mounted on glass slides by following the method of Puchtler *et al.,* [288] and Junqueira *et al.,* [289]. The slides were treated with different solutions for different time periods and the details are given in Table 2.8. After staining, the slides were mounted with DPX (Dibutyl phthalate, Polystyrene, Xylene) and coverslips were placed carefully on the top of the stained samples in such a way so as to avoid entrapment of air bubbles.

Table 2.8: Series of events during picrosirius red staining.

Solution	Time exposed	Purpose
Xylene	3 mins	To remove the wax from the slides
Xylene	3 mins	
Absolute alcohol	1 min	To gradually rehydrate tissue sections
70% v/v alcohol	30 seconds	
Distilled water	1 min	To remove any debris from the slides
Weigert's hematoxylin	8 mins	To stain the cell nuclei purple or blue
Running tap water	10 mins	To remove excess stain
Picrosirius red stain	1 hour	To stain the collagen fibres red
Acidified water	3 mins	To remove excess stain
Acidified water	3mins	
70% v/v alcohol	dunk	To gradually dehydrate tissue sections
Absolute alcohol	30 seconds	
Xylene	10 seconds	To dehydrate tissue samples and remove any residual stains or impurities
Xylene	dunk	

Slides analysed and Image acquisition:

The DPX mounted slides were left air dried for 24 hours before imaging with a light microscope Motic BA210 series (Motic, Xiamen, China) with integrated ColorVu camera. Images were taken at different objective magnifications and analysed using ImageJ software (National Institute of Health).

2.3.13 Histochemical staining of decellularised SVT:

Materials

PicoGreen™ ds-DNA fluorescent stain:

Quant-iT™ PicoGreen™ ds DNA assay kit (P11496) was purchased from Invitrogen (ThermoFisher Scientific) and stored at -20 °C until use.

4′,6-diamidino-2-phenylindole (DAPI):

DAPI staining solution (ab228549) 10mM solution in water was purchased from abcam, UK and stored at -20 °C until use.

Tris-EDTA (TE) buffer, pH 7.5

The buffer contained 10 mM Tris-Cl, pH 7.5 and 1mM EDTA

TE buffer was prepared by adding 10 mL of 1M stock solution of Tris-Cl (pH 7.5) and 2 mL of 500 mM stock solution of EDTA in 1 L distilled water. The pH of the solution was adjusted to 7.5 with the help of HCl and stored at 4 °C for upto 3 months.

The effectiveness of the decellularisation methods to decellularise sheep vaginal tissues (SVT) was determined by detecting the presence of cellular remnants in the treated tissue samples. The presence of cells was quantified by measuring double-stranded DNA (ds-DNA) in the decellularised tissue samples using PicoGreen™ ds-DNA fluorescent stain following the technique of Gagna *et al.,* [290]. The staining procedure was performed on 5 μm thick tissue sections mounted on glass slides as described in Table 2.9.

Table 2.9: Series of events during PicoGreen™ ds-DNA fluorescent staining.

Solution	Time exposed	Purpose
Xylene	3 mins	To remove the wax from the slides
Xylene	3 mins	
Absolute alcohol	1 min	To gradually rehydrate tissue sections
70% v/v alcohol	30 seconds	
Distilled water	1 min	To remove any debris from the slides
PicoGreen ds-DNA fluorescent stain (1:200 dilution in TE buffer) (λ_{ex} 480nm, λ_{em} 520nm)	30 mins (incubation in a moisture chamber in total darkness at room temperature)	To stain the ds DNA green
TE buffer	5 mins	To wash off excess dye
TE buffer	5 mins	
DAPI (1:800 dilution in PBS) (λ_{ex} 359 nm, λ_{em} 457 nm)	15 mins (incubation in a moisture chamber in total darkness at room temperature)	To counterstain cell nuclei blue
TE buffer	3 mins	To remove excess stain
TE buffer	3 mins	
70% v/v alcohol	dunk	To gradually dehydrate tissue sections
Absolute alcohol	30 seconds	
Xylene	10 seconds	To dehydrate tissue samples and remove any residual stains or impurities

The samples were mounted in DPX and coverslips were placed carefully on the top of the stained samples in such a way so as to avoid entrapment of air bubbles.

Imaging:

Histofluorescence images of the samples were captured using an Olympus IX73 inverted microscope (Life Science Solutions, GB) and a RETIGA 6000 (Imaging®) interfaced to a Dell computer using Micro-Manager V 1.4.23 20210215 software. The images were captured at different objective magnifications and analysed using ImageJ software (National Institute of Health).

2.3.14 Immunohistofluorescence (IHF) staining of TE vaginal models:

Materials

Primary antibodies:
The details of the primary antibodies used is given in Table 2.10.

Table 2.10: List of primary antibodies used.

Antibody	Details	Isotype	Supplier	Dilution
Anti-Ki67 antibody (ab15580)	Rabbit polyclonal to Ki67	IgG	Abcam, UK	1:100 in PBS
Recombinant Anti-Cytokeratin 10 antibody (ab76318)	Produced recombinantly Rabbit monoclonal [EP1607IHCY] to Cytokeratin 10-Cytoskeleton marker	IgG	Abcam, UK	1:100 in PBS
Cytokeratin 19 antibody [NBP1-78278SS]	Rabbit polyclonal to cytokeratin 19	IgG Unconjugated BSA free	Novus Biologicals, UK	1:100 in PBS

Secondary antibody:

The secondary antibody used for all three primary antibodies was donkey anti-rabbit IgG H&L Polyclonal (λ_{ex} 652 nm, λ_{em} 668 nm) (Alexa Fluor® 647) preadsorbed (ab150063) purchased from Abcam, UK and used at a dilution of 1:200.

Trypsin/ calcium chloride ($CaCl_2$) solution:

The solution was prepared by first making two separate stock solutions of trypsin and $CaCl_2$. 50 mg of bovine trypsin (T1426, Sigma Aldrich, UK) was added to 10mL distilled water and mixed. The solution was then kept at -20 °C to completely dissolve the trypsin. $CaCl_2$ stock solution was prepared by dissolving 0.1g $CaCl_2$ in 10 mL distilled water and dissolved. Then the working solution was prepared by adding 1 mL from each stock solution to 8mL distilled water. The solution was stored at -20 °C until use.

Methodology:

The immunohistofluorescence (IHF) staining of decellularised SVT and TE vaginal models was performed on 5µm thick tissue sections mounted on glass slides. Similar protocol was used for deparaffinisation of glass slides for all three antibodies mentioned in Table 3.9. Slides were first deparaffinised in xylene and then rehydrated using a graded series of ethanol (100% to 95% to 70%). The slides were the washed with distilled water to remove any ethanol or debris. The tissue sections on the slides were outlined by marking with the Dako hydrophobic marking pen (NGAIO Diagnostics) to prevent wastage of any reagents and antibodies by forming a water-repellent barrier around the tissue sections. A trypsin-mediated antigen retrieval was performed by adding 100 µL of trypsin/$CaCl_2$ solution onto each tissue section in a humidified chamber and incubated for 20 mins at 37°C. Slides were then washed thrice with PBS for 5 mins each.

The tissue sections were then permeabilised by treating with 0.5% v/v Tween 20 for 20 mins at room temperature. Slides were again washed with PBS containing 0.025% v/v Triton X100 thrice for 5 mins each. Sections were then blocked for non-specific background staining by adding 100 µL serum-free protein blocking buffer (ab64226, Abcam UK) to each sample for

30 mins at room temperature. Washing was done three times with PBS containing 0.025% v/v Triton X100 for 5 mins each.

Then primary antibody (any of those mentioned in Table 3.10) was applied 100 µL to each sample and incubated overnight at 4 °C in a humidified chamber. After incubation, washing was done thrice with PBS containing 0.025% v/v Triton X100 for 5 mins each. Secondary antibody was added 100 µL to each sample and incubated for 1 hour in a humidified chamber at room temperature. Again, washing was done thrice with PBS containing 0.025% v/v Triton X100 for 5 mins each. The slides were then counterstained with DAPI for 30 mins in a dark humidified chamber, later mounted with DPX and imaged with an epifluorescence microscope (Olympus IX73) as described in section 2.3.13.

While performing IHF staining, troubleshooting was done at different stages of the staining protocol described here. A trypsin-mediated antigen retrieval was performed on the tissue sections instead of a heat-mediated antigen retrieval method as described above. This was used because the tissue sections were fragile especially samples from the wound models and the wound models with biomaterial implantation. At this stage, it was observed that if the heat treatment was used, it caused the tissue sections to detach from the surface of glass slides. Hence, I optimised the antigen retrieval step by using a mild trypsin mediated treatment at 37°C for 20 mins.

Optimisation for blocking the non-specific binding of antibodies in tissue sections was also done by using a pre-made protein blocking buffer as described above. This caused improved staining of the targeted antigen without any non-specific binding or background staining. This step further improved my method for measuring the fluorescence intensity of the specific markers as the background fluorescence value calculated from each image analysed was zero.

2.3.15 Preparation of estradiol-17β concentrations for induction studies:

Estradiol-17β was purchased from Sigma-Aldrich, UK. A stock solution (stock A) was prepared by solubilising 0.002 g estradiol in 1 mL absolute ethanol and then 9 mL distilled water was added to get the concentration of 2 x 10^{-3} g/mL. Then a second stock solution (stock B) was prepared in sterile PBS using serial dilutions to get a concentration of 2 x 10^{3} pg/mL. The working solutions of estradiol-17β were prepared separately in Green's media at five different concentrations (25, 50, 100, 200 and 400 pg/mL) and were added to TE vaginal models culture media after raising the models to ALI models for estradiol-17β induction studies. Models were cultured in different oestradiol concentrations for three weeks in ALI

culture conditions. Estradiol-17β concentrations were based on clinical definitions of borderline (11-44 pg/mL), normal menstruating female follicular phase (21-251 pg/mL) and "supraphysiological" (258- 498 pg/mL) estradiol-17β serum levels, as recommended by the Endocrine Society guidelines [291].

2.3.16 Statistics

Statistical analysis was performed using GraphPad Prism V9.1.0 (216). A one-way analysis of variance (ANOVA) was performed using Welch test to analyze the difference between the means (represented as mean ± SD) of groups. Three or more groups were compared using Dunnett's post hoc test and a $p < 0.05$ was considered statistically significant for differences between means of each group. All experiments were run in triplicate ($N = 3$) with three samples for each parameter ($n = 9$).

2.4 Results:

2.4.1 Decellularisation of sheep vaginal tissues (SVT):

The tissue engineered vaginal models in this PhD project were developed by using decellularised sheep vaginal tissues and primary sheep vaginal epithelial cells and vaginal fibroblasts isolated from the native sheep vaginal tissue. Whole sheep urogenital tracts were obtained from the local abattoir as a waste and cleaned to dissect out the vaginal tissue and tissues were obtained in large amounts. Sheep vaginal tissues (SVT) treated with two different decellularisation solutions are shown in Figure 2.6. Visible differences in the appearance of decellularised SVT were seen as compared to the native SVT as the decellularised tissues were whiter in appearance after decellularisation treatment for 5 days. In addition, the decellularised SVT were fragile and softer as could be readily seen handling them with a pair of forceps.

Figure 2.7 demonstrates the light microscopy images of primary sheep vaginal epithelial cells and vaginal fibroblasts. The isolated primary vaginal epithelial cells cultured in Green's media formed colonies of cells surrounded by the feeder layer of i3T3s after a week in culture. Vaginal epithelial cells showed typical cobblestone-like morphology exclusive to these cells. The isolated vaginal fibroblasts showed flat, elongated cell morphology.

2.4.2 Biocompatibility of decellularised SVT:

The biocompatibility of decellularised sheep vaginal tissues produced by both the detergent method and the hypertonic+ detergent method was estimated by the resazurin® assay as shown in Figure 2.8. The cellular metabolic activity increased significantly on decellularised SVT by the detergent method as compared to the DED over two weeks in ALI culture (Figure 2.8A). Visible reduction of resazurin® dye from purple to deep pink colour could be seen in TE vaginal models constructed using de-SVT by the detergent method (Figure 2.8B).

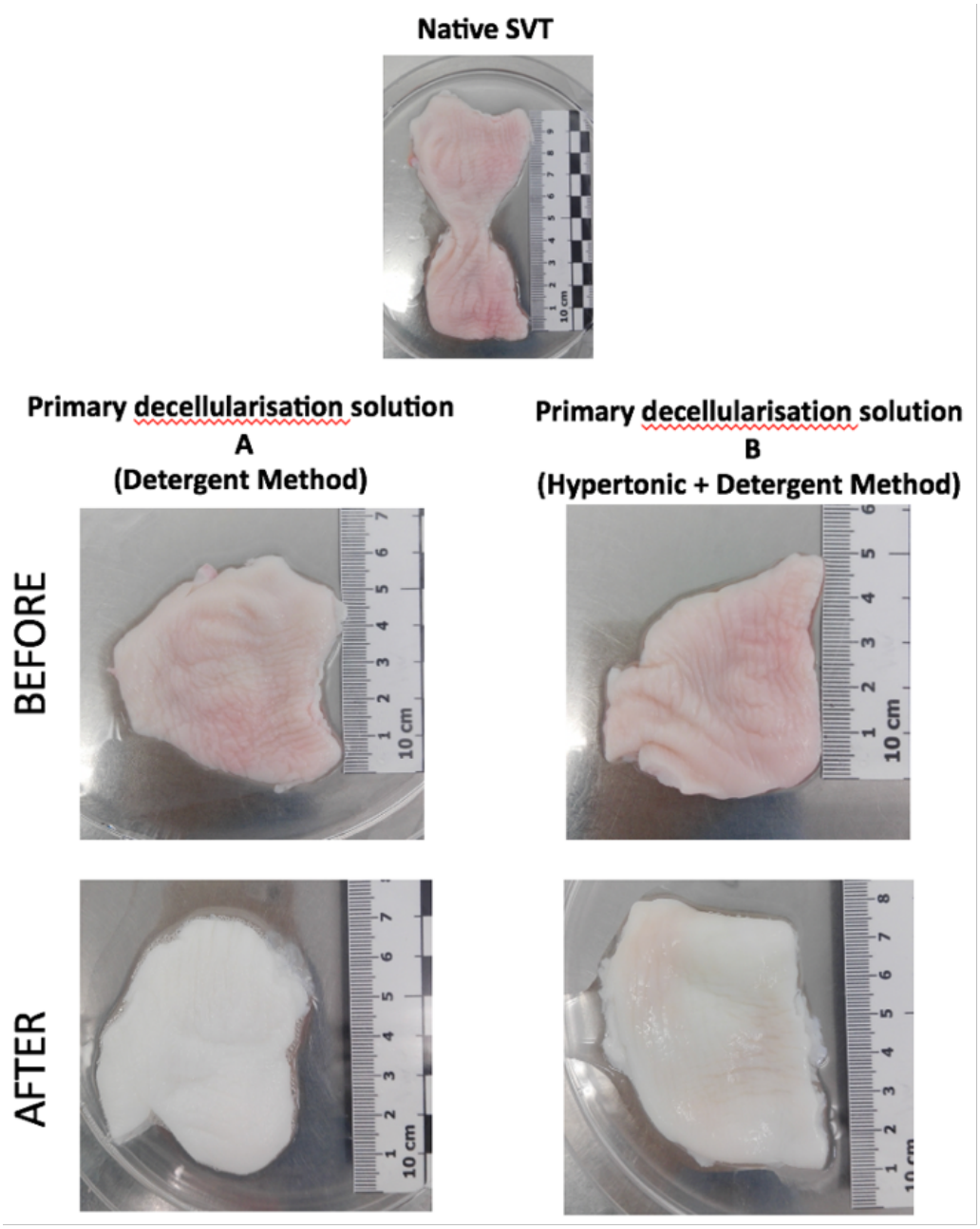

Figure 2.6: Gross appearance of the sheep vaginal tissues (SVT) before and after decellularisation in two different decellularisation solutions by two different methods (A) detergent method and (B) hypertonic+detergent method after 5 days treatment.

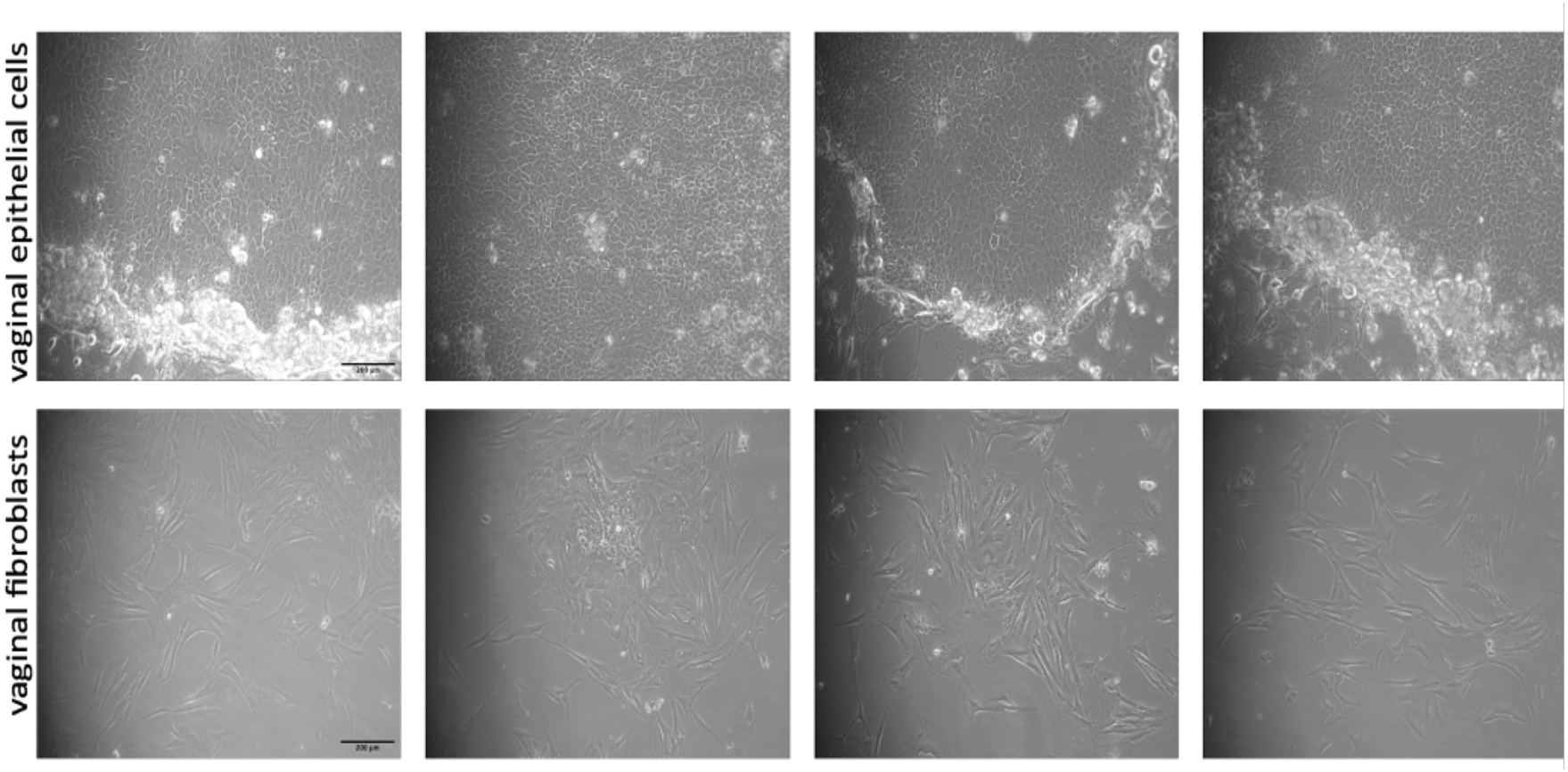

Figure 2.7: Light microscopy images of primary sheep vaginal epithelial cells and vaginal fibroblasts from native sheep vaginal tissue (SVT). Primary vaginal epithelial cells cultured on a feeder layer of i3T3 showed typical cobblestone-like morphology and vaginal fibroblasts showed typical elongated cell morphology. Scale bar=200μm (applies to all).

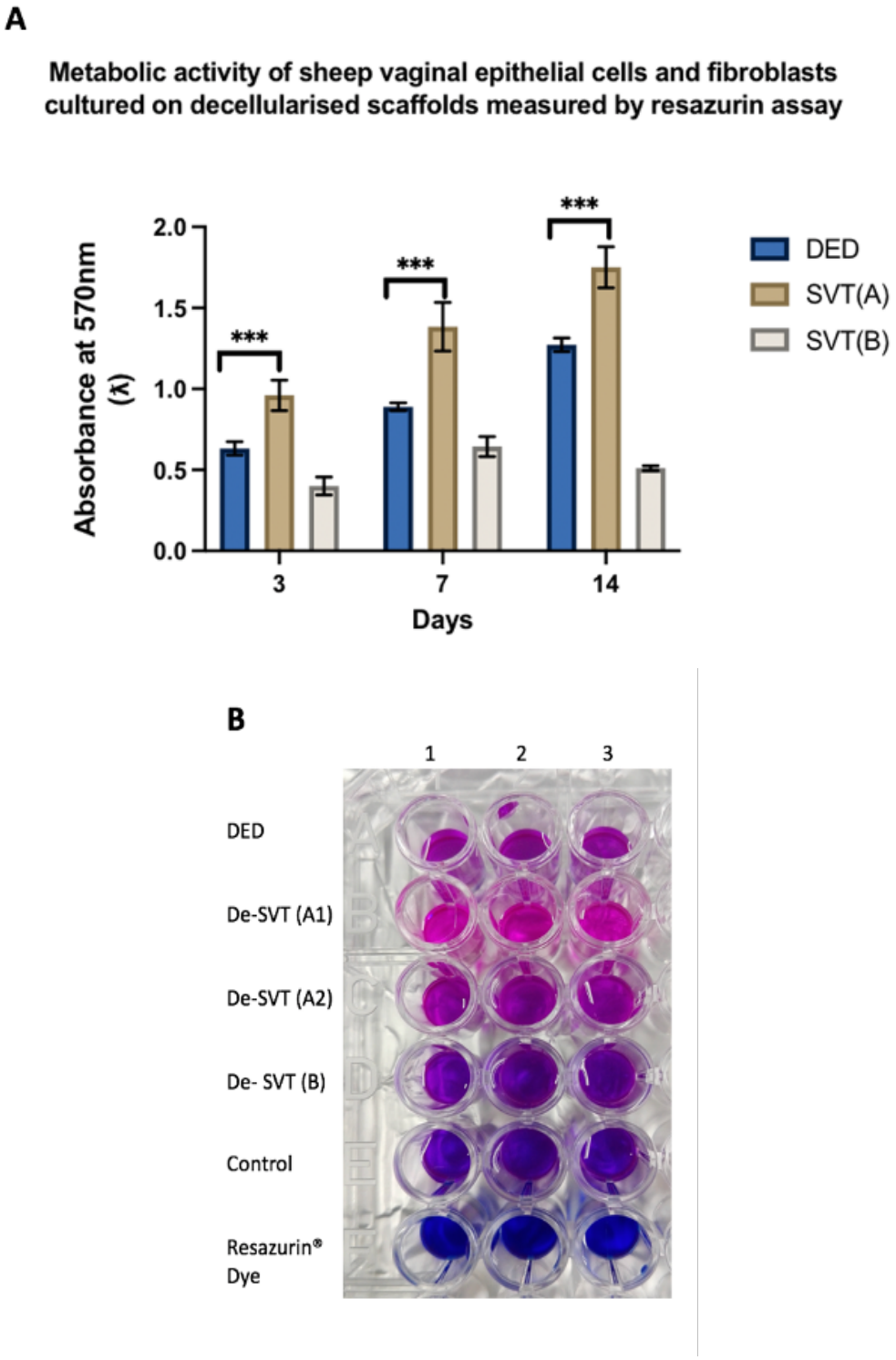

*Figure 2.8: (A) Metabolic activity of primary sheep vaginal fibroblasts and epithelial cells cultured on both de-SVT estimated by resazurin assay over 14 days (n = 9 ± SD for each group at each time point, ***p < 0.05). (B) Picture of the 96-well plate containing 100 µL of media after an hour incubation in dark with resazurin® sodium salt solution.*

**DED, de-epithelialised dermis; SVT(A1/A2), decellularisation by detergent method; SVT(B), decellularisation by hypertonic + detergent method*

2.4.3 Histological analysis of decellularised SVT:

Haematoxylin and eosin (H&E) staining of the native and decellularised SVT are shown in Figure 2.9. The native SVT showed a stratified squamous epithelium containing vaginal epithelial cells (stained purple) and an underlying fibroblast-rich lamina propria. The basal cells of the vaginal epithelium showed a continuous densely packed layer of epithelial cells. In contrast the suprabasal layers of the vaginal epithelium contained loosely packed cells that became flattened out in the superficial layers as the cells became terminally differentiated. The native vaginal epithelium consisted of a stratum of cells (7-11 layers) arranged from less differentiated basal epithelial cells towards terminally differentiated superficial layers to form a typical stratified squamous epithelium. De-SVT from the detergent method (Figure 2.9, middle row) showed an absence of vaginal epithelium as well as the cell nuclei in the lamina propria after 5 days treatment. However, the lamina propria could be seen stained deep pink showing the collagen component remained largely conserved after the decellularisation treatment. On the contrary, the hypertonic +detergent method treatment was ineffective in completely decellularising the vaginal tissues as cellular remnants (purple stained) could be seen in the lamina propria (Figure 2.9, right row).

Picrosirius red staining was performed to analyse the effectiveness of decellularisation treatments and preservance of collagen in the decellularised vaginal tissues (Figure 2.10). All tissue sections were counterstained with Weigert's hematoxylin to visualise the cell nuclei (stained brown). De-SVT by the detergent method (Figure 2.10, middle row) showed good preservance of collagen content in the lamina propria as the collagen fibres could be seen stained deep red and collagen bundles arranged in compactness. In addition, de-SVT by the detergent method resulted in complete removal of cellular components as no visible brown-stained cell nuclei could be seen even at higher objective magnifications (20X and 40X). Whereas, de-SVT by the hypertonic+detergent method resulted in (Figure 2.10, right row) inadequate removal of cellular contents from the lamina propria as brown stained nuclei could be seen remained in the ECM (pointed with arrow heads) at higher objective magnification (40X). Furthermore, the collagen bundles were seen loosely arranged in the deeper layers of the ECM which showed that the hypertonic+detergent method was more harsh as compared to the detergent method and imparted damage to the collagen content in the ECM of vaginal tissues after treatment. The histological comparison between the two decellularisation treatment methods (Figures 2.9 & 2.10) showed that the detergent method was more effective

than the hypertonic +detergent method in terms of cellular removal and preservance of ECM in vaginal tissue samples. Hence, further investigations were carried out using de-SVT by the detergent method only.

2.4.4 Histochemical analysis of decellularised SVT:

Figure 2.11 demonstrates the Picogreen™ ds-DNA fluorescent staining of decellularised SVT by the detergent method to further confirm the effectiveness of the decellularisation treatment on the molecular level. The decellularised SVT showed absence of vaginal epithelium as well as cellular contents and ds-DNA in the ECM.

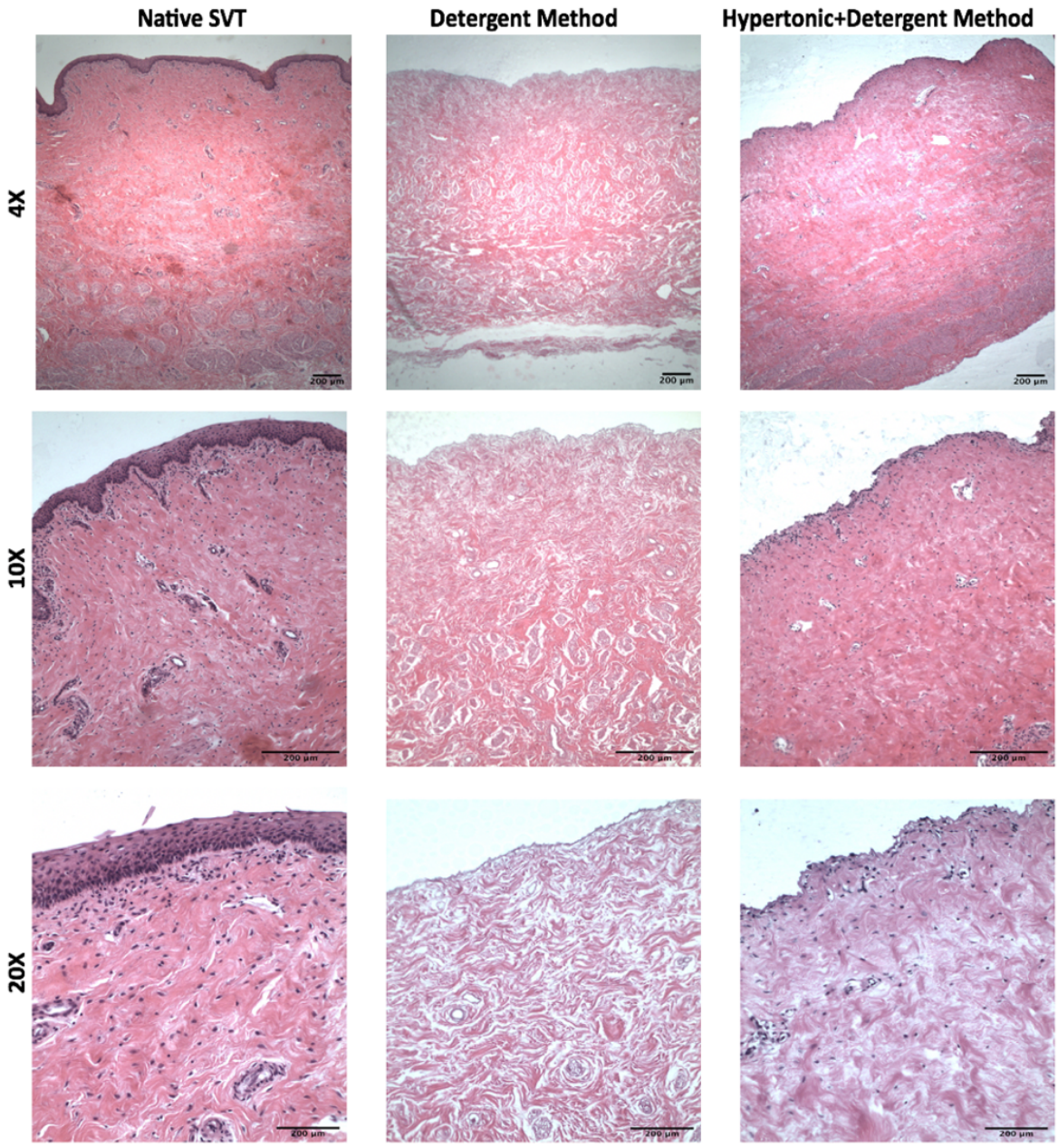

Figure 2.9: Hematoxylin and eosin (H&E) stained sections of sheep vaginal tissue (SVT) samples after 5 days treatment in two different decellularisation solutions. Native SVT showed intact vaginal stratified squamous epithelial lining, invaginations, and underlying lamina propria. Purple stained nuclei of the basal cells formed the demarcation between the epithelial tissue above and the connective tissue below. Decellularised-SVT (de-SVT) by the detergent method showed removal of epithelial lining and absence of cellular components (no noticeable purple-stained nuclei) compared to the other decellularisation technique where the cellular components were not completely removed from the connective tissue layer as purple-stained nuclei were still visible. Scale bar=200μm (applies to all).

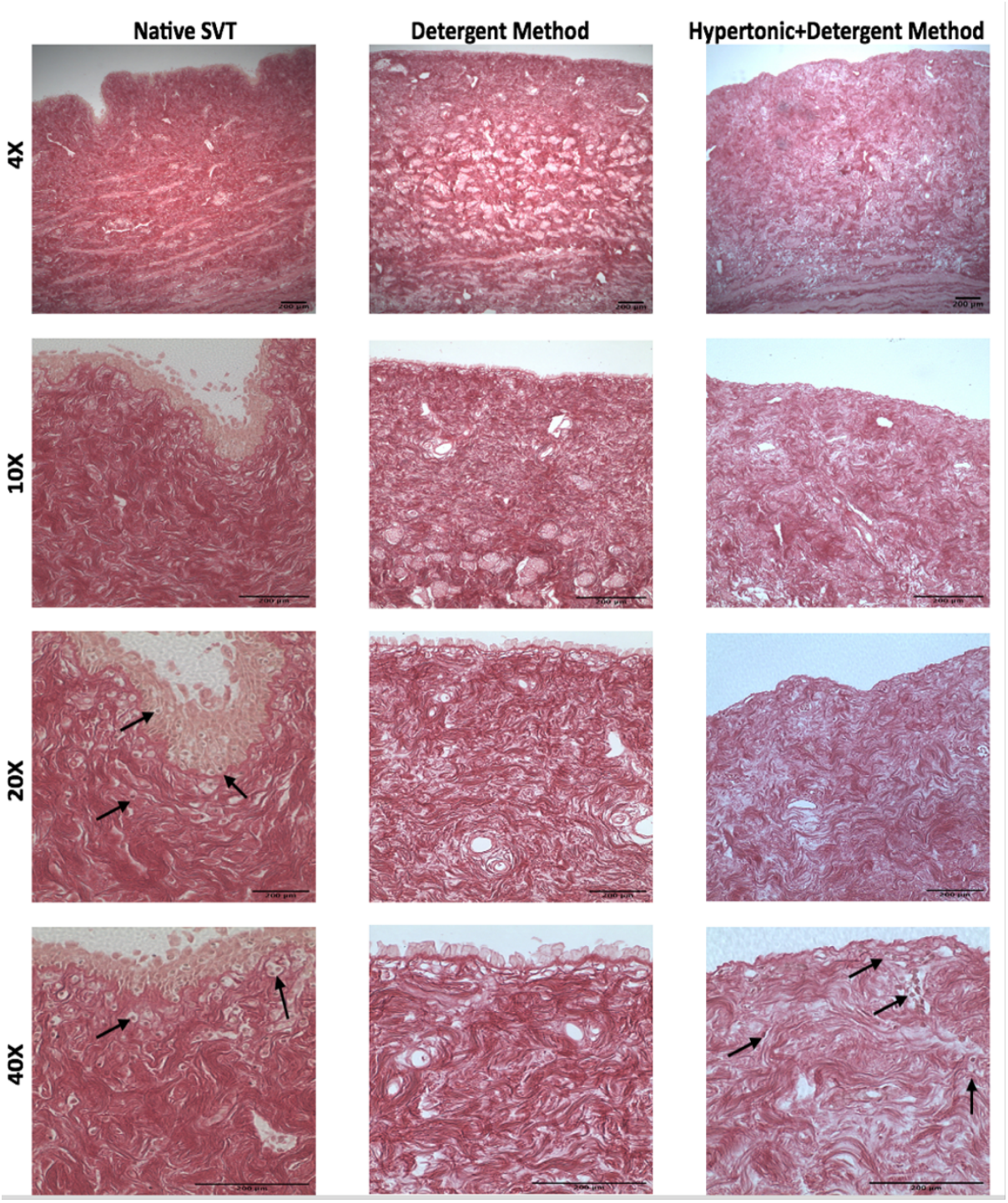

Figure 2.10: Picrosirius red staining of the native sheep vaginal tissue (SVT) and decellularised SVT after 5 days treatment in two different decellularisation solutions. The native SVT showed deep red stained collagen fibers in the extracellular matrix and cellular components could be seen stained light brown-colored nuclei (pointed with black arrow heads) in both epithelial layer and lamina propria. De-SVT by detergent method showed absence of cellular components while collagen in the matrix remained largely conserved. De-SVT by

hypertonic+detergent method showed cellular remnants (pointed with black arrow heads) in the decellularised matrix after treatment. Scale bar= 200 μm (applies to all).

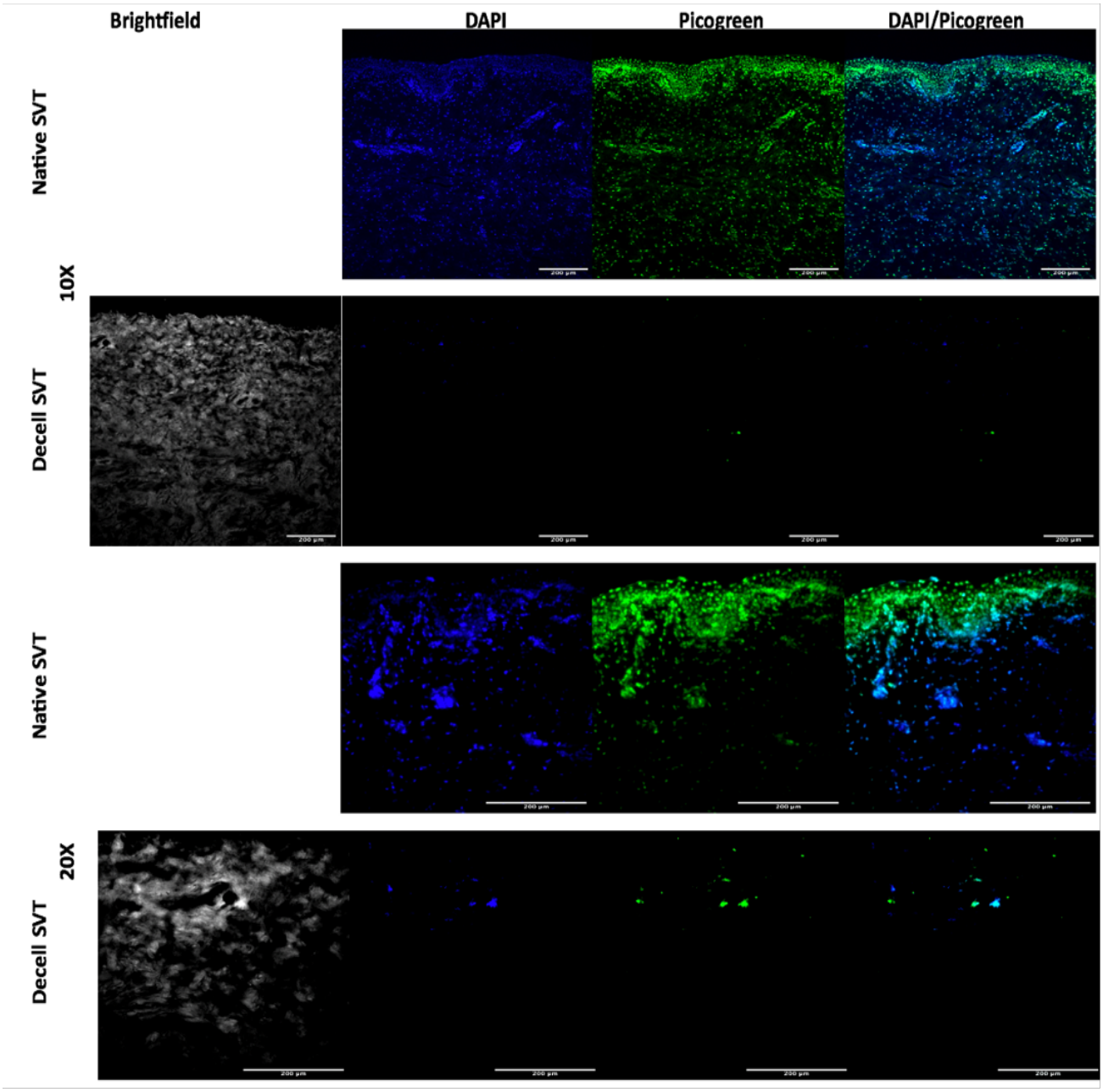

Figure 2.11: Histochemical staining of native and decellularised SVT by the detergent method. Tissue sections treated with Picogreen™ ds-DNA fluorescent stain (green channel) showed presence of cell nuclei in the native tissue and counterstained DAPI (blue channel) showed individual cells. Decellularised SVT by the detergent method showed absence of cell nuclei as well as individual cells under different objective magnifications (10X & 20X). Scale bar =200 μm (applies to all).

2.4.5 Production and characterisation of the TE vaginal models:

Tissue engineered vaginal models were cultured using primary sheep vaginal fibroblasts and vaginal epithelial cells at seeding densities of 3 x 10^5/model and 6 x 10^5/model respectively on decellularised SVT produced by the detergent method. The models were cultured up to four weeks under static ALI culture conditions and the progress of reepithelialisation of the models was monitored at different experimental time points as shown in Figure 2.12. My recellularised models showed histological similarities with the native SVT and there was a gradual thickening of a stratified epithelium over three weeks at an ALI culture. Between Days 7 and 14, the vaginal epithelium became more stratified (7–9 layers). The basal cells were seen more compactly arranged in the basal region of the vaginal epithelium whereas, the cells became dispersed in the suprabasal region as the epithelial cells started to differentiate. The superficial layer contained flattened-out, terminally differentiated epithelial cells. After 21 days in ALI, the upper layers of the TE models began to keratinise with epithelial cells appearing more flattened. The most superficial 2–3 layers of the epithelium started to flake off from the surface of the models. At Day 27, the TE vaginal models' epithelia detached from the underlying lamina propria as the integrity of the basement membrane was compromised under prolonged ALI culture.

The metabolic activity of the vaginal epithelial cells and fibroblasts cultured on de-SVT showed increasing viability up to three weeks in ALI culture under static conditions but eventually it declined beyond three weeks (Figure 2.13). Hence, the TE models were not cultured beyond three weeks in subsequent experiments.

2.4.6 Comparison of TE vaginal models cultured under static and dynamic ALI conditions:

Figure 2.14 exhibits the culturing of TE vaginal models under dynamic shear-stress ALI culture conditions. The models were cultured for five weeks under dynamic ALI culture conditions to compare the reepithelialisation of models with that of static ALI culture. The pattern of formation of a stratified vaginal epithelium on TE models was similar to that in static ALI cultures upto day 21. However, contrary to the static cultures, the TE vaginal models' epithelia continued to thicken and keratinise until day 27 in dynamic ALI cultures. The prolonged survival of TE models under dynamic conditions was attributed to the continuous fluid-shear forces generated by culturing the models on platform rocker which mimicked the native tissue dynamic microenvironment more closely in comparison with the static culture. At day 35, the

TE vaginal models' epithelia were detached from the underlying lamina propria and models could not survive beyond 4 weeks in culture. After careful considerations on both static and dynamic TE vaginal models, it was concluded to use static ALI culture conditions for our TE vaginal models as 3 weeks' time period of culture was sufficient to produce physiologically relevant TE vaginal models in subsequent experiments.

Figure 2.15 shows the comparative metabolic activity of cultured cells on TE vaginal models under static and dynamic ALI culture conditions. The metabolic activity of cells under rocking ALI culture conditions continued to increase until day 21 in a pattern similar to those under static ALI culture conditions. Beyond day 21, the metabolic activity started to decline but it was still significantly higher than that of static cultures as the models continued to thrive during week 4 in dynamic ALI cultures. At day 35, the metabolic activity was further decreased as the models could not survive beyond this time point.

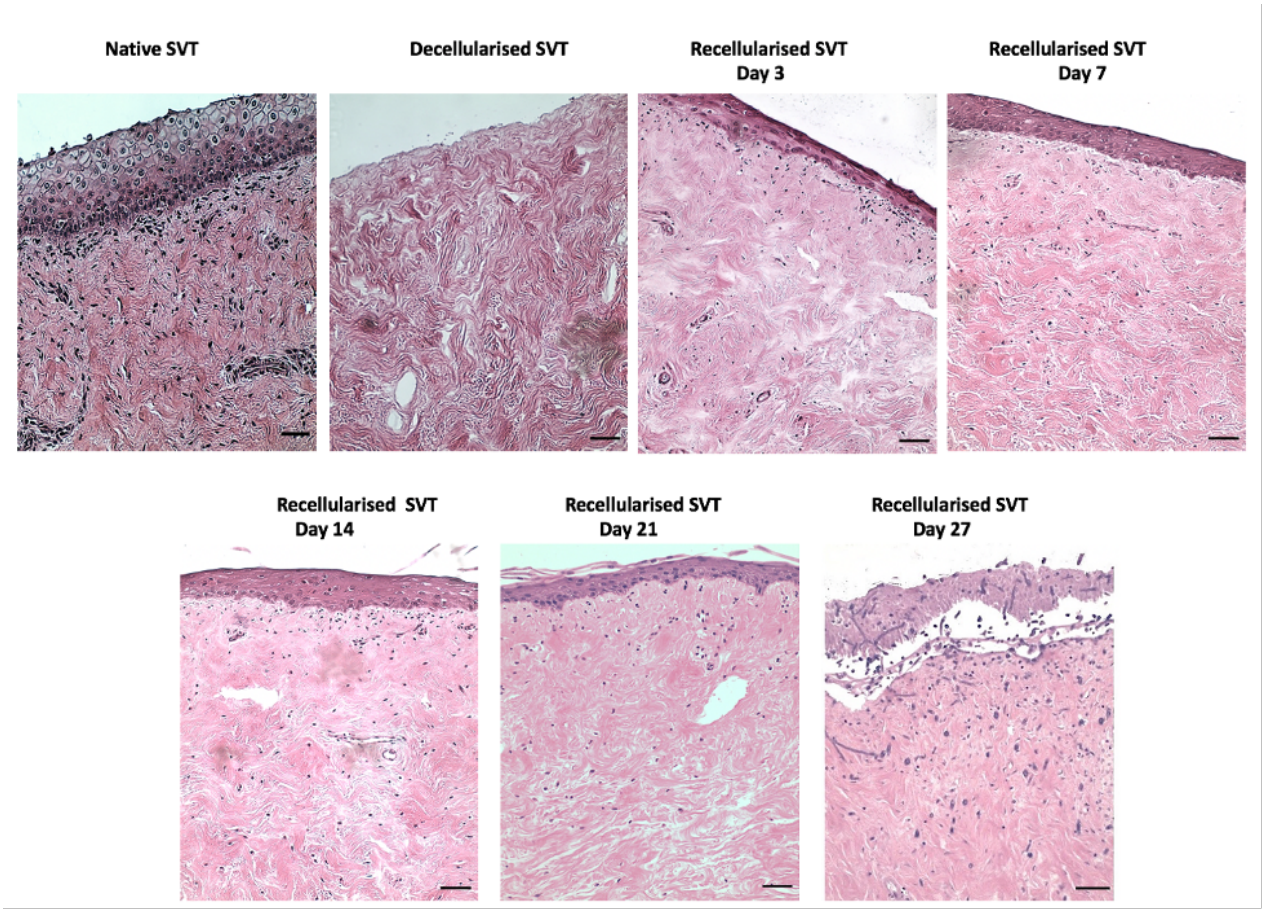

Figure 2.12: Hematoxylin and eosin (H&E) stained sections of the TE sheep vaginal models cultured in static conditions. (From top left to bottom right) De-SVT from detergent method showed absence of epithelial layer and cellular components. Recellularised tissues showed a gradual formation of a stratified epithelial layer from days 3–7 (3–5 layers) that became denser and more stratified between days 7 and 14 (7–9 layers). At day 21 of the ALI culture, superficial layers of the epithelia were seen more keratinised, and at day 27, the epithelia were observed detached from the underlying matrix (scale bar = 100 μm).

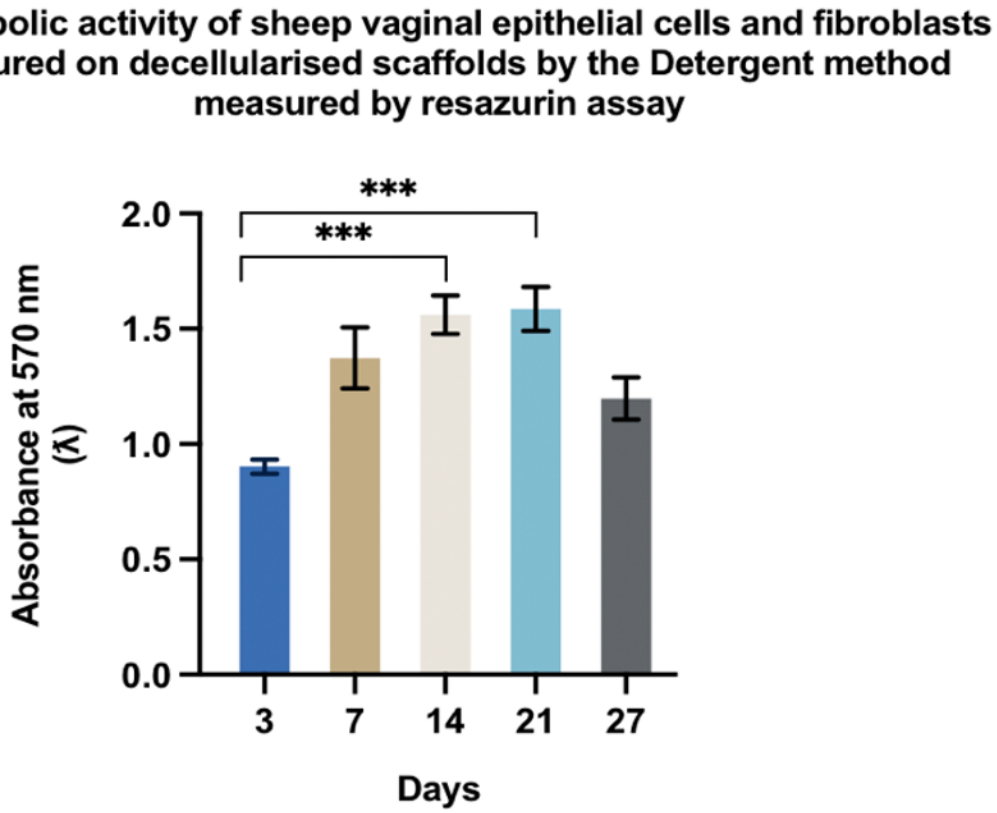

*Figure 2.13: Metabolic activity of primary sheep vaginal fibroblasts and epithelial cells cultured on the de-SVT by the detergent method under static culture conditions. The metabolic activity of cells was estimated by resazurin® assay over 27 days at ALI culture conditions (n = 9 ± SD for each group at each time point, ***p < 0.05).*

**ALI, air–liquid interface; de-SVT, decellularised sheep vaginal tissue by the detergent method*

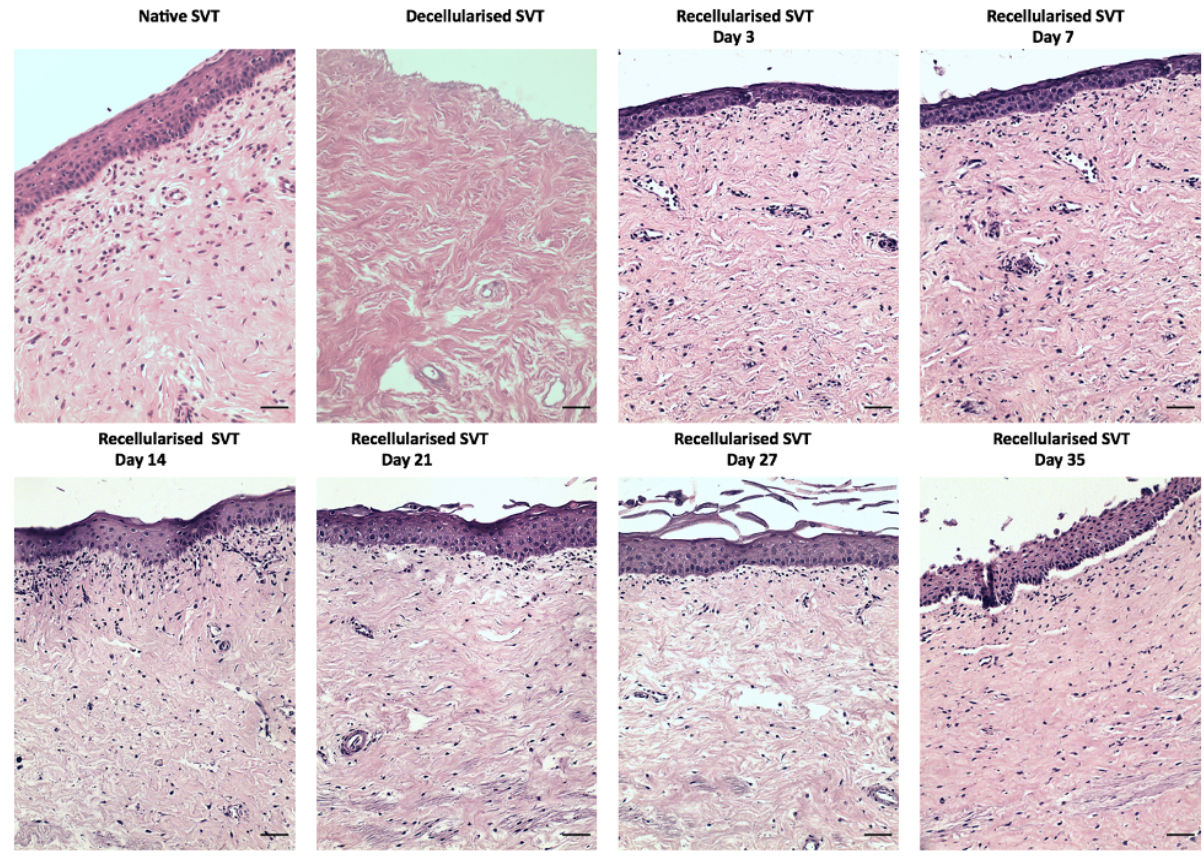

Figure 2.14: Hematoxylin and eosin (H&E) stained sections of the TE sheep vaginal models cultured in dynamic conditions. (From top left to bottom right) De-SVT from detergent method showed absence of epithelial layer and cellular components. Recellularised tissues showed a gradual formation of a stratified epithelial layer from days 3–7 (3–6 layers) that became denser and more stratified between days 7 to 21 (8–10 layers). At day 27 of the dynamic ALI culture, superficial layers of the epithelia were seen more keratinised, denser and the uppermost layers started to flake-off. At day 35 of the culture, the epithelia of the TE models were observed detaching from the underlying matrix (scale bar = 100 μm).

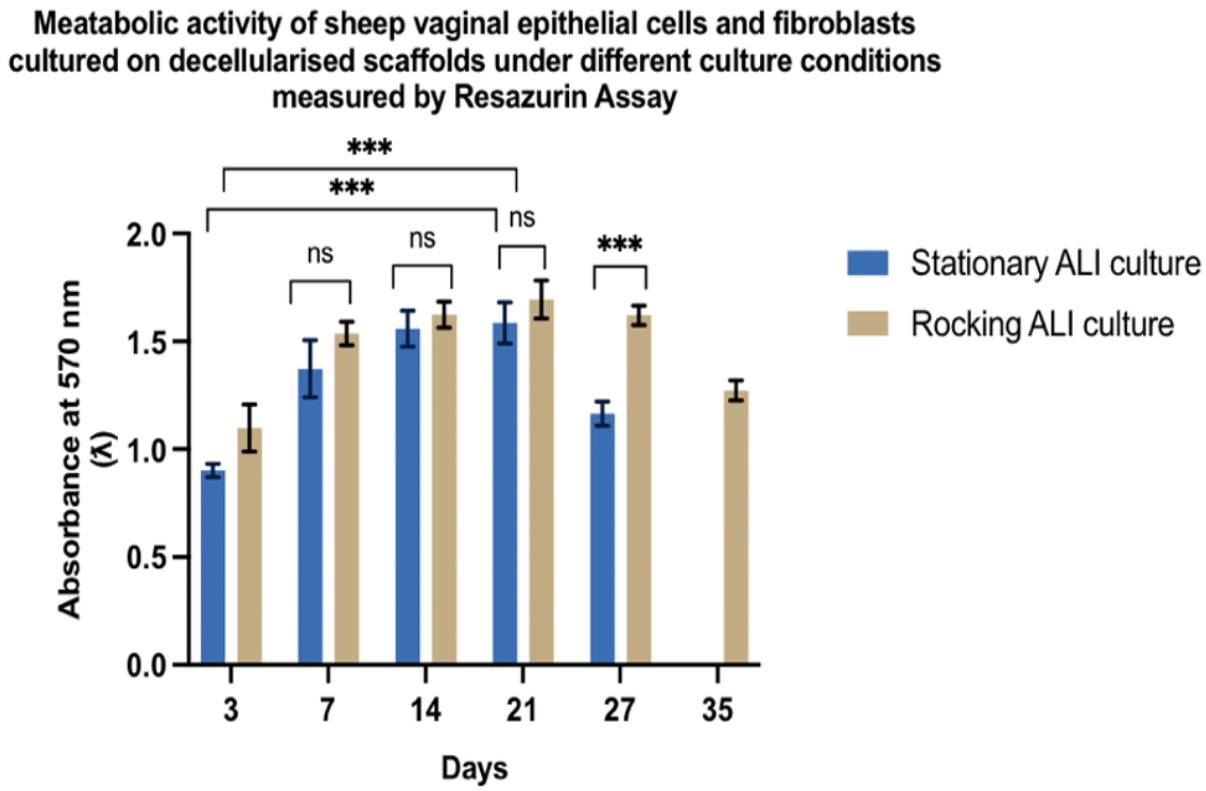

*Figure 2.15: Metabolic activity of primary sheep vaginal fibroblasts and epithelial cells cultured on the de-SVT by the detergent method estimated by resazurin® assay. The metabolic activity of cells was measured at different experimental time points under both static and dynamic ALI culture conditions over a month (n = 9 ± SD for each group at each time point, ***p < 0.05).*

**ALI, air–liquid interface; de-SVT, decellularised sheep vaginal tissue by the detergent method*

2.4.7 Production and characterisation of the TE vaginal models under estradiol-17β induction:

Figure 2.16 demonstrates the effect of different concentrations of estradiol-17β on the TE vaginal models' epithelia thickness. The histological images showed a dose-dependant response of vaginal epithelium towards increasing concentrations of estradiol-17β. There was a gradual increase in the thickness of vaginal epithelium with an increase in concentrations of estradiol-17β (from 50 to 400 pg/mL) and at the "supraphysiological" estradiol-17β concentration (400 pg/mL) there was a two-fold increase in the TE vaginal epithelium thickness compared to the control (without E_2). The average thickness of TE vaginal models' epithelia under different concentrations of estradiol-17β is given in Figure 2.18. A significant increase in the TE vaginal epithelium thickness was observed under an estradiol-17β concentration range from 100-400 pg/mL.

Additionally, the cellular metabolic activity was also influenced by the presence of estradiol-17β in the culture medium. Figure 2.17 shows that a higher concentration of estradiol-17β (from 100-400 pg/mL) increased the cellular proliferation on TE vaginal models compared to the control (without E_2). These results showed the physiological relevance of our TE vaginal models in terms of estradiol-17β responsiveness. The cultured vaginal epithelial cells and fibroblasts on de-SVT respond to estradiol-17β in a dose-dependant manner mimicking the *in vivo* cellular behaviour in our *in vitro* vaginal models.

2.4.8 Immunohistofluorescence (IHF) staining of the TE vaginal models:

Immunohistofluorescence staining of TE vaginal models was performed to detect the expression of epithelial differentiation proteins such as cytokeratins and other molecular entities such as Ki67 in TE vaginal models and compared with the native SVT. The expression of these molecular species were also detected in TE vaginal models treated in different concentrations of estradiol-17β to understand the effect of estradiol-17β induction on a molecular level that can further validate the physiological relevance of our TE vaginal models. The nuclear protein Ki67 is a promising molecular target that is associated with cellular proliferation and generally expressed in cells during the proliferative stage of the cell cycle. In native SVT and TE vaginal models, the basal epithelial cells were stained positive for Ki67 marker as shown in Figure 2.19. This is what would be expected in a stratified epithelium as cells of the basement membrane were proliferative and became more and more differentiated

in the suprabasal layers. A very few cells could be seen positive for Ki67 in the suprabasal and superficial layers of both the native SVT and TE vaginal models. Figure 2.20 demonstrates the expression of Ki67 in the TE vaginal models cultured under different concentrations of estradiol-17β. The intensity and number of cells positive for Ki67 marker increased with an increase in estradiol-17β concentration. The basal cells of the TE vaginal models' epithelia were stained intensely showing their proliferative status. With an increase in concentration of estradiol-17β (from 100 – 400 pg/mL) there was an increase in the Ki67 expression which is reflective of an increase in the number of proliferative cells in the TE models.

Cytokeratin 10 (cyt10), a marker for keratinisation, is known to be regulated by the presence of estradiol-17β in squamous epithelia of genitourinary organs in humans. Cyt10 expression is limited to the vaginal epithelial cells present in the suprabasal and superficial layers of the stratified epithelia and is an indicator of the differentiation phase in the lifecycle of epithelial cells. The native SVT and reconstructed TE vaginal models showed similar pattern of cyt10 expression in the suprabasal and superficial layers of the vaginal epithelia (Figure 2.21). As in the normal female body, cyt10 is regulated by the presence of estradiol-17β, similar findings have been reported in Figure 2.22 where an increase in the expression of cyt10 could be seen with an increase in the concentration of estradiol-17β in the culture media. These results indicated that our TE vaginal models were physiologically relevant models as the vaginal epithelial cells were responding towards estradiol-17β that can induce differentiation of squamous cells and hence, cells present in the suprabasal and superficial layers of the epithelia expressed cyt10 marker.

Cytokeratin 19 (cyt19) is typically expressed in human breast tissues and epithelia of several female reproductive organs. In non-keratinised stratified squamous epithelia such as the oral mucosa and the vaginal tissue, cyt19 has been reported to be a characteristic marker of proliferating cells in the epithelia. In the native SVT and TE vaginal models there was no cyt19 expression detected in the vaginal epithelia (Figure 2.23). However, under higher estradiol-17β concentration (100 - 400 pg/mL), a dose dependant response for cyt19 expression could be seen in the TE vaginal models' epithelia (Figure 2.24). The expression of cytokeratin 19 (cyt19) in the suprabasal and superficial epithelia of TE models cultured in high concentrations of estradiol-17β (100 - 400 pg/mL) indicated an abnormal pattern of keratin production in these models.

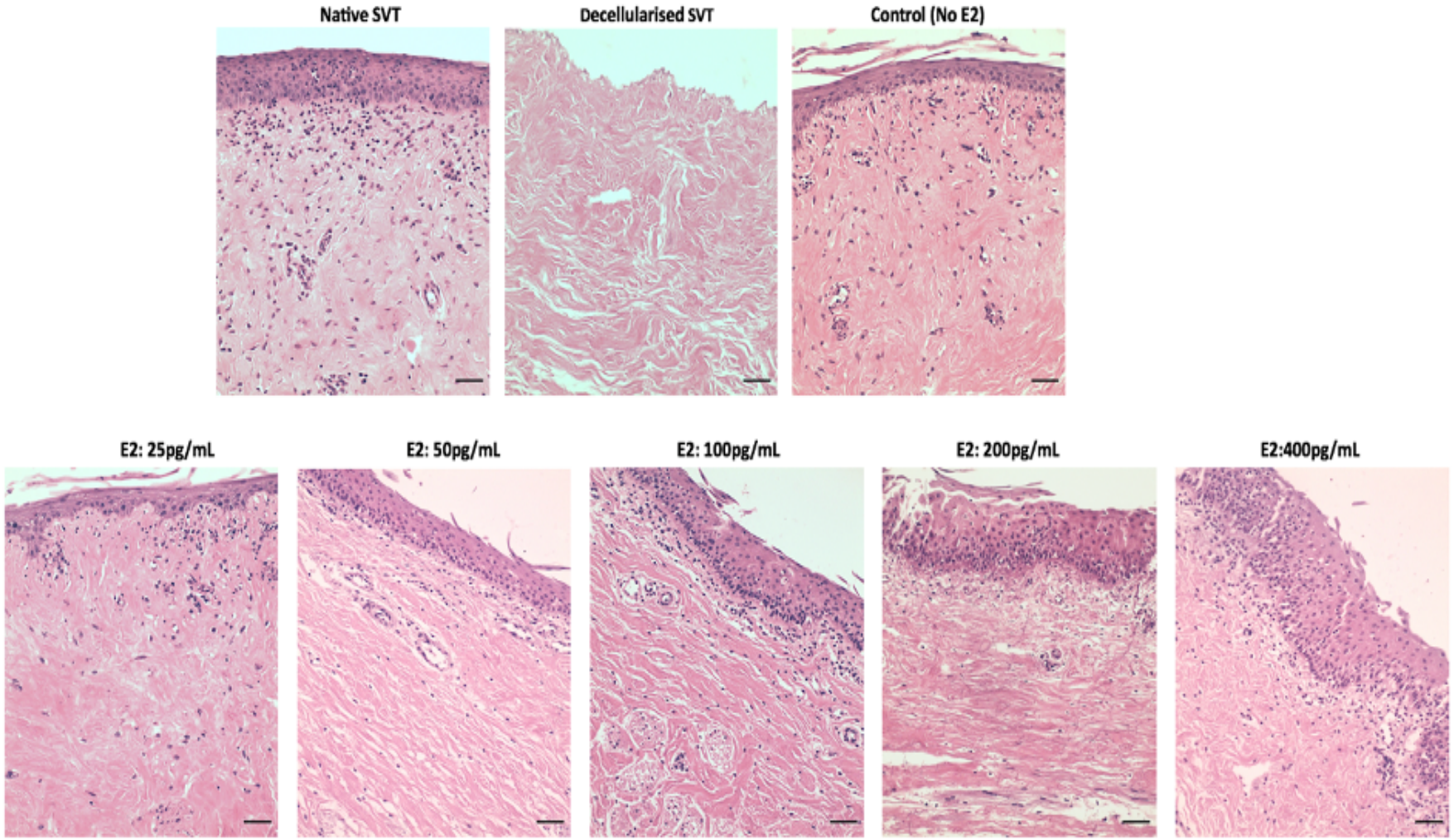

Figure 2.16: Haematoxylin and eosin (H&E) stained sections of sheep TE vaginal models after estradiol-17β induction on models cultured at air-liquid interface (ALI) upto 3 weeks under static culture conditions. TE models treated with higher concentrations of estradiol-17β [E_2] (100-400 pg/mL) showed more stratified and cornified epithelium (10-19 layers) compared to the control (without E_2) (5-7 layers). Scale bar=100μm (applies to all).

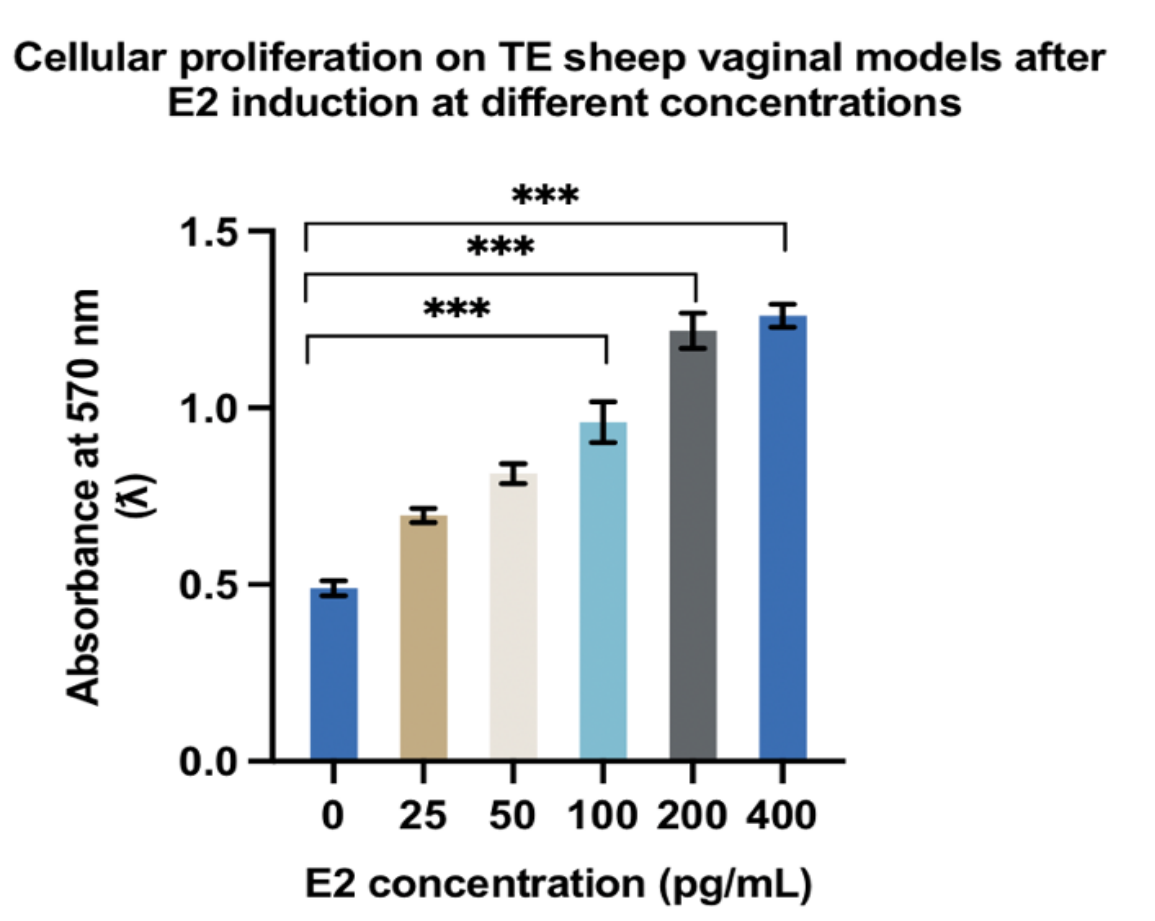

*Figure 2.17: Metabolic activity of primary vaginal epithelial cells and fibroblasts cultured on decellularised-SVT under static culture conditions under E_2 induction estimated by resazurin® assay after 3 weeks at ALI (n = 9 ± SD for each group, ***p < 0.05).*

**SVT, sheep vaginal tissue; TE, tissue engineered*

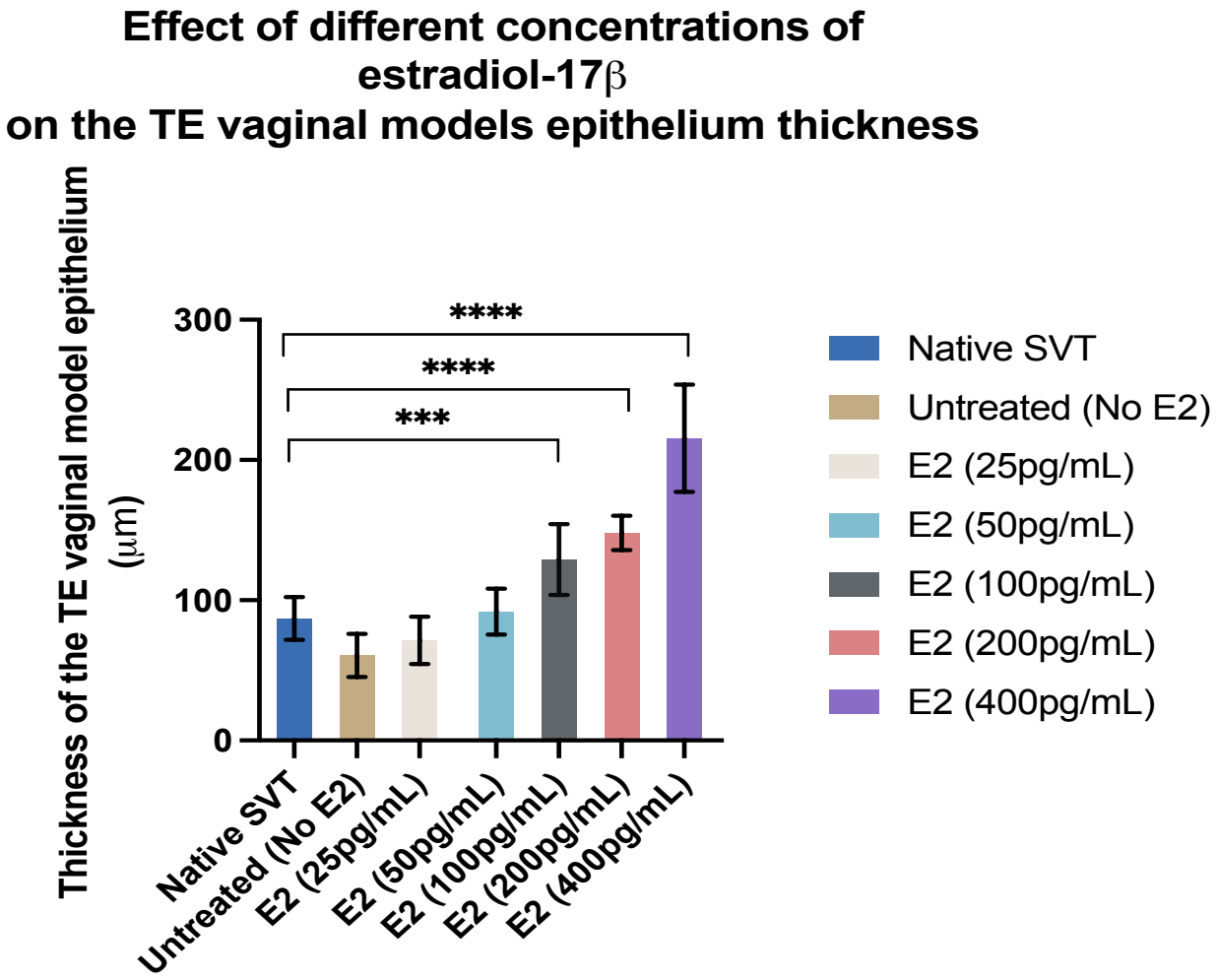

*Figure 2.18: Measurements of TE vaginal models' epithelia thickness after 3 weeks at ALI under static culture conditions (with and without E_2 induction). ($n = 9 \pm SD$ for each group, **** $p < 0.0001$, *** $p < 0.05$).*

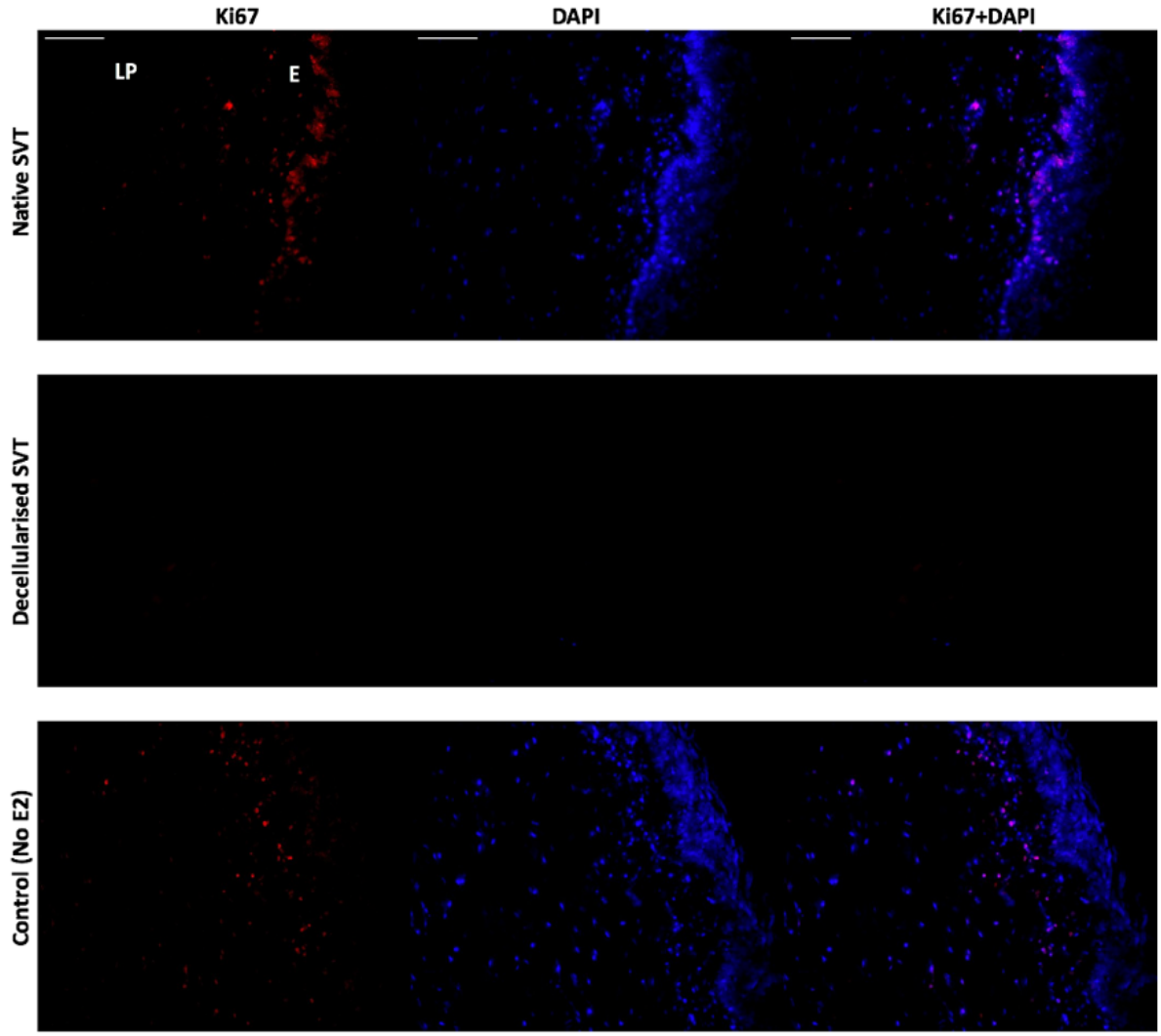

Figure: 2.19: Immunohistofluorescence detection of Ki67, a marker for proliferative cells in the TE sheep vaginal models. The basal cells of the vaginal epithelium were stained intensely for Ki67 (red channel) in the native sheep vaginal tissue (top row), whereas no cellular expression for either Ki67 or DAPI could be seen in the decellularised sheep vaginal tissue (SVT) (negative control). The expression of Ki67 in the reconstructed TE vaginal model after 3 weeks at ALI under static culture conditions showed similar pattern of expression as compared to that in the native SVT. All tissue sections were counterstained with DAPI (blue channel). Scale bar = 100 µm (applies to all).

**vaginal epithelium (E); underlying lamina propria (LP)*

DAPI, 4',6-diamidino-2-phenylindole; TE, tissue engineered

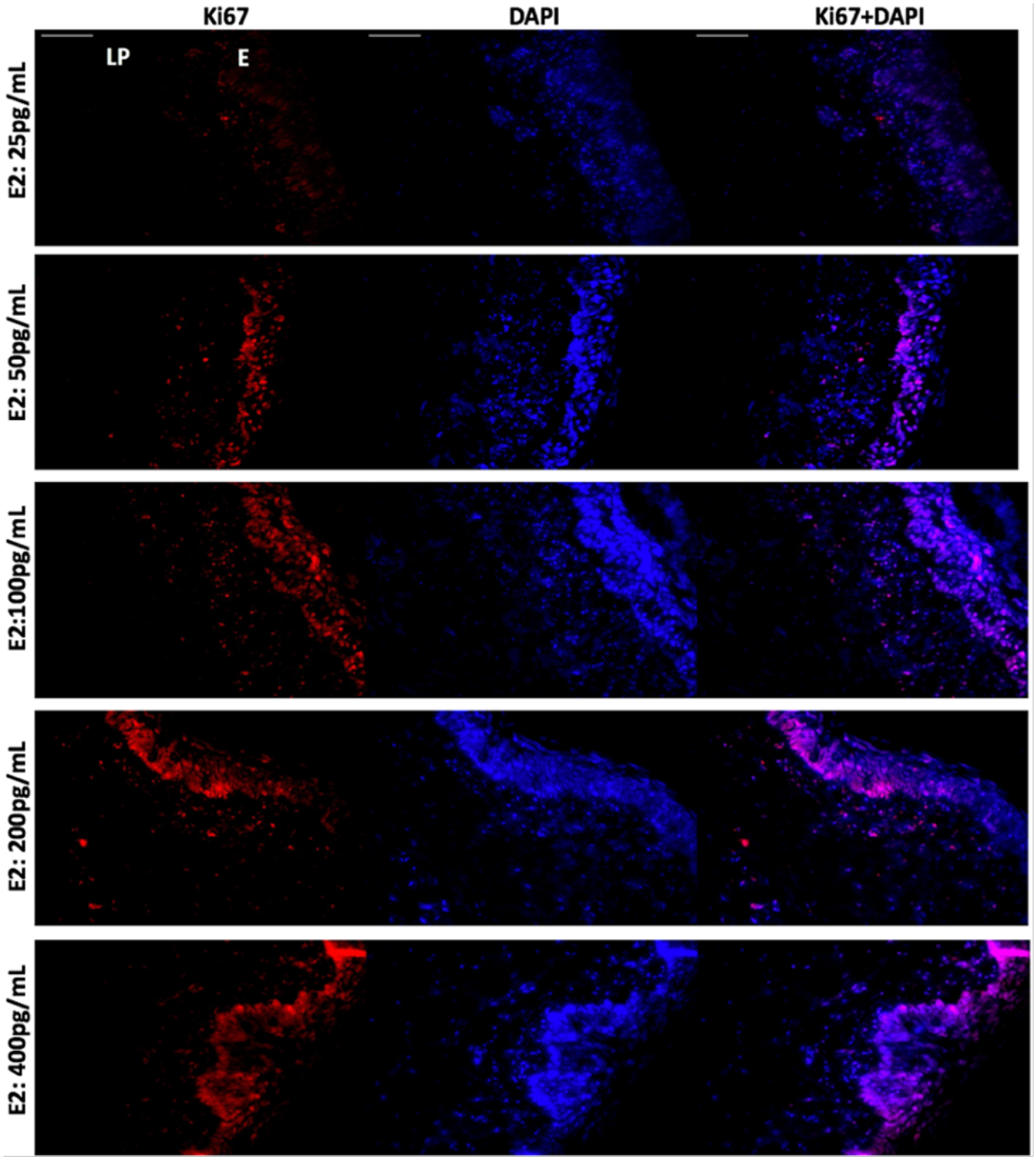

*Figure 2.20: Immunohistofluorescence detection of Ki67 in the reconstructed TE vaginal models under estradiol-17β [E_2] induction after 3 weeks at ALI under static culture conditions. A dose-dependent response of cells positive for Ki67 (red channel) could be seen with an increase in E_2 concentration. An increase in E_2 concentration (from 50 to 400 pg/ml) showed an increase in the intensity and number of positive cells for Ki67 in both the vaginal epithelium (E) and the underlying lamina propria (LP). All tissue sections were counterstained with DAPI (blue channel). Scale bar = 100 µm (applies to all).*DAPI, 4',6-diamidino-2-phenylindole; TE, tissue engineered.*

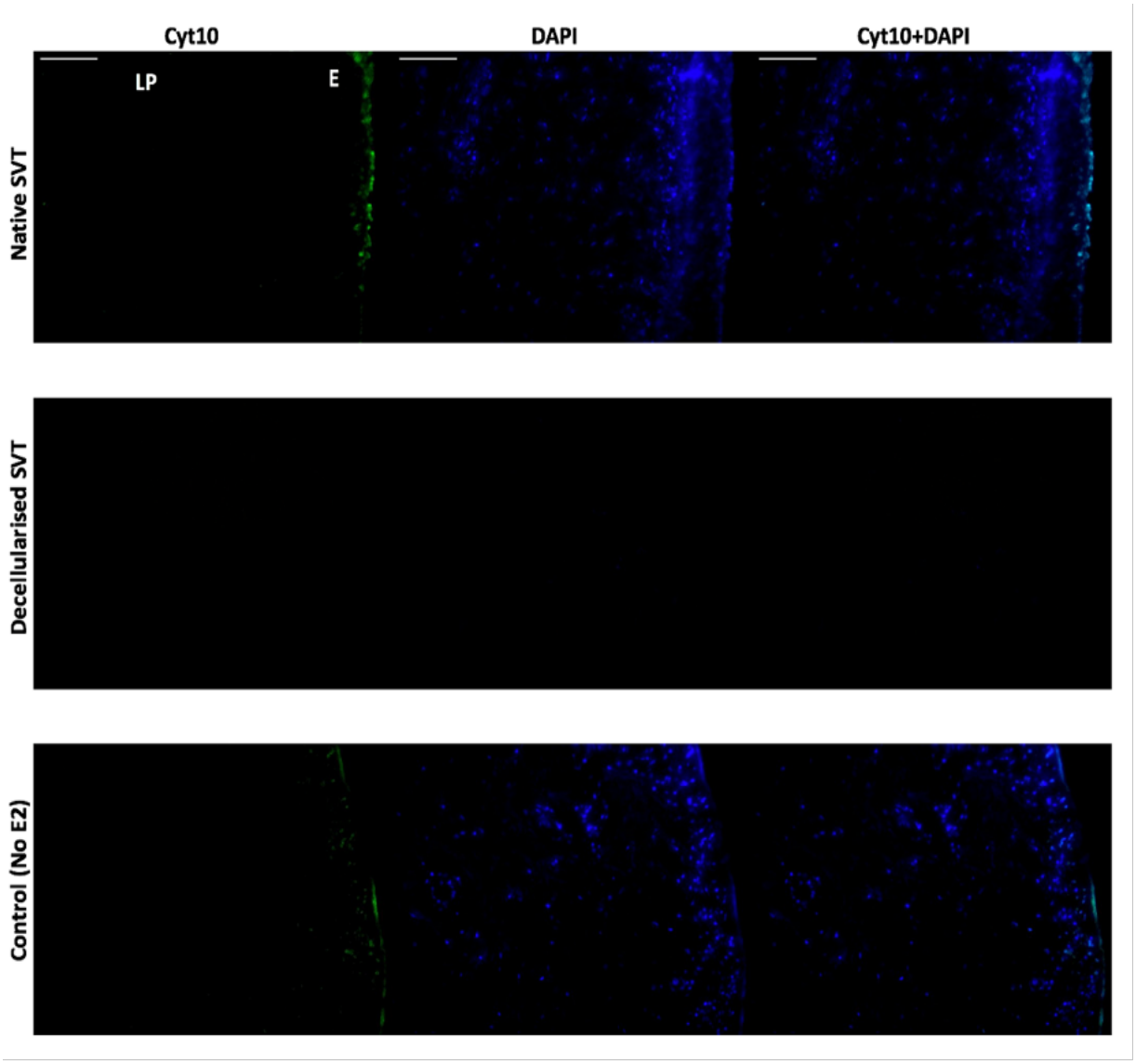

Figure 2.21: Immunohistofluorescence detection of cytokeratin 10 (cyt10), a marker of stratification in the TE sheep vaginal models. The suprabasal cells and the superficial layers of the vaginal epithelium were stained intensely for cyt10 (green channel) in the native sheep vaginal tissue (top row), whereas no cellular expression for either cyt10 or DAPI could be seen in the decellularised sheep vaginal tissue (SVT) (negative control). The expression of cyt10 in the reconstructed TE vaginal model after 3 weeks at ALI under static culture conditions showed similar pattern of expression as compared to that in the native SVT. All tissue sections were counterstained with DAPI (blue channel). Scale bar = 100 µm (applies to all).

**vaginal epithelium (E); underlying lamina propria (LP)*

DAPI, 4',6-diamidino-2-phenylindole; TE, tissue engineered

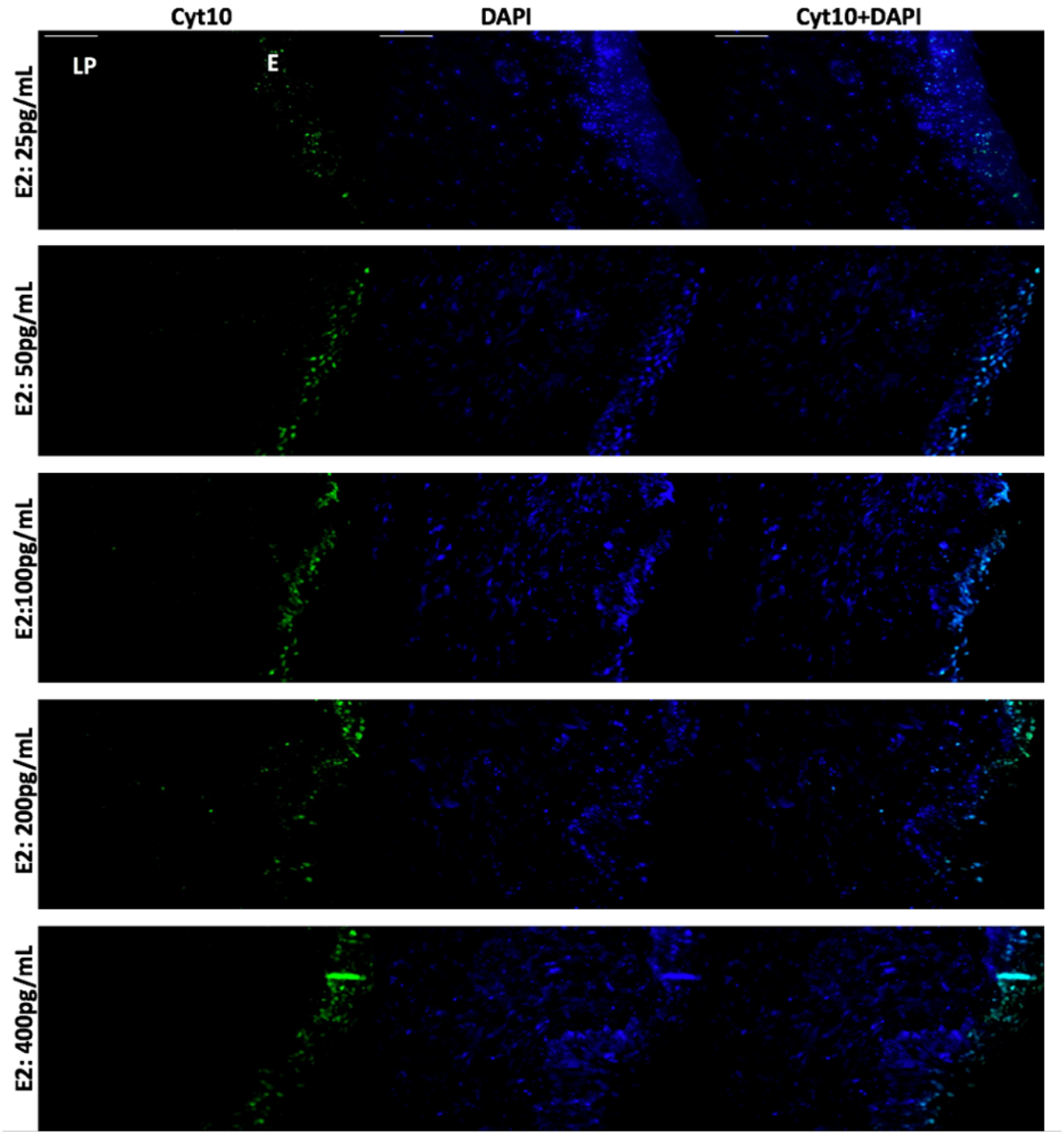

Figure 2.22: Immunohistofluorescence detection of cyt10 in the reconstructed TE vaginal models under estradiol-17β [E_2] induction after 3 weeks at ALI under static culture conditions. A dose-dependent response of cells positive for cyt10 (green channel) could be seen. Higher E_2 concentration (from 50 to 400 pg/ml) showed an increase in the intensity and number of positive cells for the expression of cyt10 in the parabasal layers of the vaginal epithelium (E) while none of the vaginal fibroblasts in the lamina propria (LP) were positive for the cyt10 expression. All tissue sections were counterstained with DAPI (blue channel). Scale bar = 100 μm (applies to all).

**DAPI, 4',6-diamidino-2-phenylindole; TE, tissue engineered*

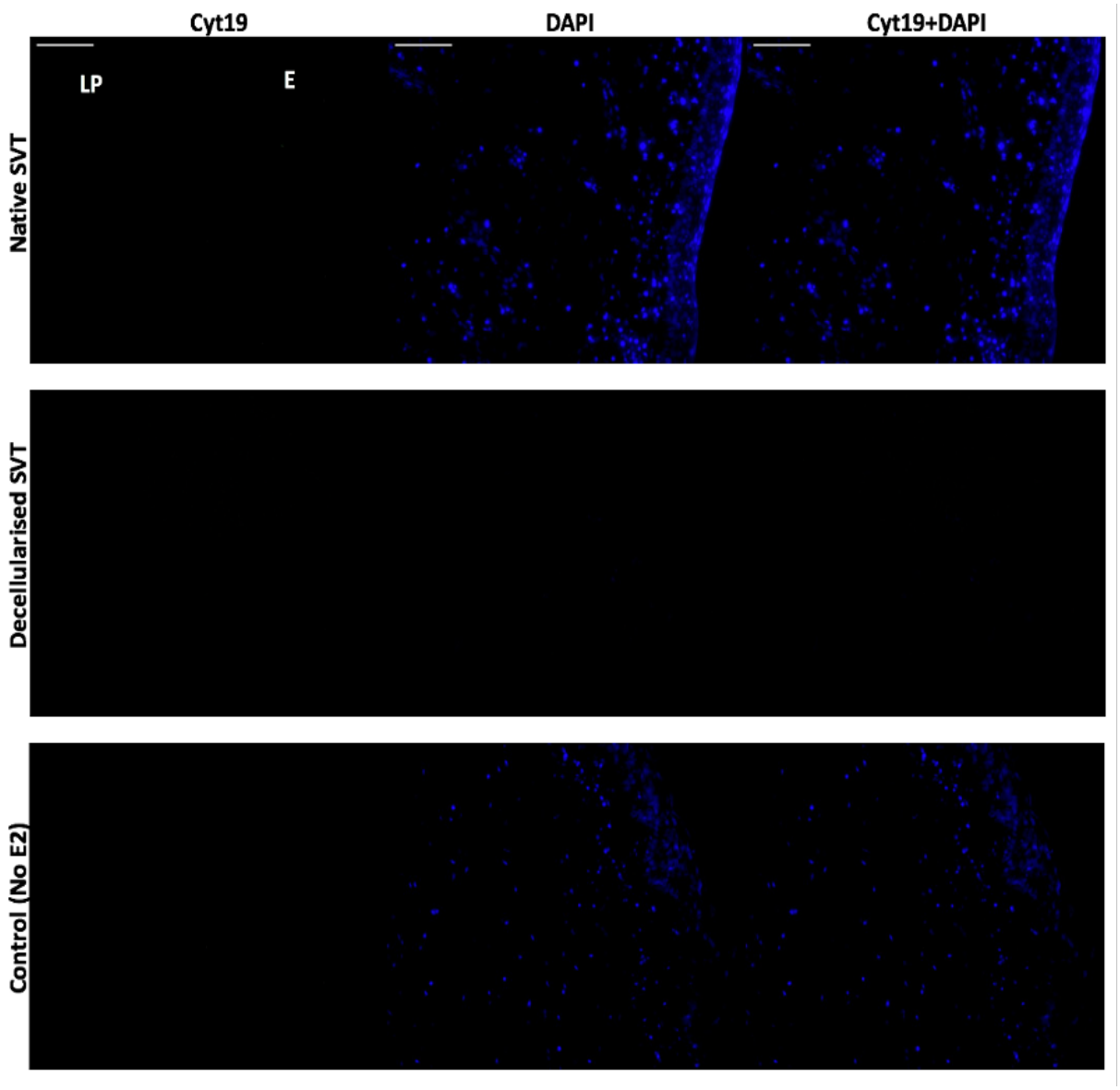

Figure 2.23: Immunohistofluorescence detection of cytokeratin 19 (cyt19) in the TE sheep vaginal models. The native SVT and TE vaginal models without estradiol-17β [E_2] did not show any cellular expression for cyt19 (either in the epithelium [E] or the lamina propria [LP]); however, the cultured cells were exhibiting DAPI (blue channel) expression (top view). In the decellularised SVT, both cyt19 and DAPI staining was absent (negative control). Scale bar = 100 μm (applies to all).

**DAPI, 4',6-diamidino-2-phenylindole; SVT, sheep vaginal tissue; TE, tissue engineered*

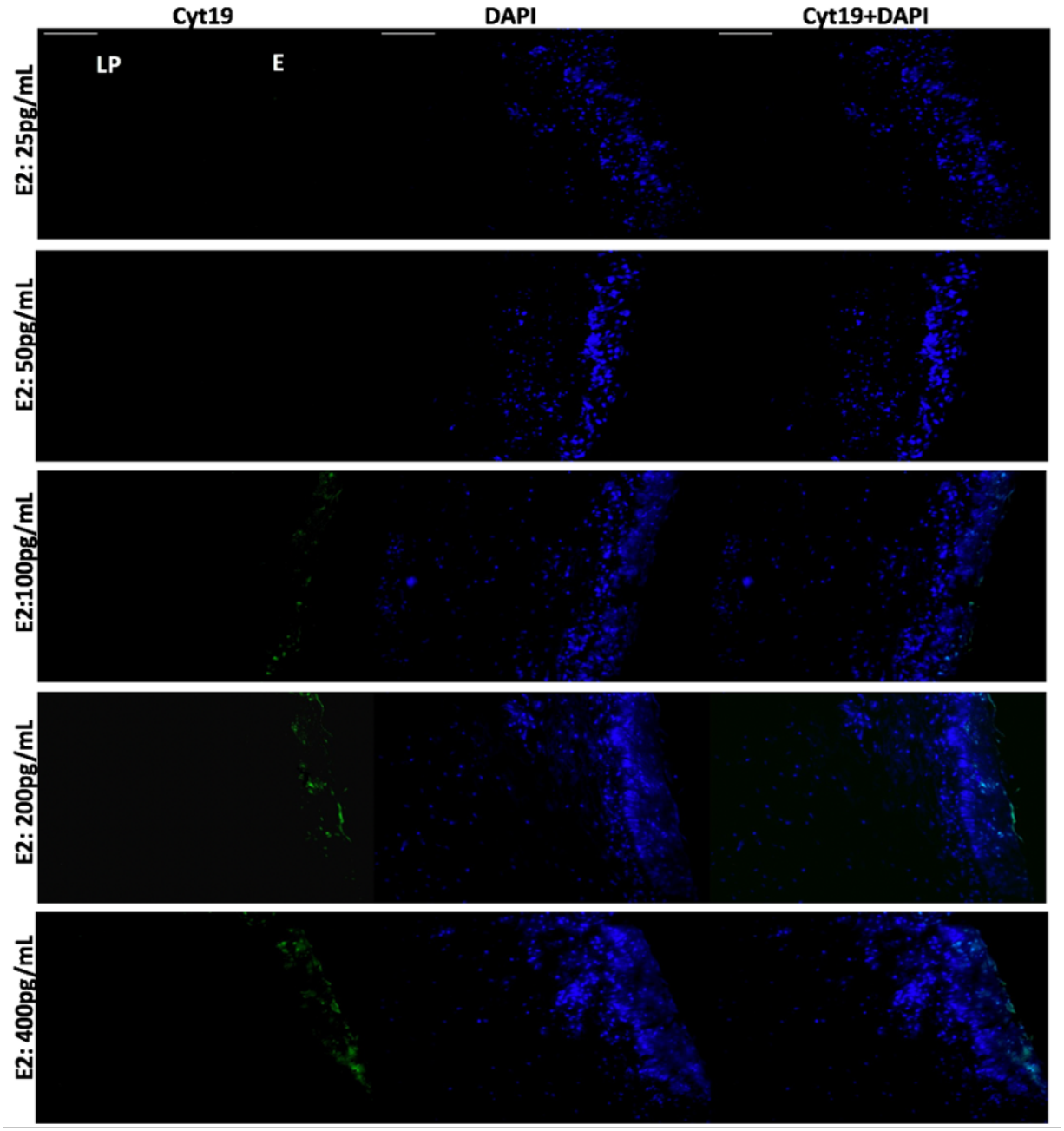

Figure 2.24: Immunohistofluorescence detection of cyt19 in the reconstructed TE vaginal models under estradiol-17β [E_2] induction after 3 weeks at ALI under static culture conditions. In the reconstructed TE sheep vaginal models, under low E_2 concentrations (25–50 pg/ml), there was no cyt19 expression (green channel) observed from the cultured cells. However, an increase in the E_2 concentration (from 100 to 400 pg/ml) induced the epithelial cells present in the transient suprabasal and superficial layers of the TE models' epithelia (E) to express cyt19 in a dose-dependent manner. All tissue sections were counterstained with DAPI (blue channel). Scale bar = 100 μm (applies to all).

**vaginal epithelium (E); underlying lamina propria (LP)*

DAPI, 4',6-diamidino-2-phenylindole; TE, tissue engineered

2.4 Discussion:

Traditionally the majority of the newly developed biomaterials and treatment therapies for use in the reconstructive procedures and tissue engineering of the native tissue are tested in animal models. In the field of urogynecological research, these animal models are valuable *in vivo* preclinical models that offer a complex biological system to test newly developed therapies for the treatment of pelvic floor dysfunctions. On the other hand, in the pharmaceutical industries, testing of compounds for vaginal applications are conventionally done on monolayer cell cultures and is the standard protocol for pharmacological preparations. These routine testing methods can predict the effectiveness and irritancy potential of novel vaginal microbicides, contraceptives, lubricants and drugs for vaginal route applications.

There are several limitations associated with the use of animal models such as high cost, rigorous ethical concerns, time consuming experiments, limited availability and requirement of additional surgical expertise and maintenance facility. More importantly, the anatomical and physiological differences in the urogenital tract among different animal species in comparison with humans can lead to misinterpretation of results as animal models are not always able to truly predict the tested outcomes in humans. These interspecies differences are a major cause of failure of tested materials and therapies in human trials. Tissue engineered (TE) *in vitro* models of the genitourinary tract and vaginal mucosa can be utilised as alternative preclinical testing models which can overcome limitations associated with the use of animal models and monolayer cell cultures. TE models are valuable tools for testing novel biomaterials and therapies by providing researchers with inexpensive high throughput data in a short amount of time without involving tough ethical regulations.

The research community in the field of women's reproductive health urgently needs access to accessible, affordable and physiologically relevant preclinical models of the vaginal tissue which can be used as an alternative to animal testing, in line with the 3Rs principles. In this study we have developed a TE vaginal model comprising of a stratified epithelium with an underlying fibroblast populated lamina propria which is structurally similar to the native vaginal tissue of sheep and human [181]. The models developed in this project were comprised of decellularised sheep vaginal tissue cultured with primary sheep vaginal epithelial cells and fibroblasts making it accessible, ethically sound and affordable. The TE models presented here

were estradiol-17β [E_2] responsive and that it has profound advantages over existing preclinical models used in the vaginal tissue research.

Existing, commercially available, *in vitro* tissue engineered (TE) vaginal models such as EpiVaginal™ developed by MatTek Corporation or the Human Vaginal Epithelium (HVE) models from Episkin are popular among the research community for toxicity and irritability studies of vaginal treatments, products and sexually transmitted infections [231], [232], [240], [243]. In addition to this, human cervico-vaginal explant cultures have long been used in vaginal tissue research for understanding the mechanism of HIV transmission and development of potential vaginal microbicides [14], [292]. These explants, *ex vivo* tissue models and *in vitro* TE models are extremely valuable tools and more relevant than 2D culture studies as these models can serve as a bridge between the cell culture and tissues *in vivo*. However, these existing models have several limitations which we aimed to overcome in this study through our tissue engineered model of the vagina.

Currently available models of the human vagina can be prohibitively expensive, have limited culture times, do not include physiologically relevant lamina propria components and either rely on immortalised cell lines or regular access to human tissue samples. The human cervico-vaginal explant cultures have short culture lives (approximately 3-4 days in culture depending upon the source) which limits their applicability for a wide range of experiments. Moreover, culturing and maintenance of polarising explants is also challenging and without the formation of a stratified vaginal epithelium in culture, these explants cannot be used in vaginal tissue studies. In the models presented here, we have used cultured expanded primary sheep vaginal cells isolated from excised sheep vaginal tissues. Both cell types showed typical morphological characteristics of each as shown in Figure 2.7. These cultured expanded cells can facilitate genetically matched models to be created, limiting the donor variability observed and enabling a reasonably high through-put of experiments. Primary sheep vaginal cells cultured on decellularised SVT showed the gradual formation of a stratified epithelium over three weeks' time in ALI culture and the resulting vaginal constructs resembled the native SVT histologically (Figure 2.12).

In the human body several organs (dermis, oral mucosa, vagina) and organ systems (digestive tract and urogenital tract) are lined by a stratified epithelium and associated fibromuscular stroma. Stratification of the vaginal epithelium is regulated by the sex steroid hormones

estradiol-17β, testosterone and progesterone. Evidence has suggested that stromal-epithelial cross-talk is critical in modulating the effects of these hormones in regulating the epithelial proliferation, differentiation and cornification [293]. Oestrogens are responsible for vaginal epithelial proliferation and stratification while progesterone acts oppositely by promoting vaginal epithelium maturation [294]. Iguchi *et al.,* [295] demonstrated that when mouse vaginal epithelial cells were cultured in isolation in 3D collagen gels, they were unable to stratify into multilayers membrane even in the presence of estradiol-17β. However, when these vaginal epithelial cells from overiectomised mice were cultured with homologous stroma and grown *in vivo*, the vaginal epithelial cells re-expressed their hormone responsiveness and stratify to form a proliferative vaginal epithelium indicating that the presence of stromal component is crucial for normal vaginal epithelial structure and function [296]. The requisite of epithelial-stromal interactions for maintaining vaginal epithelium stratification was later confirmed by Takashina *et al.,* [297] in *in vitro* studies in 3D co-culture models of mouse vaginal epithelial cells and fibroblasts. The models presented here were developed using a co-culture of primary sheep vaginal epithelial cells and fibroblasts to include the stromal component to allow the epithelial-stromal interactions necessary for the formation of a stratified vaginal epithelium *in vitro*. Figure 2.12 depicts the gradual formation of a stratified vaginal epithelium containing 7-12 layers of epithelial cells with underneath stroma populated with vaginal fibroblasts.

Managing the ethical, legal and logistical challenges associated with accessing human tissues can be a barrier to many researchers who wish to undertake *in vitro* preclinical research. In addition to this, often only small samples of vaginal tissues can be obtained which are usually donated following gynecological surgery where patient to patient variability can be very high and vaginal pathology is common. As a result, the models were developed by utilising waste animal tissue from the local abattoir, making them widely accessible and affordable. Sheep and human vaginal tissues have comparable reproductive anatomy, equivalent epithelial morphology and structural similarities [149]. For these reasons, sheep are commonly used animal models for *in vivo* studies on vaginal tissue mechanics, testing novel therapeutic agents and vaginal irritants as well as testing potential biomaterials and therapies for the management of pelvic organ prolapse and other vaginal abnormalities [148], [298], [299]. The pathophysiology and risk factors of pelvic organ prolapse (POP) including connective tissue content, hormonal changes and tissue turnover share marked similarities in humans and sheep [300]. In addition, sheep are the only vertebrates that can develop spontaneous prolapse with risk factors similar to those in humans [301]. The use of sheep vaginal tissue and primary sheep

vaginal cells to develop physiologically relevant TE vaginal models in this project is based on these urgings.

It has been well established that the function and physiology of the human vagina is influenced not only by the epithelium but also the underlying connective tissue component, the lamina propria and the ability to model the full-thickness vaginal wall is valuable for many applications including studies into pelvic organ prolapse, cancer and vaginal infection. Here, the TE models were developed using decellularised sheep vaginal matrices to provide homologous stromal component to the reconstituted vaginal epithelium which can recapitulate the microenvironment of the vaginal fibroblasts similar to the native SVT. Decellularised scaffolds are known to retain the complex biomolecular and physical cues of the native tissue extracellular matrix (ECM), that have previously been shown to redirect cell growth and viability by providing a natural microenvironment [302]. The TE vaginal matrices were successfully decellularised in five days using low concentrations of detergent mix (0.25 - 0.5% v/v Triton X100 and 0.25% wt/v sodium deoxycholate) to limit the possible harmful effects on the ECM (Figure 2.6).

Several studies have suggested that a combination of physical and chemical factors result in efficient decellularisation of organs and tissues [303]. Based on these suggestions, i combined the physical motion of a platform rocker with the chemical (a combination of ionic and nonionic detergents) action to achieve decellularisation of native sheep vaginal tissues. Sheep vaginal tissues were treated with two different decellularisation solutions and incubated on a Platform rocker that provided a rocking movement to facilitate faster diffusion of chemicals into the tissues to achieve quicker decellularisation in 5 days. This method worked superior to the previously described method by Zhang *et al.,* [275] as the decellularisation of vaginal matrices was achieved in 5 days as compared to 10 days. Previous work by Zhang *et al.,* [275] to prepare porcine acellular vaginal matrix utilised a combination of physical, chemical and enzymatic treatment to achieve effective decellularisation of the porcine vaginal tissue in 10 days.

The objective criteria to assess the efficacy of decellularisation protocol as described by *Crapo et al.,* [274] was proposed as follows: i) absence of visible nuclear material; ii) DNA content should be <50 ng/mg ECM dry weight; and iii) DNA fragment lengths should be <200 bp. It should be kept in mind that these criteria were outlined for those decellularised organ and tissue matrices intended for *in vivo* studies such as xenogeneic implantation to minimise the chances

of immune rejection post-implantation. However, my aim to develop decellularised sheep vaginal tissue in this project was to develop TE *in vitro* vaginal models to study expression of biomolecules and cellular response towards female steroid hormone estradiol-17β. Hence, i characterised the decellularised matrices on the basis of absence of visible nuclear material using H&E staining and picogreen™ staining as shown in Figures 2.9 and 2.11 respectively. Both the H&E and DAPI staining revealed that no visible cellular remnants were present in the decellularised vaginal matrices treated with the detergent method. Although DAPI is the classical financially beneficial DNA-binding fluorescent dye that binds selectively to the AT-rich regions in the minor groove of the DNA [304], further validation of the presence/absence of the DNA content in the decellularised matrices presented here were carried out using a superior picogreen™ ds-DNA histochemical staining. Picogreen™ ds-DNA fluorescent stain is an ultrasensitive ds-DNA probe that yields a 1000-fold stronger fluorescence emission when bound to ds-DNA. In addition to this, it can detect a wide-range of DNA concentrations using a single-dye concentration and is also DNA base-sequence insensitive [305]. Figure 2.11 depicts absence of cellular contents in the detergent method treated decellularised vaginal matrices under low magnification and even under higher magnification acceptable removal of cells was observed with both DAPI and picogreen™ histochemical staining.

During the process of tissue decellularisation, preservation of the composition and three-dimensional ultrastructure of the native ECM is highly desirable as these factors influence cell migration, proliferation and differentiation in the TE constructs. The decellularised vaginal matrices retained good amount of normal collagen content as shown by sirius red staining in Figure 2.10. The histological analysis of decellularised tissue samples revealed that the detergent method was superior to the hypertonic+detergent method in terms of both efficient cellular removal (absence of visible cell nuclei) and preservence of collagen matrix in the ECM.

Previously described commercial TE vaginal models are developed using either collagen gels (VEC-100-FT and VLC-100-FT by MatTek) [228] or polycarbonate membrane filters (SkinEthic™ HVE from EpiSkin) [306]. These substrates are not as relevant as the decellularised tissues presented here. One of the main advantages of using decellularised vaginal tissues compared to synthetic materials as scaffolds in vaginal tissue engineering is that they retain various growth factors that are conducive to the development of tissue engineered constructs similar to the native tissue histoarchitecture. These features were captured in the TE vaginal models presented here as shown in Figure 2.12. Here, i have shown that my

decellularised tissues retained the normal collagen content and ECM microenvironment that supported the cellular proliferation and metabolic activity of cultured vaginal fibroblasts and epithelial cells for up to 3 weeks without any loss of TE models' epithelial integrity.

Longer culture times are required for some research applications where observations and information are wanted on long term effects of vaginal treatment or infection. The ability to culture our TE vaginal models for 21 days under static conditions presents a clear advantage over explanted tissue cultures, which can be kept alive for a maximum of 4-7 days [221] or EpiVaginal™ tissues which can only be cultured for a week [228].

Evidence has suggested that those tissues and organs which are subjected to a dynamic environment *in vivo* (for example; small intestine) when modelled *in vitro*, form tissue constructs with improved cellular differentiation and stratified epithelial linings under dynamic culture conditions compared to static conditions [307]. The human pelvic floor is subjected to dynamic forces throughout the lifetime of an individual. TE vaginal models presented here were cultured under both static and dynamic culture conditions to compare the progress of the development of a fully differentiated vaginal epithelium and to test the survival time period of models (Figures 2.12 & 2.14). I have reported an increase in the survival time period of TE vaginal models from 3 weeks to 4 weeks under dynamic culture conditions provided by the shear forces of the culture media when models were cultured on a Platform rocker. In addition, cellular metabolic activity also remained significantly higher beyond 3 weeks in dynamic cultures compared to the static ones. However, no differences in the stratification and differentiation of the vaginal epithelium could be seen as TE models under both culture conditions developed a fully stratified vaginal epithelium. These results were not consistent with previous work by Cattan *et al.,* [308] on *in vitro* uroepithelium differentiation in a human tissue engineered tubular genitourinary graft. Their study on developing TE genitourinary grafts demonstrated that mechanical stimuli mediated by flow perfusion can induce terminal urothelium differentiation and basement membrane formation in in vitro urologic conduit. On the contrary, cultured vaginal epithelial cells differentiation and stratification in my TE vaginal models remained unaffected by employing dynamic fluid shear stimuli in comparison with static culture conditions. Hence, for the suitability of the experimental setup, static culture conditions were maintained to culture TE vaginal models for subsequent experiments.

The human vaginal epithelium is composed of 7-14 layers of non-keratinised stratified squamous epithelial cells that is associated with an underlying lamina propria richly supplied with blood vessels through a basement membrane junction [230]. In a healthy menstruating female, the thickness of the vaginal epithelium changes considerably during different phases of the menstrual cycle and in post-menopausal women, an overall thinning of the vaginal epithelium has been reported in tissue biopsies. The hormonal status (*e.g.,* fertile adult, menopause or pregnancy) of an individual affects the histoarchitecture of the vaginal wall which is regulated by the ovarian steroids, estradiol, testosterone and progesterone. Buchanan *et al.,* [309] first explored the role of estradiol 17-β [E_2] in promoting vaginal epithelium stratification, proliferation and cytodifferentiation *in vivo* in mouse models. Their studies suggested that under E_2 stimulation, both uterine and vaginal epithelial cells differentiate, proliferate and an increase in vaginal epithelial thickness could be seen in explanted tissues from mice. Similar results were obtained in the current study which is the first *in vitro* model to mimic the *in vivo* physiological response of the vaginal epithelium towards E_2 induction. Figure 2.16 shows that in the absence of E_2, the vaginal epithelium in our TE models consisted of 3-5 layers of squamous epithelial cells while models treated with E_2 concentrations between 100 and 400 pg/mL displayed an increase in epithelium thickness (10-19 layers). E_2 also resulted in a significant increase in cell proliferation on TE vaginal models over three weeks' time (Figure 2.17).

Previously, Pessina *et al.,*[310] reported that oestradiol administration (15 or 45 μg estradiol/d) in ovariectomized rats restored the thickness of the vaginal epithelium (10 cell layers) after hormone replacement therapy (HRT) compared to the control group (1-2 cell layers) treated with the vehicle only. I have reported similar effects of estradiol 17-β [E_2] *in vitro* in my TE sheep vaginal models as the models responded in a dose-dependent manner towards E_2. This data shows that the TE models closely resembled the native vaginal tissue in terms of oestradiol responsiveness and hence can be utilised as an *in vitro* preclinical testing model for vaginal microbicides in place of animal testing where hormone responsive behavior is desirable.

The proliferative and differentiation response of vaginal epithelium under E_2 stimulation is highly complex and involves the formation of multiple suprabasal epithelial cell layers. This process is mainly controlled by the regulatory signals and oestrogen receptor-α (ERα) present in both the vaginal epithelium and the lamina propria [309]. Evidence has suggested that the crosstalk between the oestrogen receptor-α (ERα) present in the vaginal epithelium and the

lamina propria is crucial in maintaining the oestradiol-responsiveness of the vaginal epithelial cells to form a stratified squamous vaginal epithelium. Studies by Tsai *et al.,* [311] demonstrated this significant interaction between the epithelial ERα and stromal ERα in directing vaginal epithelium proliferation, stratification and differentiation. They showed that isolated mouse vaginal epithelial cells *in vitro* failed to stratify or cornify under E_2 induction [311]; but when the same unresponsive mice vaginal epithelial cells were cultured on homologous lamina propria and grown *in vivo*, they restored their normal morphology and oestrogen-responsiveness [296]. Based on these studies the TE vaginal models developed in this project utilised decellularised homologous vaginal tissues as scaffolds. The models were oestradiol-responsive suggesting the essential cues from the lamina propria were retained in the deceullularisation process and were able to influence epithelial cell behavior (Figure 2.16).

Molecular understanding of the effects of reproductive hormones on the vaginal epithelium microenvironment could enhance our knowledge of the pathophysiology of vaginal diseases and improve treatments. Identifying molecular targets such as epithelial differentiation proteins (cytokeratins), involucrin and other secretory polymeric immunoglobulin receptors are key to understanding mechanisms of cell growth and differentiation, tumorigenesis and/or toxicity of drugs. One of the attractive therapeutic targets for developing targeted molecular therapies is Ki67, owing to its high sensitivity towards cell proliferation.

Ki67 antigen is a nuclear protein which is expressed in all the active phases of the cell cycle outside of the resting phase G0 [312]. Expression of the Ki67 in tissue biopsies is strongly associated with the proliferative cell population and in routine pathological investigations, it is widely used as a proliferation marker [313]. It has been demonstrated that in the normal tissue epithelia, Ki67 expression is strongly associated with the basal proliferating epithelial cells and the expression gets weaker as the cells started to mature and form suprabasal and superficial layers [165]. Multiple clinical laboratories have reported successful use of Ki67 as a diagnostic and prognostic marker for the identification and scoring of various malignancies.

Baldassarre *et al.,* [314] compared the Ki67 expression in vaginal tissue biopsies from pre-menopausal (pre-M) and post- menopausal (post-M) women undergoing hysterectomy for vaginal prolapse. They reported a higher expression of Ki67 positive nuclei per mm of the vaginal mucosa of pre-M tissues (E_2 125.4± 35.2 pg/mL) compared to the post-M (E_2 26.7± 15.1 pg/mL). Similar results were shown in this study in the *in vitro* TE sheep vaginal models

(Figures 2.19 & 2.20). TE vaginal models presented here were positive for Ki67 expression in fibroblasts within the lamina propria and the epithelial cells in basal and suprabasal layers of the epithelium. As the models were treated with increasing doses of E_2, Ki67 expression increased demonstrating higher levels of epithelial cell proliferation which in turn increased epithelium thickness as shown in Figure 2.20.

Other therapeutic targets such as cytokeratins are a group of cell structural proteins and their main role is in maintaining the structural integrity of the epithelia by forming the cytoskeleton of the epithelial cells [315]. Moll *et al.,* [316] reported that the cytokeratins are specifically expressed in different epithelia and their distribution is highly specific in the epithelial tissue. Expression of the cytokeratin 10 is associated with the grade of differentiation of squamous cells in the epithelia and is expressed in well-differentiated regions of the stratified epithelium [317]. Cytokeratin 19 has not been reported in the epidermis of adult human skin [318] rather its expression is strictly limited to the non-keratinised epithelia such as the oral mucosa and the vaginal tissue and specifically found in the periderm and transiently superficial layers of the epithelium [319].

To further evaluate the physiological relevance of our models, i compared the expression of cytokeratins 10 and 19 in my TE SVT models with the expression of same cytokeratins in the native human vaginal tissue reported in the literature. Huszar *et al.,* [320] documented that the cytokeratin 10 (cyt10) is typically expressed in the suprabasal layers of cornifying stratified epithelia (as opposed to non-keratinised differentiation). Figure 2.21 demonstrates that the cytokeratin 10 expression in the models presented here showed an expression pattern with similar distribution and intensity as in the native sheep vaginal tissues. In models treated with higher concentrations of E_2 (100-400 pg/mL) as shown in Figure 2.22, i observed more cyt10 positive cells indicating an increase in the quantity of suprabasal cornifying cells following E_2 treatment which is in agreement with the results demonstrated in *in vivo* studies [309].

The expression of cytokeratin 19 (cyt19) in the models was observed only under higher E_2 concentration (100-400 pg/mL) and only in the suprabasal transient and superficial layers of the epithelium suggesting that these epithelial cells acquired an abnormal phenotype (Figure 2.24). Previously, Zuk *et al.,* [321] have shown the expression of cyt19 in different epithelial layers in their 3D *in vitro* cervical cancer tissue models and similar findings have been reported in literature on breast cancer cells containing oestrogen receptor (ER) that expressed cyt19 marker under E_2 induction. Choi *et al.,*[322] have documented the upregulation of cytokeratin

19 gene expression by oestrogen in MCF-7 cells suggesting the key role of oestrogen in cytoskeletal and nuclear matrix reorganization in the epithelia of mammary tissues. Induction of normal epithelial cell transformation into an abnormal phenotype has not been reported previously, however, the expression of cyt19 in the models suggested that this might be a transitional epithelium. My models could be used to carry out further studies on the dedifferentiation and abnormal epithelial transformation under "supraphysiological" concentrations of E_2 as these models allowed me to culture normal epithelial cells under a range of physiological conditions for 3 weeks.

The mechanism of E_2-induced epithelial cell proliferation has its clinical implications as this is the key mechanism regulating the controlled cellular differentiation processes in the female genitalia and any alterations in the normal regulatory process may lead to the development of endometrial, vaginal and/or cervical cancers [323]. To the best of my knowledge, the model presented here is the first *in vitro* hormone-responsive model that depicts the direct regulation of cytokeratins 10 and 19 by estradiol-17β [E_2] in a dose-dependent manner.

The complete TE vaginal epithelium response towards E_2 induction involves a series of events that includes epithelial proliferation, stratification and differentiation mediated by the presence of ERα in both the epithelium and the lamina propria. E_2 induction elicited epithelial proliferation by binding with epithelial and lamina propria ERα in the TE models and triggered Ki67 expression in cells of basal layers which gradually became more intense at higher E_2 concentrations as shown in my models. The TE vaginal model's epithelia were more stratified under E_2 induction and this formation of multiple suprabasal layers provides such stratified tissue organisation similar to the native vaginal tissue. TE vaginal epithelial differentiation may then be elicited by the direct action of E_2 that triggered expression of differentiation-type cyt10 and a higher E_2 concentration caused abnormal transformation of some epithelial cells in the transient suprabasal cells that expressed cyt19 and hence, the formation of a highly stratified epithelium comparable to the fully mature vaginal epithelium could be seen in the models.

These results are in agreement with other *in vivo* studies in rat models [230], [309] where the fundamental role of oestradiol in stimulating cellular proliferation and differentiation in the vaginal epithelium has been reported. This is the first *in vitro* vaginal model of animal origin to clearly depict E_2 responsiveness in a manner similar to the native vaginal tissue.

Chapter 3:

Developing tissue engineered wound vaginal models

3.1 Aim:

To develop and characterise full-thickness (FT) and partial-thickness (PT) tissue engineered wound vaginal models.

The specific objectives to achieve were:

- To analyse different stages of the wound healing process in full-thickness (FT) and partial-thickness (PT) tissue engineered wound vaginal models
- To compare the histology and cell viability of full-thickness (FT) and partial-thickness (PT) tissue engineered wound vaginal models
- To determine the effect of female sex steroid estradiol-17β on the wound healing process in TE wound vaginal models
- To determine the expression of key regulatory markers during the wound healing process with and/or without estradiol-17β

3.2 Introduction:

Wounds are heterogeneous and the process of wound healing is a highly complex, well-orchestrated event which involves multiple biochemical and physical factors to achieve substantial wound healing [324]. These factors include local and recruited cell populations, both progenitor and differentiated cell types, cytokines and chemokines and relevant enzymes and components of the extracellular matrix [325].

The process of wound healing is broadly divided into key stages: haemostasis and clot formation, inflammation, proliferation and granulation tissue formation and finally a remodeling phase to partially or fully restore functionality of the wounded tissue as described by Gonzalez *et al.,* [326] and shown in Figure 3.1.

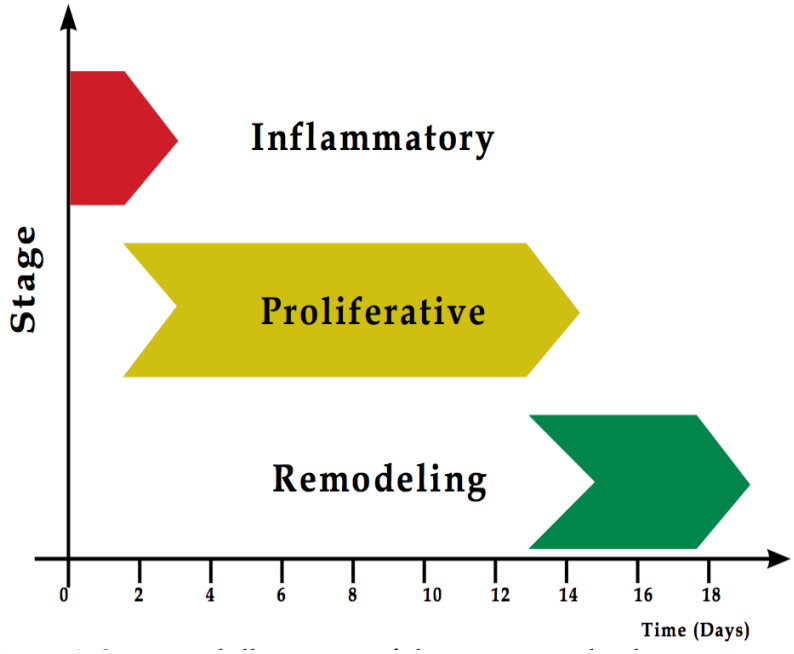

Figure 3.1: Sequential illustration of key stages involved in the process of wound repair. Reproduced with permission from [326].

Wound healing is a complex fibroproliferative response that is mediated through growth factors and cytokines *in vivo* and these stages may overlap depending on the nature of injury and tissue type. In addition to this, extrinsic factors such as suturing, or application of topical healing compounds can also affect the rate at which wounds heal. Several complications can arise due to any abnormality in the normal wound healing process. These include development of infection, chronic wound formation, fibrosis or scar tissue formation or hypertrophic scars and keloids at the wound site [327]. Other deviations in wound healing may include excessive contractility and granulation tissue formation with impaired collagen accumulation at the injury site that can block re-epithelialisation and may result in altered connective tissue properties. Research on wound healing process elucidates the underlying mechanism and factors influencing the wound repair and can assist to develop new therapies and treatments for the management of wounds.

A brief overview of the wound healing assays:

Current interest in the area of wound healing is focused on evolving approaches to promote regenerative healing in humans. For this, numerous models, both *in vivo* and *in vitro* have been developed with distinguished and specialised features to recapitulate the complex biomechanical environment of wound repair *in vivo*.

In vitro wound healing models:

The 3Rs of animal experimentation has urged the scientific community to develop alternatives to animal models to reduce the number of animals used for scientific research.

Monolayer cell culture assays:

Conventional 2D monolayer cell culture assays have been widely used to study the mechanism of wound repair *in vitro*. These assays allow to investigate the response of individual cell populations towards an injury in terms of cellular proliferation or cell migration and also enable to detect the production of cytokines or other biomolecules in 2D systems in response to injury. However, these 2D culture systems are unable to recapitulate the complexity of *in vivo* environment due to their simplicity of design. As these 2D culture systems lack the complex extracellular matrix component that provides the paracrine and autocrine factors and interact with different cell types to promote wound healing *in vivo*, these assays are inadequate and can only be employed in preliminary initial screening of different compounds. Moreover, it has been well established that cells behave differently when cultured in 3D complex matrices as opposed to tissue culture plastics. Hence, these 2D wound healing assays are limited in their applicability.

In vitro scratch assay:

The first stage in the wound healing process is the migration and proliferation of adjacent cell populations into the wounded area which makes the migration phase as the limiting event in wound healing. Therefore, *in vitro* assays studying the wound healing process were developed based on the migration assays as these assays are simple, inexpensive and uses common supplies available in most cell culture laboratories.

The basic principle behind migration assays is to deliberately disrupt a confluent cell monolayer culture with any chemical and/or mechanical means to create a standardised region of artificial gap or scratch under defined conditions. This is followed by analysing and documenting the migration of cells into this formerly cell-populated area to close the gap [328]. In this manner, the scratch assay can mimic the migration of cells *in vivo* to some extent. Moreover, improvisation of the simple scratch assay by coating the monolayer culture of cells

with ECM-derived components can enable to study the regulation of cell migration by cell-matrix interaction in real-time imaging [329].

Several modifications of the conventional scratch assay have enabled researchers to track migration of individual cells in response to exogenous compounds. This assay can also permit the immunocytochemical analysis of different proteins on cellular migration. Treating cells *via* gene transfection can allow for investigations into the effects of exogenous genes on the migration pattern of these cells that could be monitored with the help of time-lapse microscopy imaging [328]. Table 3.1 enlists advantages and limitations of common wound healing assays in 2D.

Table 3.1: 2D in vitro wound healing assays.

Method	Description	Advantages	Limitations
Scratch assay	Scratching of confluent cell monolayer with the help of a serological pipette tip or cell scarper	Easy to use, required equipment is easily available in cell culture laboratories	Irregular formation of scratch Disruption of ECM coating
Stamping	Applying pressure on cells in a defined region on cell monolayer culture	Possibility of formation of any shape ECM coating remains intact	Irregularities in manual pressure applied
Thermal wounding	Applying excessive heat in a defined region on cell monolayer culture	*In vitro* model to study thermo-mechanical damage to cells	Difficulty in restraining the thermal effect to a particular area
Electrical wounding	Applying pulses of high voltage to a defined region on cell monolayer culture	Ability to control and measure cell growth and destruction by impedance	Detachment of confluent cell layer

Optical wounding	Applying laser to create a wounded area on a defined region on cell monolayer culture	High reproducibility and controlled exposure	Heating up of the culture dish can affect cell viability

Limitations of 2D scratch assays:

There are several limitations associated with *in vitro* scratch assay compared to the other available methods. Major disadvantage includes chances of irregular dimensions of scratch formation on the monolayer culture while doing manual wounding with the help of a serological pipette tip or cell scraper. This manual wounding can also cause disruption of ECM coatings on the cell monolayer that can impede migration data analysis [330]. Another disadvantage includes the accumulation of removed cells on the edges of scratch after introducing artificial gap onto the cell monolayer. These clusters of removed cells can affect consequent migration and proliferation of cells and hence can obstruct data acquisition in real-time analysis.

In addition to this, as 2D *in vitro* scratch assay is performed on cell monolayers, there is an absence of tissue gradient and stratification which are the key attributes of cells and tissues *in vivo*. Hence, the cellular response in 2D cultures towards injury is not true representation of the *in vivo* wound healing response. Moreover, as no chemical gradient is established in monolayer cultures hence no cellular response towards chemotaxis could be investigated in 2D scratch assays.

3D in vitro wound healing models:

In recent years, there has been an increased shift from 2D wound models to 3D *in vitro* wound healing models based on the fact that cells, specifically fibroblasts (one of the key players in wound healing process) cultured in 3D matrices acquire a completely distinctive morphology, metabolic activity, proliferative rate and migration behavior as compared to their 2D cultured equivalents [331]. Grinnell [332] reported that there was a dramatic phenotypic change occurred from fibroblasts to myofibroblasts when fibroblasts were cultured in 3D matrices exposed to mechanical tensions. The migrating fibroblasts differentiation to myofibroblasts has been reported in granulation tissue formation *in vivo* that leads to wound contraction. Indeed,

the migration and proliferation of cells towards the injury site occurs in the presence of other surrounding cell types and ECM in a true *in vivo* situation. This complex microenvironment could only be served *in vitro* using 3D wound healing models.

The most popular is the tissue engineered human skin that was developed to recapitulate key structural and functional aspects of natural skin to serve as skin substitutes. These 3D tissue engineered skin equivalents have not only been utilised as graft materials for dermal reconstructive surgeries but are now emerging as *in vitro* preclinical testing model systems as shown in Figure 3.2 [333].

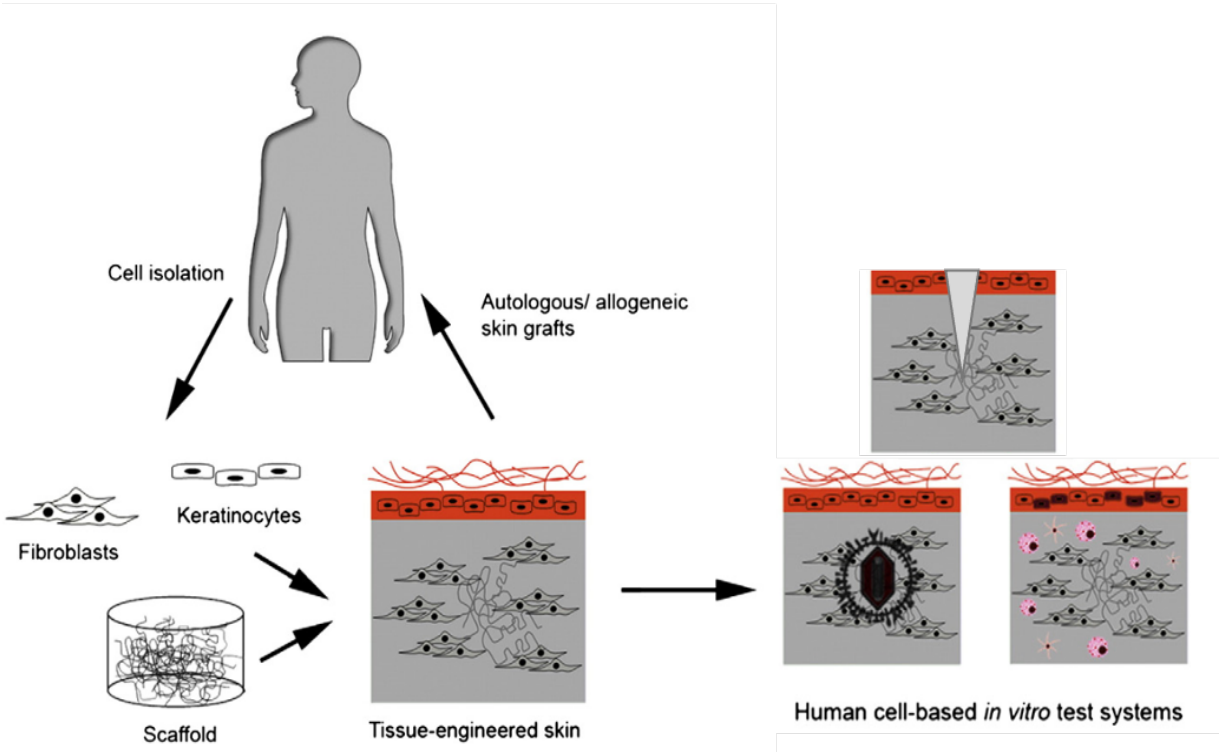

Figure 3.2: Schematic of potential applications of tissue engineered dermal constructs. Adapted from [333].

In routine pharmacological research, testing of different compounds is usually performed on skin substitutes composed only of an epidermal layer supported on synthetic membranes, however other preclinical testing protocols require the addition of connective tissue component. Nolte *et al.,* [334] have studied the key role of dermal fibroblasts differentiation in the formation chronic wounds and scar tissue formation in dermal wound healing. In this context, fibroblasts have recently been receiving a lot more attention due to their interactions

with keratinocytes during wound healing [335] and their positive influence on keratinocytes proliferation *in vitro* by secreting soluble growth factors in culture. Using skin substitutes, it was demonstrated that the crosstalk between fibroblasts and keratinocytes is essential to maintain natural epidermal histogenesis [336]. Hence, full-thickness dermal substitutes containing both the dermal and an epidermal component are desirable to study key mechanism of wound healing *in vitro*. Table 3.2 demonstrates the list of commercially available partial-thickness (PT) and full thickness (FT) dermal substitutes.

Table 3.2: Commercially available in vitro partial-thickness (PT) and full thickness (FT) dermal substitutes [333].

Brand name/manufacturer	Scaffold material	Cell source	Dermis
Episkin™/L'Oreal Nice, France	Collagen	Keratinocytes (mammary/abdominal samples obtained from healthy consenting donors during plastic surgery)	No
Skinethic™ RHE/L'Oreal, Nice, France	Polycarbonate membrane	Keratinocytes (neonatal foreskin tissue or adult breast tissue)	No
Epiderm™/MatTek Corporation, Ashland MA, USA	Collagen-coated, polycarbonate membrane	Human keratinocytes (neonatal foreskin, adult breast skin)	No
EpiDermFT™/MatTek Corporation, Ashland MA, USA	Collagen	Human keratinocytes (neonatal foreskin, adult breast skin), human fibroblasts (neonatal skin, adult skin)	Yes
EST-1000/CellSystems, Troisdorf, Germany	Polycarbonate membrane	Keratinocytes (neonatal foreskin)	No
AST-2000/CellSystems, Troisdorf, Germany	Collagen	Human keratinocytes Human fibroblasts	Yes
Phenion® FT Model/Henkel AG&Co.KGaA Duesseldorf, Germany	Bovine, cross linked, lyophilized collagen	Primary human keratinocytes (neonatal foreskin), human fibroblasts (neonatal foreskin)	Yes
StrataTest®/Stratatech Corporation Madison WI, USA	Collagen I	immortalized, human NIKS® keratinocytes dermal fibroblasts	Yes

Wound healing in pelvic floor reconstruction:

The process of wound healing in pelvic floor reconstruction is highly complex and is subjected to constant motion and weight bearing due to changes in the intraabdominal pressure and upright posture. On one hand, the elasticity and high vascularity of the vaginal tissue and associated fascia is a favorable factor in wound healing, mobility and weight bearing properties remain unfavorable. In addition, presence of any pre-existing vaginal pathology or introduction of graft materials for reconstructive procedures add further complexity to this process. Vaginal wound healing is affected by three main factors: nature of the native tissue and the surrounding microenvironment, material used for the repair (implant) and the surgical technique involved.

Pelvic floor disorders (PFDs) and impact on wound healing:

As Ulmsten [337] identified the "defective connective tissue profile" as the representative feature of pelvic floor dysfunctions, the compromised connective tissue have an impact on vaginal tissue wound healing. Several studies have reported differences in the amount of collagen in ECM in patients suffering from POP and SUI [338]. An increased expression of collagen type III in women with POP that results in an altered collagen I/III ratio correlates with the weakened connective tissue and impaired wound healing [339]. Surgical treatment for POP often requires patients' autologous fascia or vaginal connective tissue to reinforce the prolapsed pelvic organs and wound healing plays a critical role in the outcome of such procedures. Throughout the lifetime of an individual, the quality of wound healing changes considerably and ranges from an ideal wound healing in vaginal connective tissue to impaired healing in old age which became worsen if there is pre-existing vaginal pathologies [340].

In vivo rat model of vaginal wound healing:

Novel therapies and biomaterials developed for use in the pelvic floor reconstructive procedures are often tested in subcutaneous animal models. Shveiky *et al.,* [341] developed a rat vaginal injury model to investigate factors that determine age-related impaired vaginal wound healing *in vivo*. Macrophages play a key role in the inflammatory response towards injury and display remarkable plasticity in terms of their phenotype during the wound healing process [342]. The M1 phenotype which is associated with proinflammatory response that is expressed during the early stages of wound healing which later shifted towards M2 phenotype associated with tissue remodeling and healing [343]. This shift from M1 to M2 phenotype is crucial in complete recovery and healing of wounds. Studies have suggested that aging delays the macrophage polarisation from M1 to M2 and a prolonged M1 phenotype can impair wound healing [344]. Similar observations were demonstrated by Menachem-Zidon *et al.,* [345] in *in vivo* rat vaginal wound healing model.

In vivo rabbit menopause model of vaginal wound healing:

Since the majority of the pelvic reconstructive surgeries are performed in postmenopausal women, it is imperative to understand how oestrogen deficiency can affect the vaginal wound healing process. A number of studies performed mostly on cutaneous tissue have elucidated the role of oestrogens in wound healing process which is substantially protracted in their

absence [346]. Clinical data has suggested an improvement in cutaneous wound healing in elderly patients after administration of topical oestrogens [347]. Abramov *et al.,* [348] studied the process of vaginal incisional wound healing in a rabbit menopause model equivalent to human surgical menopause. Their results suggested that hypoestrogenism caused a significantly delayed wound healing in the vagina of oophorectomised rabbits histologically which was associated with increased neutrophil elastase activity and fibronectin degradation.

In vitro tissue engineered vaginal wound healing models:

This chapter has demonstrated the development and characterisation of tissue *engineered in vitro* vaginal wound model using decellularised sheep vaginal tissues and primary sheep vaginal epithelial cells and fibroblasts. The TE vaginal wound models presented here were developed to study the underlying complex mechanism of vaginal wound healing in a rapid, simple and cost-effective *in vitro* models. In addition, the effect of oestrogens on the vaginal wound healing process was investigated without the inherent heterogeneity of *in vivo* models. The TE *in vitro* vaginal models presented here were appropriate to study the mechanism of action of oestrogens which is complicated in *in vivo* models without any involvement of ethical considerations that are associated with *in vivo* animal studies.

3.3 Materials and Methods:

3.3.1 Primary sheep vaginal epithelial cells and fibroblasts and decellularised sheep vaginal tissues:

Primary sheep vaginal epithelial cells and fibroblasts were isolated and maintained as stated in sections 2.3.4 and 2.3.5 and decellularised sheep vaginal tissues were prepared by the detergent method as detailed in section 2.3.5.

3.3.2 Developing and culturing tissue engineered (TE) wound vaginal models:

A schematic of the key stages involved in the development of TE full-thickness and partial-thickness wound vaginal models is shown in Figure 3.3.

De-epithelialised, decellularised sheep vaginal tissues (de-SVT) were sterilised as stated in section 2.3.5. Tissue sections were cut (1.5 x 1.5 cm^2) aseptically with the help of sterilised surgical scalpel blades and placed in a 6-well culture plate with the basement membrane side facing upwards.

Sterilised chamfered surgical stainless-steel rings containing an internal diameter of 8 mm were placed on top of each de-SVT in such a way such to ensure a tight seal around the edges of the rings. Each ring was seeded with a 500 µL co-culture cell suspension of primary vaginal fibroblasts and epithelial cells (between passage 2-3) in Green's media at a seeding density of 3 x 10^5/model and 6 x 10^5/model respectively. While 4 mL Green's media was added to the outside of rings to stop leakage of the cell solution from within the rings. The cultures were incubated at 37°C with 5% CO_2 overnight.

After 24 hrs, the rings were removed with the help of sterile forceps and culture plates re-incubated in same conditions overnight. After 3 days in submerged culture conditions, the models were carefully and aseptically transferred to sterile petri dishes under biosafety Class II laminar flow hood. With the help of a sterile scalpel blade, full-thickness (FT) and partial-thickness (PT) incisions were performed separately on TE models as shown in Figure 4.3. The TE wound vaginal models were then immediately transferred to sterile stainless-steel grids placed in new 6-well culture plates using a set of sterile forceps with the wounded cell seeded

side facing upwards. The wells were then topped up with Green's media to overflow the grids but not the wounded model in order to maintain an air-liquid interface (ALI).

The models were cultured in Green's media for 3 days under submerged conditions and then after placing FT and PT wounds, the models were incubated for an additional three weeks at an air-liquid interface (ALI) at 37°C with 5% CO_2 and media changed twice every week. Blanks and controls were run alongside using unwounded TE vaginal models and the native SVT. TE wound models were fixed at different time points (days 1, 7,14 and 21) in 3.7% v/v formaldehyde to trace the progress of reepithelialisation and wound healing.

To study the effect of estradiol-17β induction on wound healing in TE vaginal models, E_2 concentration 100 pg/mL of Green's media was selected as it is the reported average optimal concentration of estradiol-17β in the serum levels of pre-menopausal healthy women [349]. Whereas, the reported threshold of estradiol-17β in the serum levels of post-menopausal women (referred for HRT) is below 20 pg/mL [349] so i selected E_2 concentration of 100 pg/mL for my *in vitro* vaginal wound healing studies. E_2 (100 pg/mL Green's media) was added to the PT wound vaginal models after transferring the models to ALI and continued culturing for three weeks in standard culture conditions described above. Blanks and controls were run alongside using wounded TE vaginal models without E_2 (100 pg/mL) and the native SVT. TE wound models were fixed at different time points (days 1, 7,14 and 21) in 3.7% v/v formaldehyde to trace the progress of reepithelialisation and wound healing.

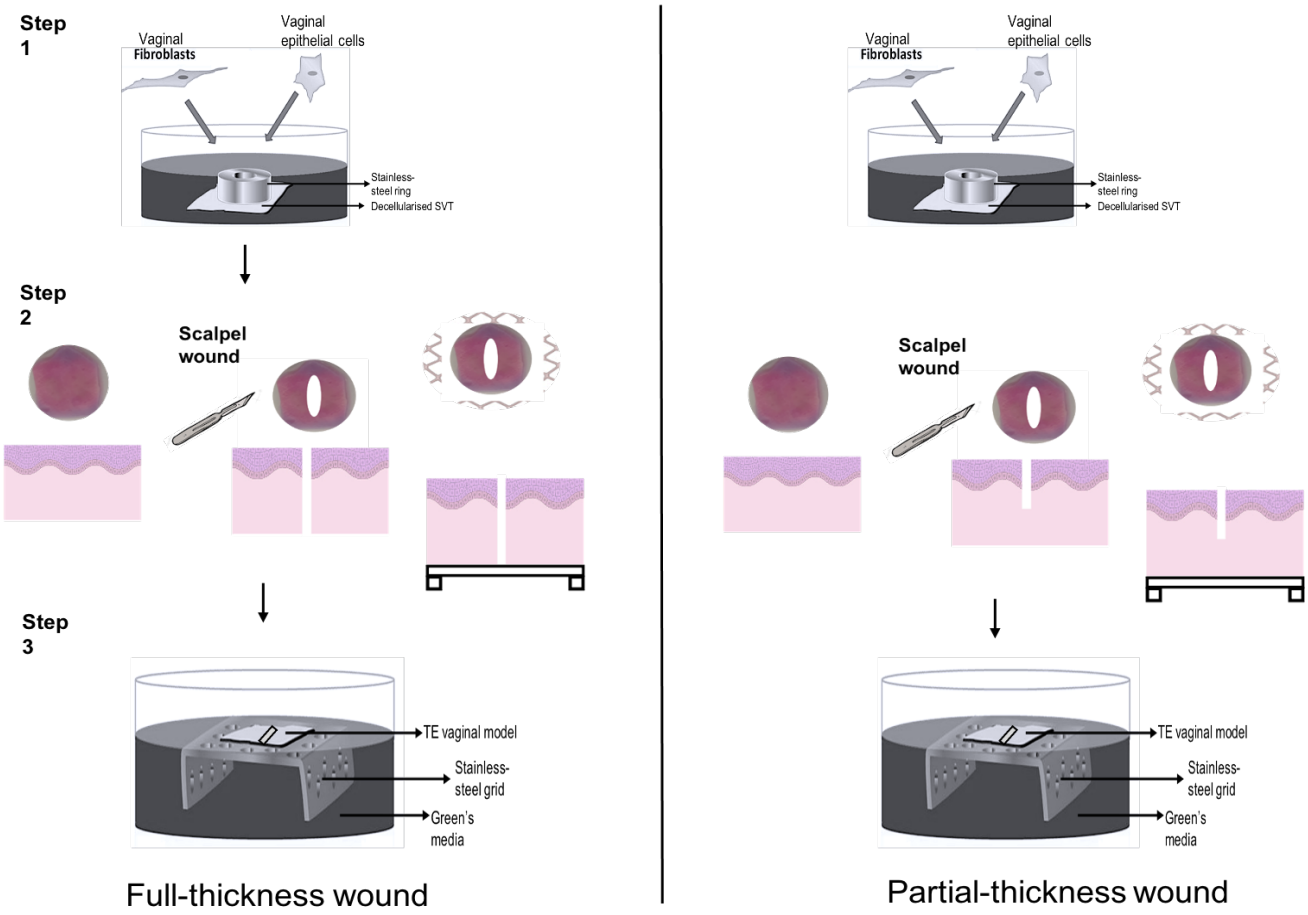

Figure 3.3: Schematic of key steps for the development of full-thickness (FT) and partial-thickness (PT) in vitro TE wound vaginal models.

3.3.3 Fixation and histological analysis of TE wound vaginal models:

The fixation, viability, tissue processing, sectioning, H&E staining and picosirius red staining of TE wound vaginal models was performed as described in sections 2.3.8 - 2.3.12.

3.3.4 Measurement of epithelia thickness in TE wound vaginal models:

All images used for the measurement of epithelia thickness in TE wound vaginal models were captured using a light microscope Motic BA210 series (Motic, Xiamen, China) with integrated ColorVu camera. Images were taken at different objective magnifications and analysed using ImageJ software (National Institute of Health).

At first, a standard image with known measurements was opened in the Image J software. Using the “line” tool from the drawing/ selection tools, the known area of measurement was

measured, and the measurement was recorded in the "known distance" in the set scale tool in the Analyze menu. The image to be analysed was then opened in ImageJ software and three random regions of epithelia were measured and recorded using the "line" tool from the drawing/ selection tools. For each parameter, three random regions on three different images were measured (*n = 9*). All experiments were performed in triplicates (*N=3*). Graphs were drawn using GraphPad Prism V9.1.0 (216) and statistical analysis was performed as described in section 2.3.16.

3.3.5 Trichrome staining:

Materials:

Masson-Goldner staining Kit:

The Masson-Goldner staining kit (1.00485) for the visualization of connective tissue with trichromic staining was purchased from Sigma-Aldrich, UK. The reagents from the kit were stored in a dry place at room temperature in dark.

The Masson-Goldner staining kit (1.00485) contained the following four reagents:

Reagent 1: Azophloxine solution (273742)

Reagent 2: Tungstophosphoric acid Orange G solution (273744)

Reagent 3: Light green SF solution (273745)

Reagent 4: Acetic acid 10% (v/v) (221040)

Weigert's hematoxylin:

Weigert's iron hematoxylin solution (HT1079) was purchased from Sigma-Aldrich, UK. The reagent was stored in a dry place at room temperature in dark. Prior to use, the reagent was filtered using a Whatman's filter paper (Grade 1, Sigma-Aldrich, UK) to separate any undissolved particles from the reagent and then used neat on the slides for staining.

Methods:

Histopathological analysis of wound healing on TE vaginal models was performed using Masson's trichrome staining following the protocol of Suvik and Effendy [350]. The slides were prepared according to the protocols described previously in section 2.3.10. Masson's trichrome staining was performed using different reagents from the Masson-Goldner staining kit for different time periods and the details are given in Table 3.3. After staining, the slides

were mounted with DPX (Dibutyl phthalate, Polystyrene, Xylene) and coverslips were placed carefully on the top of the stained samples in such a way so as to avoid entrapment of air bubbles.

Table 3.3: Series of events during Masson-Goldner Trichrome staining.

Solution	Time exposed	Purpose
Xylene	3 mins	To remove the paraffin from the slides
Xylene	3 mins	
Absolute alcohol	1 min	To gradually rehydrate tissue sections
70% v/v alcohol	30 seconds	
Distilled water	1 min	To remove any debris from the slides
Weigert's hematoxylin	5 mins	To stain the cell nuclei purple or blue
Running tap water	5 mins	To remove excess stain
1% acetic acid	30 seconds	Washing
Azophloxine solution	10 mins	To stain the muscle fibres red
1% acetic acid	30 seconds	Washing
Tungstophosphoric acid Orange G solution	1 min	To stain the erythrocytes red/orange
1% acetic acid	30 seconds	Washing
Light green SF solution	2 mins	To stain the collagen fibres green
1% acetic acid	30 seconds	Washing
70% v/v alcohol	dunk	To gradually dehydrate tissue sections
Absolute alcohol	30 seconds	
Xylene	10 seconds	To dehydrate tissue samples and remove any residual stains or impurities
Xylene	dunk	

Slides analysed and Image acquisition:

The DPX mounted slides were left air dried for 24 hours before imaging with a light microscope Motic BA210 series (Motic, Xiamen, China) with integrated ColorVu camera. Images were taken at different objective magnifications and analysed using ImageJ software (National Institute of Health).

3.3.6 Immunohistofluorescence staining of TE wound vaginal models:

Materials

Primary antibodies:

The details of the primary antibodies used is given in Table 3.4.

Table 3.4: List of primary antibodies used.

Antibody	Details	Isotype	Supplier	Dilution used
Anti-Ki67 antibody (ab15580)	Rabbit polyclonal to Ki67	IgG	Abcam, UK	1:100 in PBS
Anti-alpha smooth muscle Actin antibody [1A4] (ab7817)	Mouse monoclonal [1A4] to alpha smooth muscle Actin	IgG2a	Abcam, UK	1:100 in PBS

Secondary antibody:

The details of the secondary antibodies used against the primary antibodies enlisted in Table 3.4 is given in Table 3.5.

Table 3.5: List of secondary antibodies used.

Antibody	Details	Isotype	Supplier	Dilution used
Donkey anti- rabbit IgG H&L (Alexa Fluor® 647) preadsorbed (ab150063)	Donkey Anti-Rabbit IgG H&L (Alexa Fluor® 647) preadsorbed Polyclonal (λ_{ex} 652 nm, λ_{em} 668 nm)	IgG	Abcam, UK	1:200 in PBS

Goat Anti-Mouse IgG H&L (Alexa Fluor® 555) preadsorbed (ab150118)	Goat Anti-Mouse IgG H&L (Alexa Fluor® 555) preadsorbed (λ_{ex} 555 nm, λ_{em} 565 nm)	IgG	Abcam, UK	1:200 in PBS

4′,6-diamidino-2-phenylindole (DAPI):

DAPI staining solution (ab228549) (λ_{ex} 358 nm, λ_{em} 461 nm)10 mM solution in water was purchased from abcam, UK and stored in 10 µL aliquots at -20 °C until use. Immediately before use, 10 µL of the DAPI stock solution was defrosted at room temperature and diluted by adding in 10 mL PBS to give a working concentration of 1µg/mL. The solution was kept protected from light and used on slides placed in a dark humidified chamber.

Methodology:

The immunohistofluorescence (IHF) staining of TE wound vaginal models was performed on 5 µm thick tissue sections mounted on glass slides as detailed previously in section 2.3.14. Similar protocol was used for both antibodies on separate samples. After staining, the slides were then counterstained with DAPI for 30 mins in a dark humidified chamber, later mounted with DPX and imaged with an epifluorescence microscope (Olympus IX73).

3.3.7 Image analysis and fluorescence intensity measurement:

Immunohistofluorescence images of the samples were captured using an Olympus IX73 inverted microscope (Life Science Solutions, GB) and a RETIGA 6000 (Imaging®) interfaced to a Dell computer using Micro-Manager V 1.4.23 20210215 software. The images were taken at different objective magnifications and three random fields of view were captured on each sample and analysed. Quantification of the fluorescence was done by using ImageJ software (National Institute of Health).

The image to be analysed was opened in ImageJ software and the fluorescence region of interest was outlined using the “rectangle” drawing/selection tool. Then from the “Analyze”

menu “set measurements” was selected and three parameters “area”, “integrated intensity” and “mean grey value” were checked. The fluorescence intensity was then measured by selecting “Measure” from the “Analyze” menu. Similarly, the fluorescence intensity from three random fields of view was measured on the image and for same experimental conditions three separate experiments were performed (*n=9*). Similar protocol was followed for each parameter and experiments were run in triplicates (*N=3*). The background fluorescence was measured by selecting three regions on the image that showed no visible fluorescence and average value was calculated.

The fluorescence intensity values measured as integrated density (IntDen) were quantified as median intensity of fluorescence from each image as some regions on the image could be overexposed and the values were not true representative of actual fluorescence intensity. Hence, the mean fluorescence intensity was estimated by calculating the corrected total cell fluorescence (CTCF) by applying the following formula:

*CTCF= Integrated density – (Area of selected cell x Mean fluorescence of background readings)

Graphs were drawn for the fluorescence intensity measurements using GraphPad Prism V9.1.0 (216) and statistical analysis was performed as described in section 2.3.16.

3.4 Results:

3.4.1 Development and characterisation of TE wound vaginal models:

Full-thickness (FT) TE wound vaginal models were developed by making a clean incision through the full length of the vaginal models before transferring to ALI and the progress of wound re-epithelialisation was monitored by fixing the tissue samples at different time points. Figure 3.4 depicts the haematoxylin and eosin (H&E) stained sections of wounded models at days 1, 7. 14 and 21 following FT incision. At day 1, a clear region of gap could be seen that runs throughout the entire length of the wound in the models. After a week in ALI culture, the edges of the wounded tissue sections were observed folded and cellular migration started to become visible into the wounded region. At day 14, more cellular infiltration could be seen concentrated around the area of wound with folded edges of the tissue sections. At day 21, formation of a stratified epithelium on the basement membrane was observed that continued into the wounded area. As the wounded region ran through the entire length of the TE vaginal model, the re-epithelialisation was observed only up to halfway through the wound as the gap was seen quite big for the cultured vaginal epithelial cells and fibroblasts to completely filled in. Moreover, after 3 weeks in ALI culture the formation of a stratified squamous epithelia containing 6-9 layers of epithelial cells could be seen on TE FT wound vaginal models as presented in Figure 3.4.

Partial-thickness (PT) TE wound vaginal models were developed by making a clean incision up to halfway through the entire length of the TE vaginal models before transferring to ALI. Figure 3.5 demonstrates the series of events occurred during the PT wound healing in TE vaginal models using H&E staining over three weeks in ALI culture. At day 1, the region of wound could be seen up to halfway through the TE vaginal model. At higher magnification (20X), a higher cellular infiltration near the region of wounded area was observed and the vaginal fibroblasts could be seen clustered around the edges of the PT wound. At day 7, cellular migration and infiltration into the wounded region of the TE models were observed and beginning of the re-epithelialisation occurred as dense cellular mass was starting to form in the region of wound over the basement membrane. At day 14, cellular proliferation into the wounded region increased and the beginning of formation of a stratified epithelium (1-2 layers) could be seen extended into the wounded region. By day 21, the cellular mass appropriately covered the wounded region, and the epithelium was shown formed completely on TE PT

wound vaginal models. However, the epithelia formed on PT wound models was not able to stratify to a greater extent and only was about 1-2 layers thick and the uppermost layer was seen keratinised. The wounded region was about 70-80% healed with cellular infiltration into the gap.

The metabolic activity of primary vaginal epithelial cells and fibroblasts cultured on the FT and PT wounded vaginal models showed increasing viability up to three weeks in ALI culture as shown in Figure 3.6. The TE wound vaginal models were not cultured beyond three weeks in subsequent experiments because in case of the PT wound vaginal models, sufficient cellular infiltration and wounded area closure was observed at day 27 of the ALI culture.

Immunohistofluorescence staining for the detection of Ki67 in FT and PT wound vaginal models after 3 weeks in ALI culture was performed to detect the number of proliferating cells into and around the wounded region. Figure 3.7 demonstrates the FT and PT wound tissue sections stained with Ki67 (red channel) and counterstained with DAPI (blue channel). In both FT and PT wound models, the basal epithelial cells were stained intensely for the expression of Ki67 showing that the cells in the basement membrane were proliferative that became more and more differentiated in the suprabasal layers and a very few cells were seen positive for Ki67 expression in the suprabasal layer and visible no expression was observed in the superficial layers in both FT and PT wound vaginal models. In addition to this, no visible differences in the expression of Ki67 were observed in both FT and PT wound vaginal models after 3 weeks in ALI culture conditions.

Further quantitative analysis of Ki67 expression was performed to compare the fluorescence intensity for Ki67 expression (red channel) in FT and PT wound vaginal models and are depicted in Figure 3.8. The fluorescence intensity was measured using ImageJ software and the values were compared and graphically represented in Figure 3.8.

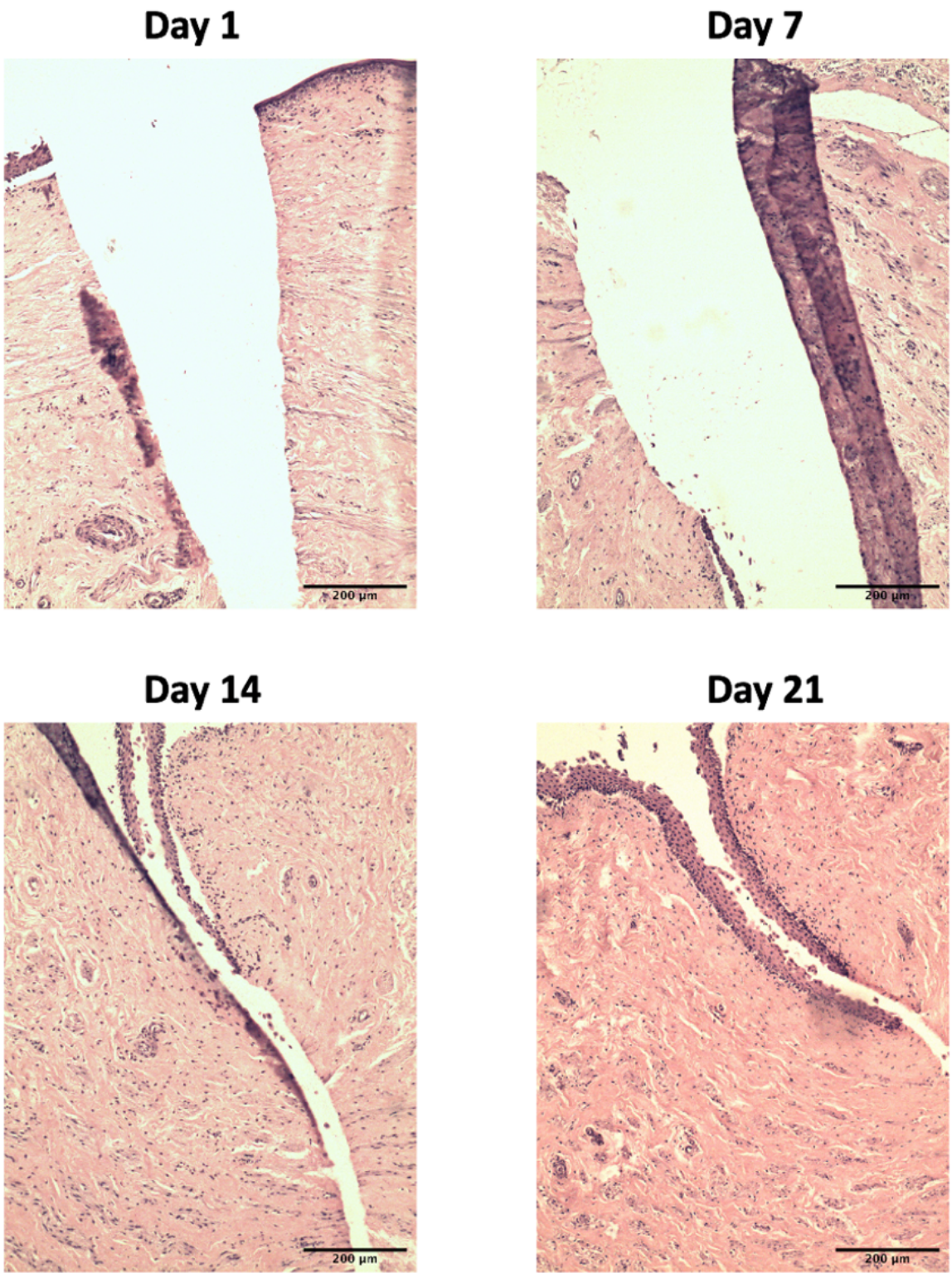

Figure 3.4: Haematoxylin and Eosin (H&E) stained sections of full-thickness (FT) vaginal wound models at different time points. Scale bar=200µm.

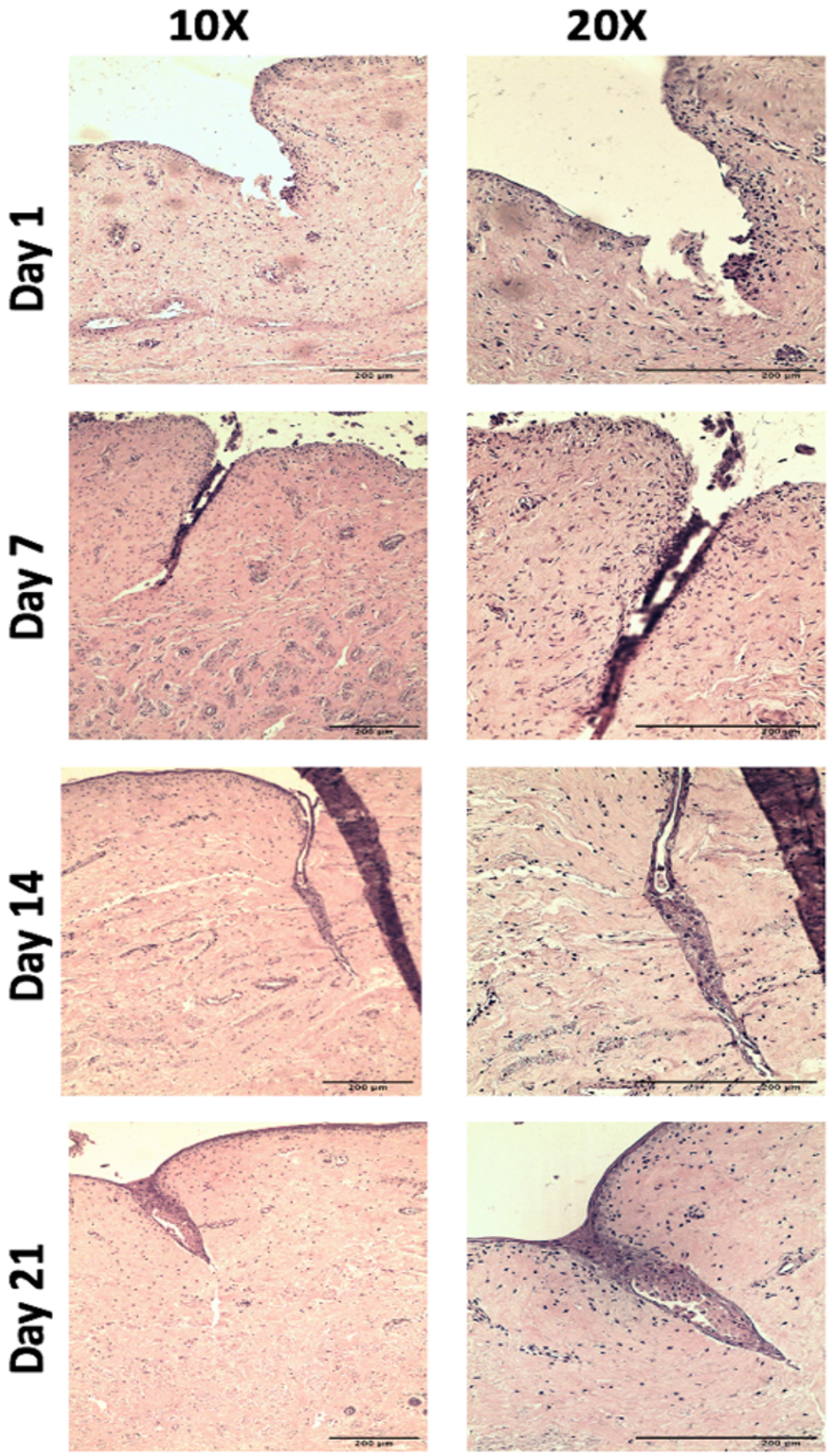

Figure 3.5: Haematoxylin and Eosin (H&E) stained sections of partial-thickness (PT) vaginal wound models at different time points. Scale bar=200 μm (applies to all).

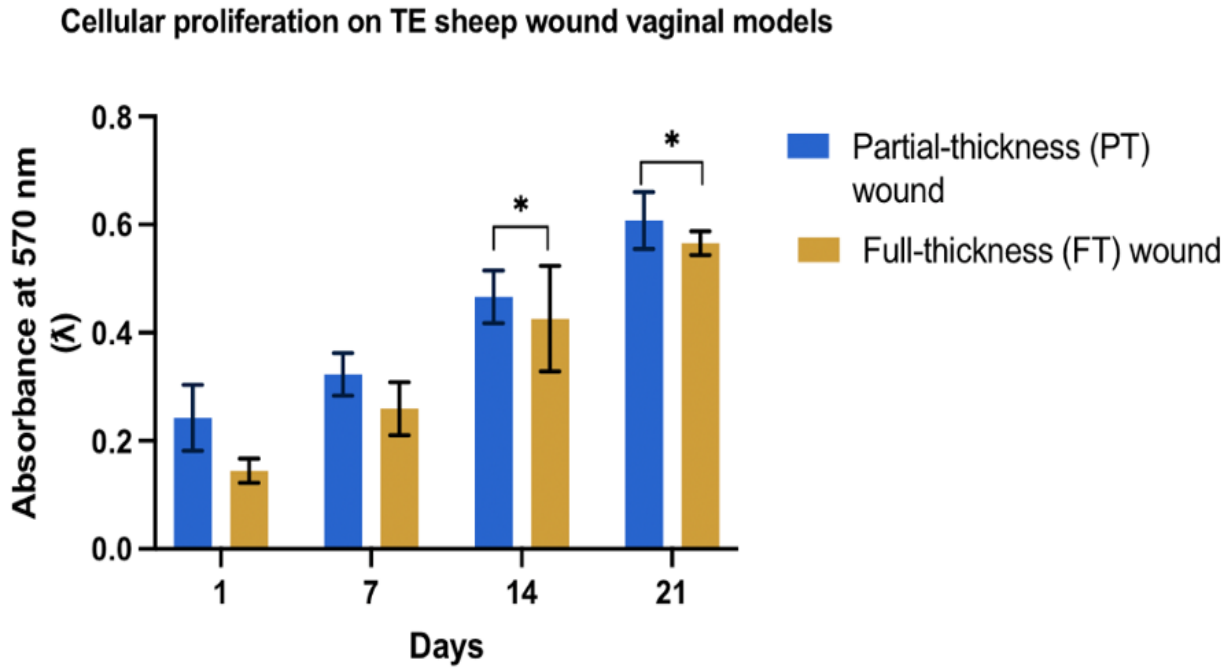

*Figure 3.6. Metabolic activity of primary sheep vaginal epithelial cells and vaginal fibroblasts cultured on FT and PT wound vaginal models at different time points as measured by the resazurin assay. (n=9 ± SD for each group, N=3, *p <0.05).*

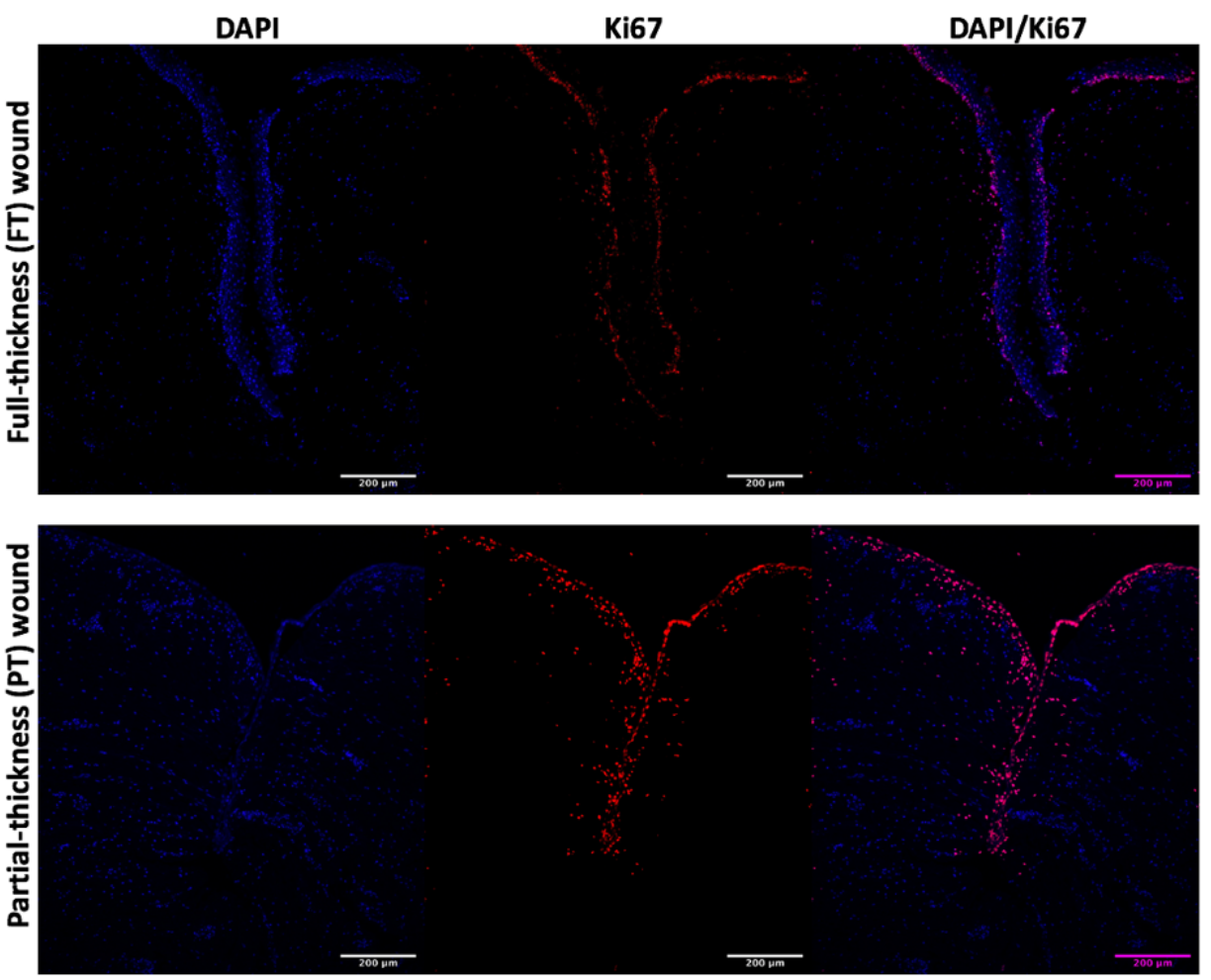

Figure 3.7: Immunohistofluorescence staining (IHF) of FT and PT wound vaginal models for the detection of Ki67 expression, a marker for proliferative cells, after 3 weeks in ALI culture conditions. The basal cells of the vaginal epithelia were stained intensely for Ki67 (red channel) in both FT and PT wound vaginal models whereas the vaginal epithelial cells present in the suprabasal and superficial layers did not show any expression for Ki67. All tissue sections were counterstained with DAPI (blue channel). Scale bar=200µm (applies to all).

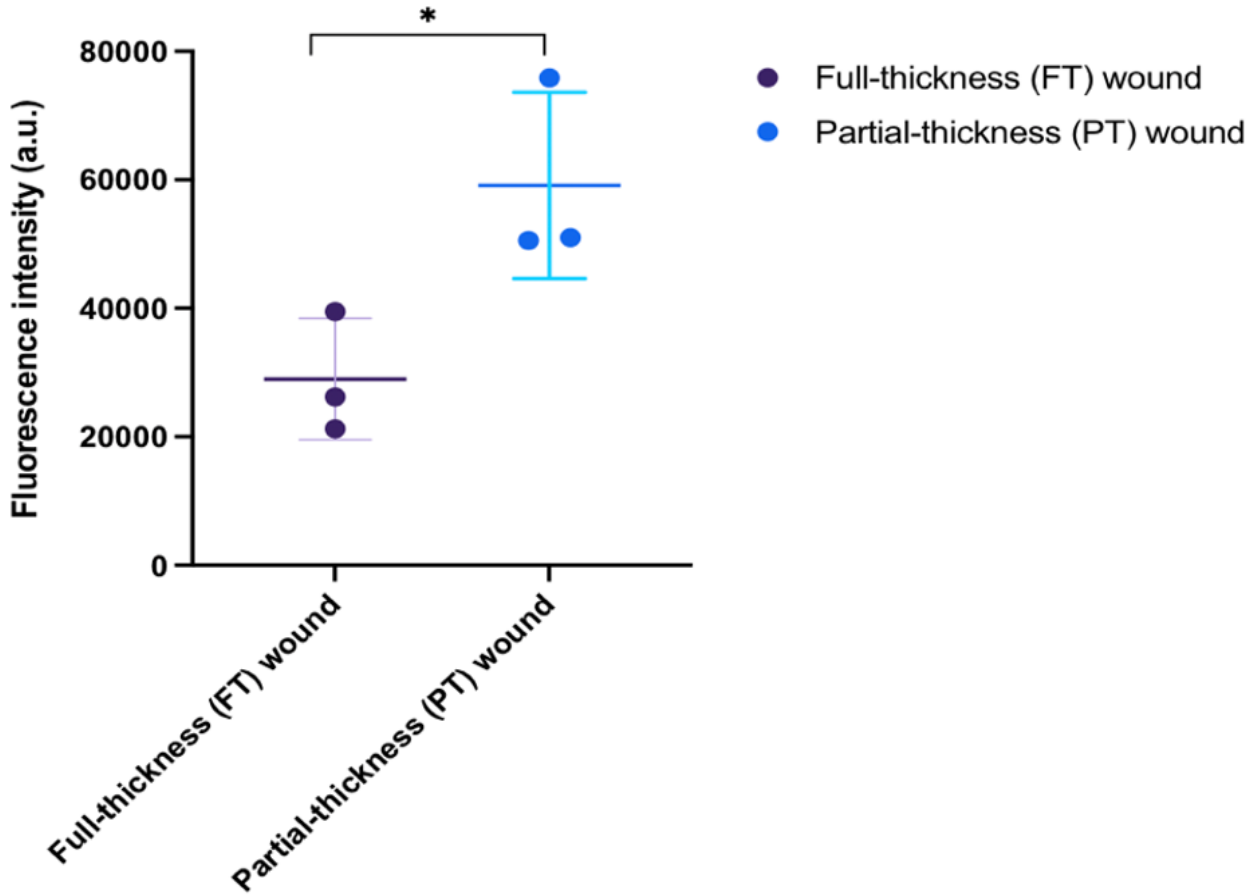

Figure 3.8: Graphical representation of fluorescence intensity of Ki67 marker expression on FT and PT wound vaginal models after 3 weeks in ALI culture conditions.
*(n=9 ± SD for each group, N=3) *p <0.05.*

3.4.2 Development and characterisation of PT wound vaginal models under estradiol-17β induction:

Figure 3.9 demonstrates the series of events monitored at different time points during the progress of PT wound healing under estradiol-17β induction in ALI cuture for upto three weeks. The concentration of estradiol-17β selected was 100 pg/mL based on the reported average serum concentration of estradiol-17β in normal healthy pre-menopausal women. The same E_2 100 pg/mL concentration was used in subsequent experiments for studying the effect of estradiol-17β on wound healing in PT TE wound vaginal models. At day 1 after the placement of PT incision on the models, the beginning of cellular migration into the wounded region was observed. The cultured vaginal epithelial cells and fibroblasts were seen

concentrated around the ridges of the PT wound. By day 7, the edges of the wounded tissue sections were appear folded and an increase in cellular infiltration and proliferation into the wounded area was observed as clumps of cells could be seen filling in the region under estradiol-17β induction. At day 14, process of re-epithelialisation began with the formation of discontinuos regions of epithelial lining closer to the wounded region. After 3 weeks, the wounded region was observed to be fully healed with the reformation of a stratified epithelium (7-9 layers) on PT wound vaginal models under estradiol-17β induction. This phase was considered as the remodelling phase as the cultured cells produced matrix resembling the native vaginal tissue ECM and a stratified epithelium that entirely covered the wounded region at the top that showed improved TE vaginal wound healing as shown in Figure 3.9.

Additionally, the metabolic activity of cultured primary vaginal epithelial cells and fibroblasts on PT wound vaginal models was also influenced by the presence of estradiol-17β (100 pg/mL) in the culture medium. Figure 3.10 shows that in the presence of estradiol-17β there was a significant increase in the cellular metabolic activity on PT wound vaginal models as compared to in the absence of estradiol-17β. These findings revealed that our PT TE wound vaginal models were estradiol-17β responsive mimicking the in vivo cell behaviour in an *in vitro* environment.

To further confirm these findings, immunohistofluorescencve staining was performed to detect the expression of Ki67 marker in the presence and absence of estradiol-17β on PT wound vaginal models. Figure 3.11 demonstrates the IHF analysis for Ki67 expression and in both PT wound model and PT wound model with E_2 (100 pg/mL) cells closer to the wounded area were observed intensely positive for Ki67 expression which showed that cells were highly proliferative around the wounded region on TE models. In the presence of E_2, the intensity of the signal was higher compared to when it is absent in the culture medium which is reflective of proliferative stimulus of E_2 on vaginal epithelial cells and fibroblasts as shown in Figure 3.11. These results were further confirmed by quantitatively measuring the fluoresence intensity for Ki67 expression with and without E_2 induction on PT wound models as shown in Figure 3.12.

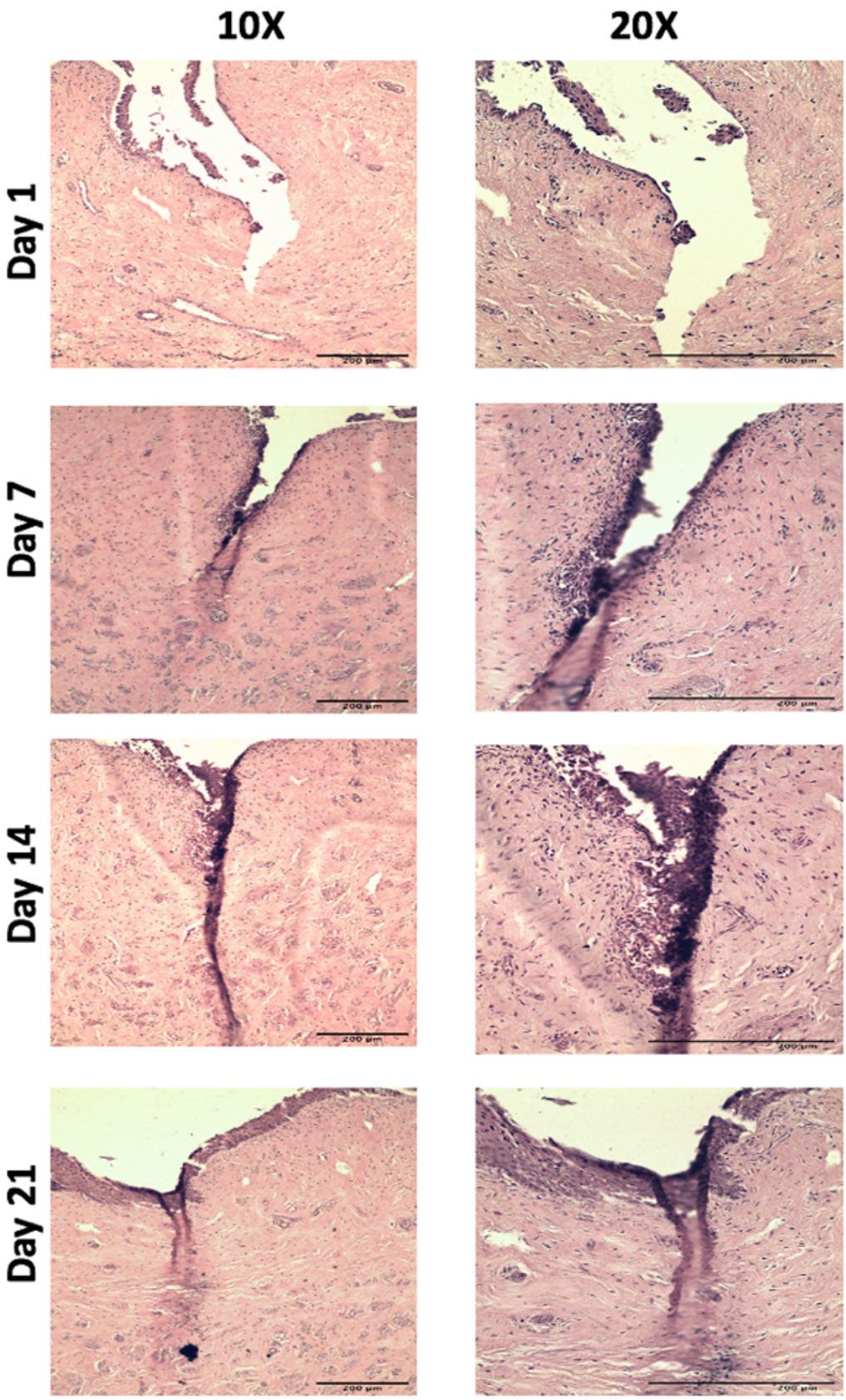

Figure 3.9: Haematoxylin and Eosin (H&E) stained sections of partial-thickness (PT) vaginal wound models under E_2 induction (100 pg/mL) at different time points in ALI culture. Scale bar= 200μm.

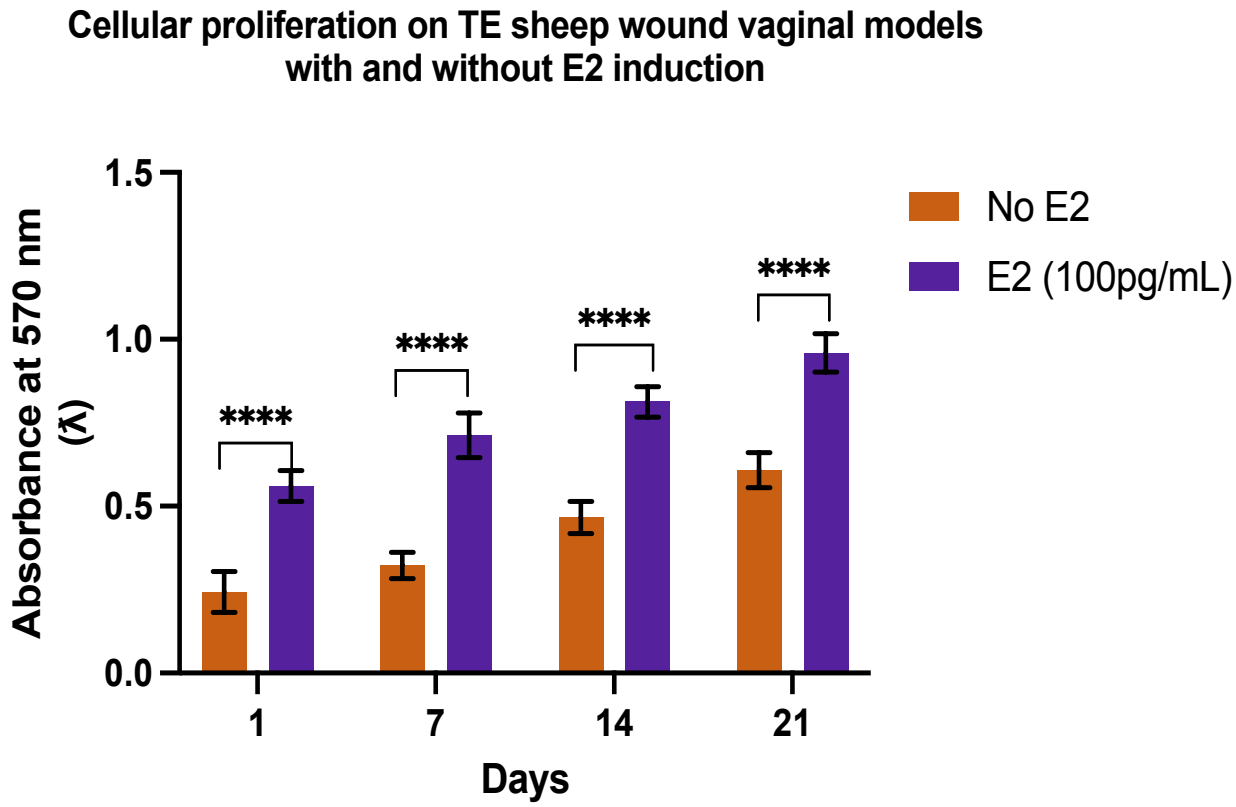

*Figure 3.10: Metabolic activity of primary sheep vaginal epithelial cells and vaginal fibroblasts cultured on PT and PT+E_2 (100 pg/mL) wound vaginal models at different time points as measured by the resazurin assay. (n=9 ± SD for each group, N=3) ****p<0.0001.*

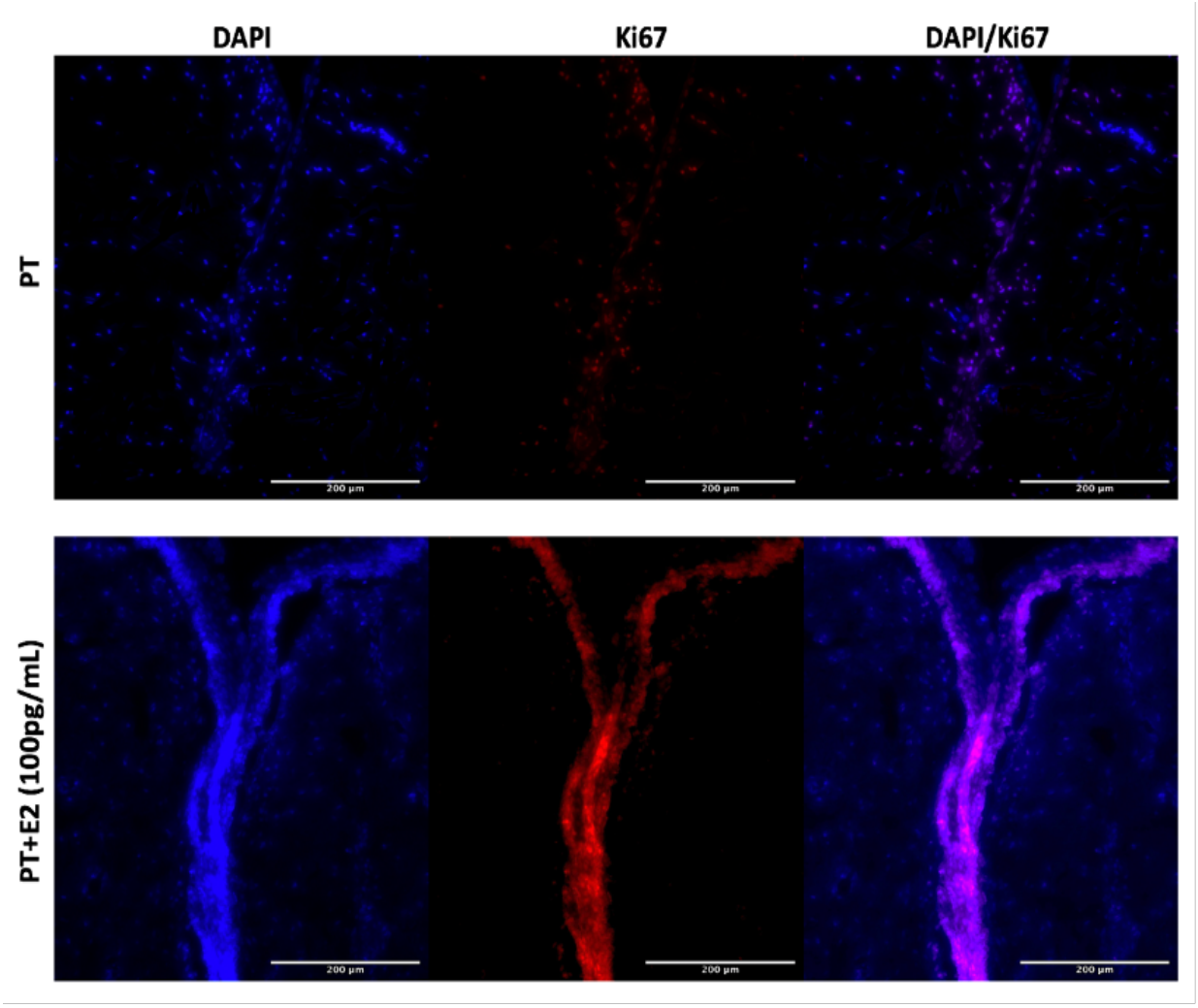

Figure 3.11: Immunohistofluorescence staining of PT and PT+E_2 (100 pg/mL) wound vaginal models for the detection of Ki67 expression after 3 weeks in ALI culture conditions. In the presence of E_2, there was an increase in the intensity and number of cells positive for Ki67 (red channel) in comparison with PT wound models cultured without E_2. Cells present in the basement membrane and within the wounded region were stained positive for Ki67 as they showed high proliferation. All tissue sections were counterstained with DAPI (blue channel). Scale bar=200 µm.

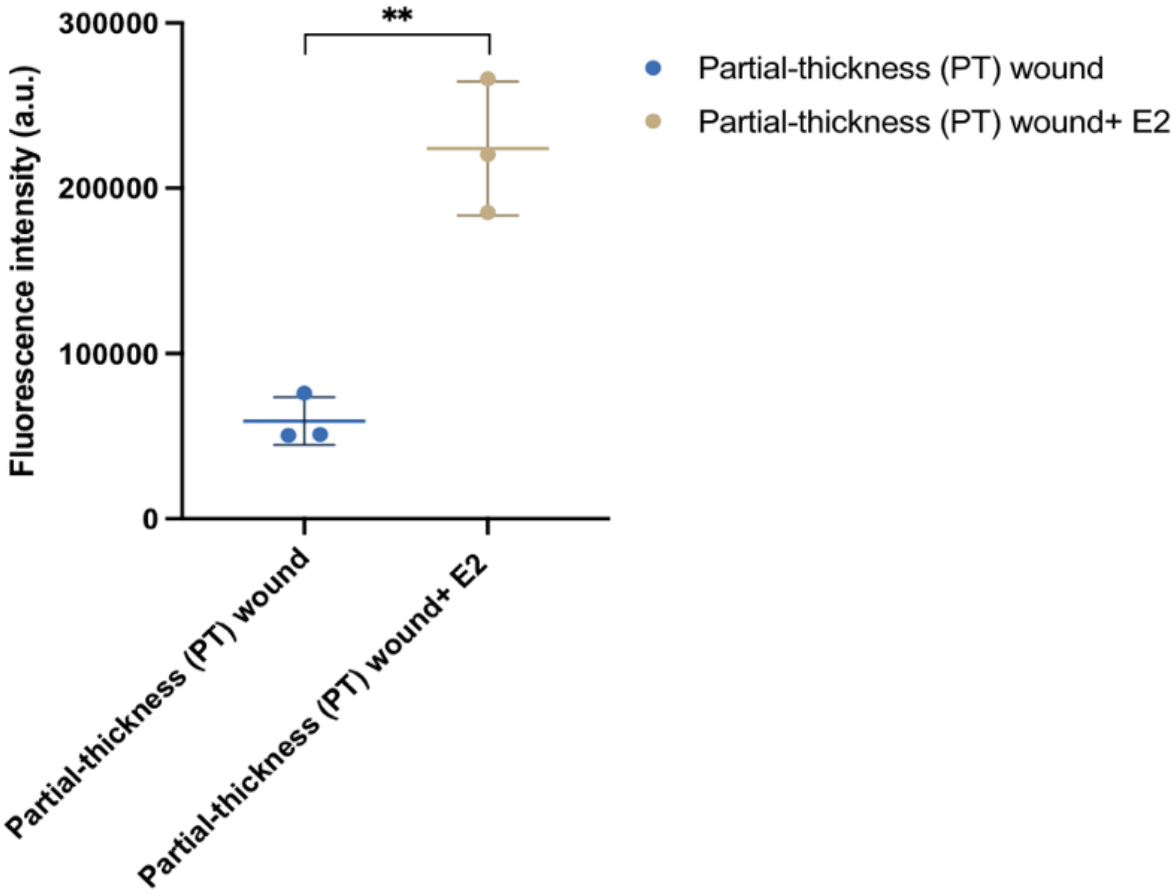

*Figure 3.12: Graphical representation of fluorescence intensity of Ki67 marker expression on PT and PT+ E_2 (100 pg/mL) wound vaginal models after 3 weeks in ALI culture conditions. (n=9 ± SD for each group, N=3) **p<0.005.*

3.4.3 Effect of estradiol-17β induction on the vaginal epithelia' thickness in PT wound vaginal models:

Comparative histological analysis of re-epithelialisation of PT TE wound vaginal models with and without E_2 induction after three weeks in ALI cultures is shown in Figure 3.13. The H&E staining of tissue sections from different samples cultured with and without E_2 revealed some common features of PT wound healing. The PT wound models cultured in the absence of E_2 showed re-epithelialisation by formation of a less stratified epithelium (2-3 layers) compared to those cultured in the presence of E_2 (7-9 layers). Moreover, the pattern of wound healing was also different in both conditions. In the presence of E_2, the edges of the PT wounded tissues appeared more folded and overlapped to completely occupy the wounded area and the stratified epithelia could be seen continuous throughout the entire length of the wound. These results

showed that wound healing in the presence of E_2 was more efficient in terms of restoration of the stratified epithelial barrier as well as wound closure *in vitro* compared to those cultured in the absence of E_2 as shown in Figure 3.13. These results were further confirmed by quantitative analysis of TE PT wound vaginal models' epithelia thickness in both conditions and the graphical representation is presented here in Figure 3.14.

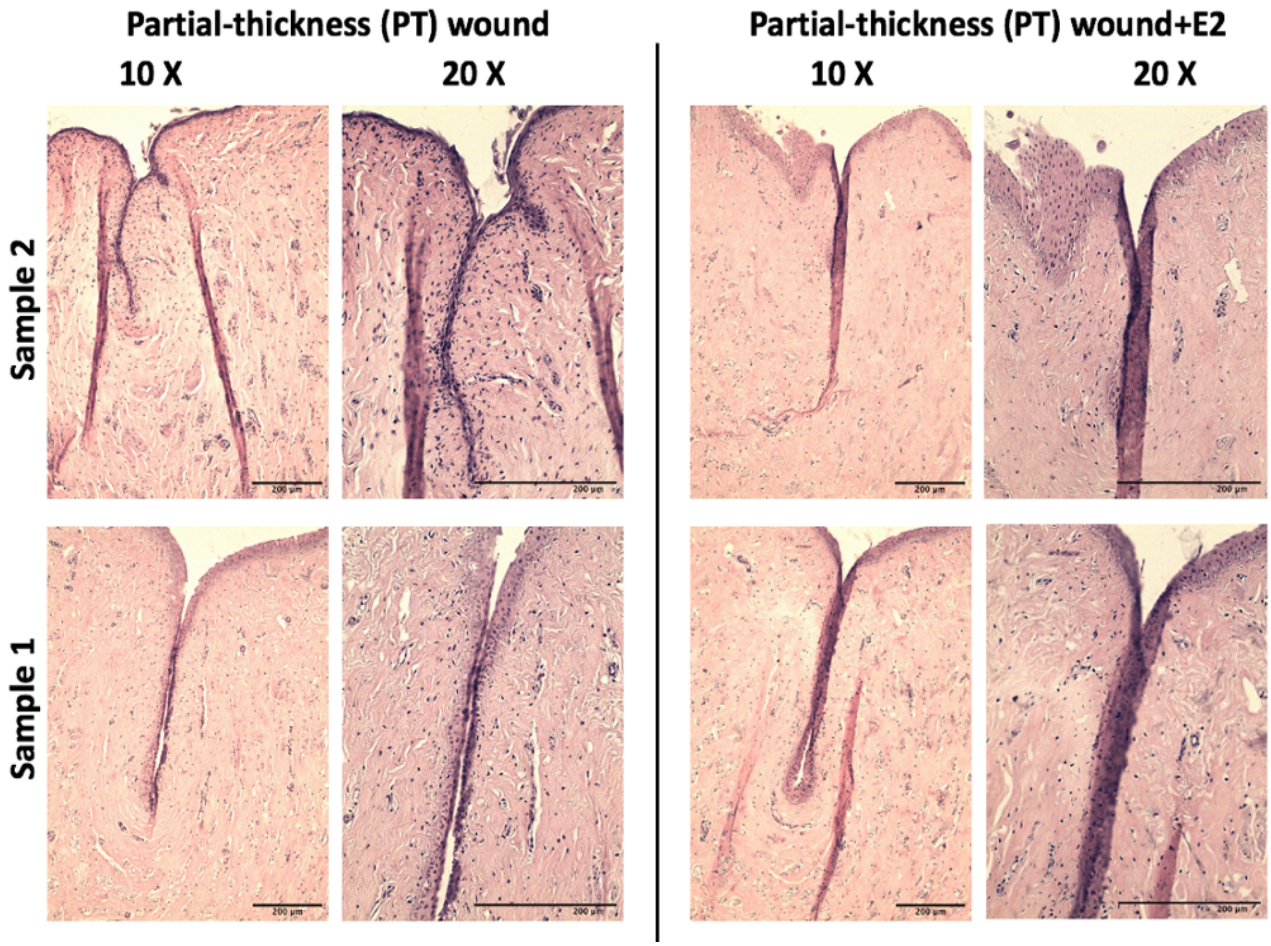

Figure 3.13: Comparative haematoxylin and eosin (H&E) stained sections of partial-thickness (PT) vaginal wound models and partial-thickness (PT) vaginal wound models under E_2 induction (100 pg/mL) after 3 weeks in ALI culture. In the presence of E_2 (100 pg/mL), an increase in the re-epithelialisation of PT TE wound models alongside an improved wound healing could be seen in different samples. Scale bar=200µm.

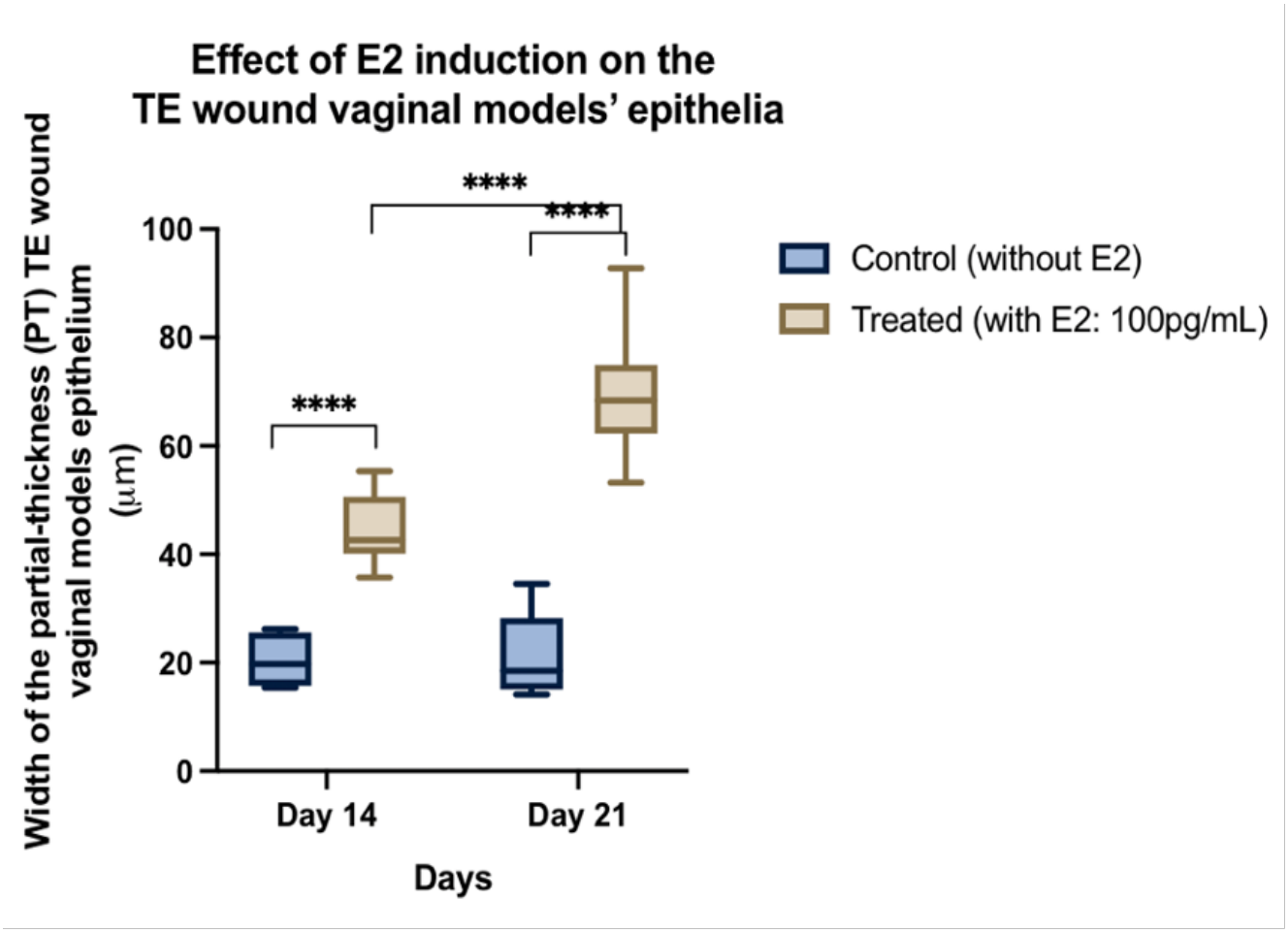

*Figure 3.14: Graphical representation of comparison of TE wound vaginal models' epithelia thickness between PT wound vaginal models and PT wound vaginal models under E_2 induction after 3 weeks in ALI culture conditions. The models' epithelia thickness was measured on nine different images for each parameter (n=9 ± SD for each group) using ImageJ software from three individual experiments (N=3), ****p< 0.0001.*

3.4.4 Demonstration of collagen changes during vaginal wound healing in in vitro PT wound models:

Masson's trichrome staining was performed to determine the density and orientation of collagen component in the lamina propria of TE PT wound vaginal models during the process of *in vitro* vaginal wound healing. Figure 3.15 demonstrates the histological analysis of PT wound vaginal models at day 14 and 21 of the ALI culture. The collagen component was stained green and/or deep green in color whereas the muscle fibres were stained red in color. It was noted that the intensity of the lightgreen SF solution (collagen dye) was increased around

the wounded region at day 21 compared to that at day 14. At day 21, re-rpithelialisation of TE PT wound models were seen and complete closure of wounded region was observed. The orientation of collagen fibres were more circular and compact near the healed area of wound as shown in Figure 3.15. In the presence of estradiol-17β (100 pg/mL) in the culture media, a visible increase in the intensity of lightgreen SF solution (collagen dye) was observed at days 14 and 21 as shown in Figure 3.16. At day 14, the tissue sections around the wounded area appeared more folded with a higher cellular migration into the wounded region compared to those without E_2 (Figure 3.15). At day 21, the collagen component surrounding the wound healing region appeared deep green in color that showed an increase in collagen deposition in the presence of E_2. Moreover, the collagen fibres were more densely packed and oriented in the form of regular bundles of fibres around the healed wounded region. In the presence of E_2, reformation of a stratified epithelium (7-9 layers) over the wounded region could be seen contrary to a thinner epithelium formation (2-4 layers) on TE wound vaginal models without E_2 (Figure 3.15 & 3.16).

These results were further confirmed by performing picrosirius red staining of PT wound models with and without E_2 (100 pg/mL). Figure 3.17 demonstrates the picrosirius red staining for collagen detection in PT wound vaginal models at different time points without E_2. The collagen fibres were stained red in color and the cellular components were stained brown. At day 14, cellular migration could be seen into the wounded region whereas the collagen fibres were arranged in an irregular manner around the wound. At day 21, re-epithelialisation of TE PT wound vaginal models was observed alongside complete closure of the wounded area. Whereas, in the presence of E_2 in the culture media, the collagen fibres around the wounded region were seemed more regularly oriented and the fibres appeared to be deep red in color (Figure 3.17). These observations showed that the density of collagen component increased in response to E_2 induction in PT wound vaginal models. Moreover in the presnece of E_2, the collagen fibres were more compactly arranged in regular bundles around the wounded region compared to without E_2 as shown in Figure 3.18.

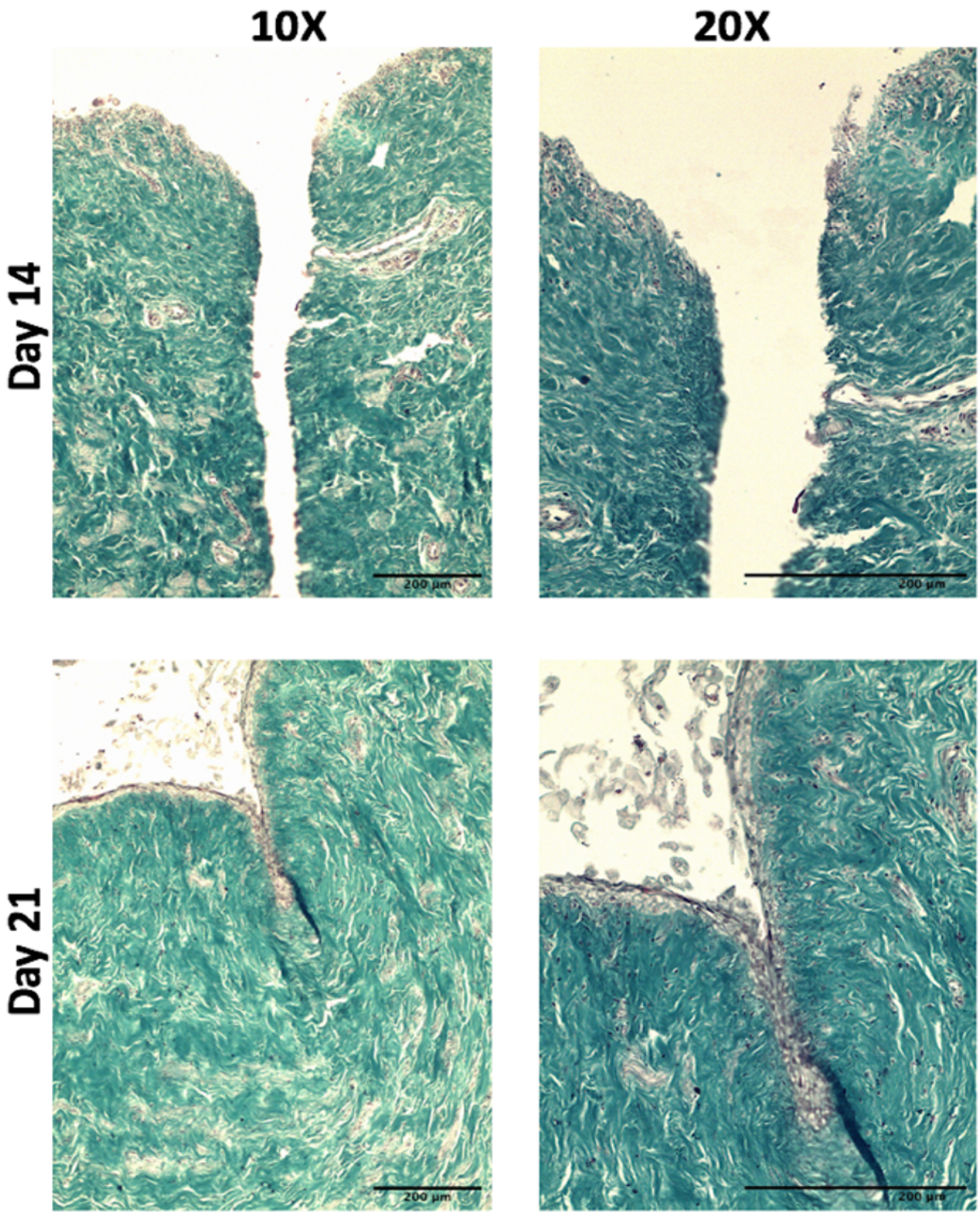

Figure 3.15: Masson's trichrome staining of partial-thickness (PT) vaginal wound models at different time points in ALI culture. The collagen component was stained green, muscle fibres stained red and cellular component was stained deep brown/black in color. The intensity of green stain was increased at day 21 compared to that at day 14. The collagen fibres were observed oriented in a tight regular pattern around the wound healing region. Scale bar=200µm.

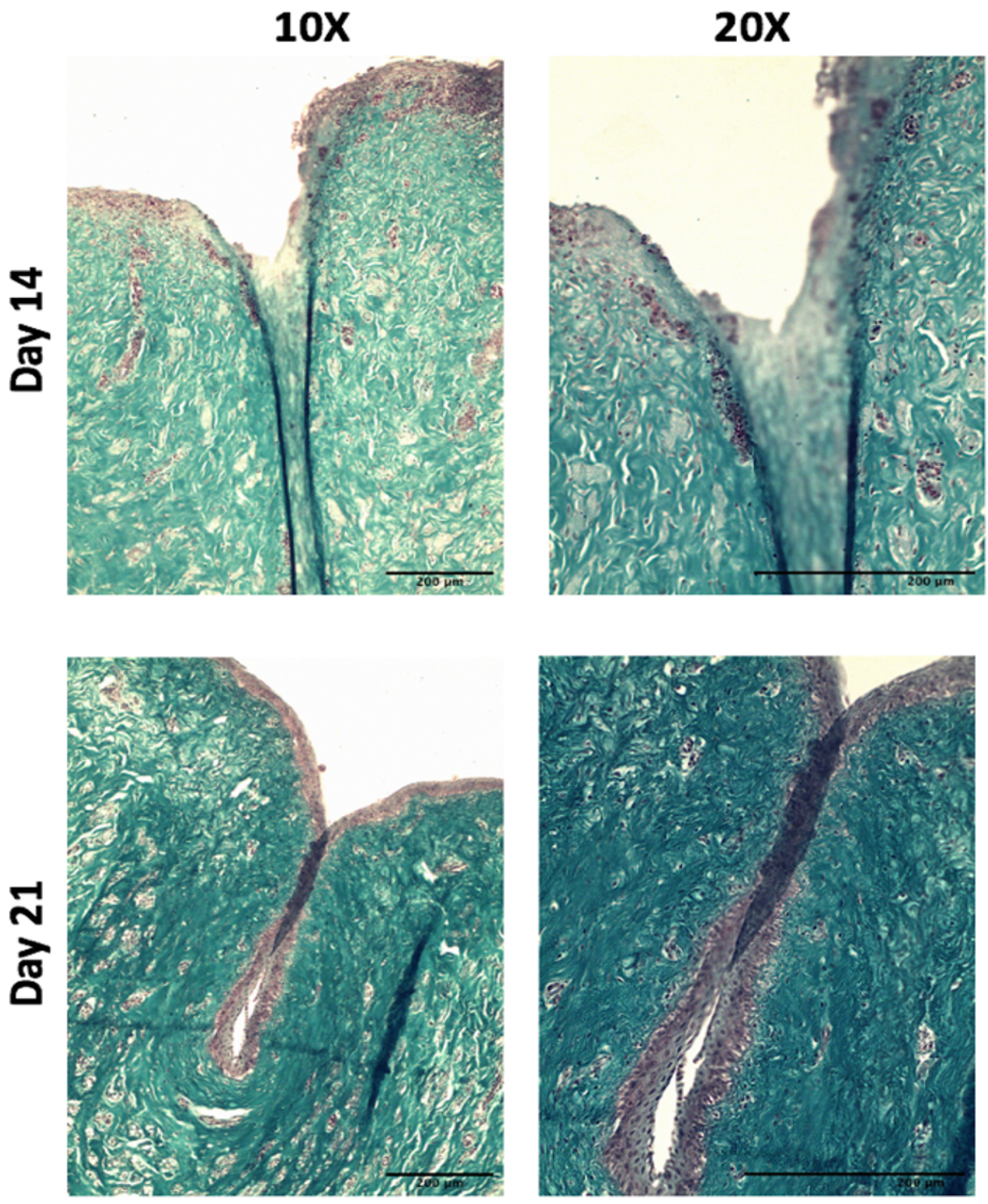

Figure 3.16: Masson's trichrome staining of partial-thickness (PT) vaginal wound models under E_2 induction (100 pg/mL) at different time points in ALI culture. The collagen component was stained green, muscle fibres stained red and cellular component was stained deep brown/black in color. In the presence of E_2, the intensity of collagen stain was observed increased and the fibres were more compactly arranged in a regular pattern surrounding the wound healing region. Scale bar=200µm.

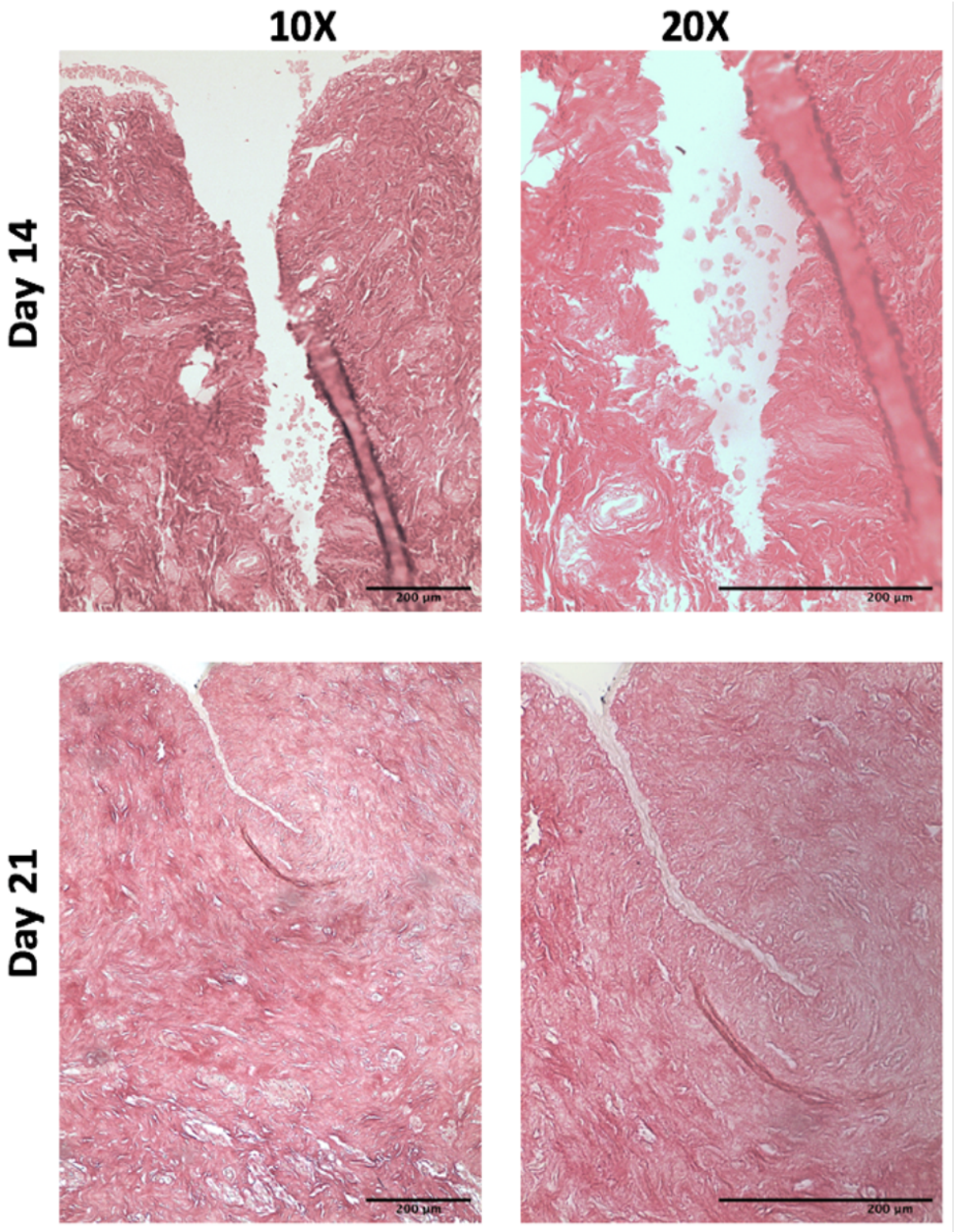

Figure 3.17: Picrosirius red staining of partial-thickness (PT) vaginal wound models at different time points in ALI culture. Collagen component was stained deep red in tissue sections. All tissue sections were counterstained with haematoxylin (cellular components appeared light brown in color). Scale bar=200µm.

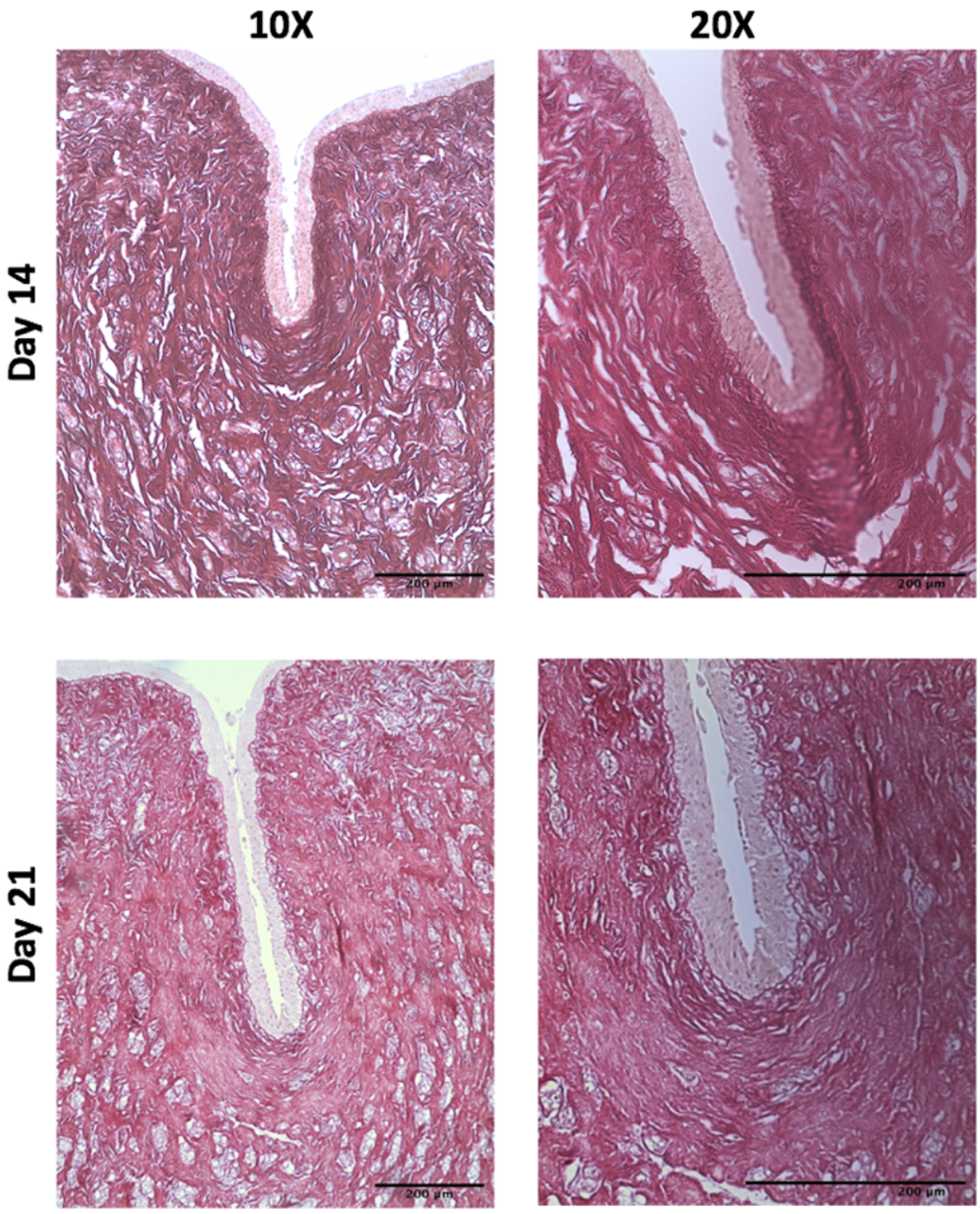

Figure 3.18: Picrosirius red staining of partial-thickness (PT) vaginal wound models under E_2 induction (100 pg/mL) at different time points in ALI culture. Collagen component was stained deep red in tissue sections. In the presence of E_2 in the culture media, the collagen fibres appeared in a regular orientation with tightly packed fibres. All tissue sections were counterstained with haematoxylin (cellular components appeared light brown in color). Scale bar=200µm.

3.4.5 Immunohistofluorescence (IHF) analysis of PT and PT+E_2 wound vaginal models:

Immunohistofluorescence analysis of PT wound vaginal models was performed to detect the expression of key proteins Ki67 and α-SM actin during the process of wound healing in the absence and presence of estradiol-17β (100 pg/mL). The nuclear protein Ki67 is generally expressed during the proliferative phase of the cell cycle and is associated with cellular proliferation. In PT wound vaginal models, the expression of Ki67 (red channel) was higher in cells closer to the wounded region with an increased expression from day 14 to day 21 as shown in Figure 3.19. At day 14, cells of the basement membrane and the surrounding region of wound were intensely positive for KI67 marker. At day 21, complete wound closure was observed and cells within the region of wound showed intense positive staining for Ki67 (Figure 3.19) . These results showed that the cultured cells were highly proliferative and migrated over the time period from day 14 to day 21 to elicit the process of wound healing in TE wound vaginal models. In the presence of E_2 (100 pg/mL), an increase in the expression of Ki67 was observed at both days 14 and 21 in PT wound vaginal models as shown in Figure 3.20. Cultured cells in the basement membrane and in the wounded region were intensely positive for Ki67 marker (red channel). Comparative analysis of these images revealed that E_2 induced the number of proliferative cells in PT wound models and played a key role in accelerating the process of wound healing and formed a stratified epithelial barrier over the wounded region with improved wound closure (Figures 3.19 & 3.20).

These results were further confirmed by quantitative analysis of fluoresence intensity (a.u.) for Ki67 expression in PT wound models with and without E_2 and the graphical representation is presented here in Figure 3.21. Analysis of the mean values revealed that the number and intensity of proliferative cells was significantly higher in PT TE models cultured with E_2 as compared to without E_2. Moreover, improved wound closure and healing was observed in models cultured with E_2.

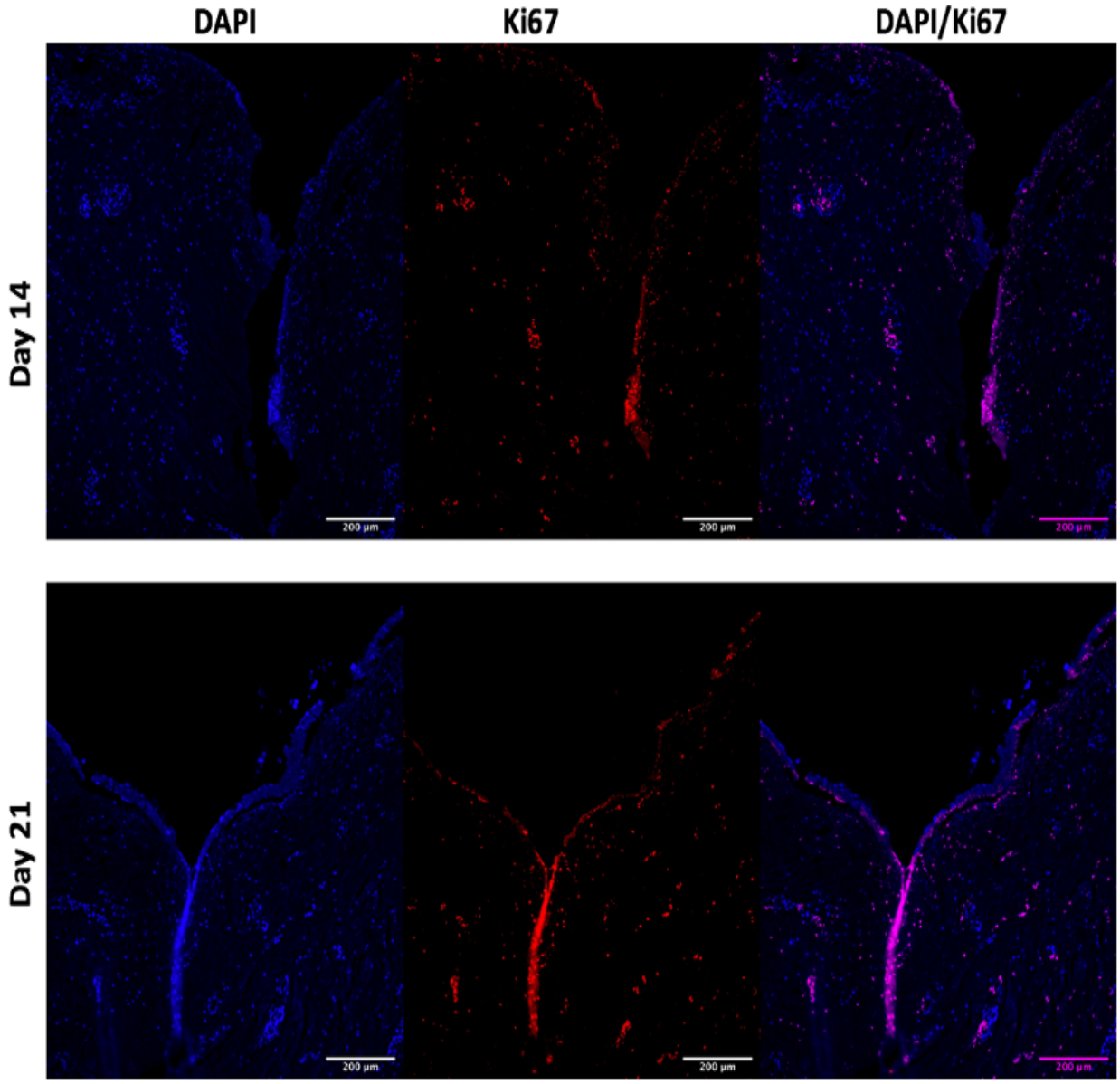

Figure 3.19: Immunohistofluorescence staining for the detection of Ki67 expression on PT wound vaginal models at different time points in ALI culture conditions. Ki67 positive cells (red channel) were more concentrated around the edges of the PT wound and in the basement membrane. All tissue sections were counterstained with DAPI (blue channel). Scale bar=200µm.

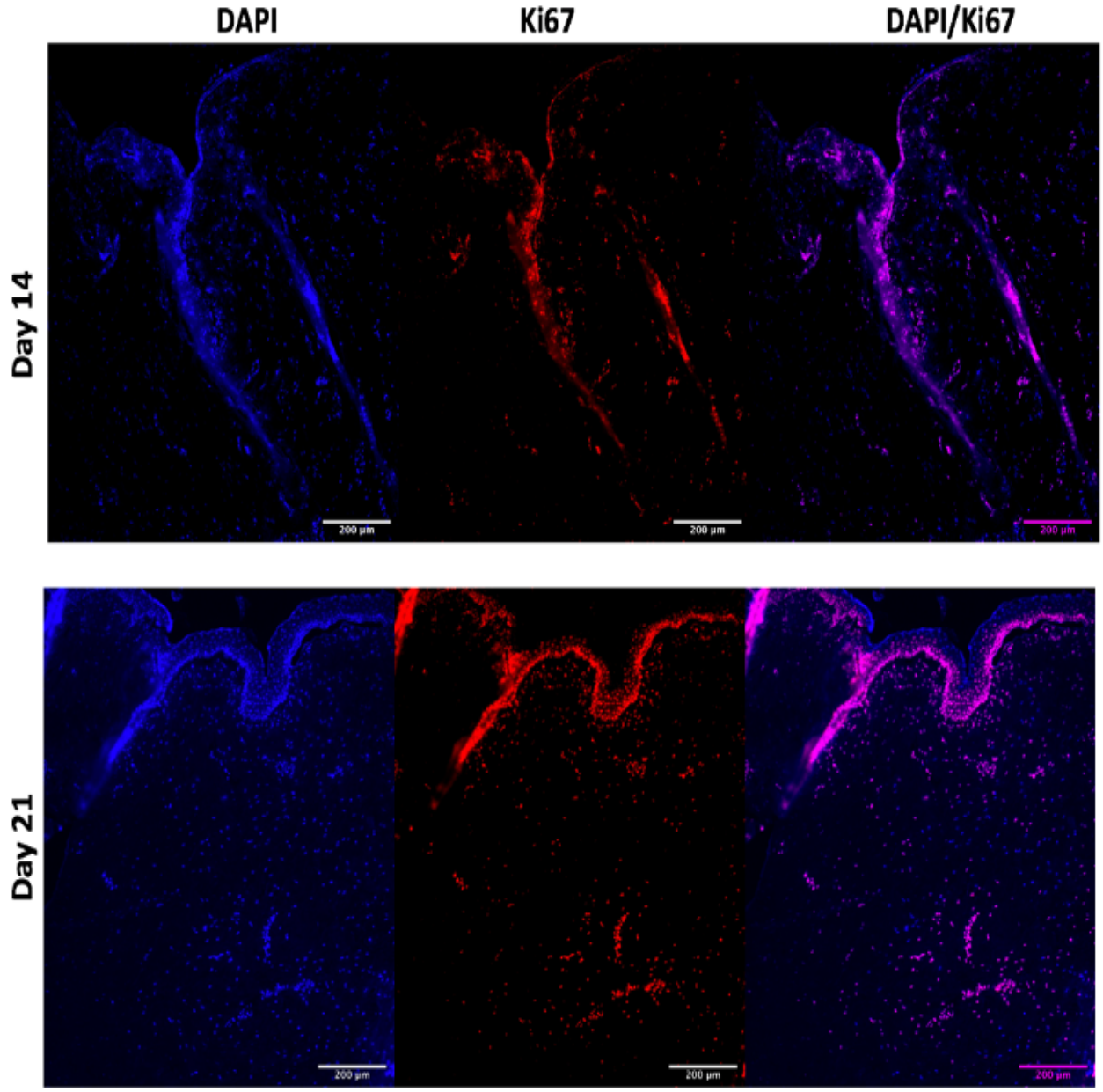

Figure 3.20: Immunohistofluorescence staining for the detection of Ki67 expression on PT wound vaginal models under E_2 induction (100 pg/mL) at different time points in ALI culture conditions. Ki67 positive cells (red channel) were more concentrated around the edges of the PT wound and in the basement membrane. In the presence of E_2, an increase in the epithelia thickness and intensity and number of proliferative cells was observed. All tissue sections were counterstained with DAPI (blue channel). Scale bar=200µm.

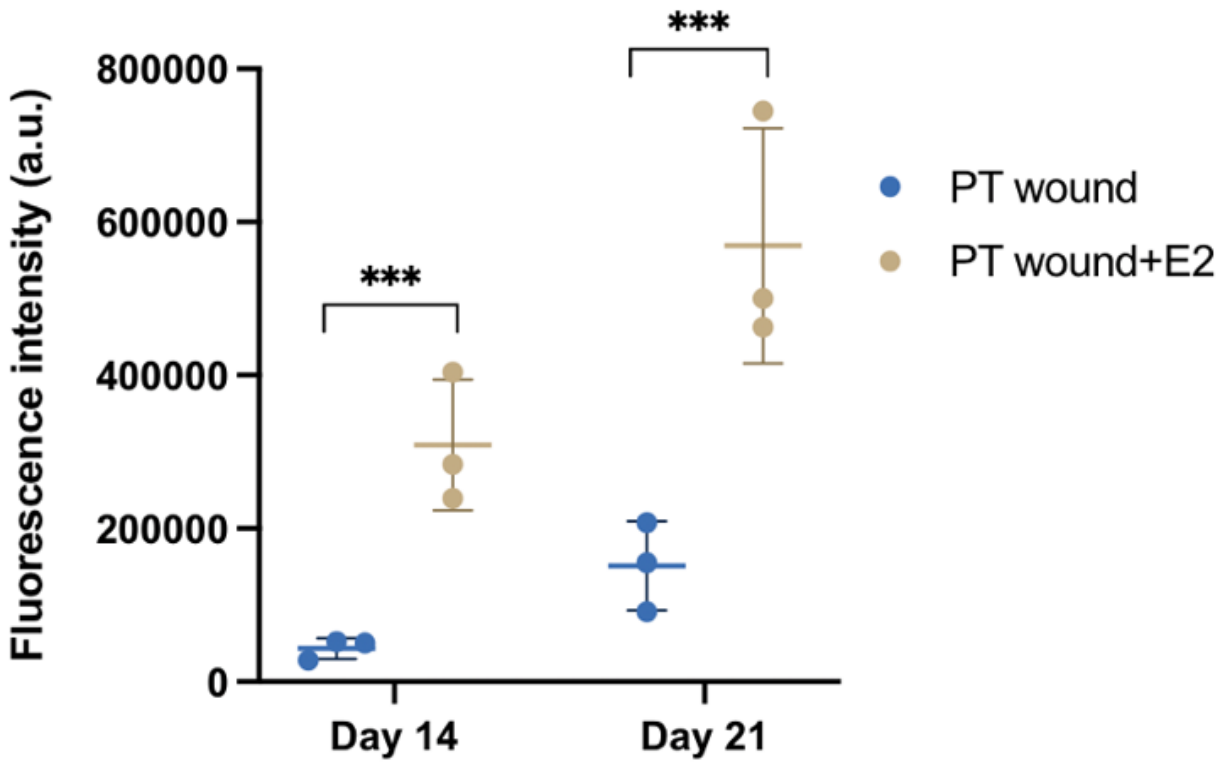

*Figure 3.21: Graphical representation of fluorescence intensity of Ki67 marker expression on PT and PT+ E_2 (100 pg/mL) wound vaginal models at different time points in ALI culture conditions. (n=9 ± SD for each group, N=3, ***p<0.005).*

3.4.6 Immunohistofluorescence (IHF) analysis of PT and PT+E_2 wound vaginal models for the detection of fibrosis marker:

Another key element in the process of *in vivo* soft tissue wound healing are the fibroblasts present in the extracellular matrix. The differentiation of fibroblasts into myofibroblasts is the key regulatory event decisive of the fate of soft tissue wound healing. Myofibroblasts are the specialised contractile fibroblasts that have predominant role in wound contractility and helaing. However, if the transition from fibroblasts to myofibroblasts remain unchecked it can lead to fibrosis and scarring. The expression of α-SM actin (α-SMA) is often used to define the myofibroblast phenotype while investigating soft tissue wound healing mechanisms.

Figure 3.22 demonstrates the IHF analysis of α-SMA expression in PT wound vaginal models at different time points in ALI culture. At day 14, the number and intensity of cells positive for α-SMA expression was higher as compared to day 21. These results showed that after two weeks in ALI culture there was an increased differentiation of fibroblasts into myofibroblasts and in turn an increased expression of α-SMA around the wounded region of the PT wound vaginal models. In the later phase of wound healing process (from days 14-21 in culture) during the granulation tissue formation, the fibroblasts were activated to transform into myofibroblasts and expressed α-SMA that played a major role in re-epithelialisation, wound contraction and granulation tissue formation that covered the wounded region as shown in Figure 3.22. On the other hand, in the presence of E_2 in the culture media, there was less transformation of fibroblasts into myofibroblast phenotype and reduced expression of α-SMA at day 14 that later reduced further at day 21 in ALI culture as shown in Figure 3.23. These results indicated that in the presence of E_2, there was a reduced risk of scarring and fibrotic tissue formation at the wounded site in PT wound models which in turn increased the likelihood for tissue remodeling and improved vaginal tissue healing. At day 21, further decline in the number and intensity of cells positive for α-SMA expression was observed which indicated that prolonged culture in the presence of E_2 in the culture media facilitated the process of re-epithelialisation, tissue remodeling and improved wound healing as shown in Figure 3.23.

These results were further confirmed by quantitative analysis of α-SMA fluorescence intensity in PT wound vaginal models with and without E_2 at different time points in ALI culture and the graphical representation is shown in Figure 3.24. The fibroblasts to myofibroblast transformation and in turn α-SMA expression was significantly higher in PT wound vaginal models in the absence of E_2 as compared to those in the presence of E_2 and hence, depicted a higher risk of fibrosis during the course of wound healing in TE models.

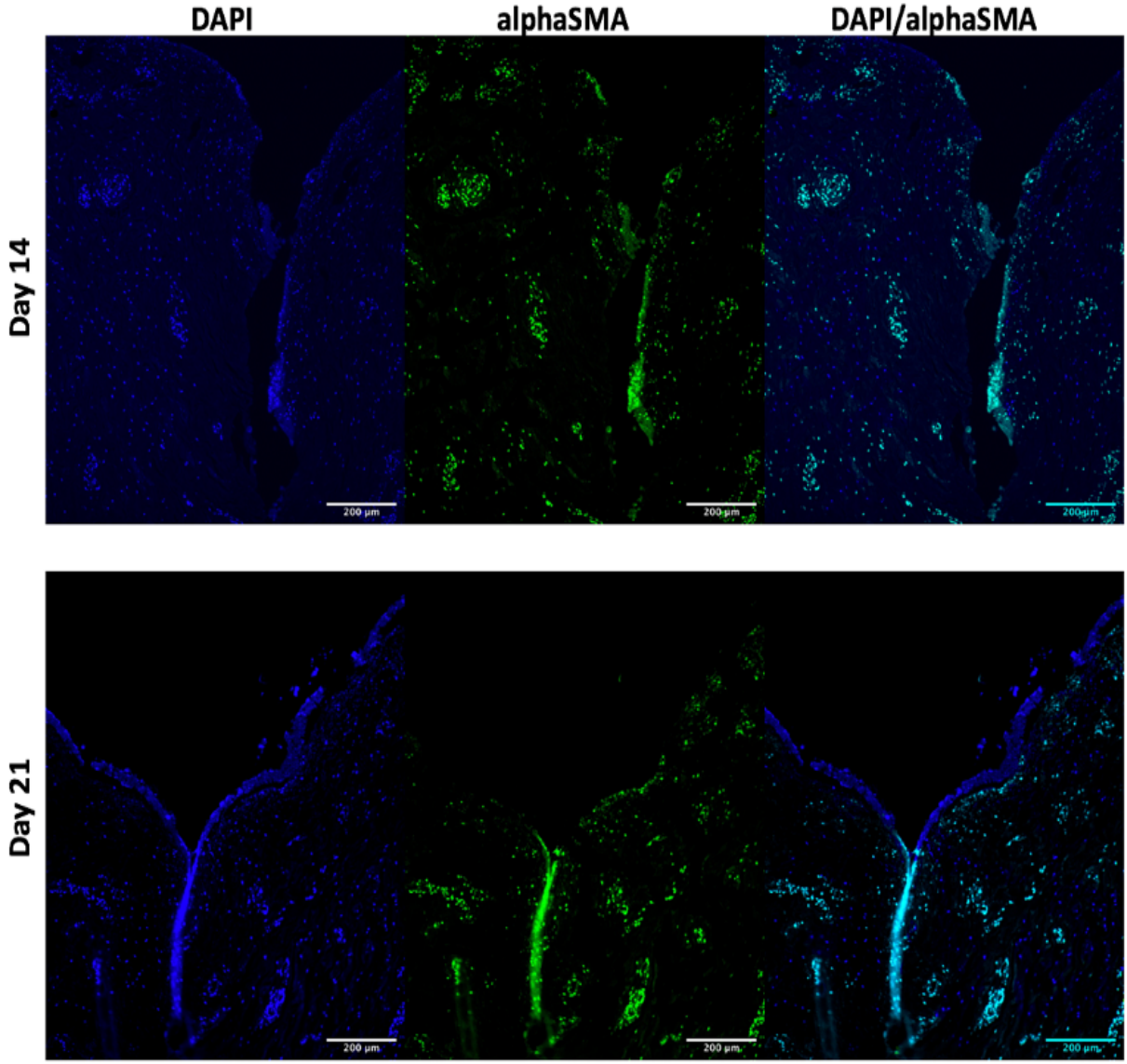

Figure 3.22: Immunohistofluorescence staining for the detection of α-SMA expression on PT wound vaginal models at different time points in ALI culture conditions. The myofibroblasts present in the models expressed the α-SMA signal (green channel) which was observed distributed in the lamina propria region. All tissue sections were counterstained with DAPI (blue channel). Scale bar=200µm.

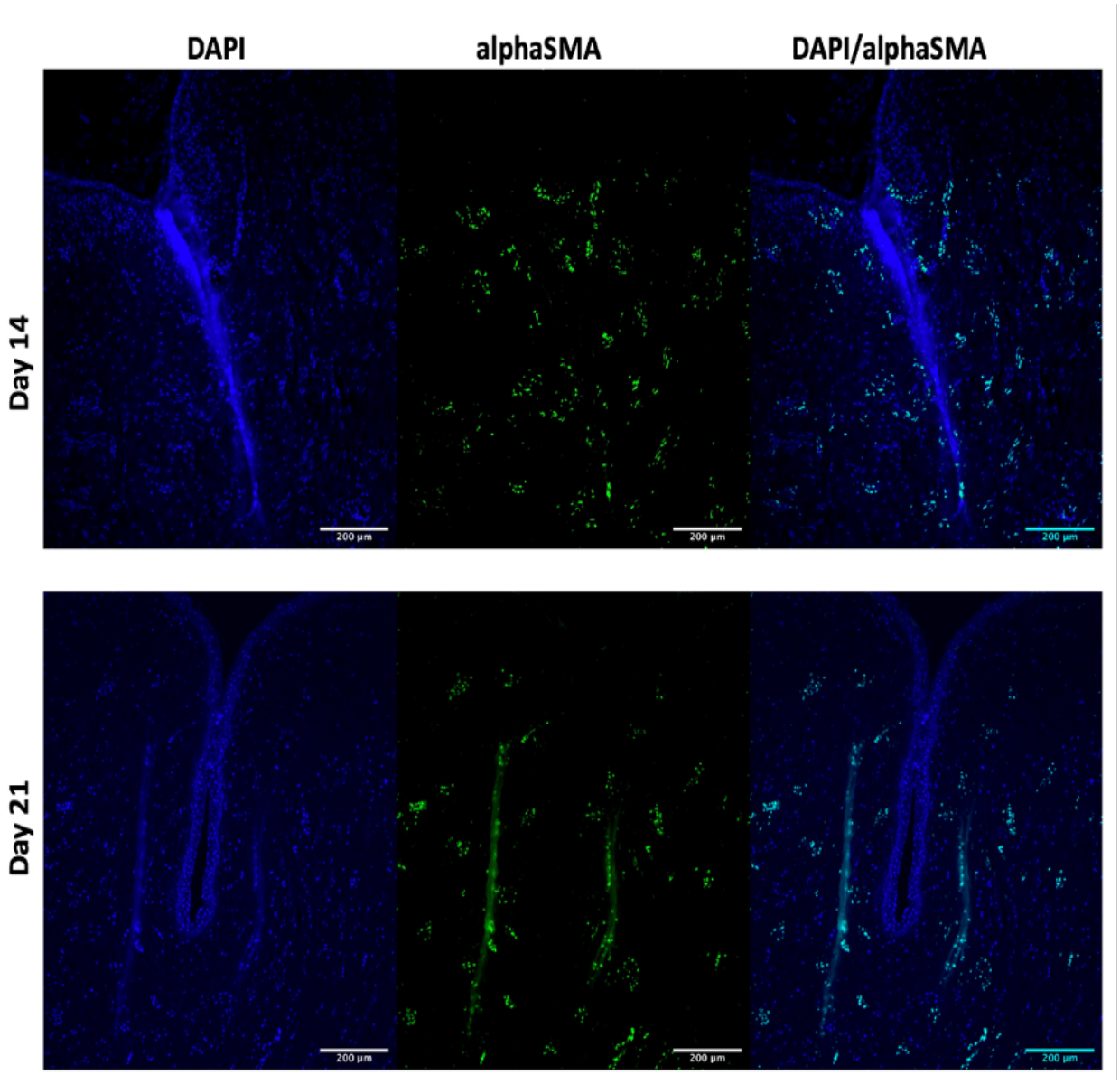

Figure 3.23: Immunohistofluorescence staining for the detection of α-SMA expression on PT wound vaginal models under E_2 induction (100 pg/mL) at different time points in ALI culture conditions. The myofibroblasts present in the models expressed the α-SMA signal (green channel) which was observed distributed in the lamina propria region whereas it was absent in the epithelial region. All tissue sections were counterstained with DAPI (blue channel). Scale bar=200µm.

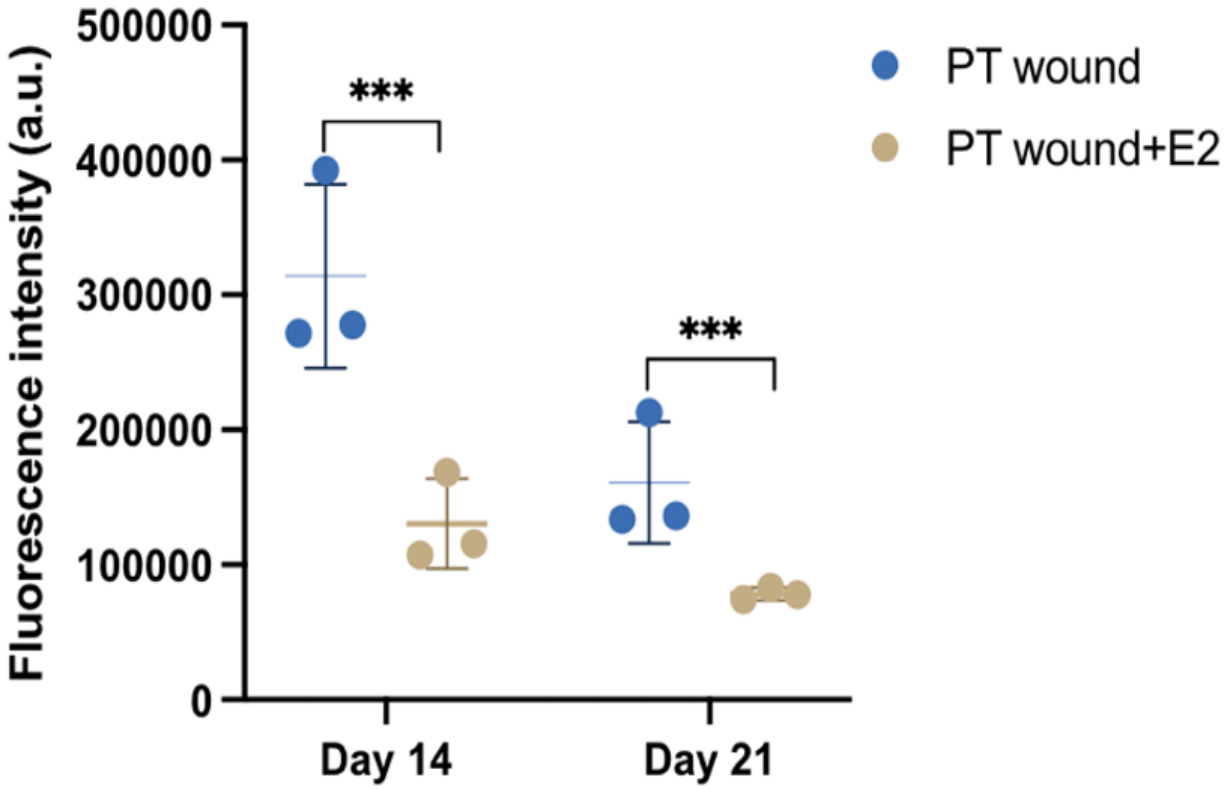

*Figure 3.24: Graphical representation of fluorescence intensity of α-SMA marker expression on PT and PT+ E_2 (100 pg/mL) wound vaginal models at different time points in ALI culture conditions. (n=9 ± SD for each group, N=3, ***p<0.005).*

3.5 Discussion:

Over the past decades, an increase in the ageing population in the western community have resulted in an increase in the number of women seeking medical attention for pelvic floor dysfunctions (PFDs) such as POP and SUI. It has been estimated that in the US alone, one in every ten women from the older population is at risk of prolapse surgery with 30 % recurrence rate [57]. The magnitude of this public health problem is gigantic, and it is highly difficult to apprehend the high failure rate of pelvic floor reconstructive surgeries due to the complex pathogenesis of PFDs. It has been postulated that the physiological process of wound healing in the vagina is a major determining factor for the outcome of these reconstructive pelvic procedures [340].

The vaginal wound healing is a complex fibroproliferative response that is mediated through the interactions between hormones, growth factors and cytokines. In elderly women, there is a high chance of impaired and protracted vaginal wound healing due to already weakened pelvic floor connective tissue that may lead to wound contraction, fibrosis, increased collagen deposition and scarring of the vaginal tissue [341]. Majority of studies on soft tissue wound healing is commonly performed in small animal models such as rats and rabbits. However, these animal models are not always true representative of the actual *in vivo* vaginal tissue wound healing process and extrapolation of animal data into clinical practice require caution. Hence, in this project TE wound vaginal models were developed using primary sheep vaginal epithelial cells and fibroblasts cultured on decellularised SVT to mirror post-injury vaginal tissue repair and recapitulate key events of *in vivo* vaginal wound healing. Moreover, as most reconstructive pelvic surgeries are undertaken in post-menopausal women, it is extremely important to understand the effect of lack of estradiol-17β on the vaginal wound healing process. Based on these annotations, the TE wound vaginal models presented here also elucidated the effects of estradiol-17β on the vaginal wound repair kinetics, a mechanism that has never been studied previously in any *in vitro* model.

Animal models of wound healing have been available for decades that have provided valuable insights into the different stages of soft tissue wound healing, yet historically the translation of identified therapies in animal models to clinical practice remains problematic [351]. Due to the logistics and ethical reasons associated with bigger animal models such as porcine, most studies

nowadays rely on investigations in smaller animal models such as mouse or rodents. The most popular dermal laboratory wound models are full-thickness excision and full-thickness incisions performed on mouse dorsal skin [352]. The popularity of excisional and incisional wounds is attributed to the fact that wounding can be performed quickly, reproducibly on different animals in a controlled manner. Furthermore, analysis could be performed easily by imaging and analysing wound closure supplemented with histological analysis to examine the process of wound healing over time. Keeping in consideration the 3Rs of animal experimentation, the TE wound vaginal models presented here are full-thickness and partial thickness incisional wounds performed on TE vaginal models to study the vaginal wound healing process *in vitro.*

The dynamic process of wound healing can be broadly divided into three different phases such as the inflammatory phase, proliferative phase and the remodeling phase as reviewed by Reinke and Sorg [353]. The understanding of the process of vaginal wound healing is based upon years of research on dermal wound healing reported in the literature. Both dermis and vaginal tissue is composed of a stratified squamous epithelial barrier and following any surgical insult, restoration of the epithelial barrier is crucial in terms of proper tissue repair and regeneration. Hence, the stages of wound repair in dermis and vaginal tissue share common similarities. In the initial stages of wound healing, the neighboring cells proliferate and migrate into the wounded region to begin covering the wounded area. The migration phase has been identified as the limiting event in wound healing and in the full-thickness (FT) and partial thickness (PT) wound models presented here the cultured cells showed migration towards the wounded area in the first week of culture in ALI in Figures 3.4 and 3.5 respectively.

In many laboratory settings, most assays developed to study wound healing are based upon migration assays in 2D cell cultures. Liang *et al.,* [328] developed the *in vitro* scratch assay to determine the migration of a single cell population into an exclusion zone created by a “scratch” onto a confluent cell monolayer. The scratch assay is the most popular migration assay among the research community due to its ease in performance, low cost, well-established and compatible with imaging of live cells during migration which enable researchers to monitor migration of single cells *in vitro*. However, as scratch assay is routinely performed on a single cell monolayer culture, hence it is impossible to determine cellular interactions between different cell types during the migration phase in wound healing. Comparable to the dermal healing, the proliferation and immigration of local vaginal fibroblasts is coordinated with the

local vaginal epithelial cells at the wound edges to ensure the process of granulation tissue formation and re-epithelialisation in the vaginal wound healing process [354]. Therefore, the coordinated migration of vaginal fibroblasts and epithelial cells was determined by performing incisions on TE vaginal models containing the full-length decellularised sheep vaginal tissue cultured with primary sheep vaginal cells as shown in Figures 3.4 and 3.5.

Abramov *et al.,* [348] conducted the comparative histological characterisation of vaginal and abdominal surgical excisional wound healing in a rabbit model. They identified common similarities in the wound healing stages in vagina and abdominal skin that included an initial inflammation, fibroblasts proliferation, neovascularization, re-epithelialisation and collagen remodeling. However, they reported the formation of a fibrinous crust in abdominal skin at days 4-7 which was absent in the vagina. Contrary to these observations, the TE wound models presented here in Figures 3.4 and 3.5 demonstrates the presence of a transient fibrinous crust in the vaginal wounds alongside a higher proliferation and migration of neighboring cells after 7 days post-injury. The lack of crust in *in vivo* vaginal wound healing is physiologically plausible as the vaginal epithelium is non-keratisnised compared to the keratinised dermal epithelium and remain unexposed to air [355]. However, as the TE wound vaginal models developed here were cultured at an ALI, i have reported the formation of a transient crust at the wound edges at day 7 most likely as a result of folding of the tissue sections around the wounded area and also air exposed at the upper region of the models.

The human body's ability to repair wounded tissue after a surgical insult is crucial in determining postoperative recovery and surgical outcome of reconstructive procedures. Extensive studies on dermal wound healing has led researchers to the development of evidence-based therapies for the management of dermal wounds. Henceforth, a reasonable approach to understand the physiology of vaginal wound healing is to compare it with dermis in order to develop wound management therapies and reconstructive procedures applicable for the female pelvic floor repair. Stunova and Vistejnova [356] have reported that the dermal fibroblasts started to migrate into acute dermal wounds within 2 days post-injury and tend to populate the wounded region by proliferation and have been identified as the main cell type of granulation tissue 4 days post-injury. In the TE vaginal models presented here, the amount of granulation tissue formed was peaked at day 14 in PT wound models' post-injury as shown in Figure 3.5. Similar observations were made in FT models, however, as the wounded region was much bigger than the PT wound models, the granulation tissue formed was mostly around the edges

of the FT wound near the folded regions of tissue sections (Figure 4.4). The difference in the timeline of granulation tissue formation could be attributed to the fact that in *in vivo* dermal wound healing, these functions are mediated by multiple growth factors such as the platelet derived growth factor (PDGF) and transforming growth factor β (TGFβ) [357]. However, in the TE wound vaginal models presented here, the cultured vaginal fibroblasts were considered to release the paracrine growth factors that facilitated granulation tissue formation.

In my TE wound vaginal models, fibroblasts proliferation continued to increase after 3 weeks post-injury in both PT and FT wound models (Figures 3.6 & 3.7) however, it was higher in PT wound models as shown in Figure 4.8. These results indicated that as the wounded region in PT models was constricted as compared to that in FT models, the migrating cells coordinated with the neighboring stromal cells and intercellular signaling pathways allowed more cells to proliferate into the wounded region to form the granulation tissue occupying the wounded area as shown in Figure 3.5. The granulation tissue formed in PT TE wound vaginal models matured progressively from days 14 to 21 in ALI post-wounding and occupied about 80% of the wounded area at day 21. Previously Abramov *et al.,* [358] reported the maturation of granulation tissue in *in vivo* vaginal excisional wound healing in a rabbit model for a longer period of time that accounted for 35 days post-wounding. Hence, my wound models allowed to investigate the formation of granulation tissue in a shorter time frame. In FT TE wound models, due to a huge gap between the two margins of the wounded region, there was an absence of granulation tissue filling up the wound rather the spurs of vaginal epithelial cells migrated along the cut margins of the wounded tissue began re-epithelialisation and formed a stratified epithelium at day 21 post-wounding (Figure 3.4).

Investigations in an *in vivo* rabbit vaginal excisional wound model by Abramov *et al.,* [358] demonstrated that the process of re-epithelialisation began shortly after the wound (about 24-48 hours) in the rabbit vagina that continued progressively by day 14 post wounding. In my TE PT and FT wound vaginal models, the beginning of the re-epithelialisation process was comparable with the previous *in vivo* findings as spurs of epithelial cells started to form along the edges of the wounded tissue within 24-hour post-injury with visible folding of the tissue margins that became more apparent at day 7 post injury (Figures 3.4 and 3.5). However, the re-epithelialisation of TE wound models was completed by day 21 post-wounding that took a bit longer than *in vivo* data reported previously. This could be attributed to the fact that the TE

wound vaginal models presented here were cultured with a co culture of only two cell types *i.e.,* primary vaginal epithelial cells and vaginal fibroblasts. Whereas in an *in vivo* environment the process of re-epithelialisation is highly orchestrated which includes synchronous interaction of epithelial cells, stromal fibroblasts, immune cells and several growth factors and vascular supply.

The mechanism of oestrogen-induced wound healing in the female urogenital tract after reconstructive procedures for the pelvic floor dysfunctions remain poorly understood. Data from clinical trials have highlighted that impaired wound healing is a leading cause of recurrence of prolapse after pelvic reconstructive surgeries and that estrogen administration may help to improve wound healing [359]. In urogynecological clinical setup, local oestrogen therapy has shown to relieve symptoms of vaginal dryness, dyspareunia, discomfort and atrophic vaginitis in postmenopausal women. Krause *et al.,* [360] reviewed the effects of vaginally administered oestrogen in postmenopausal patients referred for oestrogen replacement therapy and concluded that locally administered intravaginal oestrogen by any delivery mechanism have shown to promote vaginal cell proliferation, epithelium thickness as well as tissue compliance. Similar results were obtained in the TE wound vaginal models treated with estradiol-17β (100 pg/mL) and vaginal wound healing was histologically analysed as shown in Figure 3.9. The PT TE wound vaginal models presented here recapitulated the key stages of vaginal wound healing and models were shown to heal better with improved stratification and re-epithelialisation of the vaginal epithelium in the presence of estradiol-17β. Moreover, administration of oestrogen in the culture media of TE wound models has shown to improve the metabolic activity of cultured cells as shown in Figure 3.10.

These results were consistent with previous *in vivo* studies in animal models to determine the effect of oestrogen administration on improved vaginal wound healing. Akbiyik *et al.,* [361] studied the comparative effect of oestrogens on vaginal mucosal healing in rats after surgical interventions in young (low oestrogen level) and adult (high oestrogen levels) group of rats. They reported that in the presence of oestrogen the vaginal mucosal healing was intense and the process of re-epithelialisation and stratification was improved compared to sham. Oestrogens are also known to increase re-epithelialisation of dermal wounds by increasing the cell mitotic rate in the epidermis. Histological studies on rabbit vagina demonstrated that the vaginal wound closure, scar contraction and re-epithelialisation was significantly impaired in

ovariectomized rabbits compared to the oestrogen-administered sham-operated controls [362]. Studies in guinea pigs also revealed similar findings where improved vaginal thickness, increased smooth muscle content and increase in the toral collagen content in the vaginal wall was reported in preoperative systemic oestrogen administration [363]. Here, i have recapitulated the effects of estradiol-17β on vaginal wound healing in a TE wound model which previously has only been investigated in clinical trials or animal models. My TE models also depicted the regulatory role of estradiol-17β on the vaginal cellular proliferation at the molecular level during the process of vaginal wound repair. Here, i have shown that the presence of estradiol-17β in the culture media regulates the expression of Ki67 (cell proliferation marker) and resulted in an upregulation of Ki67 signal intensity (Figures 3.11 & 3.12) which previously was only reported from data in *in vivo* animal models [364] and/or clinical trials [365].

The morbidity associated with problems in vaginal wound healing has inspired researchers to evaluate underlying factors that result in impaired wound healing. These factors include the role of reproductive hormones such as oestrogens as well as the weakened pelvic connective tissue in wound repair. Over the years, it has been established that the high failure rate of reconstructive surgeries for pelvic organ prolapse is attributed to impaired post-operative wound healing and regeneration of the vaginal wall. Ripperda *et al.,* [366] tested their hypothesis that postoperative local oestradiol administration can lead to improved healing of injured vagina in a rat menopausal model. They concluded that acute administration of vaginal oestrogen post-injury resulted in an increase in epithelium thickness and improved epithelial barrier function over the wound.

Similar observations were made during the vaginal wound healing process in the TE models presented here. Figures 3.13 and 3.14 depicted the comparative histological analysis of TE wound vaginal model's epithelia in the presence and absence of estradiol-17β at week 3 post-injury. These results showed a positive effect of estradiol-17β on TE wound vaginal models' epithelia thickness compared to placebo. In current clinical practice, oestrogens are not consistently used to accelerate vaginal wound healing either pre- or post-operative reconstructive pelvic procedures in women. However, data from clinical trials and *in vivo* animal models as well as this current study on *in vitro* TE vaginal models collectively suggest that oestrogen administration has a favorable effect on vaginal tissue wound healing that may

help to develop hormonal therapy to reduce wound complications after reconstructive pelvic surgery.

During the process of wound healing the re-epithelialisation phase is followed by the remodelling phase (2-3 weeks post-injury) where the collagen fibres present in the ECM become thicker and are arranged in parallel to restore the tensile strength of the wounded tissue [326]. Stunova and Vistejnova [356] reviewed the role of dermal fibroblasts in the synthesis and remodelling of the ECM during the process of cutaneous wound healing. The remodelling phase is characterised by an active reorganisation of the ECM mediated by fibroblasts through secretion of various signaling molecules that increase the amount of type I fibrillar collagen to improve the tensile strength of the connective tissue surrounding the wounded region. Previously, Abramov *et al.,* [362] studied the mechanism of vaginal wound healing in oestrogen- deficient *in vivo* rabbit model and revealed that the biomechanical properties of the wounded vaginal tissue was compromised in oophorectomized rabbits post-healing.

In humans, vaginal fibroblasts isolated from patients with prolapse were reported to produce stiffer ECM containing a higher amount of collagen III and a decreased amount of fibrillar collagen content and collagen cross-linking compared to those produced by the controls (pre-menopausal) [93]. Since the altered ECM production influences tissue quality and wound repair, the impaired vaginal wound healing often leads to failure of pelvic reconstructive procedures. Vaginal fibroblasts isolated from the control group produced matrices containing collagen type I fibres and cell nuclei anisotropically aligned in a preferential direction. Similar pattern of ECM arrangement was observed in the TE wound vaginal models presented here. Masson's trichrome (Figures 3.15 & 3.16) and picrosirius red staining (Figures 3.17 & 3.18) revealed that in the presence of E_2, the process of wound healing was accelerated, and the surrounding connective tissue contained collagen fibres densely arranged in parallel bundles. The data presented here is compatible with previous investigations in a guinea pig model of vaginal surgical incision to investigate the effects of oestrogen on the healing reproductive tissues [363]. Balgobin *et al.,* [363] reported that E_2-treated animals showed a significant increase in collagen content after 21 days post injury compared to sham. They suggested that E_2 plays a major role in the connective tissue remodelling in the injured vaginal wall by not only augmenting total collagen content but also resulted in an increased matured cross-linked collagen.

The pathophysiology of POP and SUI is highly complex which is characterised by the weakened connective tissue that accounts for loss of support to the pelvic organs. In the human body, fibroblasts are the main cell type present in the connective tissue responsible for collagen metabolism and ECM remodelling that effects the quality and mechanical properties of tissues. Clinical data has suggested that the overall collagen content in the vaginal wall is lowered in patients with POP as compared to without POP [89]. Fibroblasts are highly heterogeneous in their phenotype and can transform into myofibroblasts during the process of wound healing [367]. The differentiation and transition of vaginal fibroblasts to myofibroblasts is a crucial step in ECM remodelling during the process of vaginal wound healing that determines the fate of surgical outcome.

During the process of vaginal wound healing, myofibroblasts feature higher cellular contractility by expressing alpha-smooth muscle actin (α-SMA) contractile proteins that promotes maturation of the granulation tissue and accelerates wound closure by contraction [368]. However, prolonged myofibroblast activity may lead to pathological fibrotic tissue formation and contraction at the wound site that may contribute towards post-operative tissue scarring, implant deformation and contraction that can cause chronic pain [369]. The expression of α-SMA by myofibroblasts during the process of wound repair is a hallmark of connective tissue remodeling and enhanced wound contraction. TE wound vaginal models presented here showed the highest expression of α-SMA at day 14 that continued till day 21 post injury causing wound closure and contraction (Figure 3.22).

Clinical investigations on tissue explants from prolapsed patients has shown that the prolapsed connective tissue resembles with scar or granulation tissue as it contains a lower collagen I/III ratio that imparts stiffness to the tissues compared with healthy tissue. Hence, vaginal fibroblasts isolated from prolapsed patients showed increased α-SMA expression [93]. The effect of oestrogens on the vaginal wound healing was first investigated by Sjovall [370] in a rat model. Afterwards much evidence has supported that oestrogen deficiency contributes to a delayed and/or impaired wound healing [371]. During the proliferation and remodelling phase in dermal wound healing, oestrogens have been reported to impart mitogenic effects on keratocytes promoting cellular migration and reduce fibrosis by modulating the fibroblasts differentiation to myofibroblasts and downregulate the expression of α-SMA [359]. Similar findings have been reported here in *in vitro* TE wound vaginal models. In the presence of E_2,

the α-SMA expression was significantly decreased in TE wound models at days 14 and 21 compared to the control (without E_2) as shown in Figures 3.23 & 3.24. In my models, E_2 has shown to downregulate the α-SMA expression from cultured vaginal (myo)fibroblasts that reduced the degree of wound contraction that can relieve the extent of fibrotic tissue formation. These results have clinical significance in developing therapies and implants for reconstructive procedures for the pelvic floor repair where normal vaginal wound healing alongside reduced scarring is desirable to achieve successful surgical outcome.

The strength of TE wound vaginal model presented here includes the ability to study the process of vaginal wound healing on an accelerated time scale of 3 weeks which otherwise would have been impossible while using animal models that require longer time periods of healing followed by elaborated histological evaluation and data acquisition. These wound vaginal models were cost effective, simple, reproducible and standardised to investigate factors that affect vaginal wound healing. In addition, my study design allowed to investigate multiple steps in the wound healing pathway including cellular migration and proliferation, granulation tissue formation, re-epithelialisation, collagen deposition and scar formation in an *in vitro* TE vaginal model. In contrast to other studies on vaginal wound healing, i have recapitulated the vaginal tissue response to surgical insult in the presence and/or absence of estradiol-17β in *in vitro* injury models. These characteristics highly accounts for the physiological relevance of my TE wound vaginal models towards *in vivo* vaginal wound healing in pre- and postmenopausal women and can aid to develop therapies for improved vaginal tissue healing after reconstructive pelvic floor surgeries.

Chapter 4:

Developing biomaterials for the female pelvic floor repair and their preclinical testing in tissue engineered wound vaginal models

4.1 Aim:

To characterise biomaterials for potential applications in the female pelvic floor repair and to test these materials in *in vitro* tissue engineered (TE) wound vaginal models.

The specific objectives to achieve were:

- To electrospun polyurethane (PU) mesh as a potential biomaterial for the female pelvic floor repair
- To compare the mechanical properties of electrospun polyurethane (PU) with that of polypropylene (PPL) mesh
- To develop partial-thickness (PT) tissue engineered (TE) wound vaginal models for the purpose of biomaterial implantation into the models
- To compare the histology and cell viability of PT wound vaginal models with implanted biomaterials
- To determine the effect of female sex steroid estradiol-17β on the wound healing process in PT TE wound vaginal models in the presence of implanted biomaterials
- To determine the expression of key regulatory markers during the vaginal wound healing process with and/or without estradiol-17β in the presence of implanted biomaterials

4.2 Introduction:

Pelvic organ prolapse is a serious health problem that affects almost 50% post-menopausal women worldwide [1]. With a 19% lifetime risk of surgical intervention in patients with prolapse, the vaginal prolapse surgery aims to restore the anatomical support of the pelvic floor aided with implantation of vaginal mesh [372]. Until recently, the use of non-degradable lightweight polypropylene mesh implants was the most common treatment option in urogynecology surgery. However, due to a higher incidence rate (about 30%) of unacceptable post-operative mesh-specific complications, these meshes are now banned in several countries

including UK, USA, Australia and New Zealand [373]. Thus, there is a serious unmet demand for the development of new biomaterials for the treatment of POP and SUI.

PPL and related complications:

Polypropylene (PPL) is a non-degradable, inert, nontoxic synthetic material predominantly used in synthetic knitted mesh production that were first designed for use in the abdominal wall hernia repair [111]. After reports of mesh-related complications, Klinge *et al.,* [374] investigated explanted mesh used for abdominal wall hernia repair in humans during revision operations and reported severe inflammation and persistent foreign body reaction associated with implantation of non-absorbable meshes. Evidence has suggested that knitted PPL implants triggers a chronic inflammatory response at the implant site that results in contractile scar formation [375].

The use of PPL mesh grafts in pelvic floor reconstructive procedures remained popular despite absence of significant evidence-based preclinical safety studies to treat PFDs. Then until in 2008, the FDA released its first public health warning concerning the use of PPL transvaginal mesh after receiving an alarming high number of reports concerning mesh-related post-operative complications [376]. One suggested explanation is that due to the dynamic mechanical loading and unloading in the pelvic region, shear stress forces are created at the PPL mesh-tissue interface that affects the ECM components to produce stiffer collagen matrix resulting in a fibrous tissue formation [377]. In addition, the mismatch between the biomechanical properties of the PPL mesh and the native vaginal tissue results in poor mesh integration that later become exposed or erode through the vaginal wall causing tissue scarring [378].

An ideal biomaterial for the reconstruction of the weakened pelvic floor tissues should be designed like a hammock: mechanically strong and flexible under dynamic intraabdominal pressure (IAP) changes, relatively stiffer under tension and should be biocompatible and bioactive to induce an appropriate host-tissue response for proper implant integration. Although the commercial PPL meshes are biomechanically strong enough to provide the essential support to the pelvic organs however, they are relatively rigid, bioactivity is limited, and their design does not recapitulate the microstructure of the native ECM essential to restore the native tissue function. Moreover, PPL meshes are now known to have less biocompatibility

and poor tissue integration that can cause adverse prolonged proinflammatory (M1) macrophage response leading to mesh failure [379]. Therefore, it is now well understood that new mesh materials need to be designed with practical considerations of the choice of material, design of mesh, porosity, surface chemistry as well as biological response towards the mesh.

Developing new polymeric meshes using electrospinning:

Electrospinning is a highly attractive fabrication technique that is used to develop nano and microporous sheet with ultrathin polymeric fibres to produce a new generation of urogynecological meshes [380]. The basic principle behind electrospinning involves the application of an electrohydrodynamic-based electrostatic force around a syringe containing the polymer solution to draw polymeric nanofibers through a metallic nozzle tip or needle over a particular distance to be collected on a rotating metallic collector in either an aligned or a nonaligned arrangement. As a result, the meshes produced are highly porous with a large surface area to volume ratio containing interconnecting pores for higher cellular infiltration into the mesh.

Electrospinning is a versatile technology by which a wide range of materials could be produced with tunable porosity, fibre diameter, fibre alignment and interconnectivity by changing the process parameters [381]. These nanomaterials mimic the geometrical structure of native vaginal tissue ECM which are designed for improved biocompatibility pivotal to efficient tissue integration [382] and to ensure a controlled inflammatory response that favors regeneration of healthy tissue instead of scar tissue formation.

ECM-mimicking electrospun scaffolds hold the promise of a new class of pelvic floor implants that have a load-bearing function and also set the stage for the formation and regeneration of healthy soft tissue. Several FDA approved degradable polymeric materials such as polycaprolactone (PCL), polylactic acid (PLA), polylactic-co-glycolic acid (PLGA), polyurethane (PU) as well as blends of co-polymers have been explored in literature as potential biomaterials for the pelvic floor repair and summarised in Table 4.1 [133].

Table 4.1: Summary of in vivo studies of the electrospun matrices in urogynecological research [133].

Biomaterial	Aim of study	Main findings
Poly (lactic acid) (PLA)	Urogynecological alternative implant, Implants tested in subcutaneous rat models for TE applications	Cellular infiltration into the implant, tissue remodelling and collagen synthesis and neo-tissue formation
Poly (caprolactone) (PCL)	Skin TE and wound healing	Re-epithelialisation and formation of new dermal tissue, wound closure
Poly (lactic-co-glycolic acid) (PLGA)	Bladder tissue engineering, Tested in a rat model as a hybrid with bladder acellular matrix	Good integration at the implant-tissue interface, neo-tissue formation
Poly (urethane) (PU)	Urogynecological alternative implant, Tested in CAM, Soft TE in subcutaneous rat model hybrid with urinary bladder matrix	Angiogenesis and implant integration, Explants had comparable tensile strength, bioactivity and neo-tissue formation
Poly (ethyleneterephthalate) (PET)	Non-degradable mesh in subcutaneous rat model	Presence of foreign giant cells into the implant site
Silk	Vascular reconstructive conduits in rat model, Urethra reconstruction in urethral mucosal dog model	Cellular infiltration into the graft, Neo-tissue formation, absence of inflammation
Polymer blends	PLGA/acellular matrix for bladder regeneration in urinary rat model PLLA/PCL membranes for bladder tissue engineering	Bladder regeneration, micro-vascularisation Neo-tissue and matrix formation

In this chapter, electrospun thermoplastic polyurethane (TPU) mesh was fabricated as a candidate material for the treatment of PFDs. Polyurethanes (PU) are a large group of polymers that combines the mechanical properties of elastomer and thermoplastics to exhibit elasticity, mechanical strength, stability and ease in processibility [125]. Thermoplastic polyurethanes have long been successfully used as medical-grade polymers in various tissue engineering applications and reconstructive and cosmetic procedures such as breast implants [383].

Previous study from our group on PU mesh implantation in *ex-ovo* chick chorioallantoic (CAM) model have reported improved mechanical flexibility, cellular infiltration, collagen production, tissue integration and angiogenesis [384]. In addition, studies on different polymeric materials in *in vivo* rabbit abdominal wall defect models were carried out to investigate the long-term biomechanical and cellular response towards PU in comparison with PLA, PVDF and the PPL mesh [139]. Tissue explants revealed that the PU mesh implants were mechanically stable, showed better tissue integration and cellular infiltration, displayed an M2 dominant profile and showed absence of shrinkage at 90 days post-implantation. In another study from our group [385], electrospun PU mesh was implanted in a sheep model to investigate the host vaginal tissue response *in vivo.* After 6 months post-implantation, histomorphological analysis of the explanted sheep vaginal tissues showed that the PU was well tolerated without any adverse effects on the vaginal mechanical properties. In addition, an early stage M2 macrophage response was observed in PU implanted samples compared to the conventional lightweight PPL mesh. Thus, PU scaffolds hold promising mechanical and biochemical properties to be explored as a potential candidate material for future applications in reconstructive pelvic procedures.

Clinically relevant models for material testing:

Ideally, newly developed biomaterials should be tested initially in preclinical *in vitro* models and later in animal models that represents the real anatomical situation of the PFDs in humans as closely as possible. Biomaterials designed for the pelvic floor repair are usually tested in subcutaneous animal models and occasionally in more expensive urogenital-organ models of rabbits, sheep or porcine [149]. Subcutaneous animal models are used for testing biocompatibility, host tissue response, implant integration, neovascularisation and post-surgical wound healing. The use of organ-specific models provides additional insights into the long-term dynamic biomechanical behavior of implants into the pelvic floor. Indeed these *in*

vivo models are valuable preclinical models to determine the biological and biomechanical behavior of pelvic floor implants.

Nevertheless, in the early stages of biomaterial development, what is needed is an efficient, inexpensive, fast and physiologically relevant *in vitro* model of the vaginal tissue to discriminate between materials that are biocompatible with the vaginal tissue and are suitable for later implantation in *in vivo* models. This strategy will help to reduce the need for animal testing in urogynecology research and to provide researchers with inexpensive and accessible *in vitro* testing models for early investigations into biocompatibility and tissue response towards newly developed pelvic implants. In this chapter, biomaterials designed for intended implantation into the pelvic floor were tested in *in vitro* TE wound vaginal models derived from sheep vaginal tissue and cells to evaluate the cellular and host-tissue response towards these materials.

4.3 Materials and Methods:

4.3.1: Selection of biomaterials for implantation:

Polyurethane (PU) Z3 polymer was selected as the comparative biomaterial for the commercial Gynemesh® that is composed of PPL material. PU was selected based on previous work within our group that showed that PU Z3 has desirable mechanical properties as well as good biocompatibility and tissue integration in *in vivo* rabbit model [139] and *ex-ovo* CAM assay [384].

PPL mesh:

Commercial Gynemesh® was purchased from Ethicon™ in 2017 before the implementation of ban on the sale of PPL meshes for POP repair later in 2019. The mesh was stored in a dry place at room temperature and used for research purpose only within our group. In this project the Gynemesh® was used as supplied in comparison with PU polymeric mesh to study the process of vaginal wound healing in *in vitro* TE model.

Polyurethane (PU) Z3:

PU Z3 was purchased from Biomer technology LTD, Cheshire, UK in the form of polymer granules and stored at 4 °C until use. A sacrificial layer of poly-(L)-lactic acid (PLA) was first electrospun to form a fibrous sheet on the aluminum foil to provide a no-contact surface to electrospun PU to maintain the microarchitecture of the fibrous PU sheet. Poly-(L)-lactic acid (PLA) was purchased from Sigma-Aldrich, UK having a density of 1.24 g/cm^3 and molecular weight (Mw) 55-90 KDa. The polymer granules were stored in air-tight plastic bottle at 4 °C until use.

4.3.2 Preparation of polymer solutions:

Polymer solutions were separately prepared for poly-(L)-lactic acid and polyurethane (PU) Z3. PLA was dissolved in dichloromethane (DCM) (40042, Sigma-Aldrich, UK) at a concentration of 10% wt/v at room temperature. The solution was left overnight on a benchtop shaker to allow for complete dissolution.

For polyurethane Z3, a solvent mix was first prepared containing 70% v/v *N, N*-Dimethyl formamide (DMF) (227056, Sigma-Aldrich, UK) and 30% v/v tetrahydrofuran (THF) (Sigma-Aldrich, UK) at room temperature. PU granules were then added at a concentration of 8% wt/v of the solvent mix and dissolved. The solution was left to achieve homogeneity on a benchtop shaker overnight.

4.3.3 Electrospinning:

PU mesh and PLA sacrificial layer was electrospun using the electrospinning setup illustrated in Figure 4.1 and handled in a sterile laminar flow culture hood.

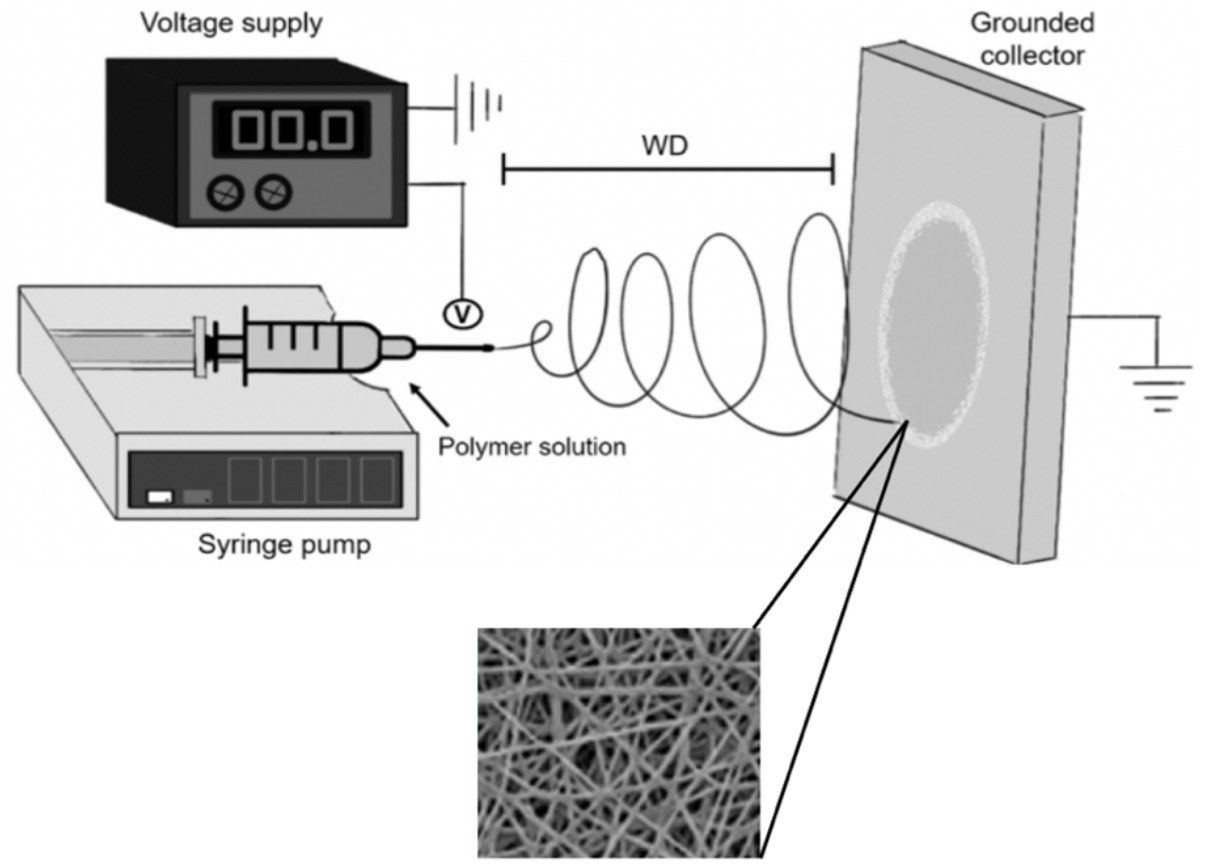

Figure 4.1: Illustration of the electrospinning setup.

Initially a sacrificial PLA layer was electrospun by spinning a total of 8 mL PLA polymer solution. PLA polymer in solution was loaded 2 mL into four individual 5 mL syringes containing blunt tipped 21 guage (G) needles (I & J Fisnar, Wayne, New Jersey) and fixed at

an equal level in a programmable Aladdin 100, Genie™ Plus (Kent Scientific, USA) syringe pump. The polymer solution was electrospun horizontally and delivered at a pump rate of 40 μL/min per syringe using an accelerating voltage of 17.4 kV DC from a voltage supply (Brandenburg, Alpha series III) across the electrospinning setup. The microfibres were collected over an aluminum foil wrapped earthed mandrel (160 mm in length and 80 mm in diameter) rotating at a speed of 265 rpm. The working distance (WD) between the tip of the needles and the collector was maintained at 20 cm provided with a 30% humidity inside the fume cabinet. After electrospinning of the PLA sacrificial layer, the voltage was disconnected, and the syringes were replaced with PU polymer solution containing syringes to continue electrospinning.

Electrospinning of 8% wt/v PU Z3 polymer solution was carried out in continuation over the PLA sacrificial layer. Total 80 mL of PU Z3 polymer solution was electrospun in two turns (20 mL each turn) by loading 5mL of solution into four individual syringes. The PU solution was delivered at a pump rate of 40 μL/min per syringe using an accelerating voltage of 20 kV DC across the electrospinning setup. The collector was set to rotate at 265 rpm and the distance between the tip of the needles and the mandrel was maintained at 24 cm. After electrospinning, the polymer sheet was allowed to dry in a fume cabinet overnight at room temperature. The PLA acted as a sacrificial layer and due to the difference of polarity with that of PU, it was easier to separate the PU layer from above the PLA layer by peeling off with the help of sterile forceps.

4.3.4: Scanning Electron Microscopy (SEM):

Scanning electron microscopy was performed to image the ultrastructure of PPL and PU Z3 meshes. The polymer samples were first cut circular with a diameter of 20 mm and then mounted on 12.5 mm metallic stubs with the help of a double-sided sticky sheet. The samples were then sputter coated with 25 nm gold using Edwards sputter coater S150B, (Crawley, England). The samples were then taken out and imaged under a high vacuum at different magnifications using FEI XL-20 scanning electron microscope (Philips, Cambridge, United Kingdom). The accelerating voltage was maintained between 10-15 kV and a laser spot size at 2 and 3 A˚. The images were then analysed using ImageJ software (National Institute of Health).

4.3.5: Mechanical testing of polymers:

Both PU Z3 and PPL were subjected to uniaxial linear and cyclic ramp test to determine the mechanical properties of the polymers. The samples were cut into 0.5 x 1.0 cm^2 pieces and their thickness was measured using a handheld micrometer screw gauge. The samples were then individually clamped vertically in a tensiometer (BOSE Electroforce instruments, Minnesota, USA) and were subjected to ramp test using a 22 N load. For uniaxial linear testing, the samples were elongated at a rate of 0.1 mm/s until the maximum point of stretch allowed using 22N load in the tensiometer. For the cyclic testing, each sample was stretched at a rate of 1 mm/s by applying a uniaxial force using the 22N load upto 25% displacement from its original length for 50 cycles. The values were standardised by using the width and thickness of polymers and reported as N/mm^2. The data was plotted as stress vs strain graphs using the GraphPad Prism V9.1.0 (216) for each polymer and statistical analysis was performed as described in section 3.3.16.

For PU, the initial linear gradient (represented as red line) on the curve was reported as the Young's modulus E (N/mm^2) referred to as "comfort-zone tangent modulus" due to the fact that it is an elastomeric polymer. The elastomeric polymers exhibit stiffness at the very initial timepoint of first stretch. Beyond this initial stretch, these elastomers behave as stretchable polymers with flexible microfibre ultrastructure. Hence, for the purpose of this PhD project and to compare it with a non-elastomeric polymer such as PPL, this region was selected as the slope region to calculate the YM.

For PPL, as commercial Gynemesh®have variation in its architecture due to the randomly distributed knitted pattern, the YM values were calculated from the slope at the linear gradient (represented as a red line) and referred to as "stress-zone tangent modulus" on the stress/strain curve. PPL mesh exhibited high stiffness during this region, whereas in various other regions plastic deformation could be expected that resulted in a sudden drop in stiffness of the polymer. The tensile strength (TS) was calculated as the average force per unit area (F/A) of both polymers at the calculated Young's modulus (E) region of slope on the stress/strain curve. This was due to the fact that the breaking point for both polymers could not be achieved with the 22N load available for these mechanical testing. Hence, the TS for both polymers is reported as an average tensile strength (TS) and not the Ultimate tensile strength (UTS). As I could not

determine the breaking point of PU and PPL due to the limitation of the tensiometer, the values for TS measured were the average values calculated at the YM.

The displacement at the TS was reported as strain that the polymer can withheld at that particular point before further stretching to achieve the breaking point. In the cyclic ramp test, the plastic deformation of PPL polymer was reported as the initial linear region on the cyclic graphs where the absence of stretchability could be seen increasing in subsequent cycles.

4.3.6 Primary vaginal epithelial cells and decellularised vaginal scaffolds:

Primary sheep vaginal epithelial cells and fibroblasts were isolated and maintained as discussed in sections 2.3.4 and 2.3.5. Sheep vaginal tissues were collected and decellularised using the detergent method discussed in section 2.3.5.

4.3.7 Developing and culturing tissue engineered (TE) partial-thickness (PT) wound vaginal models:

Tissue engineered (TE) wound vaginal models were developed and seeded with a co-culture cell suspension of primary vaginal epithelial cells and fibroblasts in Green's media as detailed in section 3.3.2. The models were cultured in submerged culture conditions for 3 days and incubated at 37 °C with 5% CO_2.

4.3.7.1 Biomaterial implantation in TE wound models:

After 3 days incubation, the models were aseptically transferred to sterile petri dishes under biosafety Class II laminar flow hood. With the help of sterile scalpel blade, partial-thickness (PT) incisions were performed separately on TE models as shown in Figure 4.2. Both biomaterials were cut 1 cm^2 x 0.1 cm^2 in the shape of small rectangles with the help of a pair of sterile scissors. The samples were then UV sterilised under a biosafety Class II laminar flow hood followed by washing with sterile PBS three times and then transferred to sterile petri plates until implantation.

After performing the incisions, the biomaterials (PPL and PU Z3) to be tested were separately implanted into the gaps created within the TE vaginal models in the direction of the incision as illustrated in Figure 4.1. The TE wound vaginal models with material implantation were then immediately transferred to sterile stainless-steel grids placed in new 6-well culture plates using

a set of sterile forceps with the wounded cell-seeded side alongside biomaterial implanted facing upwards. The models were cultured at an air-liquid interface (ALI) for up to 3 weeks and analysed at different time points as detailed in section 3.3.2.

4.3.7.2 Estradiol-17β induction studies on wound healing in the presence of implanted biomaterial on TE vaginal models:

To study the effect of estradiol-17β induction on wound healing in TE vaginal models with implanted biomaterials, E_2 concentration 100 pg/mL of Green's media was selected as discussed in section 3.3.2. The models were cultured in the presence of E_2 (100 pg/mL) at an ALI for 3 weeks and analysed at different time points as detailed previously in section 3.3.2 to trace the progress of wound healing in the presence of implanted biomaterials.

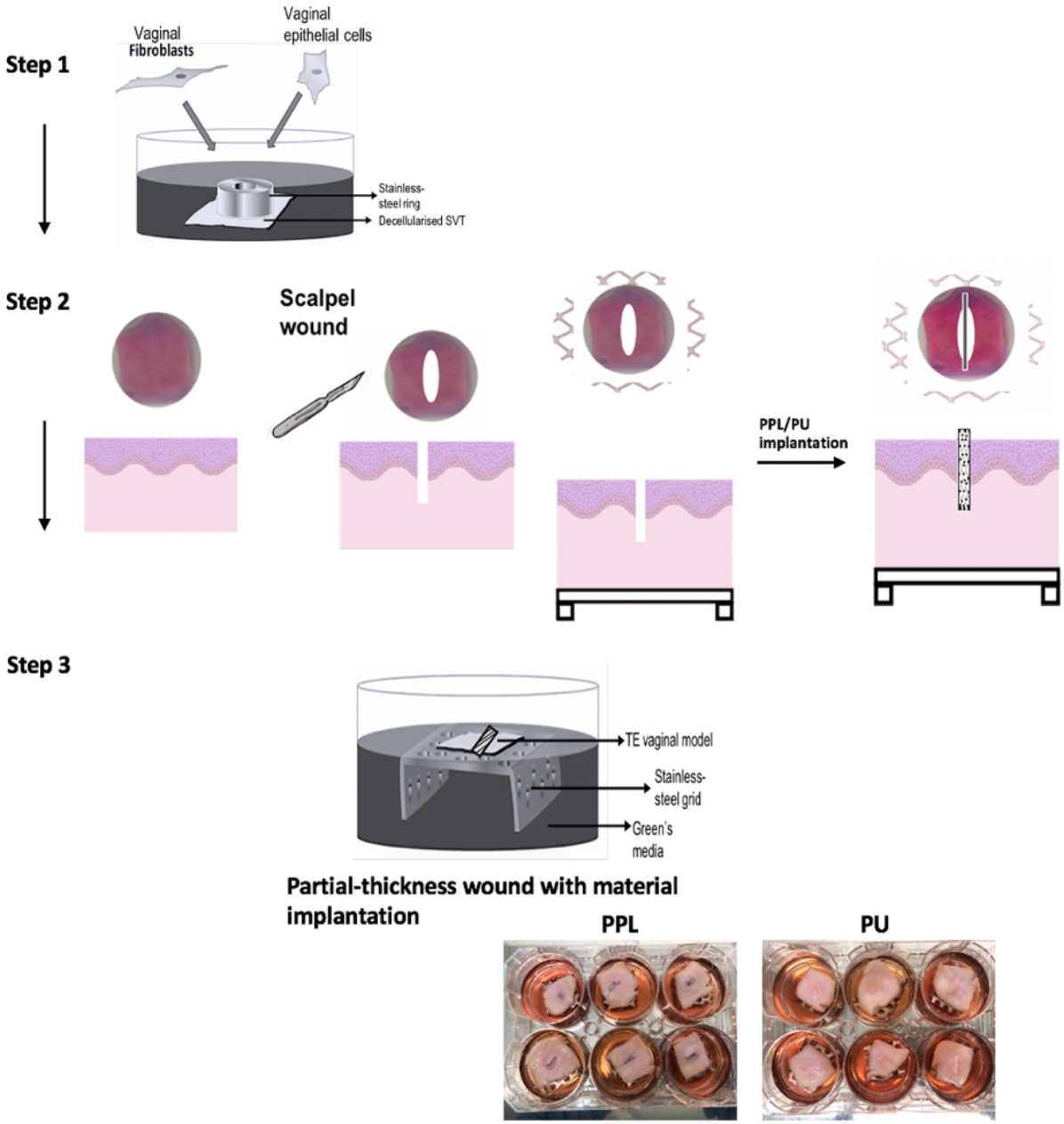

Figure 4.2: Schematic of key steps in the development of in vitro partial-thickness (PT) tissue engineered (TE) wound vaginal models for preclinical testing of the impact of biomaterials implantation on the process of vaginal wound healing.

4.3.8 Tissue fixation and histological analysis:

The fixation, viability, tissue processing and sectioning, H&E staining and picosirius red staining was performed as described in sections 2.3.8 - 2.3.12. The trichrome staining on tissue sections was performed as detailed in section 3.3.5. Images were taken as detailed in section 2.3.12.

4.3.9 Immunohistofluorescence (IHF) staining:

Details of the primary and secondary antibodies used are outlined in section 3.3.6 along with the methodology. The images were analysed and the fluorescence intensity measurements were taken as described in section 3.3.7.

4.4 Results:

4.4.1: Microstructutre of biomaterials:

Figure 4.3 demonstrates the microstructure of PPL mesh and PU Z3 electrospun polymeric sheet under scanning electron microscope (SEM) at different magnifications. The ultrastructure of commercial PPL based Gynemesh® exhibited a knitted monofilament macroporous mesh architecture with variable pore sizes throughout the entire mesh. The knitted region was observed tightly woven into a condensed pattern with intercalating regions of monofilament fibres. SEM images of electrospun 8% PU Z3 showed randomly arranged polymer fibres forming a microporous sheet with an average mean pore size of about 15-35 μm ± 5.1. The porosity was randomly distributed throughout the polymer sheet with maximum pore sizes in the range of 20-25 μm. The ultrastructure of PU Z3 resembled the native ECM organisation in terms of heterogeneity, porosity and interconnectivity that has a significant effect on host cell infiltration and immune response towards the implanted biomaterials.

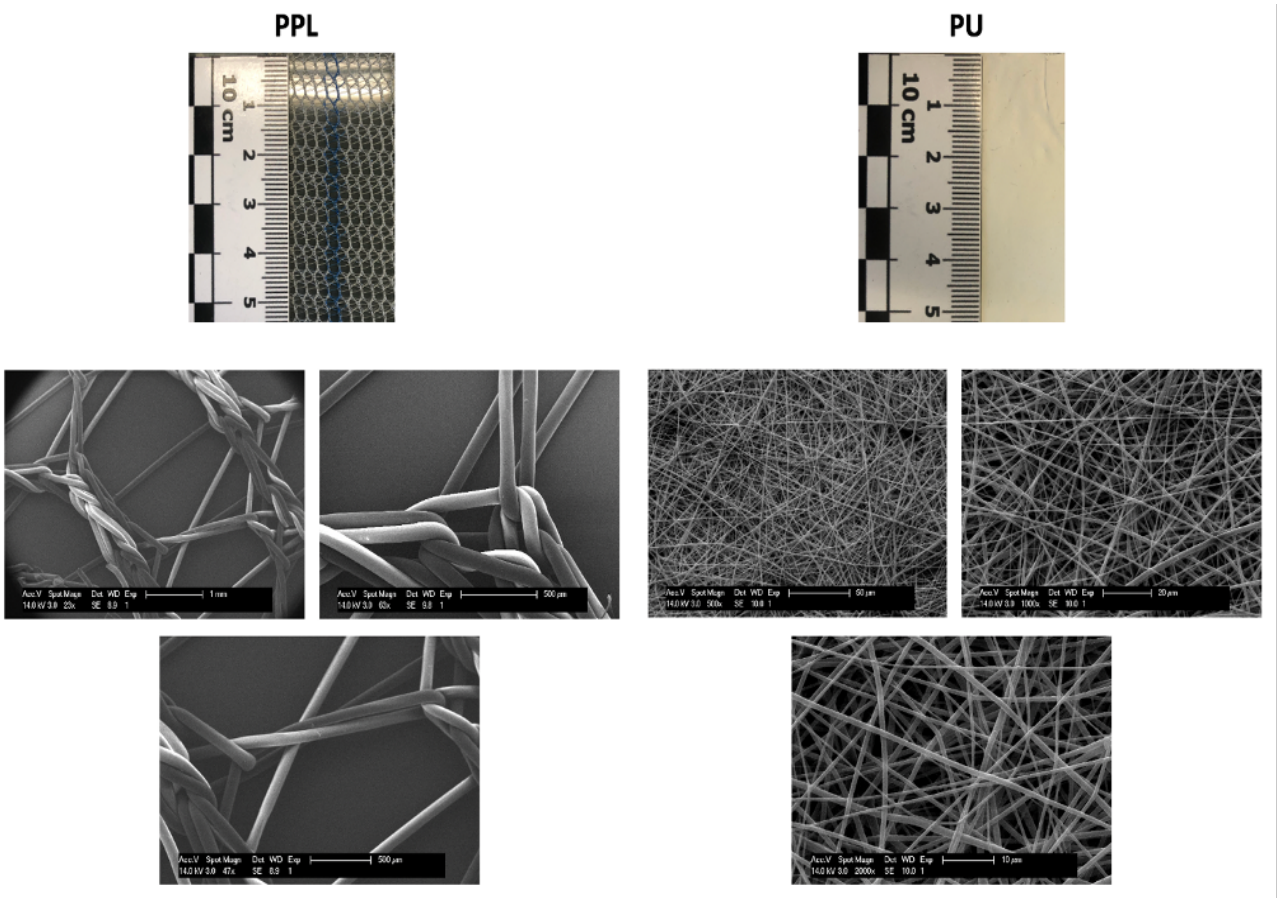

Figure 4.3: Scanning electron microscopy (SEM) of commercial polypropylene (PPL) Gynemesh® and electrospun 8% wt/v polyurethane (PU) Z3.

4.4.2: Mechanical properties of biomaterials:

The stress-strain curves of the uniaxial linear tensiometry of both PPL mesh and PU Z3 are shown in Figure 4.4 and the average values for Young's modulus (YM), tensile strength (TS) and strain for both biomaterials is graphically presented in Figure 4.5. There was a significant difference between the two biomaterials with respect to Young's modulus calculated at the subsequent tangent gradients and the average YM values for both polymers was around 10.19-12.037 N/mm^2 which is significantly higher than the average YM values for healthy native vaginal tissue fascia (6.4-10.1 N/mm^2). These values indicated that both PPL mesh and PU Z3 are mechanically strong biomaterials desirable to provide adequate support to the prolapsed pelvic floor fascia and muscles. The average tensile strength (TS) for PPL mesh (5.65 ± 0.51 N/mm^2) calculated at the slope region was significantly higher than the PU Z3 (3.26 ± 0.46

N/mm^2). These values indicated that the PPL mesh showed a much stiffer behavior than PU Z3. Nevertheless, both biomaterials have been shown to withstand the dynamic pressure changes experienced in the intraabdominal cavity that is reflected in their high strain values as graphically shown in Figure 4.5.

Figure 4.6A demonstrate the stress-strain curves for both PPL mesh and PU Z3 when subjected to cyclic uniaxial ramp tensile testing and the Young's modulus (YM) values for the 1st, 2nd and 3rd cycles are shown graphically in Figure 4.6B. The PPL mesh showed no significant difference in the average YM values calculated for cycle 1 and 2 of the cyclic tensile testing. However, the PPL mesh displayed an initial region of deformation (indicated as red lines) on the cyclic tensile testing graphs for PPL. These results showed that there was a significant deterioration in the mechanical properties of PPL mesh subjected to cyclic loading and unloading and the material displayed a permanent deformation under the applied dynamic force.

On the contrary, there was a significant difference in the average YM values calculated for PU Z3 between cycles 1 and 2 of the cyclic ramp testing. This phenomenon is expected of an electrospun elastomeric polymer where an initial stretching of the polymer sheet caused a derangement of the randomly aligned polymer fibres resulting in an initial decline in YM however, subsequent cycles showed no further decline in the YM values for PU Z3 and the values were comparable to those of PPL mesh. In addition, no initial region of deformation was observed in cyclic testing of PU Z3. This data showed that the PU Z3 retained its mechanical properties when subjected to dynamic loading and unloading and displayed a high elasticity and stretchability behavior. This mechanical property is promising to PU Z3 as a potential candidate material for future implantation into anatomical sites subjected to dynamic pressure changes such as the female pelvic floor.

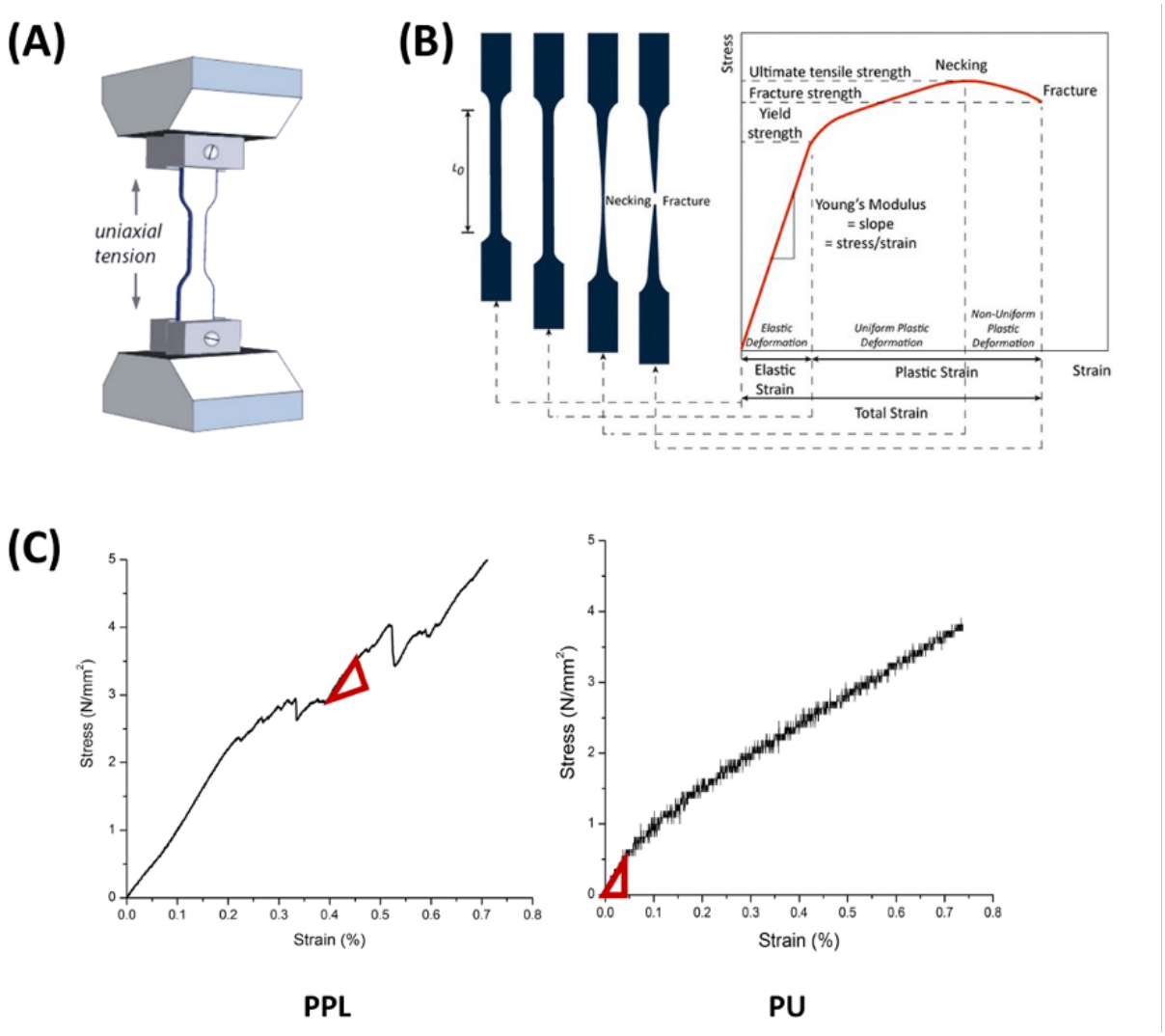

Figure 4.4: (A)Uniaxial linear ramp test for PPL and PU Z3 biomaterials. (B) Illustration of different stages during the uniaxial stretching of tested materials. (C) Stress vs strain plots for PPL and PU by non-cyclic uniaxial ramp tensile testing. The slope region is marked with the red outline. For PU, the initial region called as the "comfort-zone tangent modulus" was calculated as it is an elastomeric polymer whereas for PPL the "stress-zone tangent modulus" was calculated due to its non-elastomeric behavior.

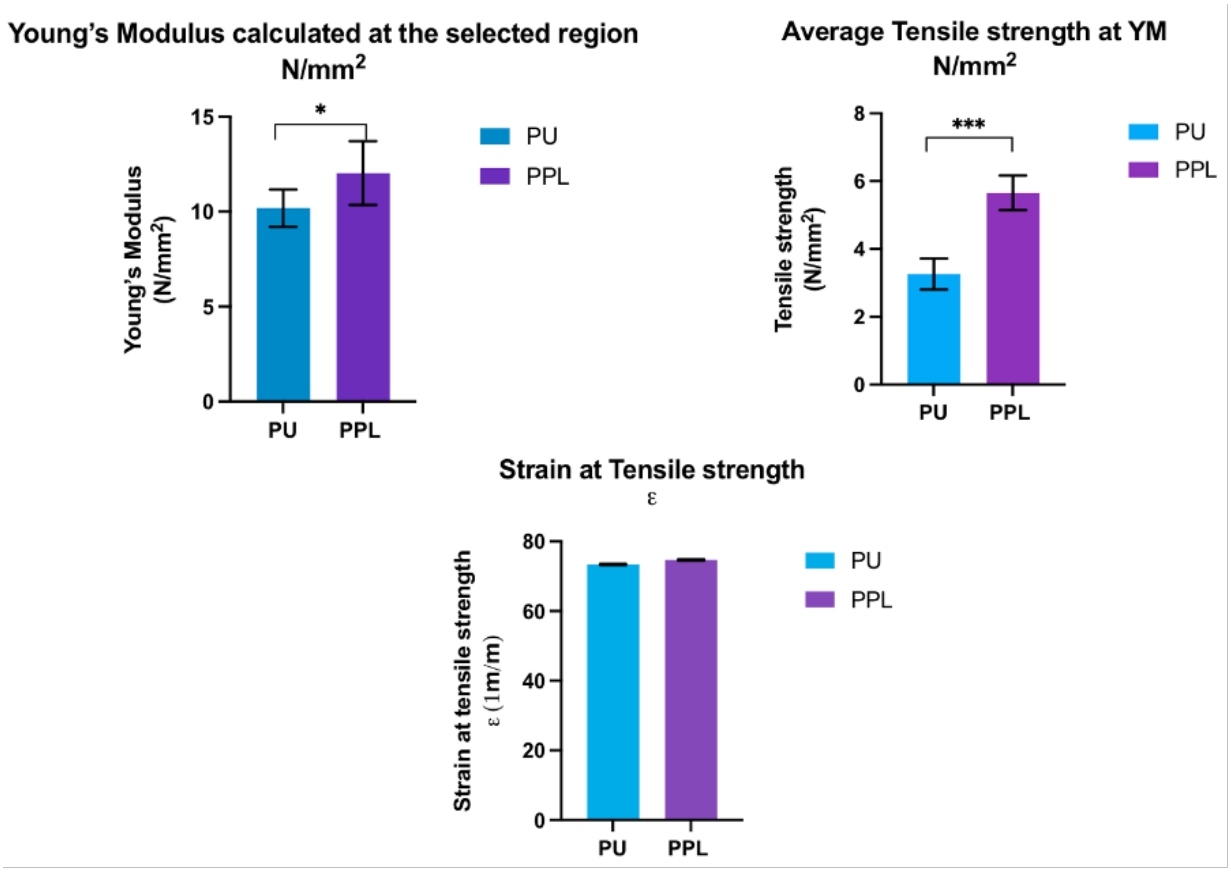

*Figure 4.5: Graphical representation of the values for the mechanical properties of PPL and PU Z3 electrospun polymers. The values were calculated from the stress vs strain plots for non-cyclic uniaxial ramp test. (n=9 for each group ± SD,*p<0.05, ***p< 0.005).*

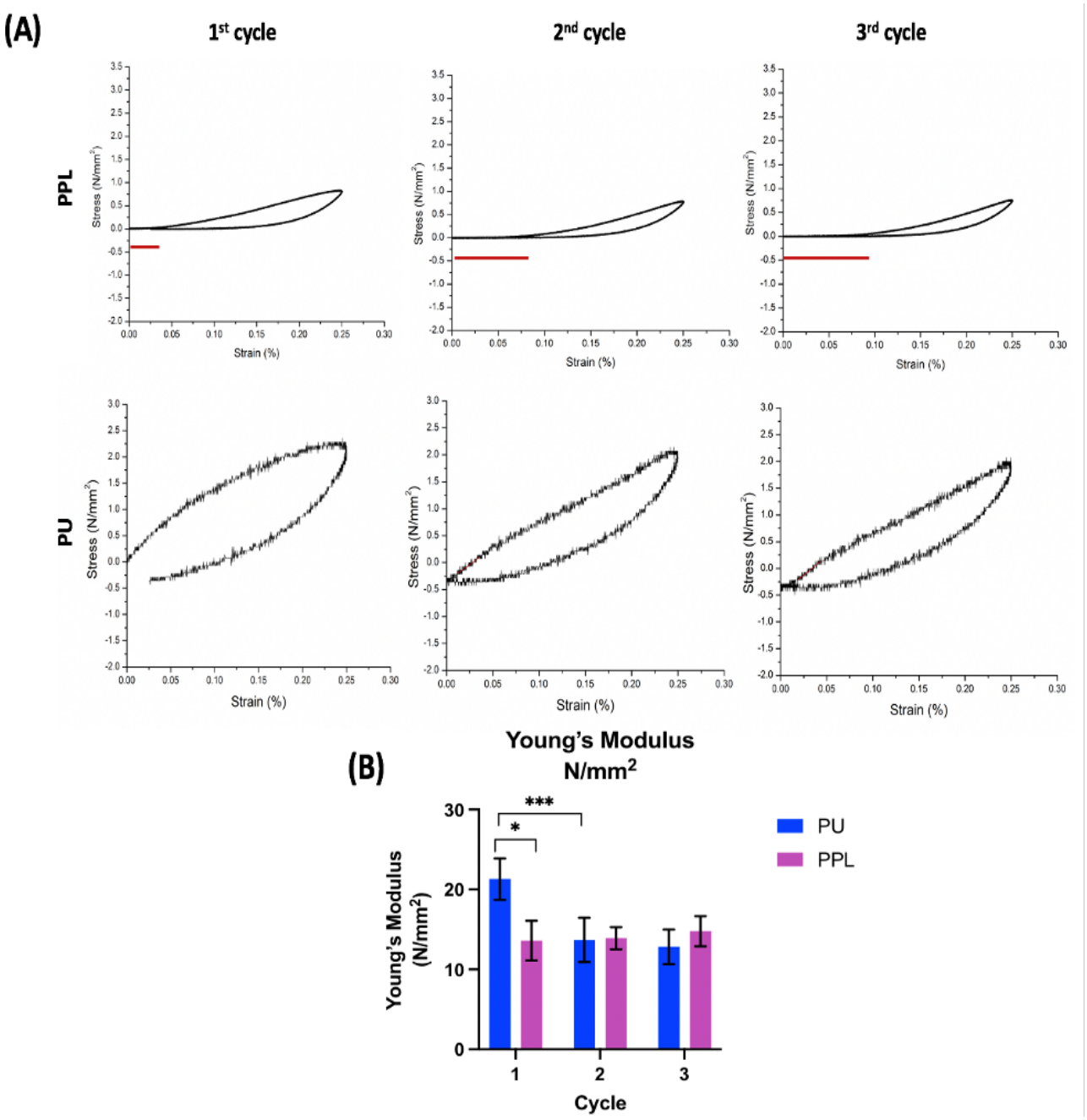

*Figure 4.6: Cyclic uniaxial ramp test for PPL and PU Z3. (A) Stress vs strain plots of the 1st, 2nd and 3rd cycles of stretching for PPL and PU Z3. The deformation in the polymer ultrastructure has been shown via red line indicating the region. (B) Graphical representation of the Young's modulus (YM) values for both polymers as calculated from the cyclic curves for the 1st, 2nd and 3rd cycles. (n=9 for each group ± SD, *p=0.02, ***p<0.005).*

4.4.3 Effect of biomaterial implantation in TE wound vaginal models on cellular infiltration and metabolic activity:

Figure 4.7 demonstrates the TE wound vaginal models with biomaterials implantation three weeks post-implantation under brightfield microscopy. Paraffin-embedded TE vaginal models were processed through the microtome to acquire 5 μm tissue sections and were observed under a light microscope to reveal the placement of PPL mesh and PU Z3 into the wounded region before performing any staining method for further investigations. Since subsequent staining procedures such as H&E, trichrome and picrosirius red protocols require extensive removal of paraffin and washing steps so it was impossible to image each sample along with the actual placement of implanted biomaterials within the wounded tissue region at every stage. Hence, bright field microscopy images are shown in Figure 4.7 to confirm the placement of biomaterials within the TE vaginal models before further processing.

Figures 4.8 and 4.9 depicts the haematoxylin and eosin (H&E) staining of TE wound vaginal models implanted with PPL mesh at different time points in the absence and presence of estradiol 17-β (100 pg/mL of Green's media) respectively. In the presence of PPL mesh, the process of re-epithelialisation of the TE wound models remained impaired and the vaginal epithelia seemed fragile and the tissue sections surrounding the PPL mesh region of implantation was observed deteriorated and injurious. The presence of E_2 in the culture media was shown to trigger an intense cellular infiltration and migration towards the implanted region in TE models as shown in Figure 4.9. There appeared to be an increase in the formation of clumps of vaginal epithelial cells clustered alongside the margins of the wounded region over three weeks in an ALI culture however, the formation of a healthy stratified epithelium remained nonexistent in tissue sections implanted with PPL mesh.

On the contrary, in the presence of PU Z3 implanted within the wounded TE vaginal models, formation of a healthy stratified squamous epithelia was observed over the TE models that continued within the wounded region until the implanted PU Z3 as shown in Figure 4.10. The surrounding tissue remained healthy and integral with an appropriate cellular infiltration towards the wounded region. The vaginal epithelial cells were also shown to form clusters alongside the PU biomaterial which is indicative of a positive cellular response towards PU that is prerequisite in the vaginal wound healing process. Coupled with the presence of

oestradiol 17-β (100 pg/mL of Green's media), the PU Z3 implanted TE wound vaginal models displayed the formation of a stratified epithelium on TE models beginning from week 2 in an ALI culture and continued to stratify up to three weeks post-implantation (Figure 4.11).

The collective presence of implanted PU Z3 and E_2 in the culture media increased the cellular metabolic activity in TE wound vaginal models compared to those implanted with PPL mesh as measured by the resazurin assay and shown in Figure 4.12. A continuous increase in the cellular viability was observed up to three weeks in an ALI culture for both PPL mesh and PU Z3 implanted TE models however, it was significantly higher in PU Z3 models compared to that in PPL mesh models.

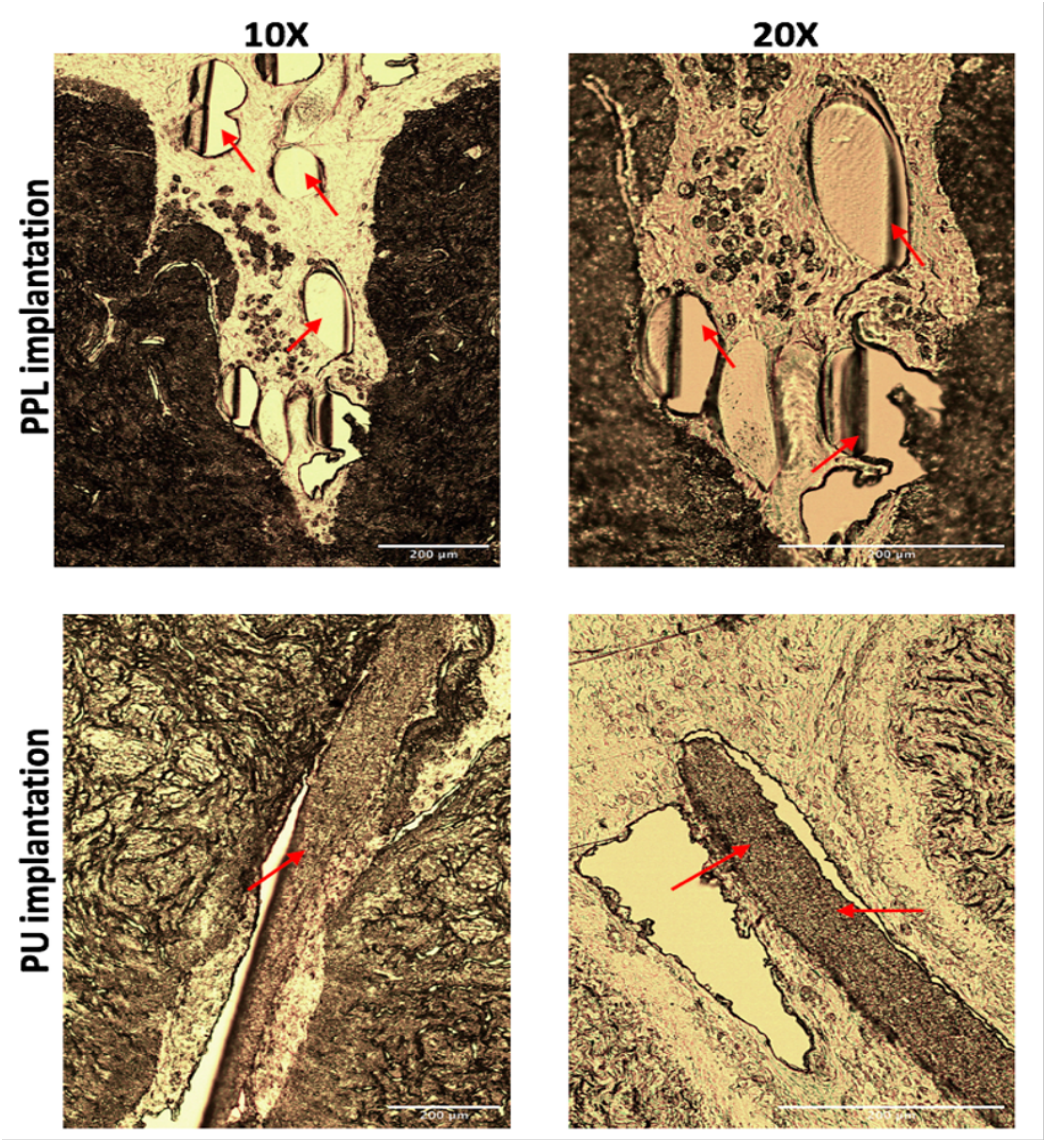

Figure 4.7: Histological analysis of PPL and PU Z3 polymers implanted in TE wound vaginal models at day 21 post-implantation under brightfield microscope. Tissue cross-sections showing that both PPL and PU Z3 remained implanted within the wounded gap region throughout the three weeks' time period at ALI culture. PPL appeared as circular regions of polymer (indicated with red arrow heads) representative of the knitted pattern present in the polymer whereas PU Z3 appeared as a microporous sheet of polymer within the wounded region (indicated with red arrow heads) in the TE vaginal models. Scale bar=200µm.

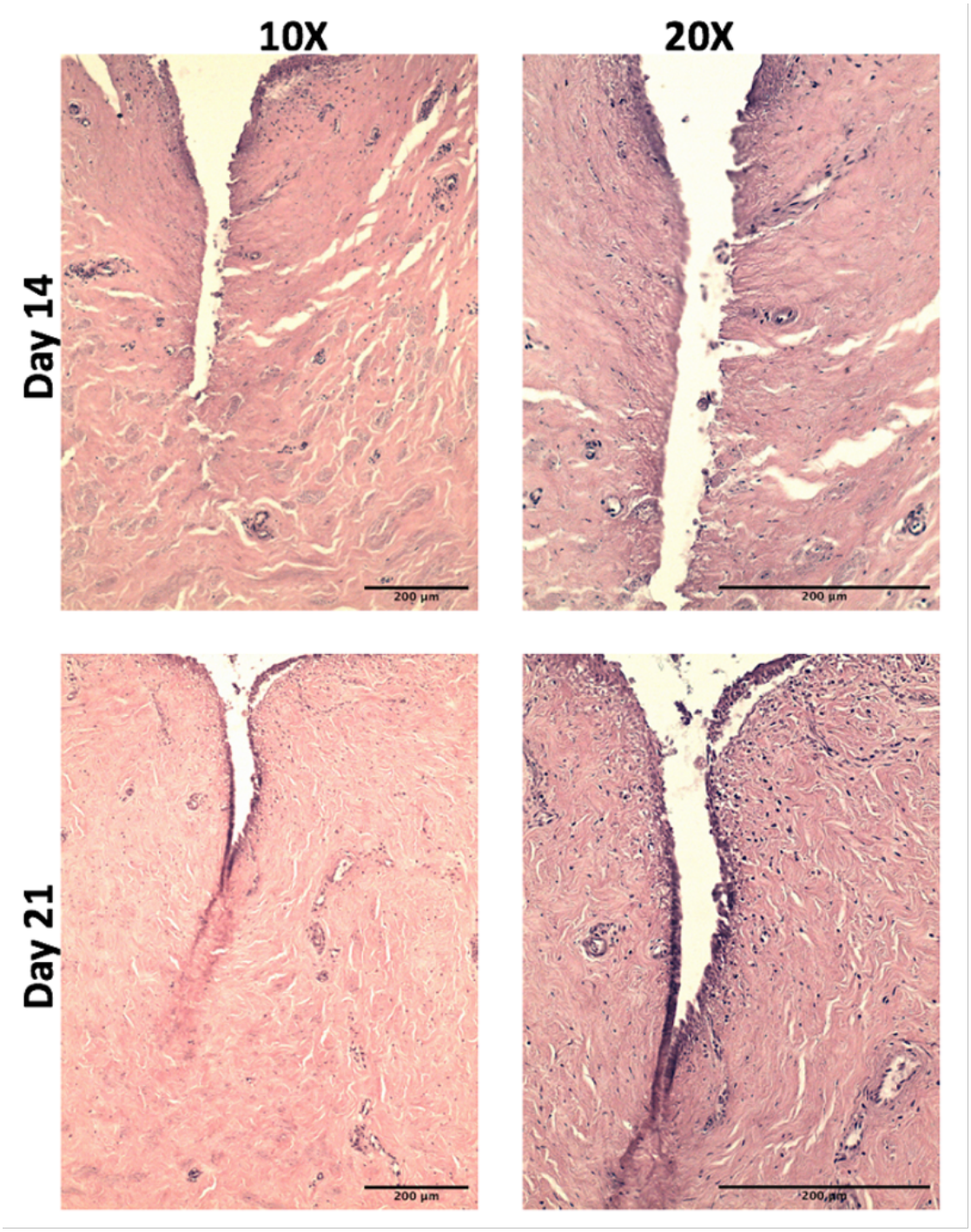

Figure 4.8: Haematoxylin and Eosin (H&E) stained tissue sections of TE wound vaginal models with PPL implantation at days 14 and 21 post-implantation. The epithelia of the models could be seen disrupted and discontinued at different regions and the wounded region was seen impaired specifically around the margins of PPL implanted region. Scale bar=200µm.

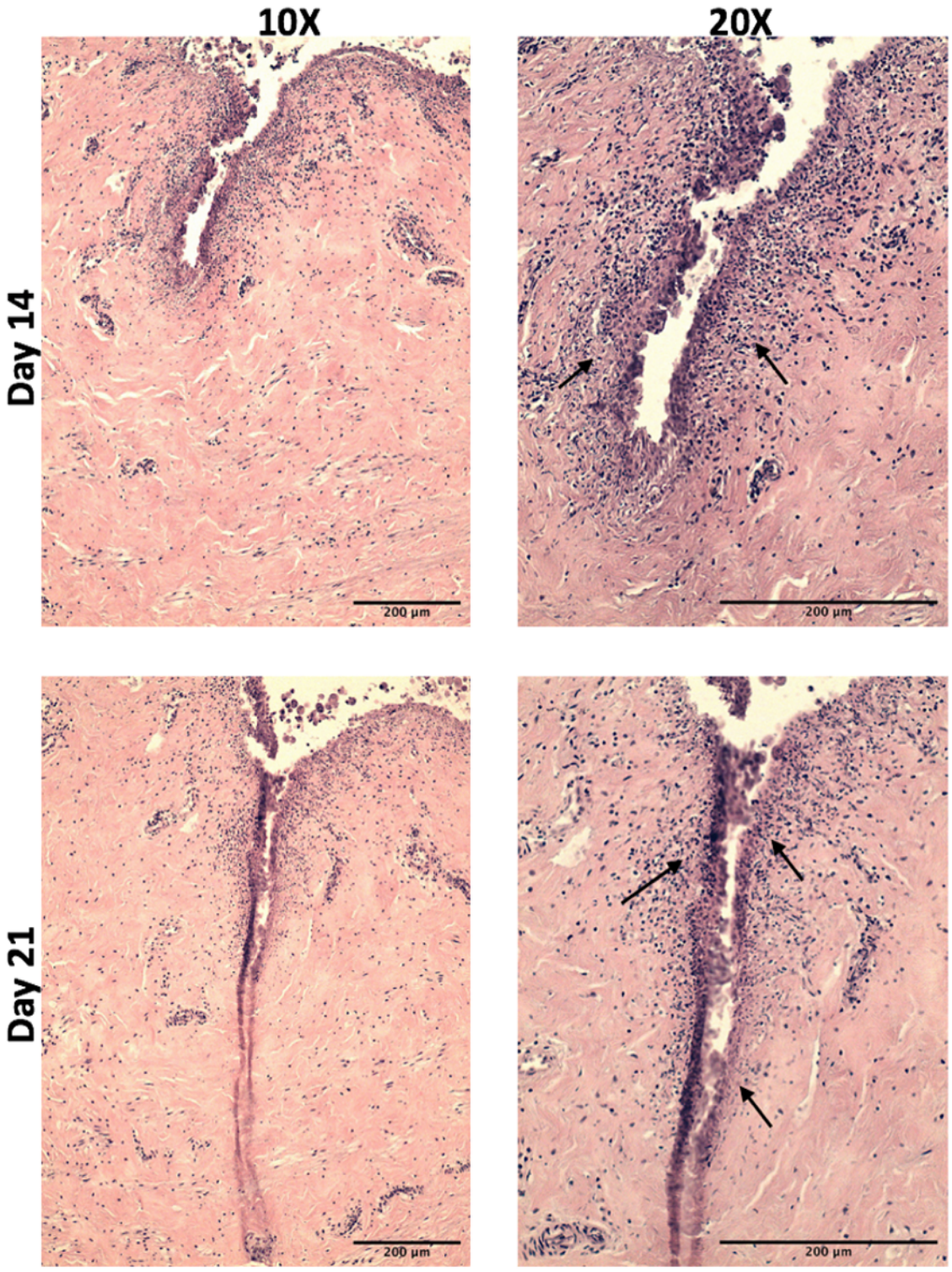

Figure 4.9: Haematoxylin and Eosin (H&E) stained tissue sections of TE wound vaginal models with PPL implantation at days 14 and 21 post-implantation cultured in the presence of estradiol-17β (100 pg/mL). An intense cellular infiltration and migration could be seen around the wounded region of the models explicitly around the PPL mesh implanted region (indicated with black arrow heads). A discontinuous epithelium was observed on the TE models with clumps of cells forming around the margins of the wounded region. Scale bar=200µm.

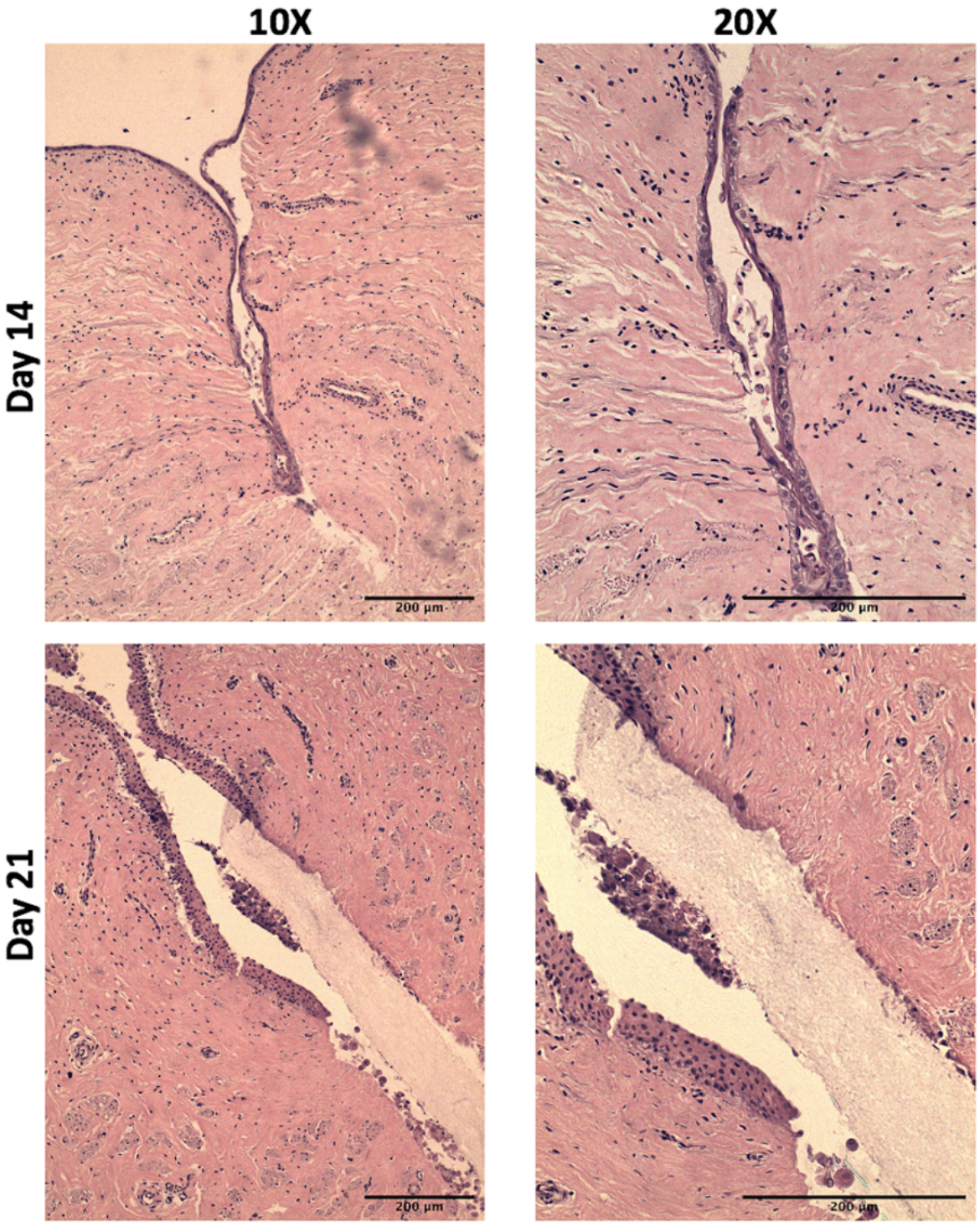

Figure 4.10: Haematoxylin and eosin (H&E) stained tissue sections of TE wound vaginal models with PU Z3 implantation at days 14 and 21 post-implantation. At day 21, re-epithelialisation of the TE wound vaginal models could be seen as the formation of a stratifies squamous epithelium was continuous over the wounded region. The surrounding tissue adjacent to the wounded region seemed healthy and populated with primary vaginal fibroblasts. PU Z3 was shown to be intact within the inner margin of the wound and was continuous with the adjacent vaginal tissue after 21 days in ALI culture. Scale bar=200µm.

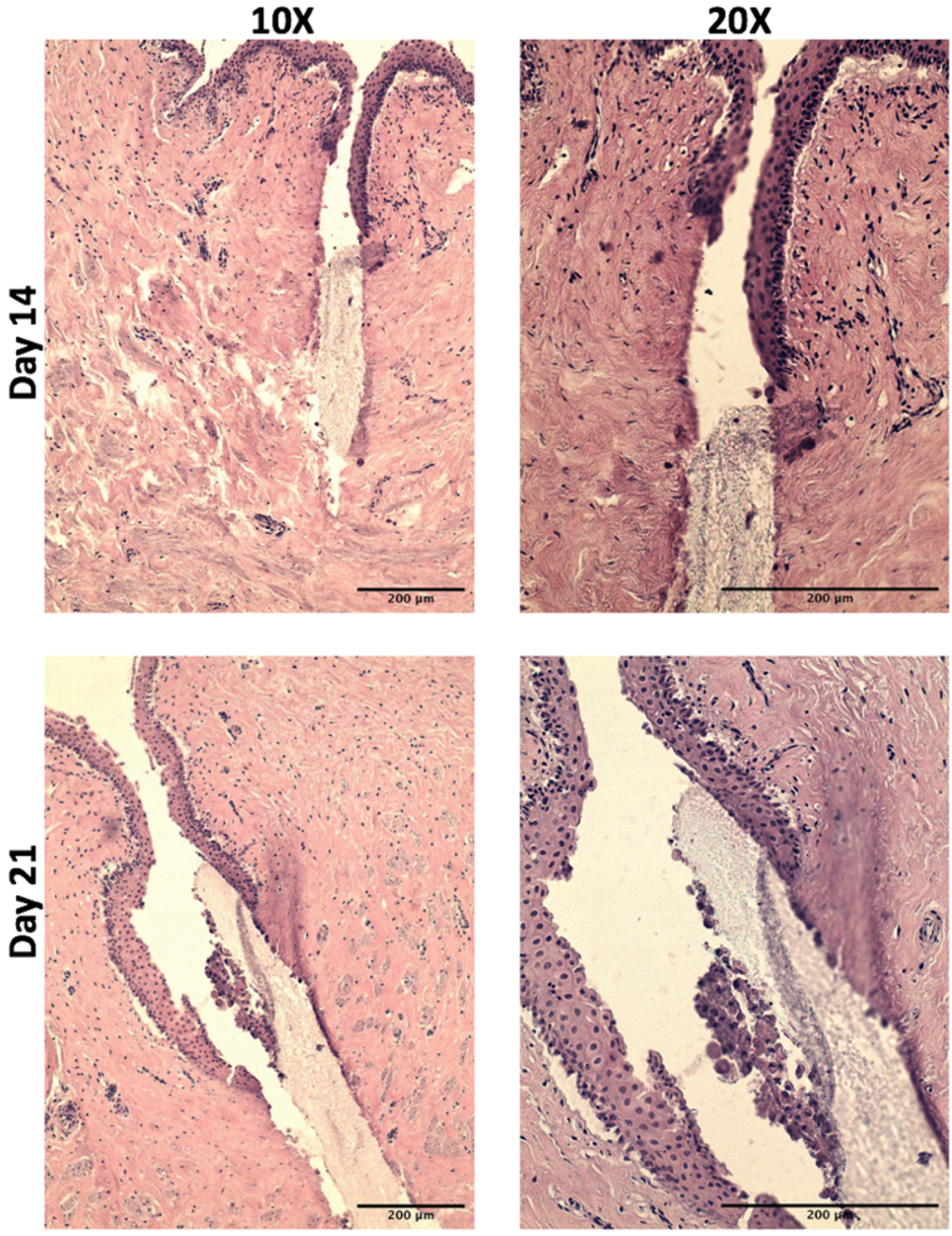

Figure 4.11: Haemetoxylin and eosin (H&E) stained tissue sections of TE wound vaginal models with PU Z3 implantation at days 14 and 21 post-implantation cultured in the presence of estradiol-17β (100 pg/mL). At day 14, a healthy stratified squamous epithelium was formed on TE vaginal models that continued until day 21 post-implantation. Scale bar=200µm.

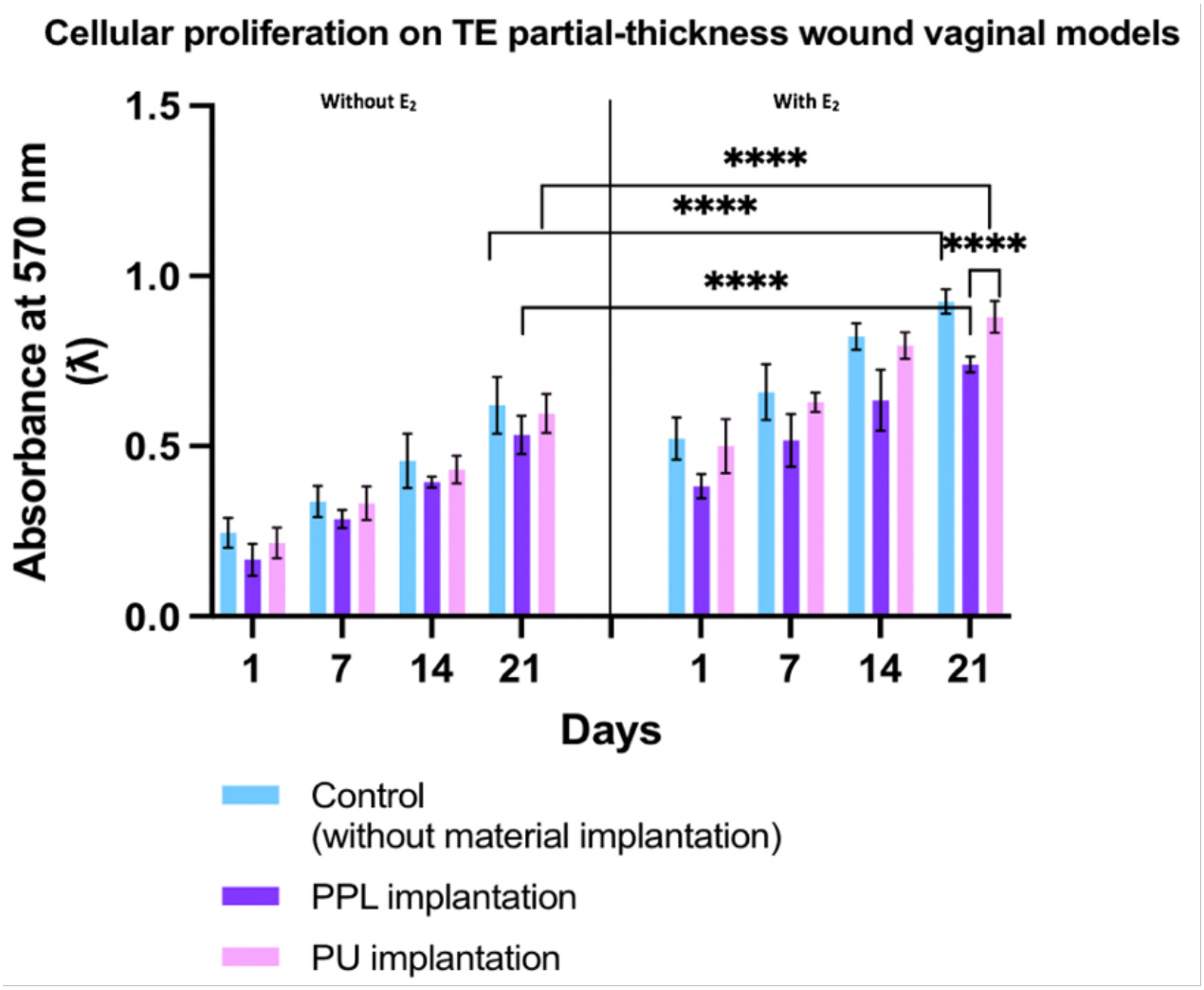

*Figure 4.12: Metabolic activity of primary sheep vaginal epithelial cells and fibroblasts cultured on TE PT wound vaginal models at different time points in ALI culture with and without biomaterials (PPL and PU Z3) implantation. The metabolic activity of the cultured cells was determined in the absence and presence of estradiol-17β (100 pg/mL). (n=9 ± SD for each group, N=3), ****p<0.0001.*

4.4.4 Demonstration of collagen changes during the vaginal wound healing process in the presence of implanted biomaterials:

The presence of biomaterials implanted into the wounded TE vaginal models also had an effect on the surrounding tissue ECM and it was determined using collagen-specific trichrome staining and picosirius red staining of the models at different time points in ALI culture.

Masson's trichrome staining was performed to determine the density and orientation of collagen fibres in the surrounding lamina propria of TE wound vaginal models during the process of *in vitro* vaginal wound healing in the presence of implanted biomaterials. The collagen component was stained green and/or deep green in color, the muscle fibres were stained red and the cellular component was stained brown/black in color. In the presence of PPL mesh implanted within the wounded region, the collagen fibres were oriented in a disordered arrangement (Figure 4.13) that appeared more oriented in the presence of estradiol-17β (100 pg/mL) in the culture media as shown in Figure 4.14. The collagen fibres were more compactly arranged and appeared deeper green in color at day 21 of PPL implantation showing an increase in collagen deposition around the wounded region in the presence of E_2 (Figure 4.14). In TE models implanted with PU Z3, an increase in collagen deposition with an increase in the formation of a stratified epithelia was observed as shown in Figure 4.15. The presence of E_2 in the culture media resulted in a more compactly arranged collagen fibres into regular circular orientation around the PU Z3 implanted wounded region (Figure 4.16). These results showed that the implantation of PU Z3 in the presence of E_2 caused an initial remodelling phase of the collagen component in the ECM of our TE models that can further influence the process of vaginal wound healing.

Picrosirius red staining of the TE wound vaginal models showed similar results for both PPL mesh and PU Z 3 implanted biomaterials. PPL mesh implanted models showed an irregular pattern of arrangement of collagen fibres in the surrounding ECM (Figure 4.17) that became more regular and denser in the presence of E_2 in the culture media as shown in Figure 4.18. Moreover, the presence of E_2 triggered the formation of a discontinous stratified epithelia on PPL implanted models that was absent in models cultured without E_2.

In TE wound vaginal models implanted with PU Z3, the collagen component appeared more denser and compact compared to PPL mesh models as shown in Figure 4.19. There was formation of continuous stratified epithelia on the models at day 14 that continued to develop and stratified into the wounded region until day 21 post-implantation. The addition of E_2 in the culture media further accelerated the process of collagen remodeling in the presence of PU Z3 implant as the collagen fibres were stained deep red in color indicating an increase in collagen production by cultured vaginal fibroblasts into ECM of the TE models as shown in Figure 4.20.

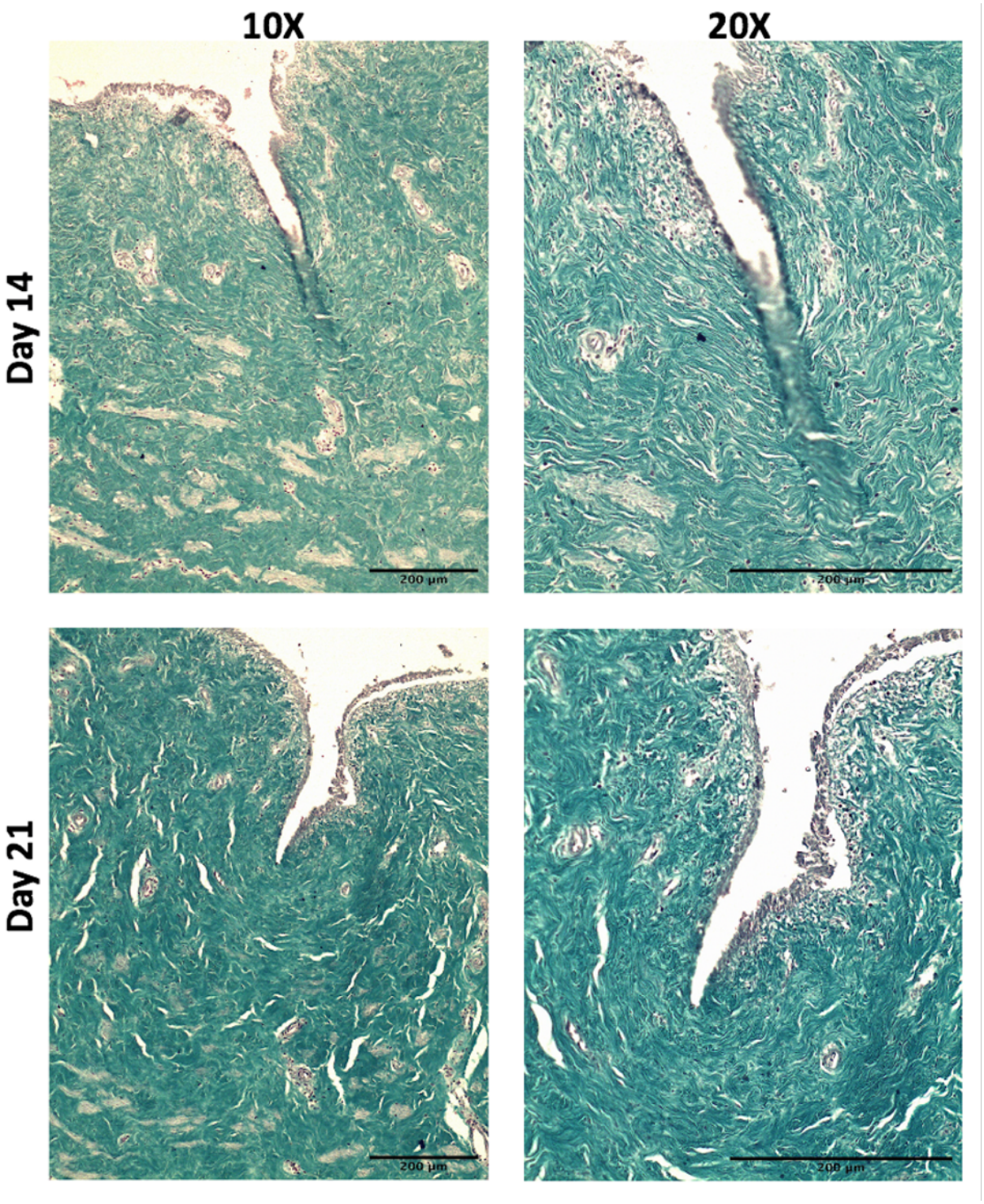

Figure 4.13: Trichrome staining of TE wound vaginal models with PPL implanted at days 14 and 21 post-implantation. The reformation of TE vaginal models' epithelia was observed disrupted in the presence of PPL implanted in the wounded region. Scale bar= 200µm.

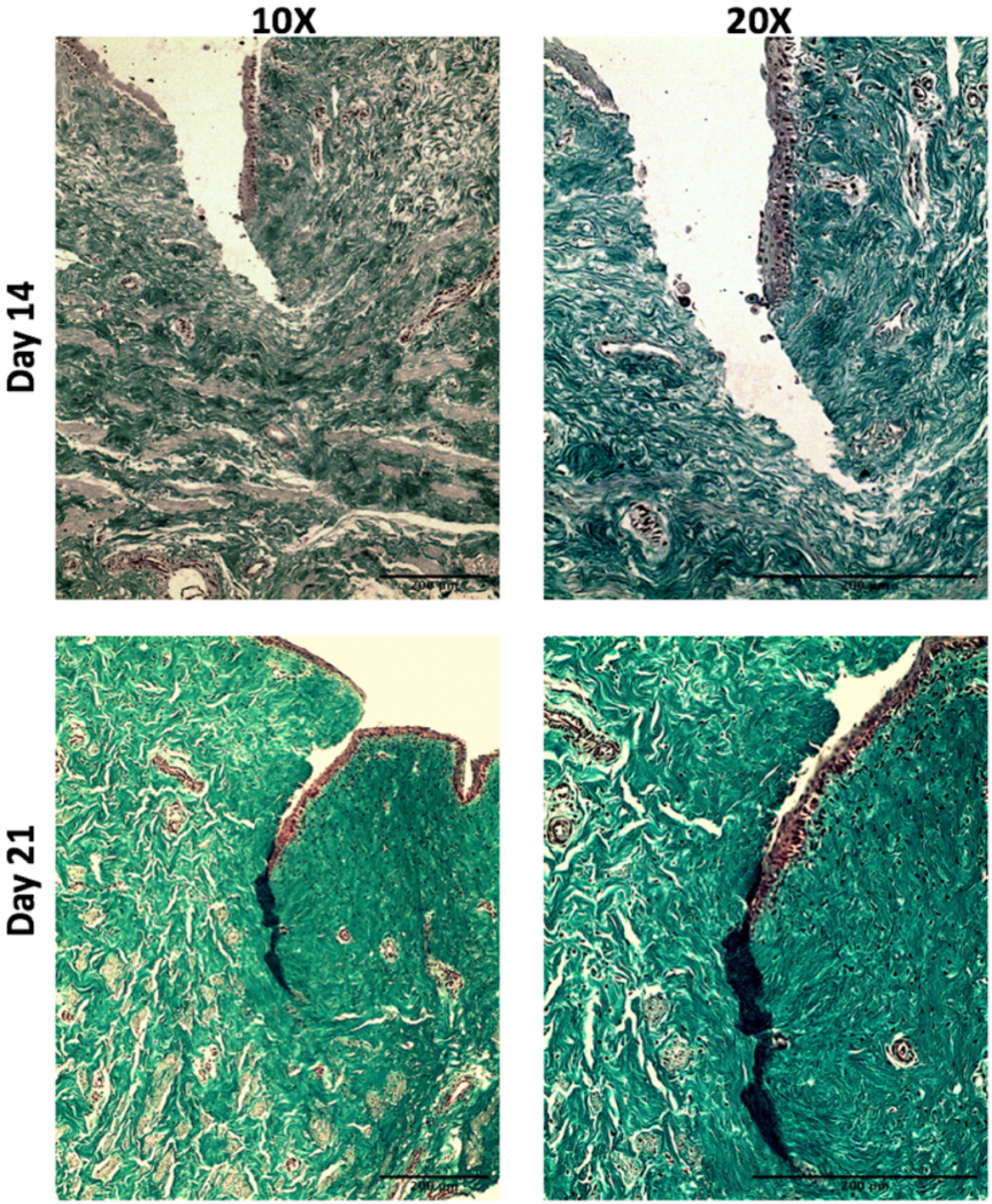

Figure 4.14: Trichrome staining of TE wound vaginal models with PPL implanted at days 14 and 21 post-implantation cultured in the presence of estradiol-17β (100 pg/mL). There was an inadequate formation of a stratified epithelia on the models and the surrounding connective tissue was stained densely with SF solution in the presence of E_2 in the culture medium. Scale bar= 200μm.

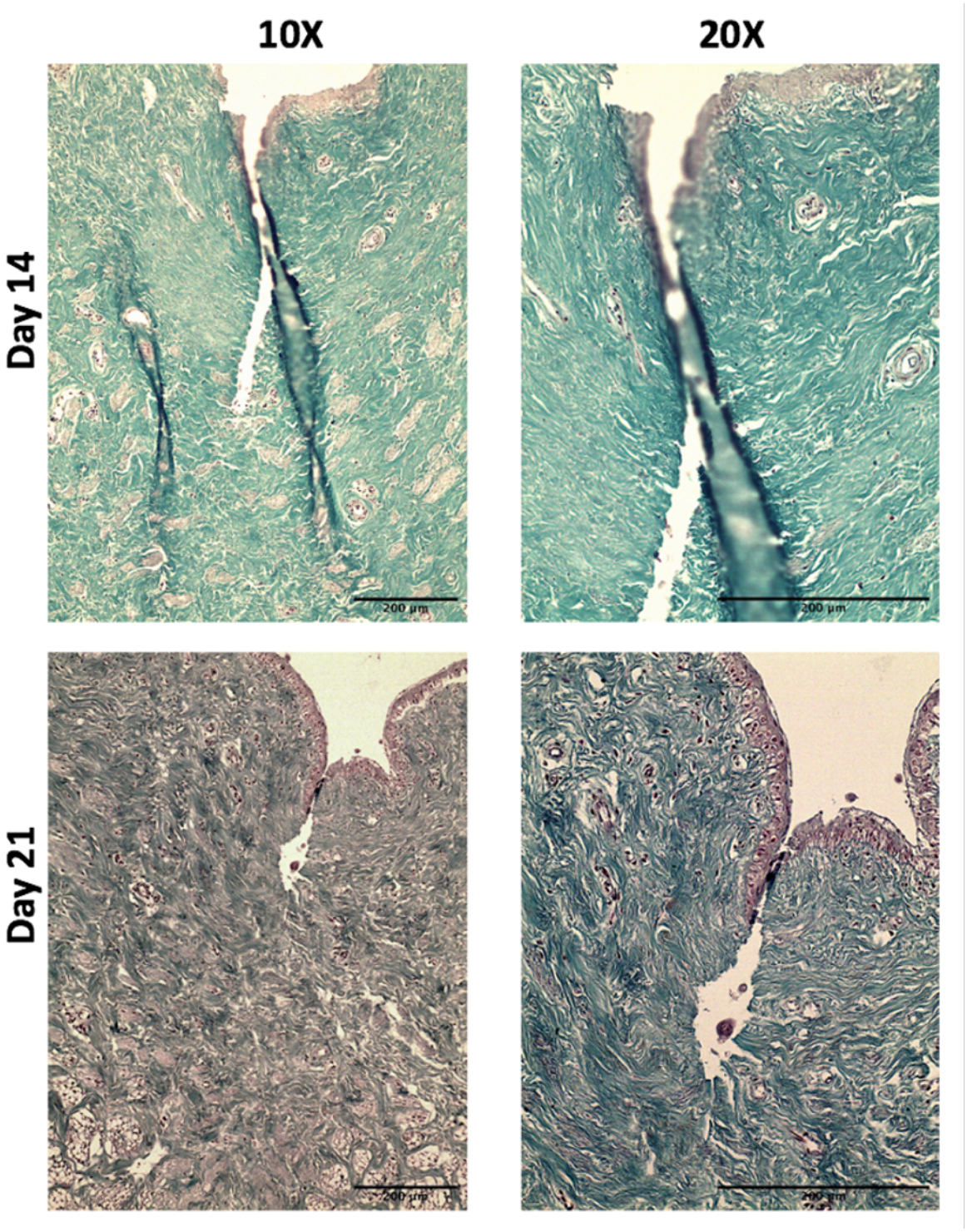

Figure 4.15: Trichrome staining of TE wound vaginal models with PU Z3 implanted at days 14 and 21 post-implantation. At day 21, formation of stratified epithelia' was observed on TE vaginal models. Scale bar= 200µm.

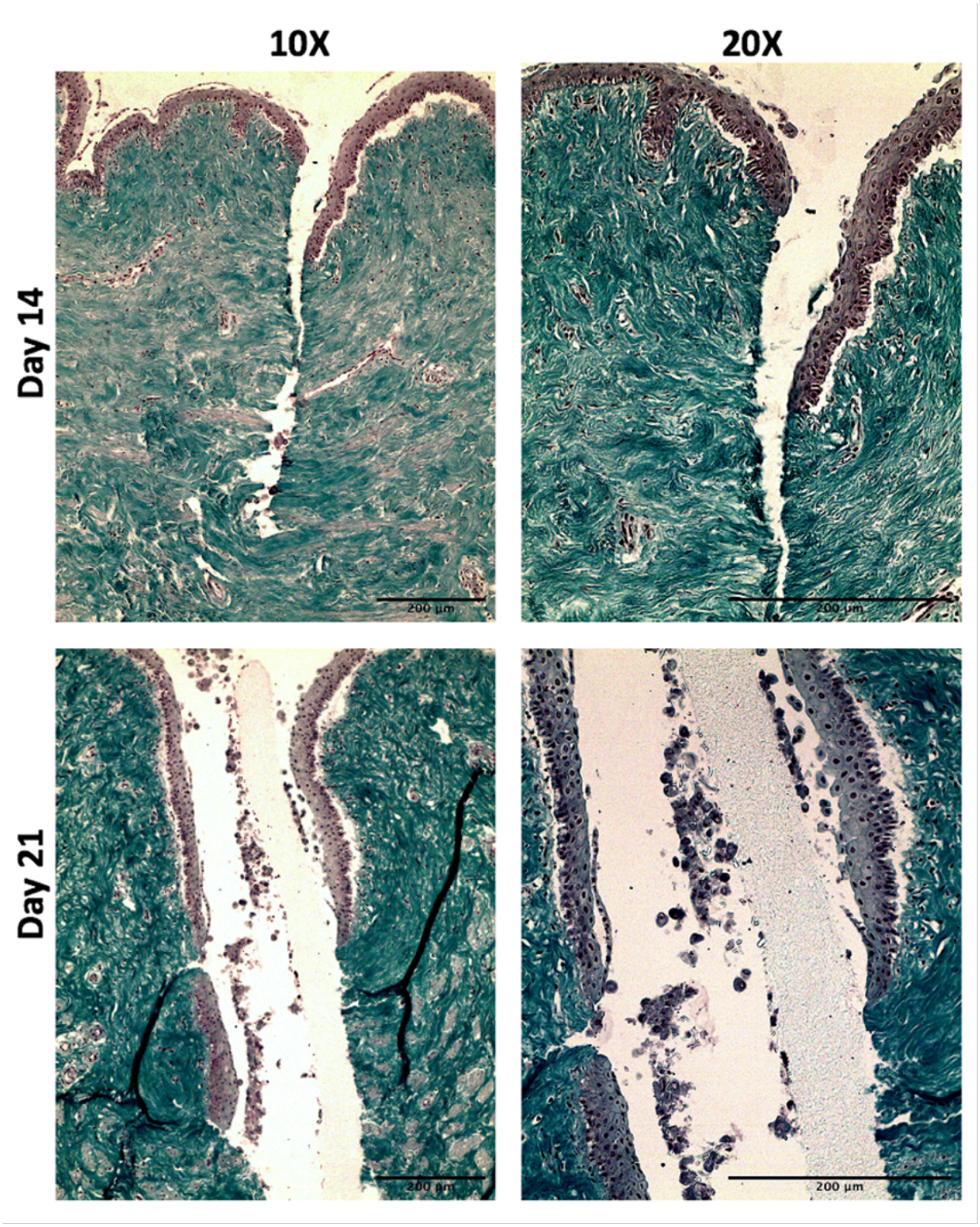

Figure 4.16: Trichrome staining of TE wound vaginal models with PU Z3 implanted at days 14 and 21 post-implantation cultured in the presence of estradiol-17β (100 pg/mL). There was an uninterrupted formation of a continuous stratified epithelia on the models and the surrounding connective tissue was stained densely with SF solution in the presence of E_2 in the culture medium. Scale bar= 200μm.

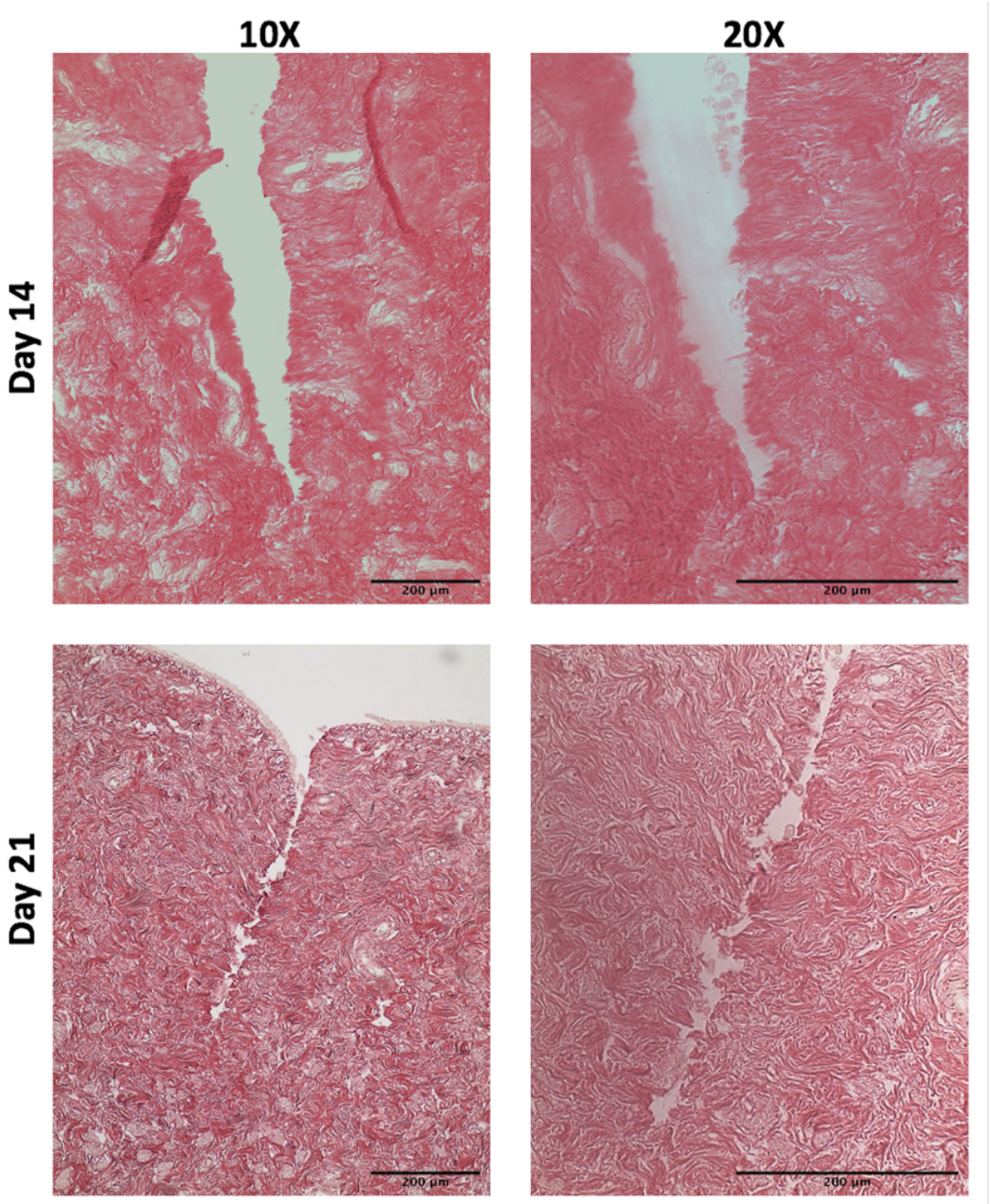

Figure 4.17: Picrosirius red staining of TE wound vaginal models with PPL implanted at days 14 and 21 post-implantation. At day 21, formation of a less stratified vaginal epithelia was observed on TE vaginal models in the presence of PPL implanted. The surrounding vaginal tissue was observed irregular and rough at the edges where the tissue was in contact with the PPL mesh. Scale bar= 200 µm.

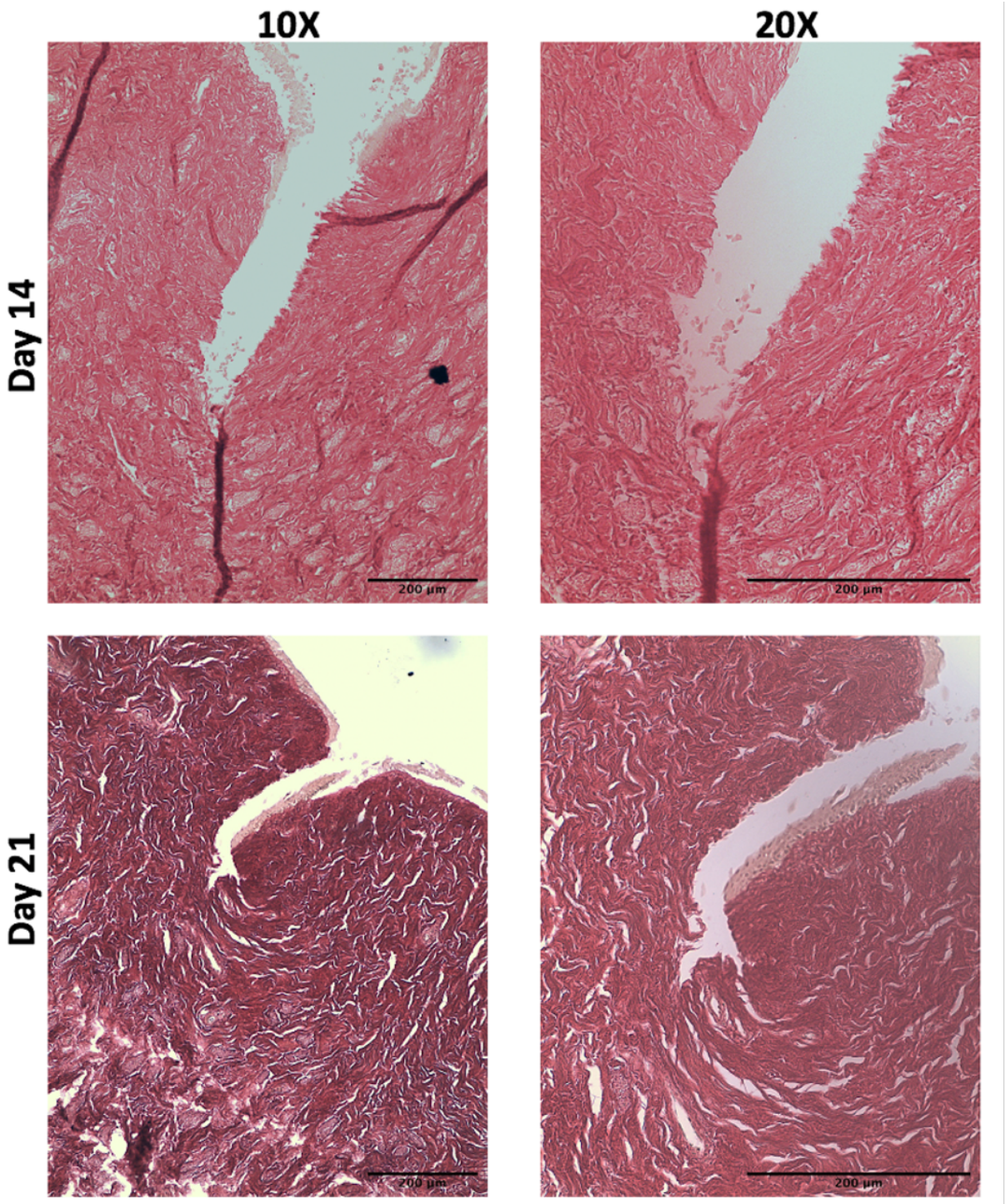

Figure 4.18: Picrosirius red staining of TE wound vaginal models with PPL implanted at days 14 and 21 post-implantation cultured in the presence of estradiol-17β (100 pg/mL). At day 21, formation of a discontinuous stratified epithelia was observed on TE wound vaginal models into the wounded region of PPL implantation in the presence of E_2. The collagen was stained bright red along the margins of the wound however, the surrounding tissue margins were observed irregular around the wounded region. Scale bar= 200 µm.

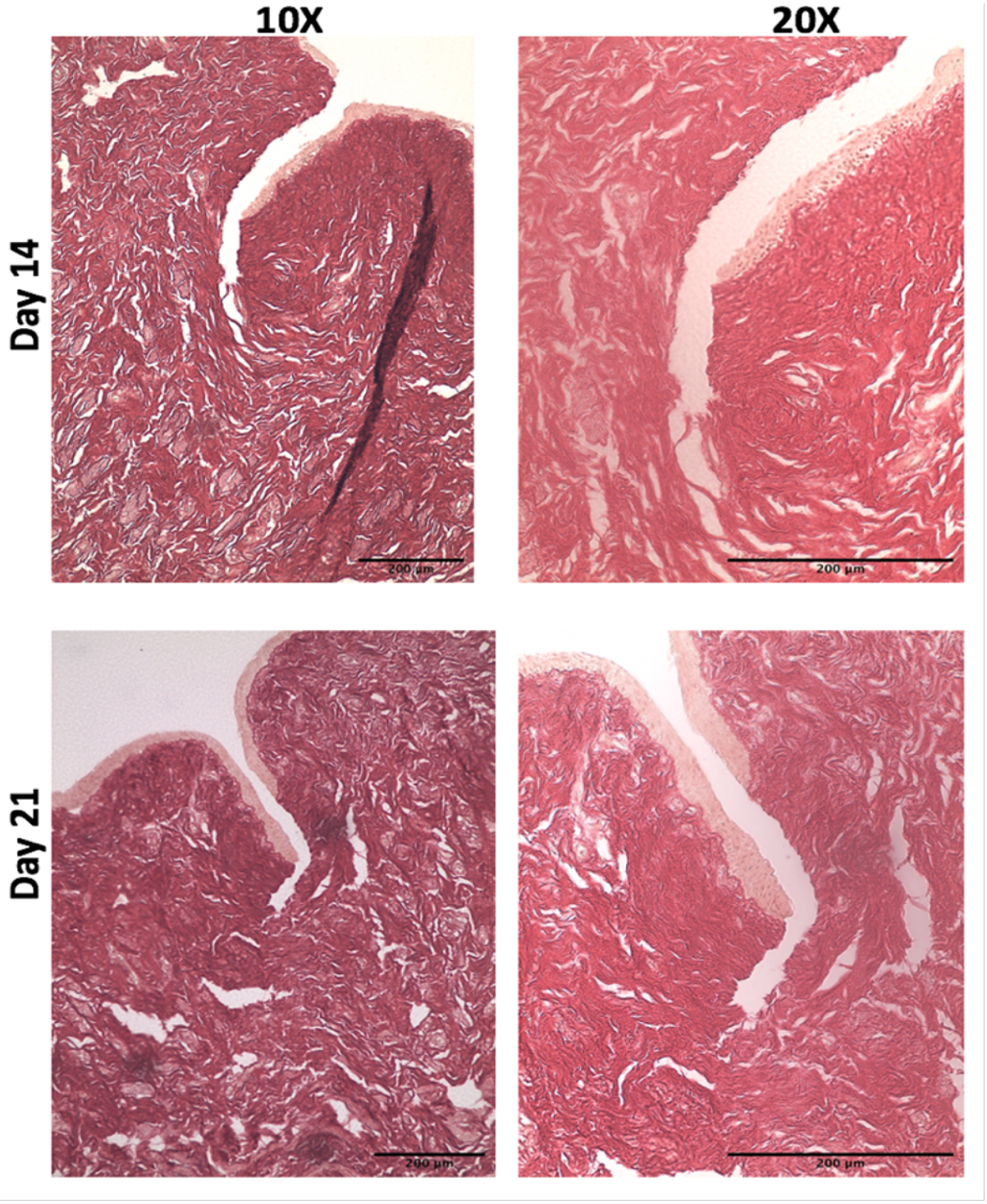

Figure 4.19: Picrosirius red staining of TE wound vaginal models with PU Z3 implanted at days 14 and 21 post-implantation. At day 14, beginning of the formation of a stratified vaginal epithelia was observed on TE vaginal models that continued to mature and stratified into the wounded region of PU implantation until day 21 in ALI culture. Scale bar= 200 µm.

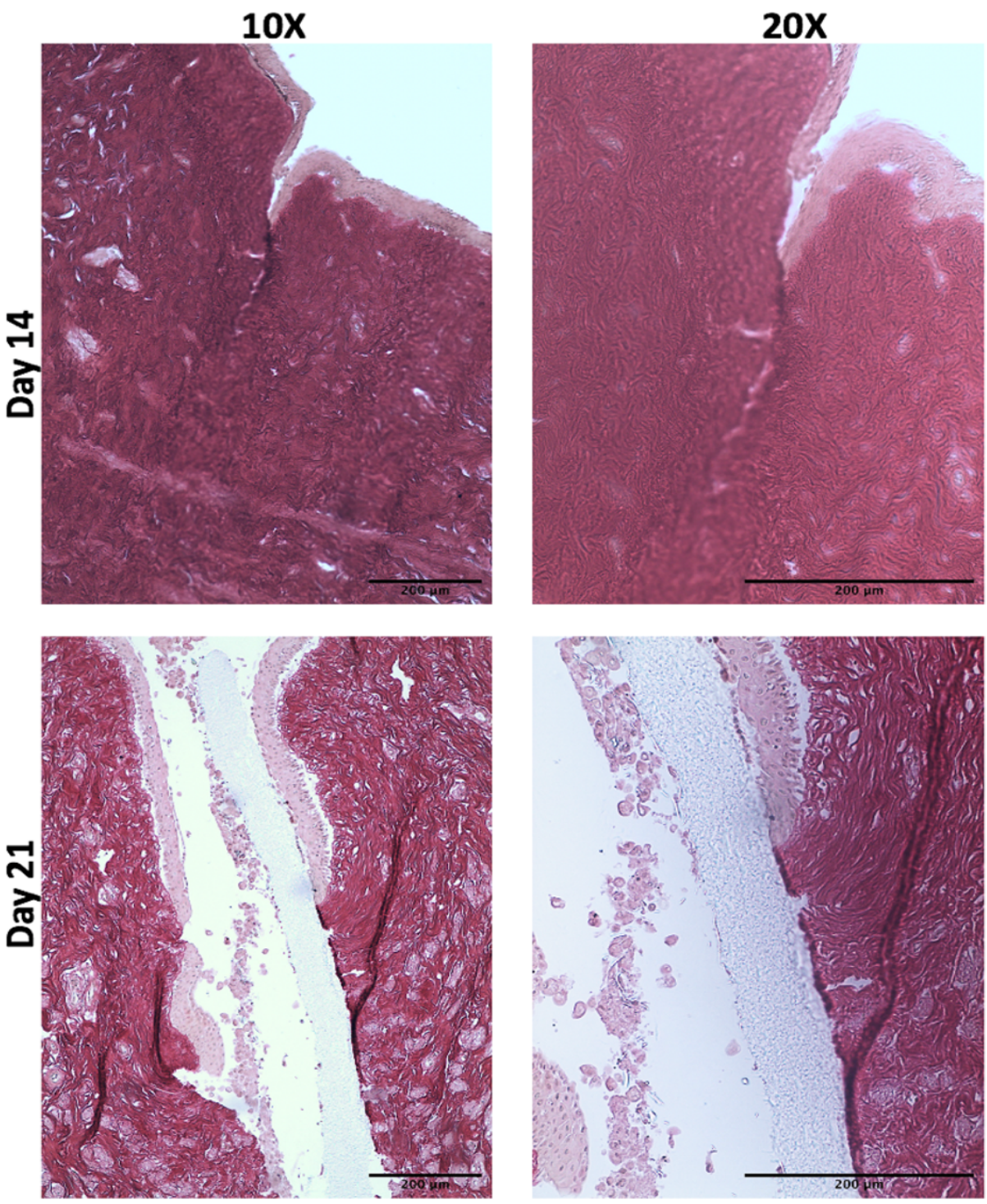

Figure 4.20: Picrosirius red staining of TE wound vaginal models with PU Z3 implanted at days 14 and 21 post-implantation cultured in the presence of estradiol-17β (100 pg/mL). At day 21, formation of a mature, highly stratified epithelia were observed on TE wound vaginal models into the wounded region of PU Z3 implantation in the presence of E_2. The collagen was stained bright red along the margins of the wound and the collagen fibres were aligned in a regular pattern. Scale bar= 200 µm.

4.4.5: Immunohistofluorescence (IHF) analysis of TE wound models with biomaterials implanted:

The effect of implanted biomaterials on cellular proliferation in TE wound vaginal models was determined by immunohistofluorescence (IHF) analysis for the detection of nuclear protein Ki67 expression. Ki67 expression is associated with the proliferative phase in the cell cycle and its expression is a reflection of number of proliferative cells present in the TE models. In the presence of PPL mesh implanted into the TE wound models, the expression of Ki67 (red channel) was increased from day 14 up to day 21 post-implantation as shown in Figure 4.21. Cells of the basement membrane that are closer to the wounded region depicted high fluorescence intensity for Ki67 expression showing their high proliferation rate in those regions. The presence of estradiol-17β (100 pg/mL) in the culture media induced an increase in the number and intensity of Ki67 posituve cells in TE wound models implanted with PPL mesh as demonstrated in Figure 4.22. Comparative imaging with PU Z3 implanted TE models revealed that the cultured cells showed higher proliferation in the areas surrounding the implanted PU Z3 as compared to that in PPL mesh implanted models (Figure 4.23). Similar pattern of increased expression and intensity of Ki67 marker was observed in TE models implanted with PU Z3 in the presence of E_2 depicting a positive effect of E_2 on cellular proliferation in the models. as shown in Figure 4.24.

These results were further confirmed by quantitative analysis of fluorescence intensity (a.u.) for Ki67 expression in TE wound vaginal models implanted with PPL and PU Z3 and the graphical representation is presented here in Figure 4.25. Analysis of the mean values revealed that the number and intensity of Ki67-positive cells was significantly higher in PU Z3 implanted models compared to PPL mesh models. Moreover, the addition of E_2 in the culture media increased the number of proliferative cells by positively influencing cellular migration and proliferation to accelerate the process of vaginal wound healing in models presented here.

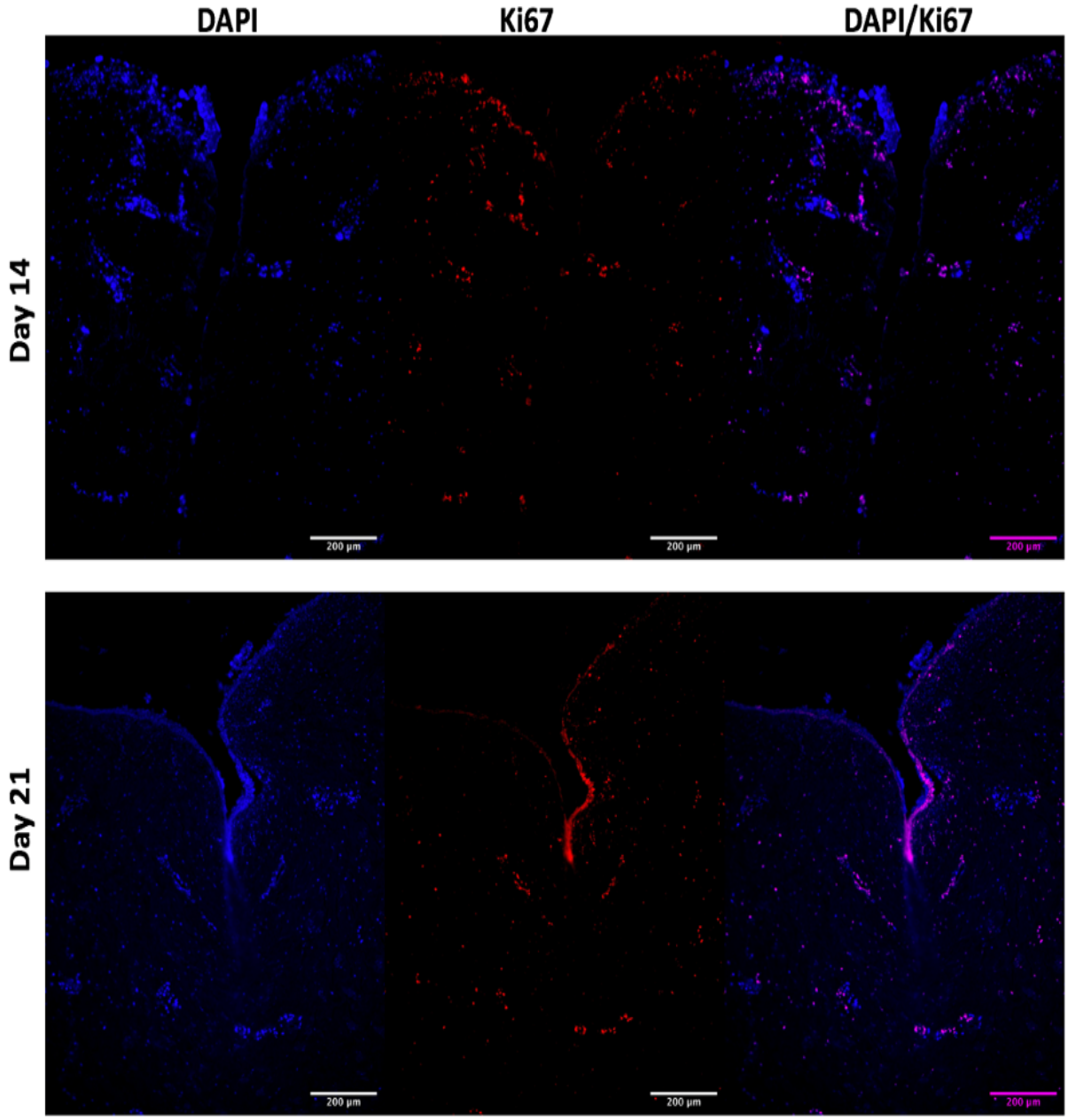

Figure 4.21: Immunohistofluorescence staining for the detection of Ki67 expression on PT wound vaginal models with PPL implantation at different time points in ALI culture. Ki67 positive cells (red channel) were more concentrated around the edges of the PT wound and in the basement membrane. All tissue sections were counterstained with DAPI (blue channel). Scale bar=200 µm.

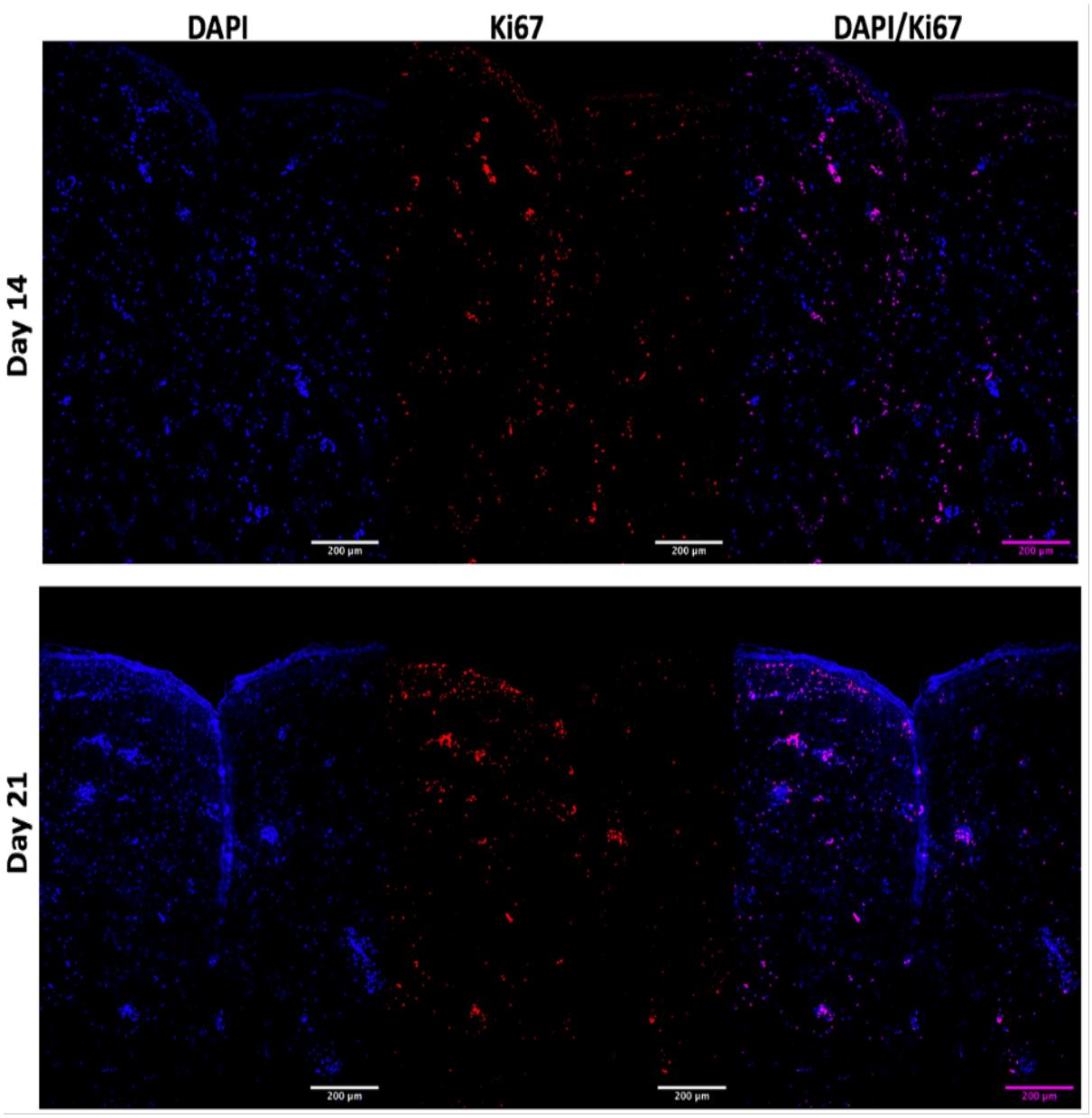

Figure 4.22: Immunohistofluorescence staining for the detection of Ki67 expression on PT wound vaginal models with PPL implantation under E_2 induction (100 pg/mL) at different time points in ALI culture. Ki67 positive cells (red channel) were more concentrated around the edges of the PT wound and in the basement membrane. In the presence of E_2, an increase in the epithelia thickness and intensity and number of proliferative cells was observed. All tissue sections were counterstained with DAPI (blue channel). Scale bar=200 µm.

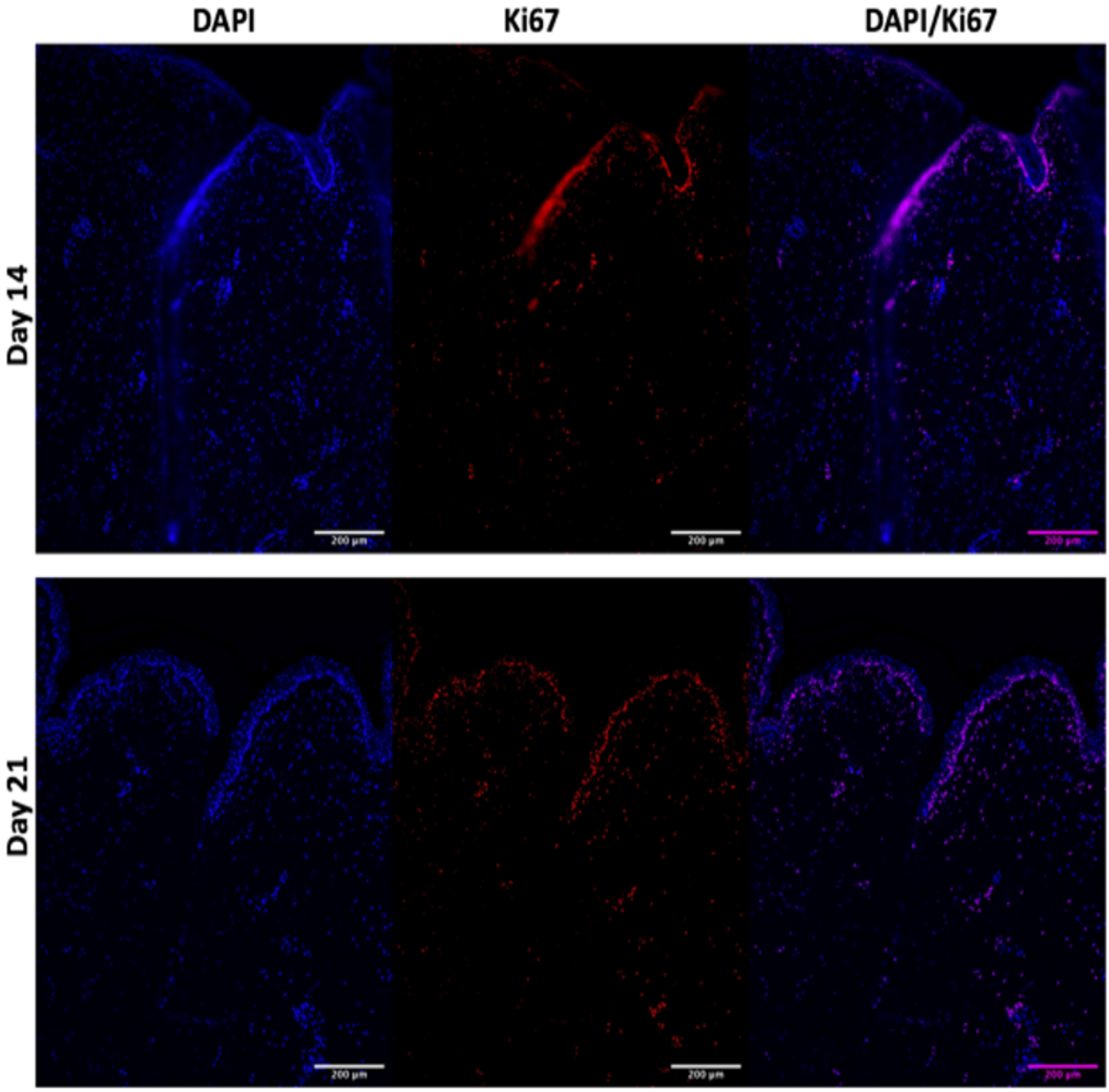

Figure 4.23: Immunohistofluorescence staining for the detection of Ki67 expression on PT wound vaginal models with PU Z3 implantation at different time points in ALI culture. Ki67 positive cells (red channel) were more concentrated around the edges of the PT wound and in the basement membrane. All tissue sections were counterstained with DAPI (blue channel). Scale bar=200 µm.

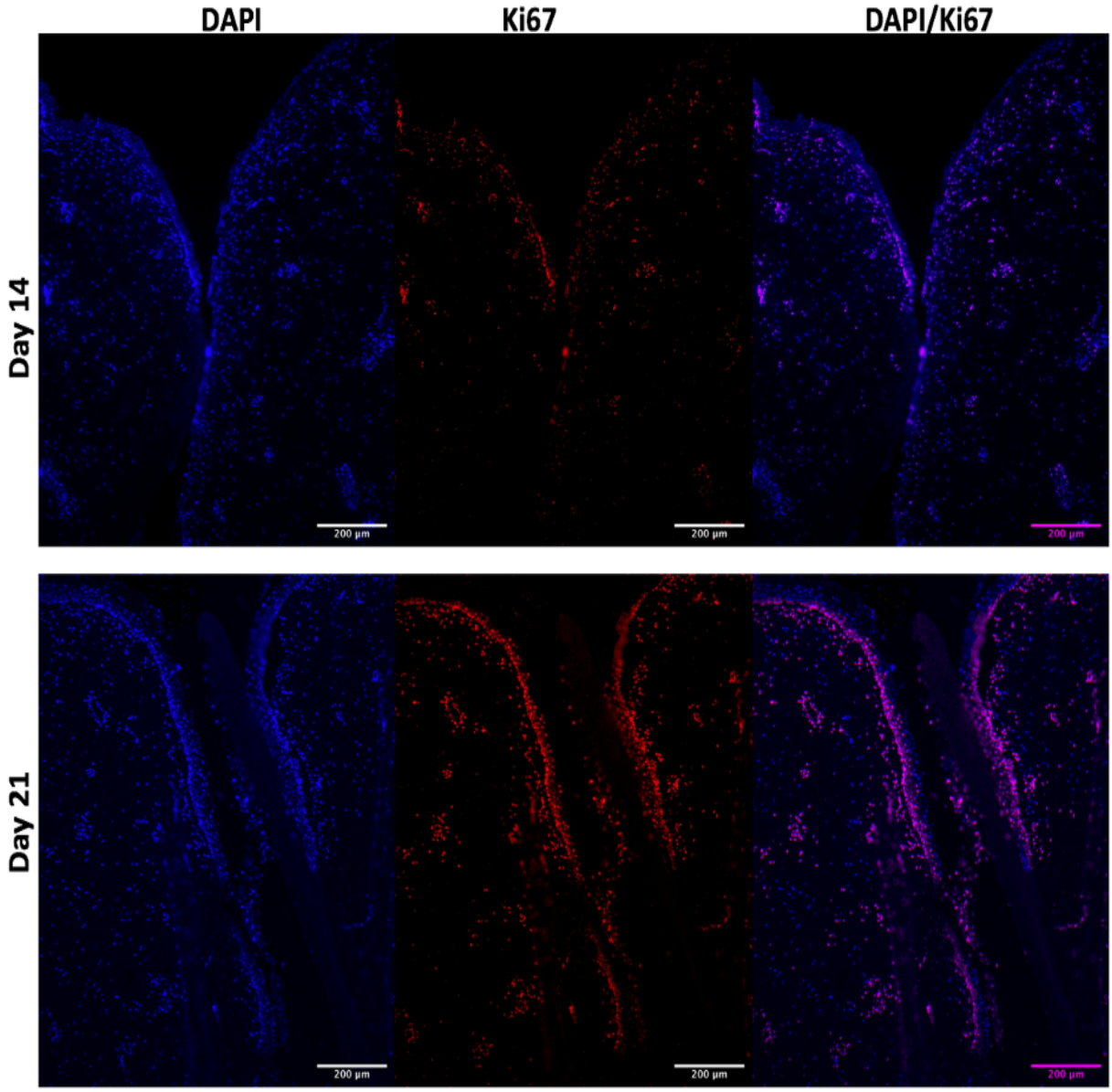

Figure 4.24: Immunohistofluorescence staining for the detection of Ki67 expression on PT wound vaginal models with PU Z3 implantation under E_2 induction (100 pg/mL) at different time points in ALI culture conditions. Ki67 positive cells (red channel) were more concentrated around the edges of the PT wound and in the basement membrane. In the presence of E_2, an increase in the epithelia thickness and intensity and number of proliferative cells was observed. Cells proliferating into the PU Z3 biomaterial were also observed positive for Ki67 expression. All tissue sections were counterstained with DAPI (blue channel). Scale bar=200 µm.

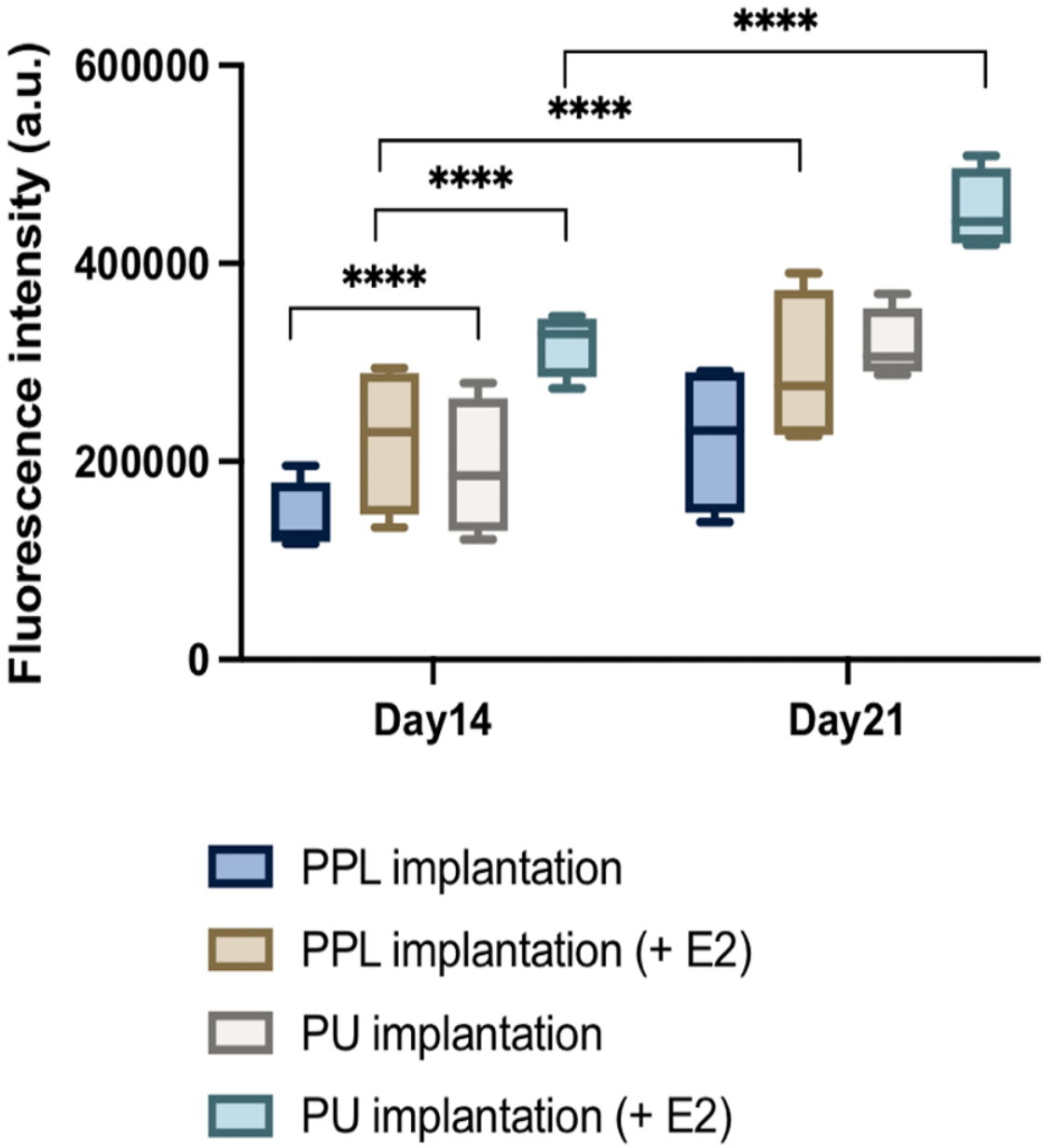

*Figure 4.25: Graphical representation of fluorescence intensity of Ki67 marker expression on PT wound vaginal models implanted with biomaterials (PPL and PU Z3) at different time points with and without E_2 (100pg/mL) in Green's media under ALI culture conditions. (n=9 ± SD for each group, N=3, ****p < 0.0001).*

4.4.6 Immunohistofluorescence (IHF) analysis of TE wound models with biomaterials implanted for the detection of fibrosis marker:

Another key consideration for appropriate vaginal tissue wound healing after biomaterials implantation into the pelvic floor accounts for the early indication of fibrosis that may later cause implant shrinkage and scar tissue formation at the implanted site. The differentiation of vaginal fibroblasts into myofibroblast phenotype is a major event in soft tissue healing process that determines the outcome of a successful wound healing and tissue remodeling post-implantation. Alpha smooth muscle actin (α-SMA) is a marker of fibrosis that is expressed by myofibroblasts and is associated with the degree of fibrotic tissue formation during the process of soft-tissue wound healing *in vivo*.

Figures 4.26 and 4.27 demonstrate the IHF analysis for the detection of α-SMA marker expression in TE wound vaginal models with PPL mesh implanted in the absence and presence of E_2 respectively. These results showed that there was an increased amount of myofibroblast transformation reflecting an increased expression of α-SMA in TE models in the presence of PPL mesh from days 14 to 21 post-implantation (Figure 4.26). However, the presence of E_2 in the culture media counteracted by decelerating the process of myofibroblast transformation with a decrease in the expression of α-SMA which in turn may reduce the risk of scarring and fibrotic tissue formation around PPL mesh implantation in our models.

In TE wound vaginal models with PU Z3 implanted, the expression of α-SMA was significantly lowered than that in PPL mesh implanted models as shown in Figure 4.28. Moreover, in the presence of E_2 in the culture media, there was less transformation of fibroblasts into myofibroblast phenotype that further reduced the expression of α-SMA in PU Z3 implanted models (Figure 4.29). These results indicated that in the presence of E_2 and PU Z3 implanted into the TE models, there was a reduced risk of scarring and fibrotic tissue formation at the wounded site which in turn increased the likelihood for tissue remodelling and improved vaginal tissue healing.

These results were further confirmed by quantitative analysis of α-SMA fluorescence intensity in TE wound vaginal models with PPL and PU Z3 implanted with and without E_2 at different time points in ALI culture and the graphical representation is shown in Figure 4.30. Results revealed that among the two biomaterials tested, the PPL mesh induced a higher vaginal

fibroblast differentiation into myofibroblasts that led to a higher risk of fibrosis and scarring during the process of vaginal wound healing in our TE models. These findings are in direct correlation with the clinical understanding of PPL mesh-related complications in patients with prolapse and are highly relevant for preclinical testing of biomaterials intended for potential applications in the female pelvic floor repair.

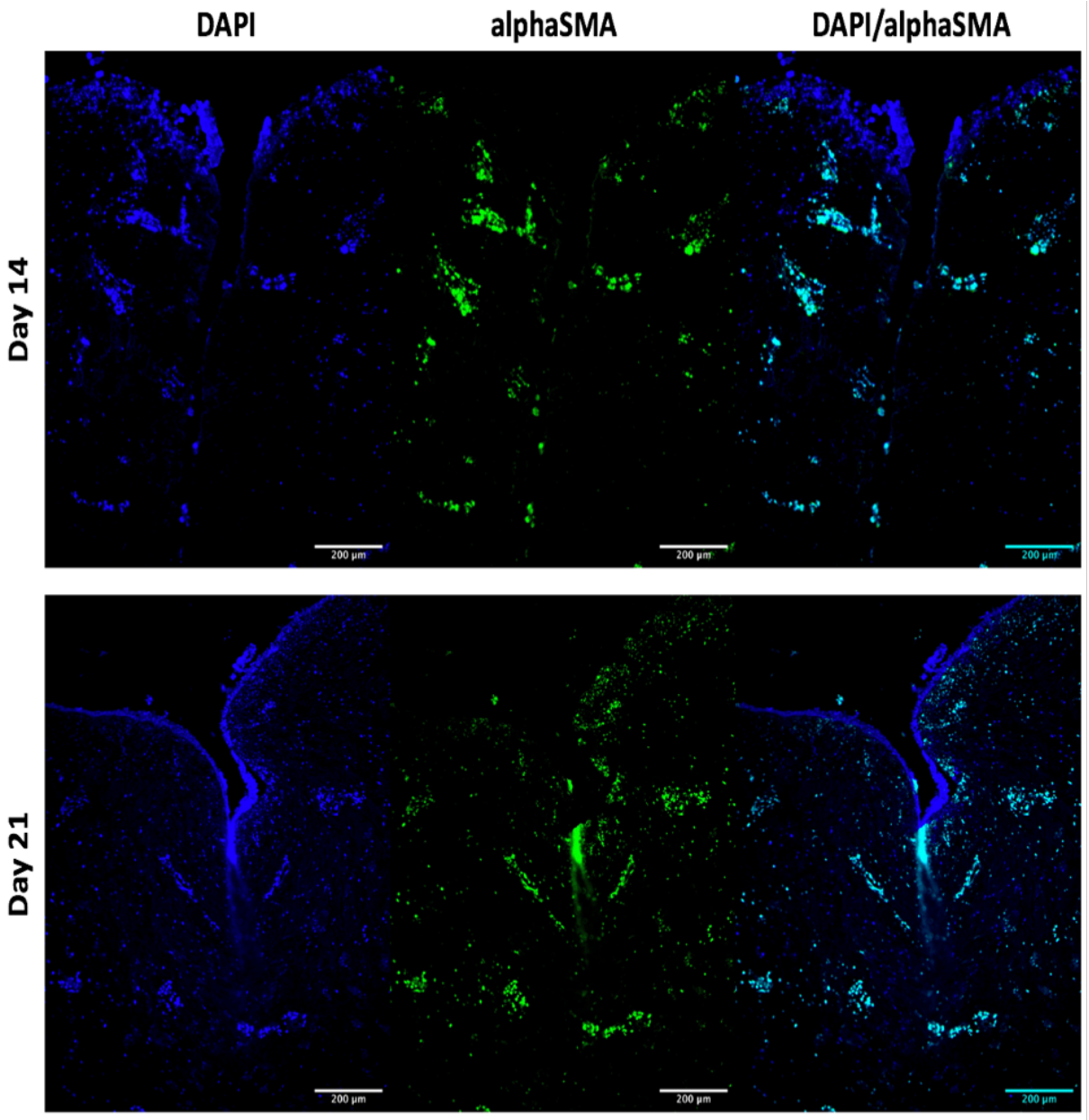

Figure 4.26: Immunohistofluorescence staining for the detection of α-SMA expression on PT wound vaginal models with PPL implantation at different time points in ALI culture conditions. The myofibroblasts present in the models expressed the α-SMA protein (green channel) which was observed distributed in the lamina propria region. All tissue sections were counterstained with DAPI (blue channel). Scale bar=200 µm.

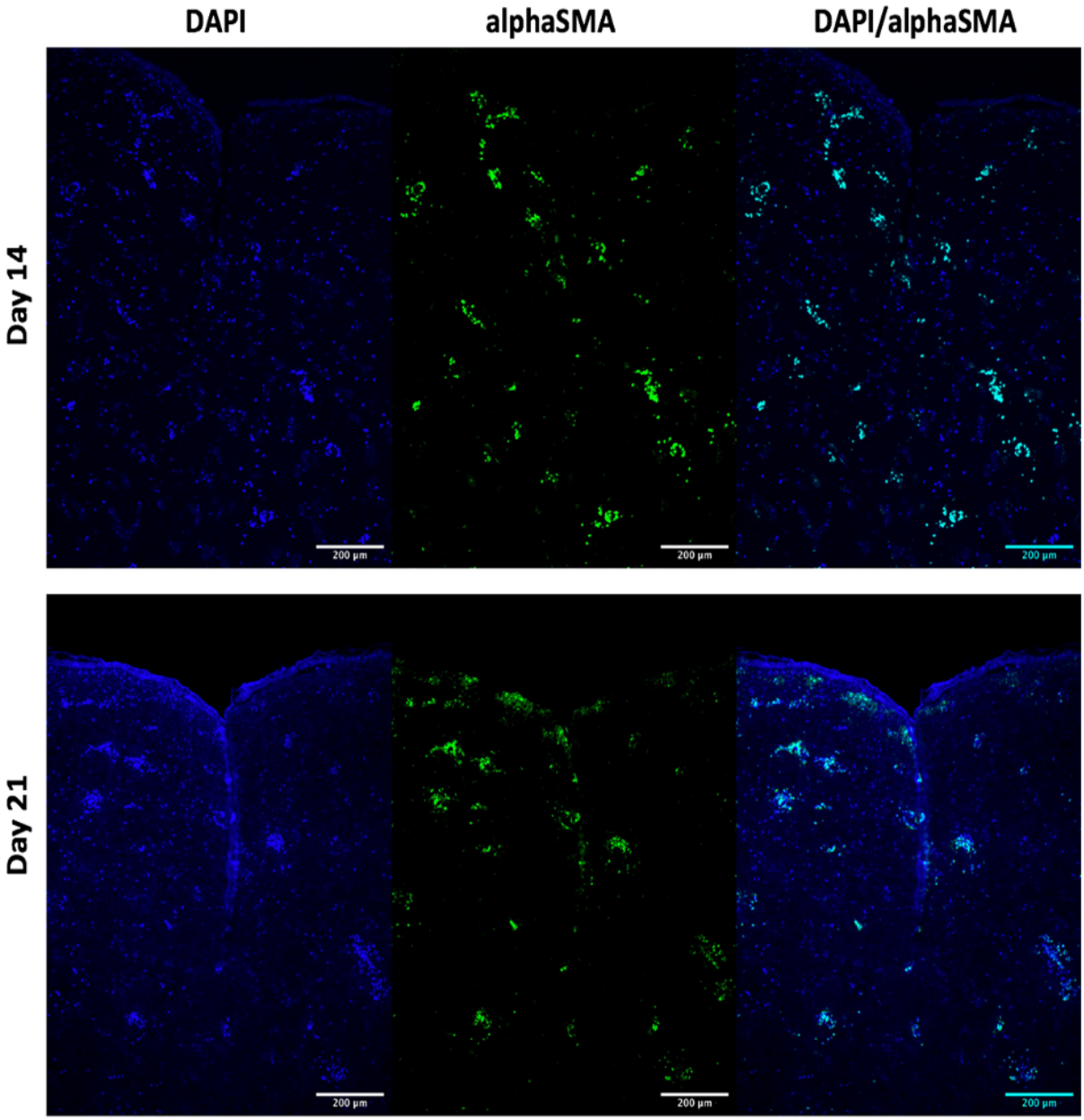

Figure 4.27: Immunohistofluorescence staining for the detection of α-SMA expression on PT wound vaginal models with PPL implantation under E_2 induction (100 pg/mL) at different time points in ALI culture conditions. The myofibroblasts present in the models expressed the α-SMA protein (green channel) which was observed distributed in the lamina propria region whereas it was absent in the epithelial region. All tissue sections were counterstained with DAPI (blue channel). Scale bar=200 µm.

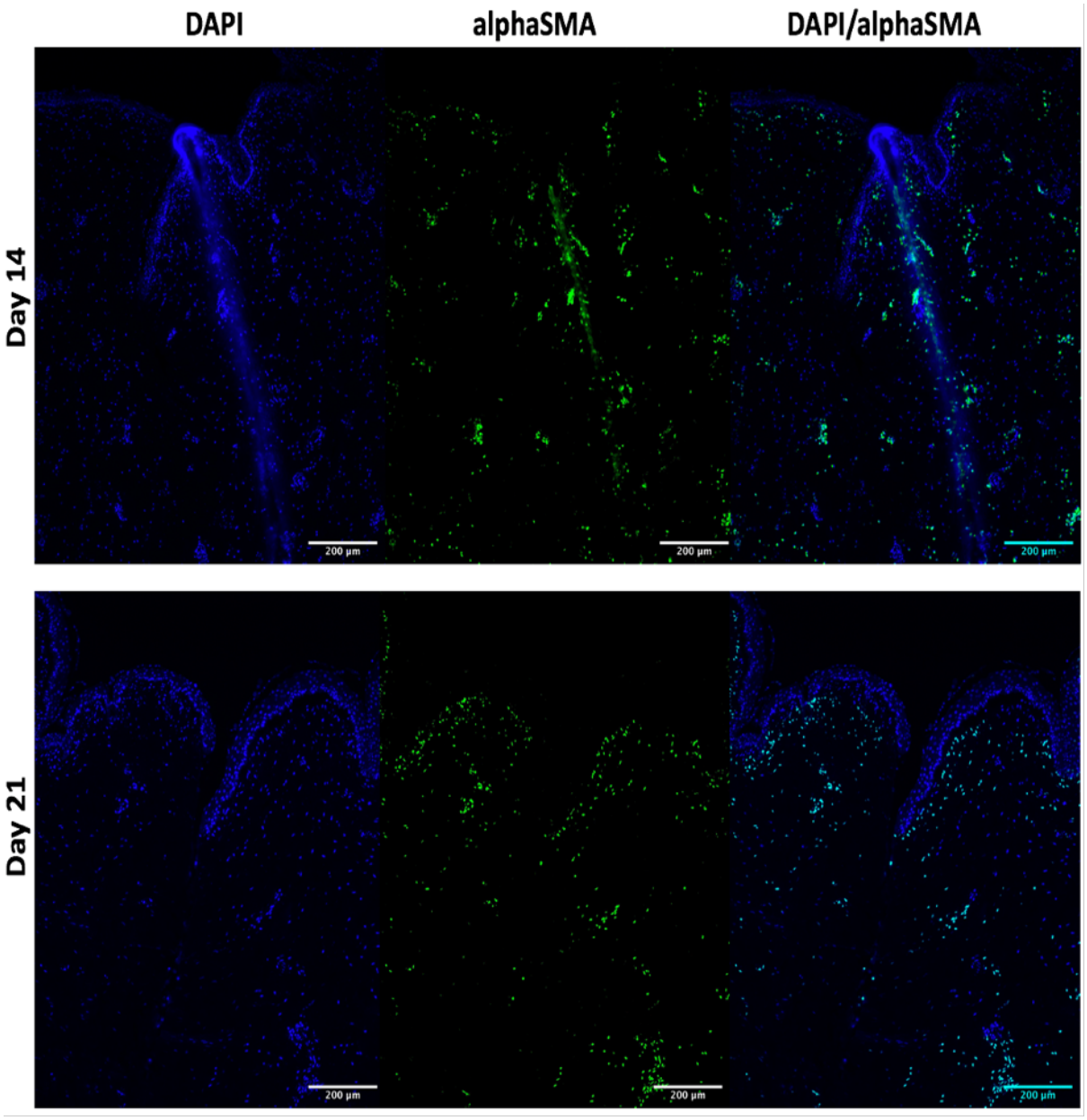

Figure 4.28: Immunohistofluorescence staining for the detection of α-SMA expression on PT wound vaginal models with PU Z3 implantation at different time points in ALI culture conditions. The myofibroblasts present in the models expressed the α-SMA protein (green channel) which was observed distributed in the lamina propria region. All tissue sections were counterstained with DAPI (blue channel). Scale bar=200 µm.

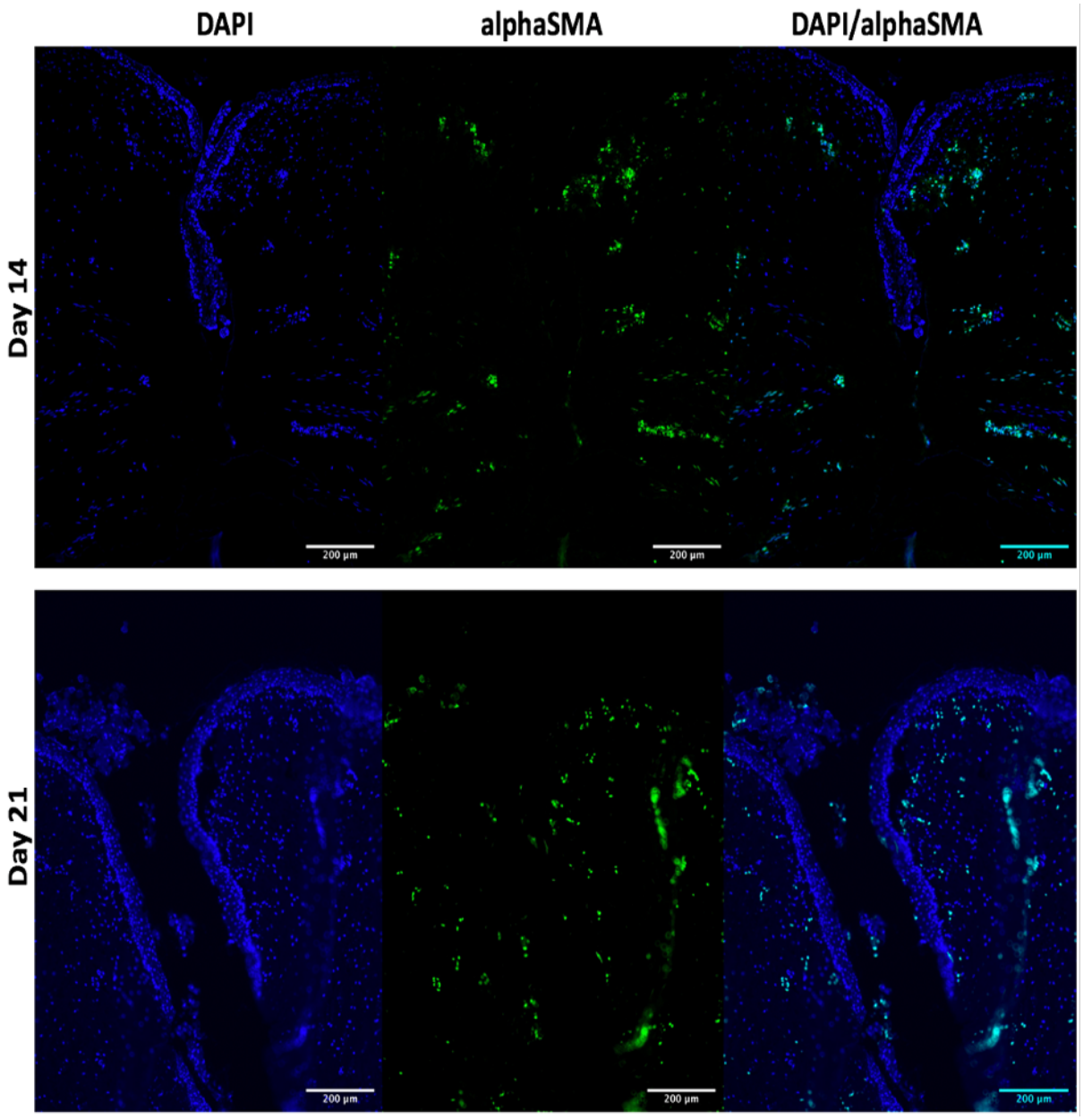

Figure 4.29: Immunohistofluorescence staining for the detection of α-SMA expression on PT wound vaginal models with PU Z3 implantation under E_2 induction (100 pg/mL) at different time points in ALI culture conditions. The myofibroblasts present in the models expressed the α-SMA protein (green channel) which was observed distributed in the lamina propria region whereas it was absent in the epithelial region. All tissue sections were counterstained with DAPI (blue channel). Scale bar=200 µm.

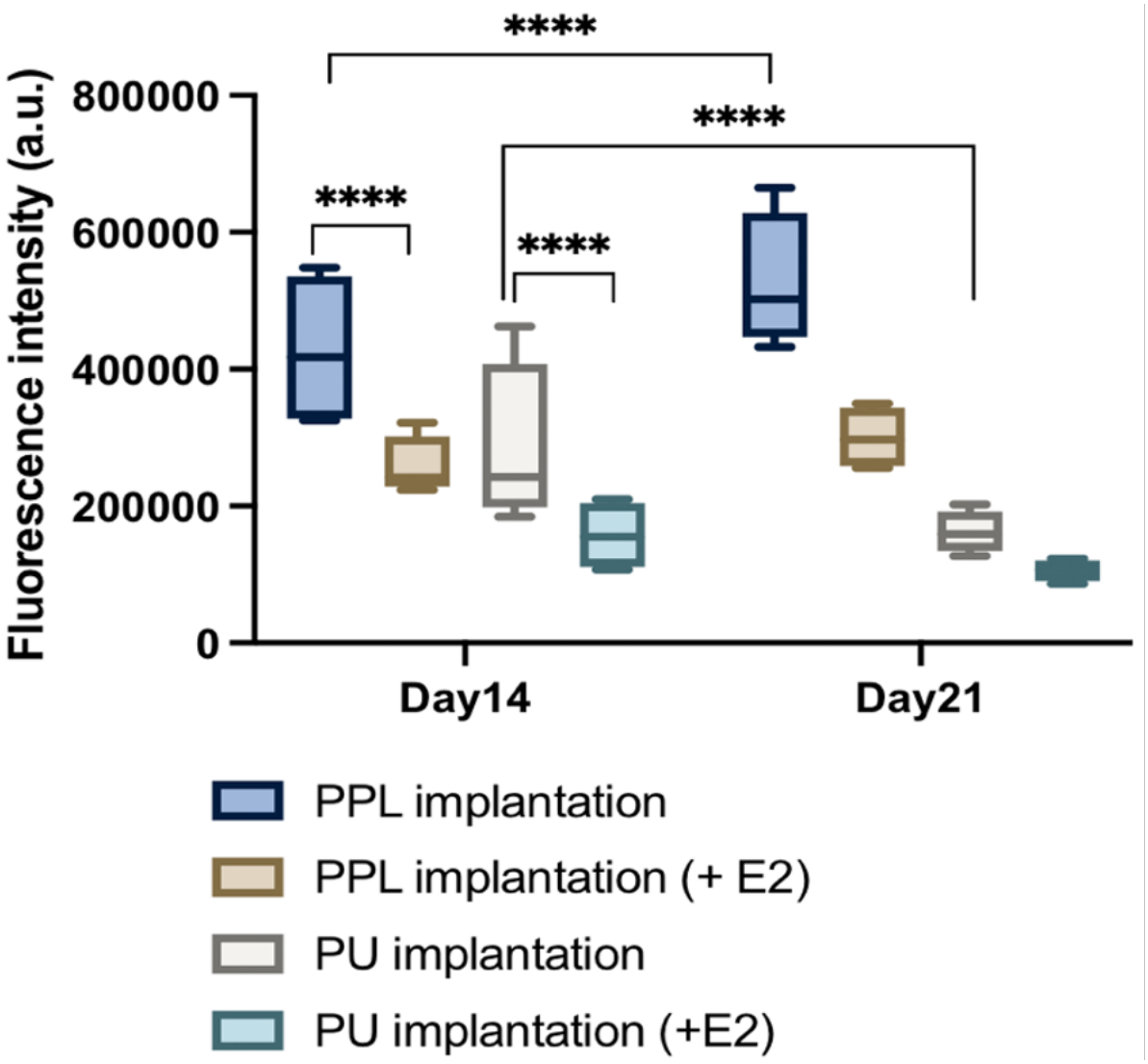

*Figure 4.30: Graphical representation of fluorescence intensity of α-SMA marker expression on PT wound vaginal models implanted with biomaterials (PPL and PU Z3) at different time points with and without E_2 (100pg/mL) in Green's media under ALI culture conditions. (n=9 ± SD for each group, N=3, ****p < 0.0001).*

4.5 Discussion:

Given the high incidence of pelvic floor disorders (PFDs) worldwide and an existing ban on the transvaginal PPL mesh implants, there is now a devastating treatment gap left in the field of urogynecology reconstructive surgeries for women suffering from POP. It is imperative to develop new materials that are safe, effective and more efficacious than the PPL mesh implants for POP and SUI repair. Pelvic organ prolapse is a disorder associated with mechanical failure of the load bearing pelvic connective tissue and fascia and requires implants for support as well as tissue regeneration. This means that the newly developed implants should not only possess appropriate stiffness, flexibility and strength but also should be biocompatible in order to recruit cells of the ECM towards the implant site for tissue repair and regeneration.

Over the years extensive work has been carried out in developing materials, including both natural and synthetic materials, for the treatment of POP and SUI. Natural materials such as autologous fascia, cadaveric dermis and acellular porcine small intestinal submucosa (SIS) have long been used in urogynecological reconstructive procedures. However, meta-analysis has shown that the use of natural materials in mid-urethral tension-free vaginal tape procedures have a high prolapse recurrence rate of about 17.9% [386]. Histologically, natural graft materials have shown a high degradation rate and poor mechanical properties and are unable to provide long-term adequate mechanical support to the prolapsed pelvic organs [387]. In recent years, a major shift in developing tissue engineered synthetic mesh scaffolds has occurred that are biocompatible, induce matrix production and neo-tissue formation and can provide long-term mechanical support to the pelvic floor.

About a decade ago, our pelvic floor research group at the Kroto research institute aimed to develop a biocompatible tissue engineered repair material (TERM) for the treatment of POP and SUI and since then have fabricated and tested several natural and synthetic polymeric materials to find the most suitable candidate material. Mangera *et al.,* [388] compared natural small intestinal submucosa (SIS) with synthetic thermoannealed poly (L) lactic acid (PLA) under free and restrained conditions to determine the response of cultured buccal fibroblasts towards both materials in terms of matrix production and changes in the biomechanical properties of scaffolds. They concluded that electrospun cell-seeded PLA is a better candidate scaffold than acellular SIS in terms of long-term success rates for POP procedures as the

polymer degrades *in vivo,* the cultured cells will have produced neo-fascia that help to support, and regenerate weakened pelvic floor connective tissue. Later Hillary *et al.,* [389] compared electrospun polymers PLA, PU Z1, PU Z3 and polymer blends with that of PPL mesh and confirmed that the PPL mesh failed mechanically under dynamic distension and inadequately supported cellular proliferation compared to electrospun matrices.

Taking into account the dynamic biomechanics of the pelvic floor muscles, new fabrication techniques such as electrospinning could be employed to design pelvic floor surgical mesh implants with improved microstructure, biocompatibility, flexibility and load-bearing properties.

The first part of this chapter was aimed at developing electrospun PU Z3 scaffold and to mechanically characterise it as a potential biomaterial for pelvic floor repair. A comparative analysis with the low weight commercial PPL mesh (Gynemesh®) was made as these PPL meshes have been used as the gold standard implant for the pelvic floor repair until their ban in 2019 by the FDA after reports of severe post-operative complications. Accordingly, all new mesh implants need to undergo intense preclinical testing to ensure their safety and suitability for implantation into the female pelvic floor. Hence, the next stage was to implant the electrospun PU Z3 into tissue engineered (TE) wound vaginal models to determine the biocompatibility and vaginal tissue response towards implanted biomaterials in *in vitro* vaginal tissue equivalents.

The first stage was to fabricate an electrospun polymer matrix with considerable flexibility and load-bearing properties to support the weakened female pelvic floor without any drastic changes in the mechanical properties to cope with the dynamic distensions experienced within the pelvic floor. For this purpose, polyurethane (PU) Z3 was selected due to its elastic behavior, strength and mechanical distensibility. Polyurethanes are a versatile group of polymers that have gained significant attention in recent years as bioactive synthetic scaffolds for tissue engineering applications [390]. Several studies have reported electrospun PU as biocompatible, non-immunogenic with tailorable biodegradability, mechanical and thermal properties that have many applications in hard and soft tissue engineering and regenerative medicine [391][392]. Previously, our group has reported that PU Z3 retained its mechanical properties

while conventional PPL mesh underwent permanent deformation after two weeks treatment under dynamic loading and unloading conditions [389].

Electrospinning is a useful fabrication technique that allows for the development of polymeric scaffolds with either an aligned, random or composite fibre arrangement resulting in a microporous scaffold that mimics the natural ECM ultrastructure. Scanning electron microscopy (SEM) images of the electrospun PU Z3 scaffold depicted a random arrangement of polymeric fibres with interconnecting microporous structure as shown in Figure 4.3. The interconnectivity and porosity are important parameters in scaffold fabrication as these affect the process of angiogenesis and neo-tissue formation following transplantation. According to Mehdizadeh *et al.,* [393] vascularisation of porous polymeric scaffolds is prerequisite for successful organ and tissue reconstruction and presents a limiting barrier for the development of clinically applicable scaffolds. The electrospun PU Z3 scaffold fabricated here contained an average pore size of about 20 - 25μm which according to the literature is favorable for vascular ingrowth, cellular infiltration and nutrient diffusion [394].

In the human body, the cell-matrix interaction is guided by the nanoscale structure of the ECM and traditionally synthetic polymeric scaffolds are aimed at replicating and mimicking the nanoscale dimensions of the natural ECM. PU Z3 electrospun scaffold was fabricated with randomly aligned polymeric fibres that recapitulated the native tissue ECM microenvironment. Moreover, the random alignment of fibres in the electrospun scaffolds results in a lower bulk density and high interconnectivity of pores that makes them preferrable for tissue engineering applications where neo-tissue formation and vascularisation is desirable post-implantation [395]. In contrast, the commercial PPL based Gynemesh® depicted a knitted macroporous structure which allows for macrophage and bacterial invasion into the mesh and increase the risk of infection and encapsulation at the implant site.

With the aim of developing degradable polymeric scaffolds for the female pelvic floor reconstructive procedures, it is crucial that the fabricated scaffolds should be biomechanically compatible with the native paravaginal fascia [396]. The load dynamics in the female pelvic floor require implants that are mechanically strong and flexible to sustain the intra-abdominal pressure (IAP) changes. As a result, it is expected that the designed materials should experience minimum changes in the microarchitecture after implantation that reduce the risk of mesh

shrinkage, plastic deformation and ultimately implant exposure through the native tissue. Lei *et al.,* [397] reported the biomechanical properties of healthy paravaginal tissue by utilising uniaxial tensile testing on vaginal tissue biopsies from pre-menopausal women and compared with those from POP patients. They reported the Young's modulus (YM) and ultimate tensile strength (UTS) values for healthy paravaginal tissues in the range of 6.65-14.35 MPa and 0.27-5.3 MPa respectively that significantly deteriorated in patients suffering from POP. My results showed that the YM and TS of PU Z3 were comparable to that of the native healthy vaginal tissue as shown in Figure 4.5.

After implantation, the biomechanical properties of implanted materials change when subjected to *in vivo* microenvironment. Current approach in developing materials is focused on replicating the biomechanical properties of the native vaginal tissue in order to provide support to the pelvic floor. In this regard, the YM of materials play an important role by not only defining the strength of a material but has also been shown to influence cellular ingrowth [388]. Hence, PU Z3 with comparable YM in the physiological range is expected to provide good cytocompatibility in my *in vitro* TE models as it offers biomechanical properties desirable for potential implantation for pelvic floor reconstructive procedures.

The elastic behavior of PPL and PU Z3 was evaluated by subjecting the biomaterials to cyclic uniaxial tensile testing and results are shown in Figure 4.6. The elastomeric PU Z3 exhibited viscoelastic behavior with minimum deformation under repeated distensions and remained flexible as shown in stress-strain curves. This is an important criterion for materials designed for the pelvic floor repair to retain their elastic behavior. In contrast, the PPL mesh showed plastic deformation immediately after first cycle of distension that continued to increase in subsequent cycles. Roman *et al.,* [398] reviewed the clinical complications associated with the design and mechanical properties of commercial PPL mesh implants for POP repair. They proposed that under dynamic pelvic floor environment, PPL mesh displayed irreversible plastic deformation that increased mesh stiffness and decreased mesh pore size and cause mesh failure leading to complications. In the data presented here, PPL mesh when subjected to cyclic distensions displayed a similar pattern of plastic deformation as reported previously.

In the earlier stages of biomaterial development, *in vitro* studies with relevant cell types are crucial to obtain a better understanding of initial cell-implant interactions such as cellular attachment, migration into the implant and production of ECM. In this chapter, i have reported

an *in vitro* TE wound vaginal model that features the complete vaginal tissue architecture including the epithelium and the lamina propria cultured with primary vaginal cells isolated from sheep. Here, i have utilised the TE wound vaginal model for implantation of biomaterials designed for the pelvic floor repair to study the vaginal cells response towards my material in comparison with PPL mesh in a physiologically relevant environment.

At present, most *in vivo* studies include small animal (rat or rabbit) models of abdominal wall defects to evaluate the effectiveness of natural and/or synthetic polymeric meshes designed for pelvic floor reconstruction rather than implantation into anatomic sites associated with PFDs. These small animal studies will remain useful to assess the biocompatibility and implant-tissue interaction *in vivo* however, they are not true representation of the pelvic floor anatomy [139]. Thus, this anatomic misrepresentation of the dynamic *in vivo* pelvic environment which is usually associated with pelvic floor fascia and muscles activity limits the effectiveness of small animal models to determine the long-term mechanical and biological outcomes of implanted materials post-operative. While large animal studies are essential to address the biomechanical aspects of POP surgery that includes the long-term mechanical support provided by the implant, angiogenesis, matrix remodelling as well as post-operative fibrous tissue formation at the implant-tissue interface. It seems rational that the implants designed for a particular anatomical site should be tested at the clinically relevant position (*i.e.,* in the pelvic floor) rather than in an entirely different anatomic position (*e.g.,* abdominal wall) [399]. However, organ-specific animal models are highly expensive, requires rigorous ethical approval, time consuming and restricted in terms of experimental repeats that limits their applicability in various laboratory setups. Hence, TE *in vitro* vaginal models are attractive alternatives for preclinical testing of biomaterials in a 3D tissue microenvironment relevant to the native vaginal tissue and help to reduce the number of animals required for testing in urogynecological research.

Comparative studies on conventional PPL meshes and electrospun scaffolds have revealed that the later allowed cellular infiltration and neo-matrix production that resulted in improved host tissue integration rather than the formation of a fibrous capsule exclusive to PPL implantation [133]. Cellular migration and proliferation in the presence of PPL mesh and PU Z3 implanted into the TE vaginal models was studied to determine the host-tissue response towards implants *in vitro*. Histological analysis revealed that the biomimetic electrospun PU Z3 scaffold did not interrupt the formation of a healthy stratified squamous epithelia on TE wound vaginal models

(Figure 4.10). The formation of stratified epithelia continued to develop within the wounded region in TE models until the PU Z3 biomaterial was reached that encountered as a physical barrier for further wound closure. On the other hand, the presence of PPL mesh implanted within the wounded region caused an interrupted irregular formation of fragile epithelia on TE wound models as shown in Figure 4.8. Previously *Liang et al.,* [400] reported similar observations in explanted vaginal tissue samples from rhesus macaque implanted with commercial Gynemesh®. Histomorphological analysis of the explanted graft-vaginal complex revealed that the Gynemesh® implanted samples had thinner epithelium compared to sham at twelve weeks post-implantation.

Reduced levels of oestrogens play an important role in the pathogenesis of POP and their presence can be key contributors in the process of optimal vaginal wound healing. Balgobin *et al.,* [363] studied the effect of estradiol-17β on the guinea pigs vaginal wound healing process in response to surgical injury. They reported that in the absence of E_2, the excised vaginal tissue epithelium was thin and largely composed of about a single cell layer whereas histomorphological analysis of E_2- administered animals showed an increase in the vaginal epithelium thickness and smooth muscle component in the muscularis region. In another *in vivo* study in the rabbit vaginal model [401], post-operative estradiol-17β administration was associated with the formation of a thicker stratified vaginal epithelium and muscularis compared to control (without E_2) eight weeks after PPL mesh implantation surgery. In the TE wound vaginal models presented here, administration of E_2 into the culture media resulted in an intense cellular proliferation and infiltration towards the PPL implanted region. Whereas, in TE wound models implanted with PU Z3, E_2 administration resulted in the formation of a thicker stratified squamous epithelia on TE models similar to those reported in aforementioned *in vivo* studies.

Previous studies from our group have reported that electrospun polymeric scaffolds supported cellular proliferation and metabolic activity in *in vitro* cell culture conditions [130], [135], [384], [388]. Electrospun polyurethanes (PU) are attractive polymeric membranes in the field of tissue engineering especially in the area of developing soft tissue wound healing products [402] as PU membranes support cell adhesion and proliferation. Gabriel *et al.,* [403] reported that the optimal pore size for electrospun PU to support fibroblasts metabolic activity and proliferation was found to be 20 μm. My results are in concordance with these findings as

among the two biomaterials tested in the TE wound models presented here, PU Z3 supported the cellular proliferation and metabolic activity more than the PPL mesh implanted models (Figure 4.12). A significant increase in the cellular metabolic activity was observed under E_2 induction in line with the findings discussed in the previous chapter.

Comparative histomorphological analysis of PU Z3 and PPL mesh implanted TE wound vaginal models presented here revealed that the collagen component in the ECM was augmented in PU Z3 models and administration of E_2 further increased collagen production (Figures 4.13 - 4.20). These results are in consistence with previous studies in animal models and hence further validate the physiological relevance of my TE wound vaginal models as a valuable preclinical testing method for biomaterials designed for pelvic floor implantation.

Clark *et al.,* [404] studied the effect of estradiol-17β on collagen metabolism and synthesis of collagen type I in the vaginal wall of rhesus macaque. They reported that E_2 administration resulted in an increase in collagen gene transcription and increased mRNA production localised to the vaginal fibroblasts present in the connective tissue of lateral vaginal walls excised from the animals. Hence, oestrogen stimulated the production of collagen in pelvic floor connective tissue.

Over the course of this study, the PPL mesh implanted TE models showed the collagen architecture in the ECM to be relatively immaturely organised (Figures 4.13 & 4.17) that became more thicker and densely packed in an aligned laminate configuration upon E_2 induction (Figures 4.14 & 4.18). A similar study by Higgins *et al.,* [401] in a rabbit vaginal model earlier concluded that oestrogen replacement administered at postoperative PPL mesh implantation surgery caused an increased collagen deposition into the PPL mesh.

Implants for the pelvic floor repair should ideally have a load bearing function along with appropriate surface chemistry and microarchitecture for cellular attachment and proliferation that can lead to repair and regeneration of the soft tissues. Electrospun PU Z3 offers a fibrous microporous surface layers that have architectural resemblance to the native tissue ECM. According to Vashaghian *et al.,* [133] such biomaterials may help to recruit M2 macrophages at the implant-tissue interface for functional tissue regeneration.

Vaginal fibroblasts play a critical role in the pelvic connective tissue quality and the transition from fibroblasts to myofibroblasts is a key event during the vaginal wound healing process and tissue remodeling after implant-based POP surgery [405]. Myofibroblasts production of alpha-SMA protein helps to repair the wounded vaginal tissue post-operative however, in case of excessive activity this can lead to fibrotic tissue formation and scarring around the implant-tissue interface that may lead to mesh shrinkage, exposure and tissue erosion. Clinical data from excised mesh-tissue complexes from patients experiencing post-operative complications revealed that the PPL mesh was associated with a higher myofibroblast activity causing a fibrotic tissue formation around the implanted mesh [369]. Here i have recapitulated similar physiological activity of myofibroblast differentiation in the presence of PPL mesh implant in my TE wound vaginal models.

Immunohistofluorescence analysis of these models showed that in the presence of PPL mesh implant there was an increased myofibroblasts differentiation activity that resulted in increased expression of α-SMA (Figures 4.26 & 4.27). Several factors can influence fibroblasts activity in the pelvic connective tissue. Studies have suggested that mechanical distensions within the pelvic floor can change the cytoskeleton transcriptional profile of the vaginal fibroblasts which in turn affect their rate of differentiation into myofibroblasts [406]. It has now been well established that vaginal fibroblasts cultured on stiffer matrices induces myofibroblasts differentiation and increased production of α-SMA [407]. Orenstein *et al.,* [408] studied the comparative histomorphological effects of synthetic PPL-based mesh implants including lightweight macroporous Gynemesh® and heavyweight microporous UltraPro® in a subcutaneous mouse model. They reported that at twelve weeks post-implantation, severe fibrosis and thick encapsulation was observed in all explanted samples. These observations can be attributed to the fact that PPL mesh is a stiffer biomaterial in comparison with polymeric PU Z3 reported here. The stiffness of the PPL mesh is a plausible underlying factor that resulted in increased myofibroblasts differentiation and α-SMA production in our PPL implanted TE wound models in comparison with PU Z3 implanted models (Figures 4.26 - 4.30). Moreover, the surface biochemistry and softer micro-fibrous architecture of the electrospun scaffolds have been reported to prevent vaginal fibroblasts differentiation into myofibroblasts as the later caused an increased risk of scar-tissue formation and contraction at the implant site.

Here, i have developed a preclinical method to evaluate newly developed biomaterials by implantation into TE wound vaginal models to determine the initial cellular and tissue response towards these biomaterials *in vitro*. Several aspects of initial host tissue-implant interactions were investigated including cellular migration, proliferation, collagen synthesis as well as vaginal wound healing and epithelia reformation in the presence of implanted biomaterials in a physiologically relevant microenvironment. I have recapitulated the native vaginal tissue ECM architecture and physiology by rendering these models as E_2 responsive and culturing them with relevant vaginal stromal and epithelial cells. Moreover, the biomaterial implanted wound models were able to discriminate between materials that are most likely to cause fibrotic tissue formation and scarring during the process of vaginal wound healing post-implantation *in vivo*. However, there were two main limitations that were identified in this study. These include the missing factors of macrophages and vasculature in the TE wound models that play an important role in host-tissue interactions with implanted biomaterials. Nevertheless, these models were developed for the purpose of initial screening of newly developed biomaterials for pelvic floor reconstructive applications. Once the preliminary biological and mechanical response of pelvic floor biomaterials will be determined using my TE wound models, further investigations will be followed using *in vivo* models. In this way, my approach was to develop these *in vitro* models to help reduce the number of animal testing in urogynecological research and to speed up the process of development and testing of much needed pelvic floor implants.

Chapter 5:
Conclusions and future work

This PhD project aimed at developing an *in vitro* tissue engineered (TE) model of the vaginal mucosa for applications in vaginal tissue research. In the field of female pelvic floor regenerative medicine, there is currently a treatment gap for women suffering from pelvic floor disorders such as pelvic organ prolapse (POP) and stress urinary incontinence (SUI). For years, the use of the polypropylene (PPL)-based vaginal mesh implants was considered to be the gold standard treatment for reconstructive pelvic procedures. However, in 2019 due to many reports of severe post-operative PPL mesh-related complications, the FDA put a ban on the use of PPL mesh in urogynecological reconstructive procedures that left patients who require surgical intervention with no alternative treatment. Currently, there is a real need to develop better biomaterials that are safe and efficient to use for implantation into the female pelvic floor. In addition, lessons that have been learnt from the vaginal mesh scandal highlighted the importance of rigorous preclinical testing of newly developed biomaterials in physiologically relevant models of the human vaginal tissue before their translation into clinics. Historically, the PPL mesh implants were originally designed for use in the abdominal hernia repair and were never tested for their use in the female pelvic floor. These anatomical differences between the abdominal wall and the dynamic pelvic floor fascia is a major cause of failure of these PPL mesh implants in the pelvic floor reconstructive procedures.

The outcomes of the project were as follows:

A physiologically relevant TE vaginal mucosa model was developed that was able to recapitulate key features of the human vaginal mucosa *in vitro*. In particular it demonstrated a positive response to the female reproductive hormone estradiol-17β [E_2] validating its physiological relevance. Then this model was used to study the process of vaginal wound healing in the presence of estradiol -17β [E_2] and showed accelerated healing. Next in this PhD project, electrospun polymeric polyurethane (PU Z3) biomaterial was developed as a potential candidate material for future applications in pelvic floor reconstructive procedures. The candidate material was structurally and mechanically tested against the conventional PPL mesh to determine the desired microarchitecture, strength and flexibility suitable to support the dynamic pelvic floor environment.

Then the two candidate biomaterials (PPL and PU Z3) were tested for their biocompatibility and host-tissue response in the TE wound vaginal model developed in this project to determine the vaginal tissue response towards implanted biomaterials in a manner similar to *in vivo* human conditions. Additionally, the contribution of estradiol -17β [E_2] to this response was investigated. The PU Z3 material was found to provoke less tissue reaction than the PPL material and the contribution of E_2 improved the response to both. The progress made in this PhD is discussed next prior to considering how these models could be used or developed further.

The TE vaginal model developed in this project was based upon decellularised sheep vaginal tissues and primary sheep vaginal epithelial cells and fibroblasts. Sheep was chosen to be the vaginal tissue donor as the sheep urogenital tract shares anatomical and histological similarities with the human tissue. Moreover, sheep vaginal tissue was collected from the local abattoir as a waste product and no additional animals were needed to be sacrificed to obtain vaginal tissues for this project. Primary sheep vaginal epithelial cells and fibroblasts were isolated and expanded in culture and were morphologically characterised. Tissue engineered vaginal models were developed by culturing these primary cells on decellularised sheep vaginal matrices and cultured at an air-liquid interface to allow for stratification of the vaginal epithelium that mimicked the histological features of the native human vaginal epithelium. The vaginal models presented here comprised of both a stratified epithelial and connective tissue component that were histologically characterised and showed an intact basement membrane within these tissue components. These features were exclusive to the TE model developed here in comparison with the commercially available Epivaginal™ models. The commercial Epivaginal™ models do not contain the lamina propria component and are developed by culturing human vaginal cells on microporous membranes and collagen gels. Hence, these commercial models lack the native vaginal tissue extracellular matrix (ECM) microarchitecture, and the cultured cells respond differently on membranes compared to their native microenvironment.

The native sheep vaginal tissues collected from the abattoir were successfully decellularised using a combination of mild anionic and cationic detergents (sodium deoxycholate and Triton X100) to ensure efficient removal of cellular components while preserving the native ECM architecture. The vaginal tissues were also treated with a strong Cambridge antibiotic solution to remove all the bacteria and native flora of the urogenital tract in order to minimise the

chances of bacterial infection during the culturing of models. The models were developed by culturing primary vaginal epithelial cells and fibroblasts on decellularised vaginal matrices. One drawback of using primary cells is that it may lead to variability between different batches of cells that may cause concerns regarding reproducibility of the experimental data. To overcome this concern, one strategy could be to use commercially available vaginal cell lines however, these cell lines are usually genetically modified and often display differences in their phenotype and physiological response in comparison with the primary vaginal cells. In this project, my strategy was to use vaginal epithelial cells and fibroblasts between passage 2-3 to develop the models in order to minimise the chances of variability among models.

A key feature of these TE vaginal models is that they could be cultured for up to three weeks in ALI culture without loss of cellular metabolic activity and epithelial membrane integrity. This is the longest culture period reported for TE vaginal models in comparison with the commercial Epivaginal™ models. This feature enabled me to investigate the process of vaginal wound healing and early tissue response towards implanted biomaterials over three weeks' time. This model could be used in a number of future *in vitro* applications where newly developed microbicides and pharmaceuticals could be tested for their long-term effects over a longer culture time period. Many commercial models are designed for immediate short-term use only. This makes them very expensive and of limited use. They have been designed primarily for pharmaceutical company use.

The effect of female reproductive hormone estradiol-17β [E_2] was investigated on TE vaginal models to demonstrate the hormone responsiveness and physiological relevance of my models. Estradiol-17β [E_2] is the main hormone responsible for maintaining a healthy pelvic fascia by retaining the thickness of the stratified squamous vaginal epithelium. Moreover, in a normal healthy individual, E_2 serum levels play a key role in maintaining the histoarchitecture of the pelvic connective tissue and collagen and elastin components. These models depicted a dose-dependent response towards E_2 concentration in the culture media as a higher E_2 concentration caused the formation of a highly stratified and thicker epithelium on the models. These results showed correlation with clinical findings as vaginal tissue biopsies from post-menopausal patients treated with E_2 have shown an improvement in the vaginal epithelium thickness and tissue histoarchitecture. Here, i have demonstrated similar findings for the first time in an *in vitro* TE model and their E_2-responsiveness determine their physiological relevance.

The TE vaginal models cultured with primary vaginal cells modelled many features of the native vaginal tissue histoarchitecture. The models depicted the stratified vaginal epithelium containing 12-15 layers of epithelial cells that were concentrated in the basement membrane and became more dispersed and flattened out in the apical layers. Moreover, the cultured vaginal epithelial cells showed E_2-sensitivity and expressed certain cytokeratins exclusive to urogenital epithelial cells expression *in vivo* such as cytokeratin 10 and 19. These cytokeratins are important diagnostic biomarkers as their expression is regulated by the E_2 serum levels.

Women suffering from pelvic floor disorders often present with a weakened connective tissue that is unable to provide adequate support to the pelvic organs. This clinical pathology has been replicated in this project by developing TE vaginal wound models and creating intentional scalpel wounds into the TE models to mimic the compromised vaginal connective tissue *in vitro.* The process of vaginal wound healing determines the outcome of any biomaterial-augmented pelvic floor reconstructive surgery and hence, is an important process that determines the success rate of these reconstructive procedures. Here, i have studied all the key stages of the vaginal wound healing process including cellular migration, proliferation as well as fibroblasts differentiation into myofibroblasts to achieve an efficient wound healing in an *in vitro* TE model. Moreover, here i have also demonstrated the effect of E_2 on the vaginal wound healing and the results have confirmed a positive effect of E_2 on the vaginal wound healing process. These findings have significant correlation with previously reported clinical findings where post-operative E_2 administration has shown improved vaginal wound healing in patients. Histological and immunohistofluorescence imaging data further confirmed that the TE wound vaginal models showed improved healing along with the formation of stratified re-epithelialisation of the wounded region in models cultured in the presence of E_2.

One interesting application of my TE wound vaginal models could be their future use in the pharmaceutical and drug discovery industry to develop and test therapeutic agents that can facilitate soft tissue wound healing. The process of wound healing is quite complex and involves a number of different cell types such as stromal cells, epithelial cells, endothelial cells, neutrophils, monocytes and macrophages that all respond in a cascade of events leading to soft tissue wound healing *in vivo*. Here, i have achieved an appropriate wound closure in my TE wound models cultured with vaginal epithelial cells and fibroblasts.

In an ideal wound healing TE model, it would be desirable to include the components of the immune system such as the neutrophils and macrophages as these cells are the key responders during an event of injury and help to recruit other stromal cells such as fibroblasts towards the wounded region. One limitation of these TE wound vaginal models is the absence of the immune component which in future i hope to include as this would enable one to study the physiological process of vaginal wound healing in more detail. Nevertheless, my aim in this PhD project was to mimic the *in vivo* process of vaginal wound healing in an *in vitro* TE model so that i was able to study the effect of E_2 without the involvement of *in vivo* physiological complexity and to correlate my findings with the clinical data. Here, i have successfully accomplished these aims by demonstrating the undeniable beneficial role of E_2 in aiding wound closure and collagen deposition in these TE wound models.

In the last section of this PhD project, i have reported for the first time the application of my TE wound vaginal models to investigate the cellular and tissue response towards implanted biomaterials in an *in vitro* model. This is the most ambitious application of my TE model as so far, this is the first model of its kind that showed the ability to discriminate between biomaterials that can cause either a fibrotic tissue response or a remodelling response post-implantation. I have achieved this by implanting potential biomaterials for the female pelvic floor repair into the wounded region of these TE models and demonstrated the cellular and tissue response by measuring the expression of alpha-smooth muscle actin (alpha-SMA), a key marker of fibrosis. In addition, i further investigated the effect of E_2 on the expression of alpha-SMA in the presence of implanted biomaterials and revealed that my electrospun polyurethane (PU) caused a lesser fibrotic response in comparison with the commercial polypropylene (PPL) mesh in our models. These findings significantly correlate with the previously reported data from animal models.

In summary, i have developed a cost-effective, efficient and physiologically relevant *in vitro* TE model for initial screening of newly developed biomaterials designed for female pelvic floor repair. My strategy was to develop this model for preclinical safety assessment of potential pelvic floor biomaterials in order to accelerate innovation and testing procedures in this challenging area of clinical need. This model provides preliminary evidence that it has the ability to evaluate biomaterials that are at risk of developing an aggravated post-operative fibrotic response without the need for animal testing. Now that this model has been developed there are many developments that can be built on it.

The model could be used to examine the effect of pre-stressing the mesh candidate materials on the vaginal tissue to study the reaction to these stressed biomaterials. Here, the approach would be to implant pre-stressed PPL mesh into the TE wound model to investigate the contribution of oxidative and mechanical stress to the vaginal tissue in the presence of PPL. This would be a step forward in replicating the *in vivo* pelvic floor conditions more accurately as pelvic implants will experience dynamic distension and oxidative-stress conditions when implanted *in vivo*. A recent study [409] by our group has reported changes in the surface properties of PPL mesh when subjected to dynamic distension under oxidative stress. This is a controversial area as manufacturers claim that the PPL mesh is totally inert. Our laboratory has used a very sensitive surface analysis technique to show that PPL subjected to mild mechanical distension (over 3 days) combined with oxidative stress (as would occur *in vivo* due to the macrophage response on the PPL mesh surface) led to surface degradation. Such changes *in vivo* could cause changes in the host tissue response to these biomaterials post-implantation.

A significant advance to these TE vaginal models could be achieved by adding the immunological components, specifically macrophages to study the initial immune response to implanted biomaterials. My proposed idea of including macrophages in the TE models developed here is that these cell types can be isolated from whole blood that can be collected from blood bank following the ethical approval from the concerned departments. Macrophages are differentiated blood cells derived from monocytes that play a major role in the activation of immune system and contribute towards inflammation, wound healing and tissue repair. Monocytes can also be isolated form buffy coat depending upon the availability of whole or pre-processed blood and can be expanded and differentiated into macrophages by culturing in 60:30:10 medium or by adding growth factors (GM-CSF or M-CSF) [410]. The idea is to include macrophages isolated from blood with a co-culture of vaginal epithelial cells and fibroblasts and culture all three cell types on decellularised sheep vaginal matrices to develop wound models. This approach would be beneficial in investigating the macrophage response towards vaginal injury and can provide in-depth details into the vaginal wound healing process in an *in vitro* model. Moreover, macrophage response towards different biomaterials can also be investigated by the addition of macrophages to TE wound vaginal models with biomaterial implantation reported in this project. Previous investigations on post-operative polypropylene mesh complications have reported a prolonged M1 type macrophage response that led to inflammation and fibrosis. It would be interesting to study the macrophage differentiation phenotype in response to PPL and PU on the wound models developed in this project.

Another advancement could be made by including the vascular network within the TE wound models to further investigate the process of vaginal wound healing. Vascular supply is crucial in wound healing as different cellular components of blood contribute towards this process via cascade of events leading to wound healing. The vasculature of native organs has complex spatial architecture that is essential for organ-specific function. The decellularised organ ECM often preserve the essential ECM composition for supporting vessel formation and similarly, the TE models developed here are based on decellularised ECM of the vaginal tissue.

In vitro modelling systems usually lack the *in vivo* vascular network, and the current challenge is to include functional microvascular networks in *in vitro* models to generate viable functional tissues. One approach is to introduce pluripotent stem cells into the models along with growth factors (such as VEGF, TGF-β) to differentiate into endothelial cells to stimulate vasculogenesis or to include HUVECs. However, these methods of vascular reconstruction using decellularised ECM is mainly restricted at the reconstruction of large blood vessels. The real perfusion function of the whole vascular network is still recognised as a major challenge. My proposed idea to include vasculature into the TE wound models developed here is to implant these models onto the chick chorioallantoic membrane (CAM). The CAM is a non-immunogenic system of live chick embryo with functional vascular network and can provide the essential blood flow via interaction with the implanted TE model. With this approach a real perfusion function of blood through the TE models could be achieved without the need for transplantation into higher animal models which require rigorous ethical approvals. While this would require further research, i suggest that it will be possible and merits investment.

In conclusion, TE vaginal models and wound models developed in this project are advancements in the field of urogynecological research as they provide physiologically relevant *in vitro* model systems for a range of applications. These applications include preclinical studies on novel vaginal therapeutics to investigate their potential effects on the histoarchitecture of the vaginal tissue and in particular to test the host-tissue response towards biomaterials developed for female pelvic floor repair.

Funding:

This PhD project was funded by the University of Sheffield Faculty of Engineering Post Graduate Research committee prize studentship.

References:

[1] A. Gomelsky, D. F. Penson, and R. R. Dmochowski, “Pelvic organ prolapse (POP) surgery: the evidence for the repairs,” *BJU Int.*, vol. 107, no. 11, pp. 1704–1719, 2011.

[2] Z. Abdool, R. Thakar, A. H. Sultan, and R. S. Oliver, “Prospective evaluation of outcome of vaginal pessaries versus surgery in women with symptomatic pelvic organ prolapse,” *Int. Urogynecol. J.*, vol. 22, no. 3, pp. 273–278, 2011.

[3] S. I. Ismail, C. Bain, and S. Hagen, “Oestrogens for treatment or prevention of pelvic organ prolapse in postmenopausal women,” *Cochrane Database Syst. Rev.*, no. 9, 2010.

[4] M. Peng *et al.*, “Rectus Fascia Versus Fascia Lata for Autologous Fascial Pubovaginal Sling: A Single-Center Comparison of Perioperative and Functional Outcomes,” *Female Pelvic Med. Reconstr. Surg.*, vol. Publish Ah, 9000.

[5] N. S. Howden, H. M. Zyczynski, P. A. Moalli, E. R. Sagan, L. A. Meyn, and A. M. Weber, “Comparison of autologous rectus fascia and cadaveric fascia in pubovaginal sling continence outcomes,” *Am. J. Obstet. Gynecol.*, vol. 194, no. 5, pp. 1444–1449, 2006.

[6] K. V Amrute and G. H. Badlani, “Female incontinence: a review of biomaterials and minimally invasive techniques,” *Curr. Opin. Urol.*, vol. 16, no. 2, pp. 54–59, 2006.

[7] C. on G. Practice, “Vaginal Placement of Synthetic Mesh for Pelvic Organ Prolapse,” *Female Pelvic Med. Reconstr. Surg.*, vol. 18, no. 1, 2012.

[8] H. Abed *et al.*, “Incidence and management of graft erosion, wound granulation, and dyspareunia following vaginal prolapse repair with graft materials: a systematic review,” *Int. Urogynecol. J.*, vol. 22, no. 7, pp. 789–798, 2011.

[9] H. N. Shah and G. H. Badlani, “Mesh complications in female pelvic floor reconstructive surgery and their management: A systematic review,” *Indian J. Urol.*, vol. 28, no. 2, pp. 129–153, Apr. 2012.

[10] M. E. Koski and E. S. Rovner, “Implications of the FDA statement on transvaginal placement of mesh: the aftermath,” *Curr. Urol. Rep.*, vol. 15, no. 2, p. 380, 2014.

[11] M. Kelly, K. Macdougall, O. Olabisi, and N. McGuire, “In vivo response to polypropylene following implantation in animal models: a review of biocompatibility,” *Int. Urogynecol. J.*, vol. 28, no. 2, pp. 171–180, 2017.

[12] M. C. Gibbons, M. A. Foley, and K. O. Cardinal, “Thinking inside the box: keeping tissue-engineered constructs in vitro for use as preclinical models,” *Tissue Eng. Part B*

Rev., vol. 19, no. 1, pp. 14–30, 2013.

[13] K. V. Greco, L. G. Jones, I. Obiri-Yeboa, and T. Ansari, "Creation of an Acellular Vaginal Matrix for Potential Vaginal Augmentation and Cloacal Repair," *J. Pediatr. Adolesc. Gynecol.*, vol. 31, no. 5, pp. 473–479, 2018.

[14] M. Merbah *et al.*, "Cervico-vaginal tissue ex vivo as a model to study early events in HIV-1 infection," *Am. J. Reprod. Immunol.*, vol. 65, no. 3, pp. 268–278, 2011.

[15] Y. Zhu *et al.*, "Ex vivo 2D and 3D HSV-2 infection model using human normal vaginal epithelial cells," *Oncotarget*, vol. 8, no. 9, pp. 15267–15282, Feb. 2017.

[16] R. M. Machado, A. Palmeira-de-Oliveira, C. Gaspar, J. Martinez-de-Oliveira, and R. Palmeira-de-Oliveira, "Studies and methodologies on vaginal drug permeation," *Adv. Drug Deliv. Rev.*, vol. 92, pp. 14–26, 2015.

[17] G.-E. Costin, H. A. Raabe, R. Priston, E. Evans, and R. D. Curren, "Vaginal Irritation Models: The Current Status of Available Alternative and In Vitro Tests," *Altern. to Lab. Anim.*, vol. 39, no. 4, pp. 317–337, Sep. 2011.

[18] F. Causa, P. A. Netti, and L. Ambrosio, "A multi-functional scaffold for tissue regeneration: The need to engineer a tissue analogue," *Biomaterials*, vol. 28, no. 34, pp. 5093–5099, 2007.

[19] J. Shepherd, I. Douglas, S. Rimmer, L. Swanson, and S. MacNeil, "Development of three-dimensional tissue-engineered models of bacterial infected human skin wounds," *Tissue Eng. Part C Methods*, vol. 15, no. 3, pp. 475–484, 2009.

[20] P. Carrier *et al.*, "Characterization of wound reepithelialization using a new human tissue-engineered corneal wound healing model," *Invest. Ophthalmol. Vis. Sci.*, vol. 49, no. 4, pp. 1376–1385, 2008.

[21] S. Sundelacruz, C. Li, Y. J. Choi, M. Levin, and D. L. Kaplan, "Bioelectric modulation of wound healing in a 3D in vitro model of tissue-engineered bone," *Biomaterials*, vol. 34, no. 28, pp. 6695–6705, 2013.

[22] S. MacNeil, J. Shepherd, and L. Smith, "Production of tissue-engineered skin and oral mucosa for clinical and experimental use," in *3D cell culture*, Springer, 2011, pp. 129–153.

[23] L. E. Smith, M. Bonesi, R. Smallwood, S. J. Matcher, and S. MacNeil, "Using swept-source optical coherence tomography to monitor the formation of neo-epidermis in tissue-engineered skin," *J. Tissue Eng. Regen. Med.*, vol. 4, no. 8, pp. 652–658, 2010.

[24] V. Hearnden *et al.*, "Diffusion studies of nanometer polymersomes across tissue engineered human oral mucosa," *Pharm. Res.*, vol. 26, no. 7, pp. 1718–1728, 2009.

[25] S. Herschorn, “Female pelvic floor anatomy: the pelvic floor, supporting structures, and pelvic organs,” *Rev. Urol.*, vol. 6, no. Suppl 5, p. S2, 2004.

[26] P. Mannella, G. Palla, M. Bellini, and T. Simoncini, “The female pelvic floor through midlife and aging,” *Maturitas*, vol. 76, no. 3, pp. 230–234, 2013.

[27] A. Huseynov *et al.*, “Developmental evidence for obstetric adaptation of the human female pelvis,” *Proc. Natl. Acad. Sci.*, vol. 113, no. 19, pp. 5227–5232, 2016.

[28] K. M. Van De Graaff, *Human Anatomy*. McGraw-Hill, 2002.

[29] M. S. Baggish and M. M. Karram, *Atlas of pelvic anatomy and gynecologic surgery*. Elsevier Health Sciences, 2015.

[30] J. A. Karam, D. V Vazquez, V. K. Lin, and P. E. Zimmern, “Elastin expression and elastic fibre width in the anterior vaginal wall of postmenopausal women with and without prolapse,” *BJU Int.*, vol. 100, no. 2, pp. 346–350, 2007.

[31] A. M. Weber *et al.*, “Basic science and translational research in female pelvic floor disorders: Proceedings of an NIH-sponsored meeting,” *Neurourol. Urodynamics Off. J. Int. Cont. Soc.*, vol. 23, no. 4, pp. 288–301, 2004.

[32] M. D. Walters and A. M. Weber, “Anatomy of the lower urinary tract, rectum and pelvic floor,” *Urogynecology Reconstr. Pelvic Surgery. St. Louis, MO Mosby*, pp. 3–13, 1999.

[33] P. Petros, “The anatomy and dynamics of pelvic floor function and dysfunction,” in *The female pelvic floor*, Springer, 2010, pp. 17–76.

[34] P. Petros, “The integral system,” *Cent. Eur. J. Urol.*, vol. 64, no. 3, p. 110, 2011.

[35] R. M. H. Power, “Embryological development of the levator ani muscle,” *Am. J. Obstet. Gynecol.*, vol. 55, no. 3, pp. 367–381, 1948.

[36] P. Thompson, “On the arrangement of the fasciae of the pelvis and their relationship to the levator ani,” *J. Anat. Physiol.*, vol. 35, no. Pt 2, p. 127, 1901.

[37] J. Ashton-Miller and J. O. L. DeLANCEY, “Functional anatomy of the female pelvic floor,” *Bø K, Berghmans B, Mørkved S, van Kampen M, Evid. based Phys. Ther. pelvic floor—Bridging Sci. Clin. Pract.*, pp. 19–33, 2007.

[38] A. E. Bharucha, “Pelvic floor: anatomy and function,” *Neurogastroenterol. Motil.*, vol. 18, no. 7, pp. 507–519, 2006.

[39] H. O. D. Critchley, J. S. Dixon, and J. A. Gosling, “Comparative study of the periurethral and perianal parts of the human levator ani muscle,” *Urol. Int.*, vol. 35, no. 3, pp. 226–232, 1980.

[40] C. Rubod, M. Boukerrou, M. Brieu, C. Jean-Charles, P. Dubois, and M. Cosson,

"Biomechanical properties of vaginal tissue: preliminary results," *Int. Urogynecol. J.*, vol. 19, no. 6, pp. 811–816, 2008.

[41] G. M. Northington, M. Basha, L. A. Arya, A. J. Wein, and S. Chacko, "Contractile Response of Human Anterior Vaginal Muscularis in Women With and Without Pelvic Organ Prolapse," *Reprod. Sci.*, vol. 18, no. 3, pp. 296–303, Dec. 2010.

[42] P. Martins *et al.*, "Biomechanical Properties of Vaginal Tissue in Women with Pelvic Organ Prolapse," *Gynecol. Obstet. Invest.*, vol. 75, no. 2, pp. 85–92, 2013.

[43] A. M. Ruiz-Zapata, A. J. Feola, J. Heesakkers, P. de Graaf, M. Blaganje, and K.-D. Sievert, "Biomechanical properties of the pelvic floor and its relation to pelvic floor disorders," *Eur. Urol. Suppl.*, vol. 17, no. 3, pp. 80–90, 2018.

[44] C. Rubod *et al.*, "Biomechanical properties of human pelvic organs," *Urology*, vol. 79, no. 4, pp. 968-e17, 2012.

[45] P. Chantereau, M. Brieu, M. Kammal, J. Farthmann, B. Gabriel, and M. Cosson, "Mechanical properties of pelvic soft tissue of young women and impact of aging," *Int. Urogynecol. J.*, vol. 25, no. 11, pp. 1547–1553, 2014.

[46] G. Rivaux, C. Rubod, B. Dedet, M. Brieu, B. Gabriel, and M. Cosson, "Comparative analysis of pelvic ligaments: a biomechanics study," *Int. Urogynecol. J.*, vol. 24, no. 1, pp. 135–139, 2013.

[47] F. Iacobellis *et al.*, "Pelvic floor dysfunctions: how to image patients?," *Jpn. J. Radiol.*, vol. 38, no. 1, pp. 47–63, 2020.

[48] R. C. Bump and P. A. Norton, "EPIDEMIOLOGY AND NATURAL HISTORY OF PELVIC FLOOR DYSFUNCTION," *Obstet. Gynecol. Clin. North Am.*, vol. 25, no. 4, pp. 723–746, 1998.

[49] B. Megabiaw *et al.*, "Pelvic floor disorders among women in Dabat district, northwest Ethiopia: a pilot study," *Int. Urogynecol. J.*, vol. 24, no. 7, pp. 1135–1143, 2013.

[50] D. Altman *et al.*, "Epidemiology of urinary incontinence (UI) and other lower urinary tract symptoms (LUTS), pelvic organ prolapse (POP) and anal incontinence (AI)," in *Incontinence: 6th International Consultation on Incontinence, Tokyo, September 2016*, International Continence Society, 2017, pp. 1–141.

[51] A. A. Dieter, M. F. Wilkins, and J. M. Wu, "Epidemiological trends and future care needs for pelvic floor disorders," *Curr. Opin. Obstet. Gynecol.*, vol. 27, no. 5, p. 380, 2015.

[52] S. S. Badalian, E. Sagayan, H. Simonyan, V. A. Minassian, and A. Isahakian, "The prevalence of pelvic floor disorders and degree of bother among women attending

primary care clinics in Armenia," *Eur. J. Obstet. Gynecol. Reprod. Biol.*, vol. 246, pp. 106–112, 2020.

[53] J.-S. Yuk, J. H. Lee, J.-Y. Hur, and J.-H. Shin, "The prevalence and treatment pattern of clinically diagnosed pelvic organ prolapse: a Korean National Health Insurance Database-based cross-sectional study 2009–2015," *Sci. Rep.*, vol. 8, no. 1, pp. 1–6, 2018.

[54] J. S. Brown, L. E. Waetjen, L. L. Subak, D. H. Thom, S. Van Den Eeden, and E. Vittinghoff, "Pelvic organ prolapse surgery in the United States, 1997," *Am. J. Obstet. Gynecol.*, vol. 186, no. 4, pp. 712–716, 2002.

[55] L. L. Subak, L. E. Waetjen, S. van den Eeden, D. H. Thom, E. Vittinghoff, and J. S. Brown, "Cost of pelvic organ prolapse surgery in the United States," *Obstet. Gynecol.*, vol. 98, no. 4, pp. 646–651, 2001.

[56] J. E. Jelovsek, C. Maher, and M. D. Barber, "Pelvic organ prolapse," *Lancet*, vol. 369, no. 9566, pp. 1027–1038, 2007.

[57] A. L. Olsen, V. J. Smith, J. O. Bergstrom, J. C. Colling, and A. L. Clark, "Epidemiology of surgically managed pelvic organ prolapse and urinary incontinence," *Obstet. Gynecol.*, vol. 89, no. 4, pp. 501–506, 1997.

[58] V. W. Sung and B. S. Hampton, "Epidemiology of pelvic floor dysfunction," *Obstet. Gynecol. Clin.*, vol. 36, no. 3, pp. 421–443, 2009.

[59] P. Abrams *et al.*, "The standardization of terminology of lower urinary tract function: report from the standardization sub-committee of International Continence Society," in *Textbook of Female Urology and Urogynecology*, CRC Press, 2010, pp. 1098–1108.

[60] M. T. Schettino *et al.*, "Risk of pelvic floor dysfunctions in young athletes," *Clin Exp Obs. Gynecol*, vol. 41, no. 6, pp. 671–676, 2014.

[61] P. Y. Noritomi, J. V. L. da Silva, R. C. A. Dellai, A. Fiorentino, L. Giorleo, and E. Ceretti, "Virtual modeling of a female pelvic floor and hypothesis for simulating biomechanical behavior during natural delivery," *Procedia CIRP*, vol. 5, pp. 300–304, 2013.

[62] M. Stone, "The Harvard Medical School family health guide." BOWKER MAGAZINE GROUP CAHNERS MAGAZINE DIVISION 249 W 17TH ST, NEW YORK, NY …, 1999.

[63] R. Kearney, R. Sawhney, and J. O. L. DeLancey, "Levator ani muscle anatomy evaluated by origin-insertion pairs," *Obstet. Gynecol.*, vol. 104, no. 1, p. 168, 2004.

[64] K. Singh, M. Jakab, W. M. N. Reid, L. A. Berger, and L. Hoyte, "Three-dimensional

magnetic resonance imaging assessment of levator ani morphologic features in different grades of prolapse," *Am. J. Obstet. Gynecol.*, vol. 188, no. 4, pp. 910–915, 2003.

[65] D. Yang, M. Zhang, and K. Liu, "Tissue engineering to treat pelvic organ prolapse," *J. Biomater. Sci. Polym. Ed.*, vol. 32, no. 16, pp. 2118–2143, 2021.

[66] S. Swift *et al.*, "Pelvic Organ Support Study (POSST): The distribution, clinical definition, and epidemiologic condition of pelvic organ support defects," *Am. J. Obstet. Gynecol.*, vol. 192, no. 3, pp. 795–806, 2005.

[67] R. C. Bump, K. Mattiasson, L. P. Bo, L. P. Brubaker, J. O. L. DeLancey, and B. L. Klarskov, "The standardization of terminology of female pelvic floor dysfunction," *Textb. Female Urol. Urogynaecology. Cardozo L, Staskin D (eds), Isis Med. Media London*, p. 1052, 2001.

[68] R. C. Bump, "The POP-Q system: two decades of progress and debate," *Int. Urogynecol. J.*, vol. 25, no. 4, pp. 441–443, 2014.

[69] B. T. Haylen *et al.*, "An International Urogynecological Association (IUGA)/International Continence Society (ICS) joint terminology and classification of the complications related directly to the insertion of prostheses (meshes, implants, tapes) and grafts in female pelvic flo," *Neurourol. Urodyn.*, vol. 30, no. 1, pp. 2–12, 2011.

[70] J. Mant, R. Painter, and M. Vessey, "Epidemiology of genital prolapse: observations from the Oxford Family Planning Association Study," *BJOG An Int. J. Obstet. Gynaecol.*, vol. 104, no. 5, pp. 579–585, 1997.

[71] E. S. Lukacz, J. M. Lawrence, R. Contreras, C. W. Nager, and K. M. Luber, "Parity, mode of delivery, and pelvic floor disorders," *Obstet. Gynecol.*, vol. 107, no. 6, pp. 1253–1260, 2006.

[72] J. O. L. DeLancey, R. Kearney, Q. Chou, S. Speights, and S. Binno, "The appearance of levator ani muscle abnormalities in magnetic resonance images after vaginal delivery," *Obstet. Gynecol.*, vol. 101, no. 1, pp. 46–53, 2003.

[73] R. E. Nappi and M. Lachowsky, "Menopause and sexuality: prevalence of symptoms and impact on quality of life," *Maturitas*, vol. 63, no. 2, pp. 138–141, 2009.

[74] G.-D. Chen, R. H. Oliver, B. S. Leung, L.-Y. Lin, and J. Yeh, "Estrogen receptor α and β expression in the vaginal walls and uterosacral ligaments of premenopausal and postmenopausal women," *Fertil. Steril.*, vol. 71, no. 6, pp. 1099–1102, 1999.

[75] L. Pandit and J. G. Ouslander, "Postmenopausal vaginal atrophy and atrophic

vaginitis," *Am. J. Med. Sci.*, vol. 314, no. 4, pp. 228–231, 1997.

[76] I. Milsom and U. Molander, "Urogenital ageing," *Br. Menopause Soc. J.*, vol. 4, no. 4, pp. 151–156, 1998.

[77] J. B. Gebhart *et al.*, "Expression of estrogen receptor isoforms α and β messenger RNA in vaginal tissue of premenopausal and postmenopausal women," *Am. J. Obstet. Gynecol.*, vol. 185, no. 6, pp. 1325–1331, 2001.

[78] D. Robinson and L. D. Cardozo, "The role of estrogens in female lower urinary tract dysfunction," *Urology*, vol. 62, no. 4, pp. 45–51, 2003.

[79] K. Aikawa, T. Sugino, S. Matsumoto, P. Chichester, C. Whitbeck, and R. M. Levin, "The effect of ovariectomy and estradiol on rabbit bladder smooth muscle contraction and morphology," *J. Urol.*, vol. 170, no. 2, pp. 634–637, 2003.

[80] M. L. Mokrzycki, K. Mittal, S. W. Smilen, A. N. Blechman, R. F. Porges, and R. I. Demopolous, "Estrogen and progesterone receptors in the uterosacral ligament," *Obstet. Gynecol.*, vol. 90, no. 3, pp. 402–404, 1997.

[81] L. Peltonen and K. Kainulainen, "Elucidation of the gene defect in Marfan syndrome Success by two complementary research strategies," *FEBS Lett.*, vol. 307, no. 1, pp. 116–121, 1992.

[82] B. Steinmann, P. M. Royce, and A. Superti-Furga, "The Ehlers-Danlos Syndrome," *Connective Tissue and Its Heritable Disorders*. pp. 431–523, 10-May-2002.

[83] M. E. Carley and J. Schaffer, "Urinary incontinence and pelvic organ prolapse in women with Marfan or Ehlers-Danlos syndrome," *Am. J. Obstet. Gynecol.*, vol. 182, no. 5, pp. 1021–1023, 2000.

[84] K. A. Connell, M. K. Guess, H. Chen, V. Andikyan, R. Bercik, and H. S. Taylor, "HOXA11 is critical for development and maintenance of uterosacral ligaments and deficient in pelvic prolapse," *J. Clin. Invest.*, vol. 118, no. 3, pp. 1050–1055, Mar. 2008.

[85] L. Kushner, M. Mathrubutham, T. Burney, R. Greenwald, and G. Badlani, "Excretion of collagen derived peptides is increased in women with stress urinary incontinence," *Neurourol. Urodyn.*, vol. 23, no. 3, pp. 198–203, 2004.

[86] B. H. Chen, Y. Wen, H. Li, and M. L. Polan, "Collagen metabolism and turnover in women with stress urinary incontience and pelvic prolapse," *Int. Urogynecol. J.*, vol. 13, no. 2, pp. 80–87, 2002.

[87] S. R. Jackson, S. D. Eckford, P. Abrams, N. C. Avery, J. F. Tarlton, and A. J. Bailey, "Changes in metabolism of collagen in genitourinary prolapse," *Lancet*, vol. 347, no.

9016, pp. 1658–1661, 1996.

[88] B. Gabriel *et al.*, “Uterosacral ligament in postmenopausal women with or without pelvic organ prolapse,” *Int. Urogynecol. J.*, vol. 16, no. 6, pp. 475–479, 2005.

[89] M. H. Kerkhof, L. Hendriks, and H. A. M. Brölmann, “Changes in connective tissue in patients with pelvic organ prolapse—a review of the current literature,” *Int. Urogynecol. J.*, vol. 20, no. 4, pp. 461–474, 2009.

[90] P. A. Moalli, S. H. Shand, H. M. Zyczynski, S. C. Gordy, and L. A. Meyn, “Remodeling of vaginal connective tissue in patients with prolapse,” *Obstet. Gynecol.*, vol. 106, no. 5 Part 1, pp. 953–963, 2005.

[91] R. Sferra *et al.*, “Neurovascular alterations of muscularis propria in the human anterior vaginal wall in pelvic organ prolapse,” *J. Anat.*, vol. 235, no. 2, pp. 281–288, 2019.

[92] A. Vetuschi *et al.*, “Changes in muscularis propria of anterior vaginal wall in women with pelvic organ prolapse,” *Eur. J. Histochem. EJH*, vol. 60, no. 1, 2016.

[93] A. M. Ruiz-Zapata *et al.*, “Vaginal fibroblastic cells from women with pelvic organ prolapse produce matrices with increased stiffness and collagen content,” *Sci. Rep.*, vol. 6, no. 1, pp. 1–9, 2016.

[94] N. A. Okeahialam, K. Dworzynski, P. Jacklin, and D. McClurg, “Prevention and non-surgical management of pelvic floor dysfunction: summary of NICE guidance,” *bmj*, vol. 376, 2022.

[95] S. Hagen and D. Stark, “Conservative prevention and management of pelvic organ prolapse in women,” *Cochrane Database Syst. Rev.*, no. 12, 2011.

[96] R. Oliver, R. Thakar, and A. H. Sultan, “The history and usage of the vaginal pessary: a review,” *Eur. J. Obstet. Gynecol. Reprod. Biol.*, vol. 156, no. 2, pp. 125–130, 2011.

[97] B. E. Arias, B. Ridgeway, and M. D. Barber, “Complications of neglected vaginal pessaries: case presentation and literature review,” *Int. Urogynecol. J.*, vol. 19, no. 8, pp. 1173–1178, 2008.

[98] L.-A. M. Hanson, J. A. Schulz, C. G. Flood, B. Cooley, and F. Tam, “Vaginal pessaries in managing women with pelvic organ prolapse and urinary incontinence: patient characteristics and factors contributing to success,” *Int. Urogynecol. J.*, vol. 17, no. 2, pp. 155–159, 2006.

[99] C. Castelo-Branco, M. J. Cancelo, J. Villero, F. Nohales, and M. D. Juliá, “Management of post-menopausal vaginal atrophy and atrophic vaginitis,” *Maturitas*, vol. 52, pp. 46–52, 2005.

[100] T. Tyagi, M. Alarab, Y. Leong, S. Lye, and O. Shynlova, “Local oestrogen therapy

modulates extracellular matrix and immune response in the vaginal tissue of post-menopausal women with severe pelvic organ prolapse," *J. Cell. Mol. Med.*, vol. 23, no. 4, pp. 2907–2919, 2019.

[101] S. D. Kleeman and M. M. Karram, "The Tension-Free Vaginal Tape Procedure," *Urol. Clin.*, vol. 38, no. 1, pp. 39–45, 2011.

[102] J. C. Burch, "Urethrovaginal fixation to Cooper's ligament for correction of stress incontinence, cystocele, and prolapse," *Am. J. Obstet. Gynecol.*, vol. 81, no. 2, pp. 281–290, 1961.

[103] U. Ulmsten *et al.*, "A multicenter study of tension-free vaginal tape (TVT) for surgical treatment of stress urinary incontinence," *Int. Urogynecol. J.*, vol. 9, no. 4, pp. 210–213, 1998.

[104] T. M. Julian, "The efficacy of Marlex mesh in the repair of severe, recurrent vaginal prolapse of the anterior midvaginal wall," *Am. J. Obstet. Gynecol.*, vol. 175, no. 6, pp. 1472–1475, 1996.

[105] C. on G. Practice, "Committee opinion no. 513: vaginal placement of synthetic mesh for pelvic organ prolapse," *Obs. Gynecol*, vol. 118, no. 6, pp. 1459–1464, 2011.

[106] P. Dällenbach, "To mesh or not to mesh: a review of pelvic organ reconstructive surgery," *Int. J. Womens. Health*, vol. 7, pp. 331–343, Apr. 2015.

[107] A. J. Wein, "Re: FDA safety communication: Update on serious complications associated with transvaginal placement of surgical mesh for pelvic organ prolapse," *J. Urol.*, vol. 186, no. 6, pp. 2328–2330, 2011.

[108] N. Y. Siddiqui and A. L. Edenfield, "Clinical challenges in the management of vaginal prolapse," *Int. J. Womens. Health*, vol. 6, p. 83, 2014.

[109] M. Llamas, "Bladder Sling Complications." Retrieved from Drugwatch: https://www. drugwatch. com/transvaginal-mesh …, 2020.

[110] M. Huebner, Y. Hsu, and D. E. Fenner, "The use of graft materials in vaginal pelvic floor surgery," *Int. J. Gynecol. Obstet.*, vol. 92, no. 3, pp. 279–288, 2006.

[111] P. K. Amid, "Classification of biomaterials and their related complications in abdominal wall hernia surgery," *Hernia*, vol. 1, no. 1, pp. 15–21, 1997.

[112] V. Sola, J. Pardo, P. Ricci, and E. Guiloff, "Tension free monofilament macropore polypropylene mesh (Gynemesh PS) in female genital prolapse repair," *Int. braz j urol*, vol. 32, no. 4, pp. 410–415, 2006.

[113] M. E. Falagas, S. Velakoulis, C. Iavazzo, and S. Athanasiou, "Mesh-related infections after pelvic organ prolapse repair surgery," *Eur. J. Obstet. Gynecol. Reprod. Biol.*, vol.

134, no. 2, pp. 147–156, 2007.

[114] P. P. Pott, M. L. R. Schwarz, R. Gundling, K. Nowak, P. Hohenberger, and E. D. Roessner, “Mechanical properties of mesh materials used for hernia repair and soft tissue augmentation,” 2012.

[115] F. Daneshgari, “Re: FDA Public Health Notification: Serious Complications Associated with Transvaginal Placement of Surgical Mesh in Repair of Pelvic Organ Prolapse and Stress Urinary Incontinence,” *Eur. Urol.*, vol. 55, no. 5, pp. 1235–1236, 2009.

[116] F. D. A. FDA, “Safety Communication: UPDATE on Serious Complications Associated With Transvaginal Placement of Surgical Mesh for Pelvic Organ Prolapse,” *AlertsandNotices/ucm262435. htm*, 2011.

[117] R. Lombardo, F. C. Burkhard, and A. Tubaro, “European Association of Urology Urinary Incontinence Guidelines Panel Group. Re: association between the amount of vaginal mesh used with mesh erosions and repeated surgery after repairing pelvic organ prolapse and stress urinary incontinence,” *Eur Urol*, vol. 75, p. 196, 2018.

[118] N. Ng-Stollmann, C. Fünfgeld, B. Gabriel, and A. Niesel, “The international discussion and the new regulations concerning transvaginal mesh implants in pelvic organ prolapse surgery,” *Int. Urogynecol. J.*, vol. 31, no. 10, pp. 1997–2002, 2020.

[119] H. H. S. Food and Drug Administration, “Obstetrical and gynecological devices; reclassification of surgical instrumentation for use with urogynecologic surgical mesh. Final order,” *Fed. Regist.*, vol. 82, no. 4, pp. 1598–1603, 2017.

[120] S. A. Powers, L. K. Burleson, and J. L. Hannan, “Managing female pelvic floor disorders: a medical device review and appraisal,” *Interface Focus*, vol. 9, no. 4, p. 20190014, 2019.

[121] K. E. MORTON, D. Davies, and J. DEWHURST, “The use of the fasciocutaneous flap in vaginal reconstruction,” *BJOG An Int. J. Obstet. Gynaecol.*, vol. 93, no. 9, pp. 970–973, 1986.

[122] A. L. Merriman and M. J. Kennelly, “Biologic grafts for use in pelvic organ prolapse surgery: a contemporary review,” *Curr. Urol. Rep.*, vol. 21, no. 12, pp. 1–7, 2020.

[123] M. E. Karlovsky, A. A. Thakre, A. Rastinehad, L. Kushner, and G. H. Badlani, “Biomaterials for pelvic floor reconstruction,” *Urology*, vol. 66, no. 3, pp. 469–475, 2005.

[124] L. A. Yurteri-Kaplan and R. E. Gutman, “The use of biological materials in urogynecologic reconstruction: a systematic review,” *Plast. Reconstr. Surg.*, vol. 130,

no. 5S–2, pp. 242S-253S, 2012.

[125] Z.-L. Farmer, J. Domínguez-Robles, C. Mancinelli, E. Larrañeta, and D. A. Lamprou, "Urogynecological surgical mesh implants: New trends in materials, manufacturing and therapeutic approaches," *Int. J. Pharm.*, vol. 585, p. 119512, 2020.

[126] S. Roman Regueros *et al.*, "Acute in vivo response to an alternative implant for urogynecology," *Biomed Res. Int.*, vol. 2014, 2014.

[127] W. Zhao *et al.*, "Periurethral injection of autologous adipose-derived stem cells with controlled-release nerve growth factor for the treatment of stress urinary incontinence in a rat model," *Eur. Urol.*, vol. 59, no. 1, pp. 155–163, 2011.

[128] X. H. Zou *et al.*, "Mesenchymal stem cell seeded knitted silk sling for the treatment of stress urinary incontinence," *Biomaterials*, vol. 31, no. 18, pp. 4872–4879, 2010.

[129] D. Hachim, S. T. LoPresti, C. C. Yates, and B. N. Brown, "Shifts in macrophage phenotype at the biomaterial interface via IL-4 eluting coatings are associated with improved implant integration," *Biomaterials*, vol. 112, pp. 95–107, 2017.

[130] N. Mangır, A. J. Bullock, S. Roman, N. Osman, C. Chapple, and S. MacNeil, "Production of ascorbic acid releasing biomaterials for pelvic floor repair," *Acta Biomater.*, vol. 29, pp. 188–197, 2016.

[131] M. Boennelycke, S. Gras, and G. Lose, "Tissue engineering as a potential alternative or adjunct to surgical reconstruction in treating pelvic organ prolapse," *Int. Urogynecol. J.*, vol. 24, no. 5, pp. 741–747, 2013.

[132] J. Whooley *et al.*, "Stress urinary incontinence and pelvic organ prolapse: Biologic graft materials revisited," *Tissue Eng. Part B Rev.*, vol. 26, no. 5, pp. 475–483, 2020.

[133] M. Vashaghian, S. J. Zaat, T. H. Smit, and J. Roovers, "Biomimetic implants for pelvic floor repair," *Neurourol. Urodyn.*, vol. 37, no. 2, pp. 566–580, 2018.

[134] A. Mangera, A. J. Bullock, S. Roman, C. R. Chapple, and S. MacNeil, "Comparison of candidate scaffolds for tissue engineering for stress urinary incontinence and pelvic organ prolapse repair," *BJU Int.*, vol. 112, no. 5, pp. 674–685, Sep. 2013.

[135] S. Roman, A. Mangera, N. I. Osman, A. J. Bullock, C. R. Chapple, and S. MacNeil, "Developing a tissue engineered repair material for treatment of stress urinary incontinence and pelvic organ prolapse—which cell source?," *Neurourol. Urodyn.*, vol. 33, no. 5, pp. 531–537, 2014.

[136] N. I. Osman, S. Roman, A. J. Bullock, C. R. Chapple, and S. MacNeil, "The effect of ascorbic acid and fluid flow stimulation on the mechanical properties of a tissue engineered pelvic floor repair material," *Proc. Inst. Mech. Eng. Part H J. Eng. Med.*,

vol. 228, no. 9, pp. 867–875, 2014.

[137] N. Mangır, C. J. Hillary, C. R. Chapple, and S. MacNeil, “Oestradiol-releasing Biodegradable Mesh Stimulates Collagen Production and Angiogenesis: An Approach to Improving Biomaterial Integration in Pelvic Floor Repair,” *Eur. Urol. Focus*, vol. 5, no. 2, pp. 280–289, 2019.

[138] S. Shafaat, N. Mangir, S. R. Regureos, C. R. Chapple, and S. MacNeil, “Demonstration of improved tissue integration and angiogenesis with an elastic, estradiol releasing polyurethane material designed for use in pelvic floor repair,” *Neurourol. Urodyn.*, vol. 37, no. 2, 2018.

[139] S. Roman *et al.*, “Evaluating alternative materials for the treatment of stress urinary incontinence and pelvic organ prolapse: a comparison of the in vivo response to meshes implanted in rabbits,” *J. Urol.*, vol. 196, no. 1, pp. 261–269, 2016.

[140] Y. Peng, R. Khavari, N. A. Nakib, T. B. Boone, and Y. Zhang, “Assessment of urethral support using MRI-derived computational modeling of the female pelvis,” *Int. Urogynecol. J.*, vol. 27, no. 2, pp. 205–212, 2016.

[141] P. A. Moalli *et al.*, “A rat model to study the structural properties of the vagina and its supportive tissues,” *Am. J. Obstet. Gynecol.*, vol. 192, no. 1, pp. 80–88, 2005.

[142] D. Ulrich *et al.*, “Changes in pelvic organ prolapse mesh mechanical properties following implantation in rats,” *Am. J. Obstet. Gynecol.*, vol. 214, no. 2, pp. 260-e1, 2016.

[143] M. Peró *et al.*, “Rabbit as an animal model for the study of biological grafts in pelvic floor dysfunctions,” *Sci. Rep.*, vol. 11, no. 1, pp. 1–9, 2021.

[144] L. N. Otto, O. D. Slayden, A. L. Clark, and R. M. Brenner, “The rhesus macaque as an animal model for pelvic organ prolapse,” *Am. J. Obstet. Gynecol.*, vol. 186, no. 3, pp. 416–421, 2002.

[145] R. M. Shaffer, R. Liang, K. Knight, C. M. Carter-Brooks, S. Abramowitch, and P. A. Moalli, “Impact of polypropylene prolapse mesh on vaginal smooth muscle in rhesus macaque,” *Am. J. Obstet. Gynecol.*, vol. 221, no. 4, pp. 330-e1, 2019.

[146] A. C. Winter, “Prolapse of the vagina and cervix in ewes,” *Vet. Annu. (United Kingdom)*, 1996.

[147] S. Emmerson *et al.*, “Composite mesh design for delivery of autologous mesenchymal stem cells influences mesh integration, exposure and biocompatibility in an ovine model of pelvic organ prolapse,” *Biomaterials*, vol. 225, p. 119495, 2019.

[148] L. Hympanova *et al.*, “Assessment of electrospun and ultra-lightweight polypropylene

meshes in the sheep model for vaginal surgery," *Eur. Urol. Focus*, vol. 6, no. 1, pp. 190–198, 2020.

[149] S. D. Abramowitch, A. Feola, Z. Jallah, and P. A. Moalli, "Tissue mechanics, animal models, and pelvic organ prolapse: a review," *Eur. J. Obstet. Gynecol. Reprod. Biol.*, vol. 144, pp. S146–S158, 2009.

[150] T. I. Valdes, D. Kreutzer, and F. Moussy, "The chick chorioallantoic membrane as a novel in vivo model for the testing of biomaterials," *J. Biomed. Mater. Res. An Off. J. Soc. Biomater. Japanese Soc. Biomater. Aust. Soc. Biomater. Korean Soc. Biomater.*, vol. 62, no. 2, pp. 273–282, 2002.

[151] D. Ribatti, "The chick embryo chorioallantoic membrane (CAM) assay," *Reprod. Toxicol.*, vol. 70, pp. 97–101, 2017.

[152] N. Mangir, A. Raza, J. W. Haycock, C. Chapple, and S. Macneil, "An improved in vivo methodology to visualise tumour induced changes in vasculature using the chick chorionic allantoic membrane assay," *In Vivo (Brooklyn).*, vol. 32, no. 3, pp. 461–472, 2018.

[153] K. J. Stepp and M. D. Walters, "Anatomy of the lower urinary tract, rectum, and pelvic floor," in *Urogynecology and reconstructive pelvic surgery*, Elsevier, 2007, pp. 17–30.

[154] P. B. Pendergrass, C. A. Reeves, M. W. Belovicz, D. J. Molter, and J. H. White, "The shape and dimensions of the human vagina as seen in three-dimensional vinyl polysiloxane casts," *Gynecol. Obstet. Invest.*, vol. 42, no. 3, pp. 178–182, 1996.

[155] J. O. L. DeLancey, "Anatomie aspects of vaginal eversion after hysterectomy," *Am. J. Obstet. Gynecol.*, vol. 166, no. 6, pp. 1717–1728, 1992.

[156] C. Caneparo, D. Brownell, S. Chabaud, and S. Bolduc, "Genitourinary Tissue Engineering: Reconstruction and Research Models," *Bioengineering*, vol. 8, no. 7, p. 99, 2021.

[157] C. F. V. Smout and F. Jacoby, *Gynaecological and Obstetrical Anatomy and Functional Histology*. The Williams & Wilkins, 1943.

[158] D. H. Owen and D. F. Katz, "A vaginal fluid simulant," *Contraception*, vol. 59, no. 2, pp. 91–95, 1999.

[159] R. Bulla *et al.*, "Mannose-binding lectin is produced by vaginal epithelial cells and its level in the vaginal fluid is influenced by progesterone," *Mol. Immunol.*, vol. 48, no. 1–3, pp. 281–286, 2010.

[160] L. Brannon-Peppas, "Novel vaginal drug release applications," *Adv. Drug Deliv. Rev.*, vol. 11, no. 1–2, pp. 169–177, 1993.

[161] A. Fadiel *et al.*, “Ezrin is a key element in the human vagina,” *Maturitas*, vol. 60, no. 1, pp. 31–41, 2008.

[162] C. A. Squier, M. J. Mantz, P. M. Schlievert, and C. C. Davis, “Porcine vagina ex vivo as a model for studying permeability and pathogenesis in mucosa,” *J. Pharm. Sci.*, vol. 97, no. 1, pp. 9–21, 2008.

[163] G. Schaller, E. Lengyel, K. Pantel, W. Hardt, and D. Mischke, “Keratin expression reveals mosaic differentiation in vaginal epithelium,” *Am. J. Obstet. Gynecol.*, vol. 169, no. 6, pp. 1603–1607, 1993.

[164] D. L. Patton, S. S. Thwin, A. Meier, T. M. Hooton, A. E. Stapleton, and D. A. Eschenbach, “Epithelial cell layer thickness and immune cell populations in the normal human vagina at different stages of the menstrual cycle,” *Am. J. Obstet. Gynecol.*, vol. 183, no. 4, pp. 967–973, 2000.

[165] K. Nilsson, B. Risberg, and G. Heimer, “The vaginal epithelium in the postmenopause—cytology, histology and pH as methods of assessment,” *Maturitas*, vol. 21, no. 1, pp. 51–56, 1995.

[166] C. D. Blaskewicz, J. Pudney, and D. J. Anderson, “Structure and function of intercellular junctions in human cervical and vaginal mucosal epithelia,” *Biol. Reprod.*, vol. 85, no. 1, pp. 97–104, 2011.

[167] W. H. Organization, *AIDS epidemic update: December 2009*. WHO Regional Office Europe, 2010.

[168] A. M. Marchiando, W. V. Graham, and J. R. Turner, “Epithelial barriers in homeostasis and disease,” *Annu. Rev. Pathol. Mech. Dis.*, vol. 5, pp. 119–144, 2010.

[169] A. Jones, “Bacterial vaginosis: a review of treatment, recurrence, and disparities,” *J. Nurse Pract.*, vol. 15, no. 6, pp. 420–423, 2019.

[170] G. Sandri, S. Rossi, F. Ferrari, M. C. Bonferoni, and C. Caramella, “Strategies to improve systemic and local availability of drugs administered via vaginal route,” in *Enhancement in drug delivery 2007*, CRC Press, Boca Raton, 2007, pp. 441–470.

[171] R. K. Malcolm, S. D. McCullagh, R. J. Morrow, and A. D. Woolfson, “21 Vagina and Uterus as Drug-Absorbing Organs,” *Enhanc. drug Deliv.*, 2007.

[172] J. A. Fernández-Romero *et al.*, “Zinc acetate/carrageenan gels exhibit potent activity in vivo against high-dose herpes simplex virus 2 vaginal and rectal challenge,” *Antimicrob. Agents Chemother.*, vol. 56, no. 1, pp. 358–368, 2012.

[173] M. R. Neutra and P. A. Kozlowski, “Mucosal vaccines: the promise and the challenge,” *Nat. Rev. Immunol.*, vol. 6, no. 2, pp. 148–158, 2006.

[174] K. L. Vincent, G. Vargas, J. Wei, N. Bourne, and M. Motamedi, “Monitoring vaginal epithelial thickness changes noninvasively in sheep using optical coherence tomography,” *Am. J. Obstet. Gynecol.*, vol. 208, no. 4, pp. 282-e1, 2013.

[175] P. Bagnall and D. Rizzolo, “Bacterial vaginosis: A practical review,” *J. Am. Acad. PAs*, vol. 30, no. 12, pp. 15–21, 2017.

[176] F. Blostein, E. Levin-Sparenberg, J. Wagner, and B. Foxman, “Recurrent vulvovaginal candidiasis,” *Ann. Epidemiol.*, vol. 27, no. 9, pp. 575–582, 2017.

[177] P. Tanmahasamut, T. Jirasawas, S. Laiwejpithaya, C. Areeswate, C. Dangrat, and K. Silprasit, “Effect of estradiol vaginal gel on vaginal atrophy in postmenopausal women: A randomized double-blind controlled trial,” *J. Obstet. Gynaecol. Res.*, vol. 46, no. 8, pp. 1425–1435, 2020.

[178] A. C. of O. and Gynecologists, “Pelvic organ prolapse,” *Female Pelvic Med. Reconstr. Surg.*, vol. 25, no. 6, pp. 397–408, 2019.

[179] G.-E. Costin, E. Hill, J. Brown, and A. J. Clippinger, “Qualification of a non-animal vaginal irritation method admitted as nonclinical assessment model (NAM) in the Incubator Phase of the United States Food and Drug Administration (US FDA) Medical Devices Development Tool (MDDT),” *Toxicol. Vitr.*, vol. 62, p. 104680, 2020.

[180] S. L. Achilles, P. B. Shete, K. J. Whaley, T. R. Moench, and R. A. Cone, “Microbicide efficacy and toxicity tests in a mouse model for vaginal transmission of Chlamydia trachomatis,” *Sex. Transm. Dis.*, pp. 655–664, 2002.

[181] J. M. McCracken, G. A. Calderon, A. J. Robinson, C. N. Sullivan, E. Cosgriff-Hernandez, and J. C. E. Hakim, “Animal Models and Alternatives in Vaginal Research: a Comparative Review,” *Reprod. Sci.*, pp. 1–15, 2021.

[182] B. J. Catalone *et al.*, “Mouse model of cervicovaginal toxicity and inflammation for preclinical evaluation of topical vaginal microbicides,” *Antimicrob. Agents Chemother.*, vol. 48, no. 5, pp. 1837–1847, 2004.

[183] O. J. D’Cruz, S. H. Yiv, B. Waurzyniak, and F. M. Uckun, “Contraceptive efficacy and safety studies of a novel microemulsion-based lipophilic vaginal spermicide,” *Fertil. Steril.*, vol. 75, no. 1, pp. 115–124, 2001.

[184] R. Liang, K. Knight, A. Nolfi, S. Abramowitch, and P. A. Moalli, “Differential effects of selective estrogen receptor modulators on the vagina and its supportive tissues,” *Menopause*, vol. 23, no. 2, pp. 129–137, 2016.

[185] T. I. Montoya, P. A. Maldonado, J. F. Acevedo, and R. A. Word, “Effect of vaginal or

systemic estrogen on dynamics of collagen assembly in the rat vaginal wall," *Biol. Reprod.*, vol. 92, no. 2, pp. 41–43, 2015.

[186] J. Simon, L. Nachtigall, R. Gut, E. Lang, D. F. Archer, and W. Utian, "Effective treatment of vaginal atrophy with an ultra-low-dose estradiol vaginal tablet.," *Obstet. Gynecol.*, vol. 112, no. 5, pp. 1053–1060, 2008.

[187] C. Falconer, G. Ekman-Ordeberg, U. Ulmsten, G. Westergren-Thorsson, K. Barchan, and A. Malmström, "Changes in paraurethral connective tissue at menopause are counteracted by estrogen," *Maturitas*, vol. 24, no. 6, pp. 197–204, 1996.

[188] P. Eckstein, M. C. N. Jackson, N. Millman, and A. J. Sobrero, "Comparison of vaginal tolerance tests of spermicidal preparations in rabbits and monkeys," *Reproduction*, vol. 20, no. 1, pp. 85–93, 1969.

[189] D. L. Patton, Y. T. C. Sweeney, L. K. Rabe, and S. L. Hillier, "Rectal applications of nonoxynol-9 cause tissue disruption in a monkey model," *Sex. Transm. Dis.*, vol. 29, no. 10, pp. 581–587, 2002.

[190] N. Promadej-Lanier *et al.*, "Development and evaluation of a vaginal ring device for sustained delivery of HIV microbicides to non-human primates," *J. Med. Primatol.*, vol. 38, no. 4, pp. 263–271, 2009.

[191] O. J. D'cruz, D. Erbeck, and F. M. Uckun, "A study of the potential of the pig as a model for the vaginal irritancy of benzalkonium chloride in comparison to the nonirritant microbicide PHI-443 and the spermicide vanadocene dithiocarbamate," *Toxicol. Pathol.*, vol. 33, no. 4, pp. 465–476, 2005.

[192] A. D. van Eyk and P. van der Bijl, "Porcine vaginal mucosa as an in vitro permeability model for human vaginal mucosa," *Int. J. Pharm.*, vol. 305, no. 1–2, pp. 105–111, 2005.

[193] K. L. Vincent *et al.*, "High resolution imaging of epithelial injury in the sheep cervicovaginal tract: a promising model for testing safety of candidate microbicides," *Sex. Transm. Dis.*, vol. 36, no. 5, p. 312, 2009.

[194] J. A. Moss *et al.*, "Pharmacokinetics of a multipurpose pod-intravaginal ring simultaneously delivering five drugs in an ovine model," *Antimicrob. Agents Chemother.*, vol. 57, no. 8, pp. 3994–3997, 2013.

[195] J. D. S. Holt *et al.*, "The sheep as a model of preclinical safety and pharmacokinetic evaluations of candidate microbicides," *Antimicrob. Agents Chemother.*, vol. 59, no. 7, pp. 3761–3770, 2015.

[196] L. Hympanova *et al.*, "Morphological and functional changes in the vagina following

critical lifespan events in the ewe," *Gynecol. Obstet. Invest.*, vol. 84, no. 4, pp. 360–368, 2019.

[197] E. Adriaens and J. P. Remon, "Gastropods as an evaluation tool for screening the irritating potency of absorption enhancers and drugs," *Pharm. Res.*, vol. 16, no. 8, pp. 1240–1244, 1999.

[198] M. M. M. Dhondt, E. Adriaens, and J.-P. Remon, "The evaluation of the local tolerance of vaginal formulations, with or without nonoxynol-9, using the slug mucosal irritation test," *Sex. Transm. Dis.*, pp. 229–235, 2004.

[199] M. M. M. Dhondt, E. Adriaens, J. Van Roey, and J. P. Remon, "The evaluation of the local tolerance of vaginal formulations containing dapivirine using the Slug Mucosal Irritation test and the rabbit vaginal irritation test," *Eur. J. Pharm. Biopharm.*, vol. 60, no. 3, pp. 419–425, 2005.

[200] B. Rizk and E. Torres, "Biocompatibility and efficacy of an isotonic buffered gel for vaginal pH balancing," *Fertil. Steril.*, vol. 110, no. 4, p. e285, 2018.

[201] J. Das Neves and M. F. Bahia, "Gels as vaginal drug delivery systems," *Int. J. Pharm.*, vol. 318, no. 1–2, pp. 1–14, 2006.

[202] M. Balls and D. W. Straughan, "The three Rs of Russell & Burch and the testing of biological products.," *Dev. Biol. Stand.*, vol. 86, pp. 11–18, 1996.

[203] J. D. Sobel, R. Tchao, J. Bozzola, M. E. Levison, and D. Kaye, "Human vaginal epithelial multilayer tissue culture," *In Vitro*, vol. 15, no. 12, pp. 993–1000, 1979.

[204] F. C. Krebs *et al.*, "Sodium dodecyl sulfate and C31G as microbicidal alternatives to nonoxynol 9: comparative sensitivity of primary human vaginal keratinocytes," *Antimicrob. Agents Chemother.*, vol. 44, no. 7, pp. 1954–1960, 2000.

[205] G. I. GORODESKI, R. L. ECKERT, W. H. UTIAN, and E. A. RORKE, "Maintenance of in Vivo-Like Keratin Expression, Sex Steroid Responsiveness, and Estrogen Receptor Expression in Cultured Human Ectocervical Epithelial Cells*," *Endocrinology*, vol. 126, no. 1, pp. 399–406, Jan. 1990.

[206] I. S. Dixon and M. A. Stanley, "Immunofluorescent studies of human cervical epithelia in vivo and in vitro using antibodies against specific keratin components.," *Mol. Biol. Med.*, vol. 2, no. 1, pp. 37–51, 1984.

[207] G. I. Gorodeski, M. F. Romero, U. Hopfer, E. Rorke, W. H. Utian, and R. L. Eckert, "Human uterine cervical epithelial cells grown on permeable support–a new model for the study of differentiation," *Differentiation*, vol. 56, no. 1–2, pp. 107–118, 1994.

[208] N. Rajan *et al.*, "Characterization of an immortalized human vaginal epithelial cell

line," *J. Urol.*, vol. 163, no. 2, pp. 616–622, 2000.

[209] G. I. Gorodeski *et al.*, "Characterization of paracellular permeability in cultured human cervical epithelium: regulation by extracellular adenosine triphosphate," *J. Soc. Gynecol. Investig.*, vol. 1, no. 3, pp. 225–233, 1994.

[210] G. I. Gorodeski, "Estrogen increases the permeability of the cultured human cervical epithelium by modulating cell deformability," *Am. J. Physiol. Physiol.*, vol. 275, no. 3, pp. C888–C899, 1998.

[211] M. Kaminsky, M. M. Szivos, K. R. Brown, and D. A. Willigan, "Comparison of the sensitivity of the vaginal mucous membranes of the albino rabbit and laboratory rat to nonoxynoxynol-9," *Food Chem. Toxicol.*, vol. 23, no. 7, pp. 705–708, 1985.

[212] G. N. Milligan, K. L. Dudley, N. Bourne, A. Reece, and L. R. Stanberry, "Entry of Inflammatory Cells Into the Mouse Vagina Following Application of Candidate Microbicides: Comparison of Detergent-Based and Sulfated Polymer–Based Agents," *Sex. Transm. Dis.*, vol. 29, no. 10, pp. 597–605, 2002.

[213] F. C. Krebs *et al.*, "Comparative in vitro sensitivities of human immune cell lines, vaginal and cervical epithelial cell lines, and primary cells to candidate microbicides nonoxynol 9, C31G, and sodium dodecyl sulfate," *Antimicrob. Agents Chemother.*, vol. 46, no. 7, pp. 2292–2298, 2002.

[214] J. E. Cummins Jr *et al.*, "Preclinical testing of candidate topical microbicides for anti-human immunodeficiency virus type 1 activity and tissue toxicity in a human cervical explant culture," *Antimicrob. Agents Chemother.*, vol. 51, no. 5, pp. 1770–1779, 2007.

[215] C. G. Fink, G. H. Thomas, J. M. Allen, and J. A. Jordan, "Metaplasia in endocervical tissue maintained in organ culture–an experimental model," *BJOG An Int. J. Obstet. Gynaecol.*, vol. 80, no. 2, pp. 169–175, 1973.

[216] M. E. R. O'Brien *et al.*, "Glycoprotein patterns in normal and malignant cervical tissue," *Cancer Lett.*, vol. 58, no. 3, pp. 247–254, 1991.

[217] Q. Hu *et al.*, "Blockade of attachment and fusion receptors inhibits HIV-1 infection of human cervical tissue," *J. Exp. Med.*, vol. 199, no. 8, pp. 1065–1075, 2004.

[218] N. Richardson-Harman *et al.*, "Multisite comparison of anti-human immunodeficiency virus microbicide activity in explant assays using a novel endpoint analysis," *J. Clin. Microbiol.*, vol. 47, no. 11, pp. 3530–3539, 2009.

[219] P. Gupta *et al.*, "Use of frozen–thawed cervical tissues in the organ culture system to measure anti-HIV activities of candidate microbicides," *AIDS Res. Hum. Retroviruses*, vol. 22, no. 5, pp. 419–424, 2006.

[220] R. M. Machado, A. Palmeira-de-Oliveira, L. Breitenfeld, J. Martinez-de-Oliveira, and R. Palmeira-de-Oliveira, "Optimization and Application of In Vitro and Ex Vivo Models for Vaginal Semisolids Safety Evaluation," *J. Pharm. Sci.*, vol. 108, no. 10, pp. 3289–3301, 2019.

[221] D. J. Anderson, J. Pudney, and D. J. Schust, "Caveats associated with the use of human cervical tissue for HIV and microbicide research," *AIDS*, vol. 24, no. 1, p. 1, 2010.

[222] C. C. Hsu, J. Y. Park, N. F. H. Ho, W. I. Higuchi, and J. L. Fox, "Topical vaginal drug delivery I: effect of the estrous cycle on vaginal membrane permeability and diffusivity of vidarabine in mice," *J. Pharm. Sci.*, vol. 72, no. 6, pp. 674–680, 1983.

[223] N. F. H. Ho *et al.*, "Systems approach to vaginal delivery of drugs III: Simulation studies interfacing steroid release from silicone matrix and vaginal absorption in rabbits," *J. Pharm. Sci.*, vol. 65, no. 11, pp. 1578–1585, 1976.

[224] K. Berginc, N. Škalko-Basnet, P. Basnet, and A. Kristl, "Development and evaluation of an in vitro vaginal model for assessment of drug's biopharmaceutical properties: Curcumin," *AAPS pharmscitech*, vol. 13, no. 4, pp. 1045–1053, 2012.

[225] I. O. C. Thompson, P. Van der Bijl, C. W. Van Wyk, and A. D. Van Eyk, "A comparative light-microscopic, electron-microscopic and chemical study of human vaginal and buccal epithelium," *Arch. Oral Biol.*, vol. 46, no. 12, pp. 1091–1098, 2001.

[226] B. E. Hjelm, A. N. Berta, C. A. Nickerson, C. J. Arntzen, and M. M. Herbst-Kralovetz, "Development and Characterization of a Three-Dimensional Organotypic Human Vaginal Epithelial Cell Model1," *Biol. Reprod.*, vol. 82, no. 3, pp. 617–627, Mar. 2010.

[227] J. Barrila *et al.*, "Organotypic 3D cell culture models: using the rotating wall vessel to study host–pathogen interactions," *Nat. Rev. Microbiol.*, vol. 8, no. 11, pp. 791–801, 2010.

[228] "EpiVaginal in vitro 3D Tissues | MatTek Life Sciences." [Online]. Available: https://www.mattek.com/products/epivaginal/. [Accessed: 07-Jun-2020].

[229] S. Ayehunie, C. Cannon, K. LaRosa, J. Pudney, D. J. Anderson, and M. Klausner, "Development of an in vitro alternative assay method for vaginal irritation," *Toxicology*, vol. 279, no. 1–3, pp. 130–138, 2011.

[230] A. Machado and J. das Neves, "Tissue-based in vitro and ex vivo models for vaginal permeability studies," *Concepts Model. Drug Permeability Stud.*, pp. 273–308, 2016.

[231] S. Ayehunie, C. Cannon, S. Lamore, M. Klausner, and J. Kubilus, "EpiVaginal™ Human Vaginal-Ectocervical Tissue Models for Irritation and HIV-1 Studies," *Fertil. Steril.*, vol. 84, p. S60, 2005.

[232] A. Seyoum, K. Joseph, H. Patrick, C. Chris, L. Sarah, and K. Mitchell, "Irritation testing of contraceptive and feminine-care products using epivaginal™, an in vitro human vaginal–ectocervical tissue model," *Toxicol. Lett.*, no. 164, p. S224, 2006.

[233] K. Noguchi, K. Tsukumi, and T. Urano, "Qualitative and quantitative differences in normal vaginal flora of conventionally reared mice, rats, hamsters, rabbits, and dogs," *Comp. Med.*, vol. 53, no. 4, pp. 404–412, 2003.

[234] K. J. Looker, A. S. Magaret, K. M. E. Turner, P. Vickerman, S. L. Gottlieb, and L. M. Newman, "Global estimates of prevalent and incident herpes simplex virus type 2 infections in 2012," *PLoS One*, vol. 10, no. 1, p. e114989, 2015.

[235] E. A. Aisenbrey and W. L. Murphy, "Synthetic alternatives to Matrigel," *Nat. Rev. Mater.*, vol. 5, no. 7, pp. 539–551, 2020.

[236] C. Grammen, P. Augustijns, and J. Brouwers, "In vitro profiling of the vaginal permeation potential of anti-HIV microbicides and the influence of formulation excipients," *Antiviral Res.*, vol. 96, no. 2, pp. 226–233, 2012.

[237] G. I. GORODESKI, R. L. ECKERT, W. H. UTIAN, L. SHEEAN, and E. A. RORKE, "Cultured human ectocervical epithelial cell differentiation is regulated by the combined direct actions of sex steroids, glucocorticoids, and retinoids," *J. Clin. Endocrinol. Metab.*, vol. 70, no. 6, pp. 1624–1630, 1990.

[238] M. Cremel *et al.*, "Characterization of CCL20 secretion by human epithelial vaginal cells: involvement in Langerhans cell precursor attraction," *J. Leukoc. Biol.*, vol. 78, no. 1, pp. 158–166, 2005.

[239] A. D. Van Eyk and P. Van der Bijl, "The culture of human buccal and vaginal epithelial cells for permeability studies.," *SADJ J. South African Dent. Assoc. Tydskr. van die Suid-afrikaanse Tandheelkd. Ver.*, vol. 53, no. 11, pp. 497–503, 1998.

[240] M. R. Clark, T. J. McCormick, G. F. Doncel, and D. R. Friend, "Preclinical evaluation of UC781 microbicide vaginal drug delivery," *Drug Deliv. Transl. Res.*, vol. 1, no. 2, pp. 175–182, 2011.

[241] O. J. D'Cruz and F. M. Uckun, "Mucosal safety of PHI-443 and stampidine as a combination microbicide to prevent genital transmission of HIV-1," *Fertil. Steril.*, vol. 88, no. 4, pp. 1197–1206, 2007.

[242] A. S. Ham *et al.*, "Development of a combination microbicide gel formulation

containing IQP-0528 and tenofovir for the prevention of HIV infection," *J. Pharm. Sci.*, vol. 101, no. 4, pp. 1423–1435, 2012.

[243] M. Kaur *et al.*, "Engineering a degradable polyurethane intravaginal ring for sustained delivery of dapivirine," *Drug Deliv. Transl. Res.*, vol. 1, no. 3, p. 223, 2011.

[244] M. R. Clark, M. M. Peet, S. Davis, G. F. Doncel, and D. R. Friend, "Evaluation of rapidly disintegrating vaginal tablets of tenofovir, emtricitabine and their combination for HIV-1 prevention," *Pharmaceutics*, vol. 6, no. 4, pp. 616–631, 2014.

[245] H. Fatakdawala and S. A. Uhland, "Hydrogen peroxide mediated transvaginal drug delivery," *Int. J. Pharm.*, vol. 409, no. 1–2, pp. 121–127, 2011.

[246] C. T. Alves, X.-Q. Wei, S. Silva, J. Azeredo, M. Henriques, and D. W. Williams, "Candida albicans promotes invasion and colonisation of Candida glabrata in a reconstituted human vaginal epithelium," *J. Infect.*, vol. 69, no. 4, pp. 396–407, 2014.

[247] S. K. McQuillan and S. R. Grover, "Dilation and surgical management in vaginal agenesis: a systematic review," *Int. Urogynecol. J.*, vol. 25, no. 3, pp. 299–311, 2014.

[248] W. H. Hendren and A. Atala, "Use of bowel for vaginal reconstruction," *J. Urol.*, vol. 152, no. 2, pp. 752–755, 1994.

[249] A.-M. Amies Oelschlager, A. Kirby, and L. Breech, "Evaluation and management of vaginoplasty complications," *Curr. Opin. Obstet. Gynecol.*, vol. 29, no. 5, pp. 316–321, 2017.

[250] W. C. Lin, C. Y. Y. Chang, Y. Y. Shen, and H. D. Tsai, "Use of autologous buccal mucosa for vaginoplasty: a study of eight cases," *Hum. Reprod.*, vol. 18, no. 3, pp. 604–607, 2003.

[251] J. K. Parsons, S. L. Gearhart, and J. P. Gearhart, "Vaginal reconstruction utilizing sigmoid colon: complications and long-term results," *J. Pediatr. Surg.*, vol. 37, no. 4, pp. 629–633, 2002.

[252] A. M. Raya-Rivera *et al.*, "Tissue-engineered autologous vaginal organs in patients: a pilot cohort study," *Lancet*, vol. 384, no. 9940, pp. 329–336, 2014.

[253] H. Orabi, I. Saba, A. Rousseau, and S. Bolduc, "Novel three-dimensional autologous tissue-engineered vaginal tissues using the self-assembly technique," *Transl. Res.*, vol. 180, pp. 22–36, 2017.

[254] S. F. Badylak, "Decellularized Allogeneic and Xenogeneic Tissue as a Bioscaffold for Regenerative Medicine: Factors that Influence the Host Response," *Ann. Biomed. Eng.*, vol. 42, no. 7, pp. 1517–1527, 2014.

[255] S. F. Badylak, "Xenogeneic extracellular matrix as a scaffold for tissue

reconstruction," *Transpl. Immunol.*, vol. 12, no. 3, pp. 367–377, 2004.

[256] T. W. Gilbert, T. L. Sellaro, and S. F. Badylak, "Decellularization of tissues and organs," *Biomaterials*, vol. 27, no. 19, pp. 3675–3683, 2006.

[257] M. Parmaksiz, A. E. Elcin, and Y. M. Elcin, "Decellularization of bovine small intestinal submucosa and its use for the healing of a critical-sized full-thickness skin defect, alone and in combination with stem cells, in a small rodent model," *J. Tissue Eng. Regen. Med.*, vol. 11, no. 6, pp. 1754–1765, Jun. 2017.

[258] S. L. Voytik-Harbin, A. O. Brightman, M. R. Kraine, B. Waisner, and S. F. Badylak, "Identification of extractable growth factors from small intestinal submucosa," *J. Cell. Biochem.*, vol. 67, no. 4, pp. 478–491, Dec. 1997.

[259] C. A. McDevitt, G. M. Wildey, and R. M. Cutrone, "Transforming growth factor-β1 in a sterilized tissue derived from the pig small intestine submucosa," *J. Biomed. Mater. Res. Part A*, vol. 67A, no. 2, pp. 637–640, Nov. 2003.

[260] S. F. Badylak *et al.*, "The use of xenogeneic small intestinal submucosa as a biomaterial for Achille's tendon repair in a dog model," *J. Biomed. Mater. Res.*, vol. 29, no. 8, pp. 977–985, Aug. 1995.

[261] S. F. Badylak, R. Record, K. Lindberg, J. Hodde, and K. Park, "Small intestinal submucosa: a substrate for in vitro cell growth," *J. Biomater. Sci. Polym. Ed.*, vol. 9, no. 8, pp. 863–878, Jan. 1998.

[262] H. C. Ott *et al.*, "Perfusion-decellularized matrix: using nature's platform to engineer a bioartificial heart," *Nat. Med.*, vol. 14, no. 2, pp. 213–221, 2008.

[263] J. J. Song and H. C. Ott, "Organ engineering based on decellularized matrix scaffolds," *Trends Mol. Med.*, vol. 17, no. 8, pp. 424–432, 2011.

[264] R.-N. Chen, H.-O. Ho, Y.-T. Tsai, and M.-T. Sheu, "Process development of an acellular dermal matrix (ADM) for biomedical applications," *Biomaterials*, vol. 25, no. 13, pp. 2679–2686, 2004.

[265] C. A. Harrison *et al.*, "Use of an in Vitro Model of Tissue-Engineered Skin to Investigate the Mechanism of Skin Graft Contraction," *Tissue Eng.*, vol. 12, no. 11, pp. 3119–3133, Nov. 2006.

[266] F. Chen, J. J. Yoo, and A. Atala, "Acellular collagen matrix as a possible 'off the shelf' biomaterial for urethral repair," *Urology*, vol. 54, no. 3, pp. 407–410, 1999.

[267] B.-S. Kim, J. J. Yoo, and A. Atala, "Peripheral nerve regeneration using acellular nerve grafts," *J. Biomed. Mater. Res. Part A*, vol. 68A, no. 2, pp. 201–209, Feb. 2004.

[268] L. E. Flynn, "The use of decellularized adipose tissue to provide an inductive

microenvironment for the adipogenic differentiation of human adipose-derived stem cells," *Biomaterials*, vol. 31, no. 17, pp. 4715–4724, 2010.

[269] J. Hülsmann *et al.*, "Transplantation material bovine pericardium: biomechanical and immunogenic characteristics after decellularization vs. glutaraldehyde-fixing," *Xenotransplantation*, vol. 19, no. 5, pp. 286–297, Sep. 2012.

[270] J. S. Cartmell and M. G. Dunn, "Effect of chemical treatments on tendon cellularity and mechanical properties," *J. Biomed. Mater. Res.*, vol. 49, no. 1, pp. 134–140, Jan. 2000.

[271] M. Parmaksiz, A. Dogan, S. Odabas, A. E. Elçin, and Y. M. Elçin, "Clinical applications of decellularized extracellular matrices for tissue engineering and regenerative medicine," *Biomed. Mater.*, vol. 11, no. 2, p. 22003, 2016.

[272] S. Nagata, R. Hanayama, and K. Kawane, "Autoimmunity and the Clearance of Dead Cells," *Cell*, vol. 140, no. 5, pp. 619–630, 2010.

[273] B. N. Brown, J. E. Valentin, A. M. Stewart-Akers, G. P. McCabe, and S. F. Badylak, "Macrophage phenotype and remodeling outcomes in response to biologic scaffolds with and without a cellular component," *Biomaterials*, vol. 30, no. 8, pp. 1482–1491, 2009.

[274] P. M. Crapo, T. W. Gilbert, and S. F. Badylak, "An overview of tissue and whole organ decellularization processes," *Biomaterials*, vol. 32, no. 12, pp. 3233–3243, 2011.

[275] J.-K. Zhang *et al.*, "A new material for tissue engineered vagina reconstruction: Acellular porcine vagina matrix," *J. Biomed. Mater. Res. Part A*, vol. 105, no. 7, pp. 1949–1959, Jul. 2017.

[276] J. Kapuściński and B. Skoczylas, "Fluorescent complexes of DNA with DAPI 4′,6-diamidine-2-phenyl indole 2HCl or DCI 4′,6-dicarboxyamide-2-pnenyl indole," *Nucleic Acids Res.*, vol. 5, no. 10, pp. 3775–3800, Oct. 1978.

[277] R. W. Grauss, M. G. Hazekamp, F. Oppenhuizen, C. J. van Munsteren, A. C. Gittenberger-de Groot, and M. C. DeRuiter, "Histological evaluation of decellularised porcine aortic valves: matrix changes due to different decellularisation methods☆," *Eur. J. Cardio-Thoracic Surg.*, vol. 27, no. 4, pp. 566–571, Apr. 2005.

[278] B. Mendoza-Novelo *et al.*, "Decellularization of pericardial tissue and its impact on tensile viscoelasticity and glycosaminoglycan content," *Acta Biomater.*, vol. 7, no. 3, pp. 1241–1248, 2011.

[279] K. H. Hussein *et al.*, "Sterilization using Electrolyzed Water Highly Retains the

Biological Properties in Tissue-Engineered Porcine Liver Scaffold," *Int. J. Artif. Organs*, vol. 36, no. 11, pp. 781–792, Feb. 2013.

[280] D. O. Freytes, R. M. Stoner, and S. F. Badylak, "Uniaxial and biaxial properties of terminally sterilized porcine urinary bladder matrix scaffolds," *J. Biomed. Mater. Res. Part B Appl. Biomater.*, vol. 84B, no. 2, pp. 408–414, Feb. 2008.

[281] D. A. Taylor, L. C. Sampaio, Z. Ferdous, A. S. Gobin, and L. J. Taite, "Decellularized matrices in regenerative medicine," *Acta Biomater.*, vol. 74, pp. 74–89, 2018.

[282] R. Jackson, R. P. N. Hilson, A. R. Roe, N. Perkins, C. Heuer, and D. M. West, "Epidemiology of vaginal prolapse in mixed-age ewes in New Zealand," *N. Z. Vet. J.*, vol. 62, no. 6, pp. 328–337, 2014.

[283] I. Urbankova *et al.*, "Comparative anatomy of the ovine and female pelvis," *Gynecol. Obstet. Invest.*, vol. 82, no. 6, pp. 582–591, 2017.

[284] I. O. Asencio, S. Mittar, C. Sherborne, A. Raza, F. Claeyssens, and S. MacNeil, "A methodology for the production of microfabricated electrospun membranes for the creation of new skin regeneration models," *J. Tissue Eng.*, vol. 9, p. 2041731418799851, Jan. 2018.

[285] J. G. Rheinwatd and H. Green, "Seria cultivation of strains of human epidemal keratinocytes: the formation keratinizin colonies from single cell is," *Cell*, vol. 6, no. 3, pp. 331–343, 1975.

[286] C. E. Skala *et al.*, "Isolation of fibroblasts for coating of meshes for reconstructive surgery: differences between mesh types," *Regen. Med.*, vol. 4, no. 2, pp. 197–204, Mar. 2009.

[287] A. T. Feldman and D. Wolfe, "Tissue processing and hematoxylin and eosin staining," in *Histopathology*, Springer, 2014, pp. 31–43.

[288] H. Puchtler, F. S. Waldrop, and L. S. Valentine, "Polarization microscopic studies of connective tissue stained with picro-sirius red FBA," *Beitr. Pathol.*, vol. 150, no. 2, pp. 174–187, 1973.

[289] L. C. U. Junqueira, G. Bignolas, and R. R. Brentani, "Picrosirius staining plus polarization microscopy, a specific method for collagen detection in tissue sections," *Histochem. J.*, vol. 11, no. 4, pp. 447–455, 1979.

[290] C. E. Gagna *et al.*, "Novel DNA staining method and processing technique for the quantification of undamaged double-stranded DNA in epidermal tissue sections by PicoGreen probe staining and microspectrophotometry," *J. Histochem. Cytochem.*, vol. 55, no. 10, pp. 999–1014, 2007.

[291] M. C. Leinung, P. J. Feustel, and J. Joseph, “Hormonal treatment of transgender women with oral estradiol,” *Transgender Heal.*, vol. 3, no. 1, pp. 74–81, 2018.

[292] J.-C. Grivel and L. Margolis, “Use of human tissue explants to study human infectious agents,” *Nat. Protoc.*, vol. 4, no. 2, pp. 256–269, 2009.

[293] P. S. Cooke *et al.*, “Stromal estrogen receptors mediate mitogenic effects of estradiol on uterine epithelium,” *Proc. Natl. Acad. Sci.*, vol. 94, no. 12, pp. 6535–6540, 1997.

[294] G. R. Cunha, P. S. Cooke, and T. Kurita, “Role of stromal-epithelial interactions in hormonal responses,” *Arch. Histol. Cytol.*, vol. 67, no. 5, pp. 417–434, 2004.

[295] T. Iguchi, F. D. Uchima, P. L. Ostrander, and H. A. Bern, “Growth of normal mouse vaginal epithelial cells in and on collagen gels,” *Proc. Natl. Acad. Sci.*, vol. 80, no. 12, pp. 3743–3747, 1983.

[296] P. S. Cooke, F. D. Uchima, D. K. Fujii, H. A. Bern, and G. R. Cunha, “Restoration of normal morphology and estrogen responsiveness in cultured vaginal and uterine epithelia transplanted with stroma,” *Proc. Natl. Acad. Sci.*, vol. 83, no. 7, pp. 2109–2113, 1986.

[297] R. Takashina *et al.*, “Stratification of mouse vaginal epithelium 2. Identification of factors inducing stratification,” *Biol. Reprod.*, vol. 99, no. 4, pp. 727–734, 2018.

[298] S. S. Patnaik *et al.*, “Biomechanical characterization of sheep vaginal wall tissue: a potential application in human pelvic floor disorders,” in *Summer Bioengineering Conference*, 2012, vol. 44809, pp. 1193–1194.

[299] M. Endo *et al.*, “Cross-linked xenogenic collagen implantation in the sheep model for vaginal surgery,” *Gynecol. Surg.*, vol. 12, no. 2, pp. 113–122, 2015.

[300] N. Young *et al.*, “Vaginal wall weakness in parous ewes: a potential preclinical model of pelvic organ prolapse,” *Int. Urogynecol. J.*, vol. 28, no. 7, pp. 999–1004, 2017.

[301] M. G. Mori da Cunha, K. Mackova, L. H. Hympanova, M. A. T. Bortolini, and J. Deprest, “Animal models for pelvic organ prolapse: systematic review,” *Int. Urogynecol. J.*, vol. 32, no. 6, pp. 1331–1344, 2021.

[302] T. Hoshiba, H. Lu, N. Kawazoe, and G. Chen, “Decellularized matrices for tissue engineering,” *Expert Opin. Biol. Ther.*, vol. 10, pp. 1717–1728, Dec. 2010.

[303] R. Guruswamy Damodaran and P. Vermette, “Tissue and organ decellularization in regenerative medicine,” *Biotechnol. Prog.*, vol. 34, no. 6, pp. 1494–1505, Nov. 2018.

[304] Y. Wang, H. Schellenberg, V. Walhorn, K. Toensing, and D. Anselmetti, “Binding mechanism of fluorescent dyes to DNA characterized by magnetic tweezers,” *Mater. Today Proc.*, vol. 4, pp. S218–S225, 2017.

[305] V. L. Singer, L. J. Jones, S. T. Yue, and R. P. Haugland, “Characterization of PicoGreen reagent and development of a fluorescence-based solution assay for double-stranded DNA quantitation,” *Anal. Biochem.*, vol. 249, no. 2, pp. 228–238, 1997.

[306] “SkinEthic HVE Human Vaginal Epithelium.” [Online]. Available: https://www.episkin.com/HVE-Vaginal-Epithelium. [Accessed: 05-Oct-2021].

[307] M. Schweinlin *et al.*, “Development of an advanced primary human in vitro model of the small intestine,” *Tissue Eng. Part C Methods*, vol. 22, no. 9, pp. 873–883, 2016.

[308] V. Cattan *et al.*, “Mechanical stimuli-induced urothelial differentiation in a human tissue-engineered tubular genitourinary graft,” *Eur. Urol.*, vol. 60, no. 6, pp. 1291–1298, 2011.

[309] D. L. Buchanan, T. Kurita, J. A. Taylor, D. B. Lubahn, G. R. Cunha, and P. S. Cooke, “Role of stromal and epithelial estrogen receptors in vaginal epithelial proliferation, stratification, and cornification,” *Endocrinology*, vol. 139, no. 10, pp. 4345–4352, 1998.

[310] M. A. Pessina, R. F. Hoyt Jr, I. Goldstein, and A. M. Traish, “Differential effects of estradiol, progesterone, and testosterone on vaginal structural integrity,” *Endocrinology*, vol. 147, no. 1, pp. 61–69, 2006.

[311] P.-S. Tsai, F.-D. A. Uchima, S. T. Hamamoto, and H. A. Bern, “Proliferation and differentiation of prepubertal mouse vaginal epithelial cells in vitro and the specificity of estrogen-induced growth retardation,” *Vitr. Cell. Dev. Biol.*, vol. 27, no. 6, pp. 461–468, 1991.

[312] T. Scholzen and J. Gerdes, “The Ki-67 protein: from the known and the unknown,” *J. Cell. Physiol.*, vol. 182, no. 3, pp. 311–322, 2000.

[313] F. C. Geyer, D. N. Rodrigues, B. Weigelt, and J. S. Reis-Filho, “Molecular classification of estrogen receptor-positive/luminal breast cancers,” *Adv. Anat. Pathol.*, vol. 19, no. 1, pp. 39–53, 2012.

[314] M. Baldassarre *et al.*, “Effects of long-term high dose testosterone administration on vaginal epithelium structure and estrogen receptor-α and-β expression of young women,” *Int. J. Impot. Res.*, vol. 25, no. 5, pp. 172–177, 2013.

[315] P. A. Coulombe and M. B. Omary, “‘Hard’and ‘soft’principles defining the structure, function and regulation of keratin intermediate filaments,” *Curr. Opin. Cell Biol.*, vol. 14, no. 1, pp. 110–122, 2002.

[316] R. Moll, W. W. Franke, D. L. Schiller, B. Geiger, and R. Krepler, “The catalog of human cytokeratins: patterns of expression in normal epithelia, tumors and cultured

cells," *Cell*, vol. 31, no. 1, pp. 11–24, 1982.

[317] C. Carrilho, M. Alberto, L. Buane, and L. David, "Keratins 8, 10, 13, and 17 are useful markers in the diagnosis of human cervix carcinomas," *Hum. Pathol.*, vol. 35, no. 5, pp. 546–551, 2004.

[318] M. Michel *et al.*, "Keratin 19 as a biochemical marker of skin stem cells in vivo and in vitro: keratin 19 expressing cells are differentially localized in function of anatomic sites, and their number varies with donor age and culture stage," *J. Cell Sci.*, vol. 109, no. 5, pp. 1017–1028, 1996.

[319] P. G. Chu and L. M. Weiss, "Keratin expression in human tissues and neoplasms," *Histopathology*, vol. 40, no. 5, pp. 403–439, 2002.

[320] M. Huszar, O. Gigi-Leitner, R. Moll, W. W. Franke, and B. Geiger, "Monoclonal antibodies to various acidic (type I) cytokeratins of stratified epithelia: Selective markers for stratification and squamous cell carcinomas," *Differentiation*, vol. 31, no. 2, pp. 141–153, 1986.

[321] A. K. Zuk, X. Wen, S. Dilworth, D. Li, and L. Ghali, "Modeling and validating three dimensional human normal cervix and cervical cancer tissues in vitro," *J. Biomed. Res.*, vol. 31, no. 3, p. 240, 2017.

[322] I. Choi, L. J. Gudas, and B. S. Katzenellenbogen, "Regulation of keratin 19 gene expression by estrogen in human breast cancer cells and identification of the estrogen responsive gene region," *Mol. Cell. Endocrinol.*, vol. 164, no. 1–2, pp. 225–237, 2000.

[323] S.-H. Chung, S. Franceschi, and P. F. Lambert, "Estrogen and ERα: Culprits in cervical cancer?," *Trends Endocrinol. Metab.*, vol. 21, no. 8, pp. 504–511, 2010.

[324] T. J. Shaw and P. Martin, "Wound repair at a glance," *J. Cell Sci.*, vol. 122, no. 18, pp. 3209–3213, Sep. 2009.

[325] G. C. Gurtner, S. Werner, Y. Barrandon, and M. T. Longaker, "Wound repair and regeneration," *Nature*, vol. 453, no. 7193, pp. 314–321, 2008.

[326] A. C. de O. Gonzalez, T. F. Costa, Z. de A. Andrade, and A. R. A. P. Medrado, "Wound healing-A literature review," *An. Bras. Dermatol.*, vol. 91, pp. 614–620, 2016.

[327] S. Ud-Din, S. W. Volk, and A. Bayat, "Regenerative healing, scar-free healing and scar formation across the species: current concepts and future perspectives," *Exp. Dermatol.*, vol. 23, no. 9, pp. 615–619, 2014.

[328] C.-C. Liang, A. Y. Park, and J.-L. Guan, "In vitro scratch assay: a convenient and inexpensive method for analysis of cell migration in vitro," *Nat. Protoc.*, vol. 2, no. 2,

pp. 329–333, 2007.

[329] A. Stamm, K. Reimers, S. Strauß, P. Vogt, T. Scheper, and I. Pepelanova, “In vitro wound healing assays–state of the art,” *BioNanoMaterials*, vol. 17, no. 1–2, pp. 79–87, 2016.

[330] K. P. Goetsch and C. U. Niesler, “Optimization of the scratch assay for in vitro skeletal muscle wound healing analysis,” *Anal. Biochem.*, vol. 411, no. 1, pp. 158–160, 2011.

[331] E. Cukierman, R. Pankov, D. R. Stevens, and K. M. Yamada, “Taking cell-matrix adhesions to the third dimension,” *Science (80-.).*, vol. 294, no. 5547, pp. 1708–1712, 2001.

[332] F. Grinnell, “Fibroblasts, myofibroblasts, and wound contraction.,” *J. Cell Biol.*, vol. 124, no. 4, pp. 401–404, 1994.

[333] F. Groeber, M. Holeiter, M. Hampel, S. Hinderer, and K. Schenke-Layland, “Skin tissue engineering—in vivo and in vitro applications,” *Adv. Drug Deliv. Rev.*, vol. 63, no. 4–5, pp. 352–366, 2011.

[334] S. V. Nolte, W. Xu, H.-O. Rennekampff, and H. P. Rodemann, “Diversity of fibroblasts–a review on implications for skin tissue engineering,” *Cells Tissues Organs*, vol. 187, no. 3, pp. 165–176, 2008.

[335] V. Falanga *et al.*, “Wounding of bioengineered skin: cellular and molecular aspects after injury,” *J. Invest. Dermatol.*, vol. 119, no. 3, pp. 653–660, 2002.

[336] D.-Y. Lee and K.-H. Cho, “The effects of epidermal keratinocytes and dermal fibroblasts on the formation of cutaneous basement membrane in three-dimensional culture systems,” *Arch. Dermatol. Res.*, vol. 296, no. 7, pp. 296–302, 2005.

[337] U. Ulmsten, “Connective tissue factors in the aetiology of female pelvic disorders,” *Annals of medicine*, vol. 22, no. 6. p. 403, 1990.

[338] L. De Landsheere *et al.*, “Histology of the vaginal wall in women with pelvic organ prolapse: a literature review,” *Int. Urogynecol. J.*, vol. 24, no. 12, pp. 2011–2020, 2013.

[339] S. Vishwajit, C. Fuelhase, and G. H. Badlani, “The biochemistry of wound healing in the pelvic floor: What have we learned?,” *Curr. Bladder Dysfunct. Rep.*, vol. 4, no. 1, pp. 13–19, 2009.

[340] S. al Guo and L. A. DiPietro, “Factors affecting wound healing,” *J. Dent. Res.*, vol. 89, no. 3, pp. 219–229, 2010.

[341] D. Shveiky *et al.*, “Age-associated impairments in tissue strength and immune response in a rat vaginal injury model,” *Int. Urogynecol. J.*, vol. 31, no. 7, pp. 1435–

1441, 2020.

[342] A. A. Tarique, J. Logan, E. Thomas, P. G. Holt, P. D. Sly, and E. Fantino, "Phenotypic, functional, and plasticity features of classical and alternatively activated human macrophages," *Am. J. Respir. Cell Mol. Biol.*, vol. 53, no. 5, pp. 676–688, 2015.

[343] C. J. Ferrante and S. J. Leibovich, "Regulation of macrophage polarization and wound healing," *Adv. wound care*, vol. 1, no. 1, pp. 10–16, 2012.

[344] S. Mahbub, C. R. Deburghgraeve, and E. J. Kovacs, "Advanced age impairs macrophage polarization," *J. Interf. Cytokine Res.*, vol. 32, no. 1, pp. 18–26, 2012.

[345] O. Ben Menachem-Zidon *et al.*, "Age-associated differences in macrophage response in a vaginal wound healing rat model," *Int. Urogynecol. J.*, vol. 31, no. 9, pp. 1803–1809, 2020.

[346] O. Jorgensen and A. Schmidt, "Influence of sex hormones on granulation tissue formation and on healing of linear wounds," *Acta Chir. Scand.*, vol. 124, pp. 1–10, 1962.

[347] G. S. Ashcroft, T. Greenwell-Wild, M. A. Horan, S. M. Wahl, and M. W. J. Ferguson, "Topical estrogen accelerates cutaneous wound healing in aged humans associated with an altered inflammatory response," *Am. J. Pathol.*, vol. 155, no. 4, pp. 1137–1146, 1999.

[348] Y. Abramov, B. Golden, M. Sullivan, R. P. Goldberg, and P. K. Sand, "Vaginal incisional wound healing in a rabbit menopause model: a histologic analysis," *Int. Urogynecol. J.*, vol. 23, no. 12, pp. 1763–1769, 2012.

[349] M. Notelovitz, S. Funk, N. Nanavati, and M. Mazzeo, "Estradiol absorption from vaginal tablets in postmenopausal women," *Obstet. Gynecol.*, vol. 99, no. 4, pp. 556–562, 2002.

[350] A. Suvik and A. W. M. Effendy, "The use of modified Masson's trichrome staining in collagen evaluation in wound healing study," *Mal J Vet Res*, vol. 3, no. 1, pp. 39–47, 2012.

[351] D. M. Ansell, K. A. Holden, and M. J. Hardman, "Animal models of wound repair: Are they cutting it?," *Exp. Dermatol.*, vol. 21, no. 8, pp. 581–585, 2012.

[352] R. Mohammadi, M. Mehrtash, M. Mehrtash, N. Hassani, and A. Hassanpour, "Effect of platelet rich plasma combined with chitosan biodegradable film on full-thickness wound healing in rat model," *Bull. Emerg. Trauma*, vol. 4, no. 1, p. 29, 2016.

[353] J. M. Reinke and H. Sorg, "Wound repair and regeneration," *Eur. Surg. Res.*, vol. 49,

no. 1, pp. 35–43, 2012.

[354] I. K. Cohen, R. F. Die-gelmann, W. J. Lindblad, and N. E. Hugo, “Wound healing: biochemical and clinical aspects,” *Plast. Reconstr. Surg.*, vol. 90, no. 5, p. 926, 1992.

[355] T. K. Hunt, H. Hopf, and Z. Hussain, “Physiology of wound healing,” *Adv. Skin Wound Care*, vol. 13, p. 6, 2000.

[356] A. Stunova and L. Vistejnova, “Dermal fibroblasts—A heterogeneous population with regulatory function in wound healing,” *Cytokine Growth Factor Rev.*, vol. 39, pp. 137–150, 2018.

[357] S. Porter, “The role of the fibroblast in wound contraction and healing,” *WOUNDS UK*, vol. 3, no. 1, p. 33, 2007.

[358] Y. Abramov *et al.*, “Histologic characterization of vaginal vs. abdominal surgical wound healing in a rabbit model,” *Wound repair Regen.*, vol. 15, no. 1, pp. 80–86, 2007.

[359] H.-C. Horng *et al.*, “Estrogen effects on wound healing,” *Int. J. Mol. Sci.*, vol. 18, no. 11, p. 2325, 2017.

[360] M. Krause, T. L. Wheeler, T. E. S. II, and H. E. Richter, “Local effects of vaginally administered estrogen therapy: a review,” *J. Pelvic Med. Surg.*, vol. 15, no. 3, p. 105, 2009.

[361] F. Akbiyik, Ç. G. Mesci, and Y. H. Çavuşoğlu, “Estrogen as primary factor in vaginal healing in rats,” *Eur. Rev. Med. Pharmacol. Sci.*, vol. 26, no. 5, pp. 1508–1512, 2022.

[362] Y. Abramov, A. R. Webb, S. M. Botros, R. P. Goldberg, G. A. Ameer, and P. K. Sand, “Effect of bilateral oophorectomy on wound healing of the rabbit vagina,” *Fertil. Steril.*, vol. 95, no. 4, pp. 1467–1470, 2011.

[363] S. Balgobin *et al.*, “Estrogen alters remodeling of the vaginal wall after surgical injury in guinea pigs,” *Biol. Reprod.*, vol. 89, no. 6, pp. 131–138, 2013.

[364] J. M. McCracken, S. Balaji, S. G. Keswani, and J. C.-E. Hakim, “An Avant-Garde Model of Injury-Induced Regenerative Vaginal Wound Healing,” *Adv. Wound Care*, vol. 10, no. 4, pp. 165–173, 2021.

[365] M. M. Cotreau *et al.*, “A study of 17β-estradiol-regulated genes in the vagina of postmenopausal women with vaginal atrophy,” *Maturitas*, vol. 58, no. 4, pp. 366–376, 2007.

[366] C. M. Ripperda *et al.*, “Vaginal estrogen: a dual-edged sword in postoperative healing of the vaginal wall,” *Menopause (New York, NY)*, vol. 24, no. 7, p. 838, 2017.

[367] I. A. Darby, B. Laverdet, F. Bonté, and A. Desmoulière, “Fibroblasts and

myofibroblasts in wound healing," *Clin. Cosmet. Investig. Dermatol.*, vol. 7, p. 301, 2014.

[368] B. Hinz and G. Gabbiani, "Cell-matrix and cell-cell contacts of myofibroblasts: role in connective tissue remodeling," *Thromb. Haemost.*, vol. 90, no. 12, pp. 993–1002, 2003.

[369] A. M. Artsen *et al.*, "Mesh induced fibrosis: the protective role of T regulatory cells," *Acta Biomater.*, vol. 96, pp. 203–210, 2019.

[370] A. Sjövall, "The influence of oestrogen upon the healing of vaginal wounds in rats," *Acta Obstet. Gynecol. Scand.*, vol. 27, no. 1, pp. 1–10, 1947.

[371] H. N. Wilkinson and M. J. Hardman, "The role of estrogen in cutaneous ageing and repair," *Maturitas*, vol. 103, pp. 60–64, 2017.

[372] P. L. Dwyer, "Evolution of biological and synthetic grafts in reconstructive pelvic surgery," *Int. Urogynecol. J.*, vol. 17, no. 1, pp. 10–15, 2006.

[373] E. Holt, "US FDA rules manufacturers to stop selling mesh devices," *Lancet*, vol. 393, no. 10182, p. 1686, 2019.

[374] U. Klinge, B. Klosterhalfen, M. Müller, and V. Schumpelick, "Foreign body reaction to meshes used for the repair of abdominal wall hernias," *Eur. J. Surg.*, vol. 165, no. 7, pp. 665–673, 1999.

[375] M. Yuan *et al.*, "Application of synthetic and natural polymers in surgical mesh for pelvic floor reconstruction," *Mater. Des.*, vol. 209, p. 109984, 2021.

[376] E. Mironska, C. Chapple, and S. MacNeil, "Recent advances in pelvic floor repair," *F1000Research*, vol. 8, 2019.

[377] D. R. Ostergard, "Polypropylene vaginal mesh grafts in gynecology," *Obstet. Gynecol.*, vol. 116, no. 4, pp. 962–966, 2010.

[378] K. Paul, S. Darzi, J. A. Werkmeister, C. E. Gargett, and S. Mukherjee, "Emerging nano/micro-structured degradable polymeric meshes for pelvic floor reconstruction," *Nanomaterials*, vol. 10, no. 6, p. 1120, 2020.

[379] A. L. Nolfi *et al.*, "Host response to synthetic mesh in women with mesh complications," *Am. J. Obstet. Gynecol.*, vol. 215, no. 2, pp. 206.e1-206.e8, 2016.

[380] M. Vashaghian *et al.*, "Toward a new generation of pelvic floor implants with electrospun nanofibrous matrices: A feasibility study," *Neurourol. Urodyn.*, vol. 36, no. 3, pp. 565–573, 2017.

[381] N. Bhardwaj and S. C. Kundu, "Electrospinning: a fascinating fiber fabrication technique," *Biotechnol. Adv.*, vol. 28, no. 3, pp. 325–347, 2010.

[382] M. M. Stevens and J. H. George, “Exploring and engineering the cell surface interface,” *Science (80-.).*, vol. 310, no. 5751, pp. 1135–1138, 2005.

[383] J. P. Santerre, K. Woodhouse, G. Laroche, and R. S. Labow, “Understanding the biodegradation of polyurethanes: from classical implants to tissue engineering materials,” *Biomaterials*, vol. 26, no. 35, pp. 7457–7470, 2005.

[384] S. Shafaat, N. Mangir, S. R. Regureos, C. R. Chapple, and S. MacNeil, “Demonstration of improved tissue integration and angiogenesis with an elastic, estradiol releasing polyurethane material designed for use in pelvic floor repair,” *Neurourol. Urodyn.*, 2018.

[385] L. Hympánová *et al.*, “Assessment of Electrospun and Ultra-lightweight Polypropylene Meshes in the Sheep Model for Vaginal Surgery,” *Eur. Urol. Focus*, vol. 6, no. 1, pp. 190–198, 2020.

[386] X. Jia *et al.*, “Efficacy and safety of using mesh or grafts in surgery for anterior and/or posterior vaginal wall prolapse: systematic review and meta-analysis,” *BJOG An Int. J. Obstet. Gynaecol.*, vol. 115, no. 11, pp. 1350–1361, 2008.

[387] A. J. Woodruff, E. E. Cole, R. R. Dmochowski, H. M. Scarpero, E. N. Beckman, and J. C. Winters, “Histologic comparison of pubovaginal sling graft materials: a comparative study,” *Urology*, vol. 72, no. 1, pp. 85–89, 2008.

[388] A. Mangera, A. J. Bullock, S. Roman, C. R. Chapple, and S. MacNeil, “Comparison of candidate scaffolds for tissue engineering for stress urinary incontinence and pelvic organ prolapse repair,” *BJU Int.*, vol. 112, no. 5, pp. 674–685, Sep. 2013.

[389] C. J. Hillary, S. Roman, A. J. Bullock, N. H. Green, C. R. Chapple, and S. MacNeil, “Developing repair materials for stress urinary incontinence to withstand dynamic distension,” *PLoS One*, vol. 11, no. 3, p. e0149971, 2016.

[390] B. Naureen, A. Haseeb, W. J. Basirun, and F. Muhamad, “Recent advances in tissue engineering scaffolds based on polyurethane and modified polyurethane,” *Mater. Sci. Eng. C*, vol. 118, p. 111228, 2021.

[391] J. Kucinska-Lipka, I. Gubanska, H. Janik, and M. Sienkiewicz, “Fabrication of polyurethane and polyurethane based composite fibres by the electrospinning technique for soft tissue engineering of cardiovascular system,” *Mater. Sci. Eng. C*, vol. 46, pp. 166–176, 2015.

[392] H. Janik and M. Marzec, “A review: Fabrication of porous polyurethane scaffolds,” *Mater. Sci. Eng. C*, vol. 48, pp. 586–591, 2015.

[393] H. Mehdizadeh, S. Sumo, E. S. Bayrak, E. M. Brey, and A. Cinar, “Three-dimensional

modeling of angiogenesis in porous biomaterial scaffolds," *Biomaterials*, vol. 34, no. 12, pp. 2875–2887, 2013.

[394] S. Zhong, Y. Zhang, and C. T. Lim, "Fabrication of large pores in electrospun nanofibrous scaffolds for cellular infiltration: a review," *Tissue Eng. Part B Rev.*, vol. 18, no. 2, pp. 77–87, 2012.

[395] S. Roman, N. Mangir, J. Bissoli, C. R. Chapple, and S. MacNeil, "Biodegradable scaffolds designed to mimic fascia-like properties for the treatment of pelvic organ prolapse and stress urinary incontinence," *J. Biomater. Appl.*, vol. 30, no. 10, pp. 1578–1588, 2016.

[396] A. Mangera, A. J. Bullock, C. R. Chapple, and S. MacNeil, "Are biomechanical properties predictive of the success of prostheses used in stress urinary incontinence and pelvic organ prolapse? A systematic review," *Neurourol. Urodyn.*, vol. 31, no. 1, pp. 13–21, 2012.

[397] L. Lei, Y. Song, and R. Chen, "Biomechanical properties of prolapsed vaginal tissue in pre-and postmenopausal women," *Int. Urogynecol. J.*, vol. 18, no. 6, pp. 603–607, 2007.

[398] S. Roman, N. Mangir, and S. MacNeil, "Designing new synthetic materials for use in the pelvic floor: what is the problem with the existing polypropylene materials?," *Curr. Opin. Urol.*, vol. 29, no. 4, pp. 407–413, 2019.

[399] S. Manodoro *et al.*, "Graft-related complications and biaxial tensiometry following experimental vaginal implantation of flat mesh of variable dimensions," *BJOG An Int. J. Obstet. Gynaecol.*, vol. 120, no. 2, pp. 244–250, 2013.

[400] R. Liang *et al.*, "Extracellular matrix regenerative graft attenuates the negative impact of polypropylene prolapse mesh on vagina in rhesus macaque," *Am. J. Obstet. Gynecol.*, vol. 216, no. 2, pp. 153-e1, 2017.

[401] E. W. Higgins *et al.*, "Effect of estrogen replacement on the histologic response to polypropylene mesh implanted in the rabbit vagina model," *Am. J. Obstet. Gynecol.*, vol. 201, no. 5, pp. 505-e1, 2009.

[402] Y. Wang, P. Li, P. Xiang, J. Lu, J. Yuan, and J. Shen, "Electrospun polyurethane/keratin/AgNP biocomposite mats for biocompatible and antibacterial wound dressings," *J. Mater. Chem. B*, vol. 4, no. 4, pp. 635–648, 2016.

[403] L. P. Gabriel, A. A. Rodrigues, M. Macedo, A. L. Jardini, and R. Maciel Filho, "Electrospun polyurethane membranes for Tissue Engineering applications," *Mater. Sci. Eng. C*, vol. 72, pp. 113–117, 2017.

[404] A. L. Clark, O. D. Slayden, K. Hettrich, and R. M. Brenner, “Estrogen increases collagen I and III mRNA expression in the pelvic support tissues of the rhesus macaque,” *Am. J. Obstet. Gynecol.*, vol. 192, no. 5, pp. 1523–1529, 2005.

[405] Z. Guler and J. P. Roovers, “Role of Fibroblasts and Myofibroblasts on the Pathogenesis and Treatment of Pelvic Organ Prolapse,” *Biomolecules*, vol. 12, no. 1, p. 94, 2022.

[406] A. A. A. Ewies *et al.*, “Changes in transcription profile and cytoskeleton morphology in pelvic ligament fibroblasts in response to stretch: the effects of estradiol and levormeloxifene,” *MHR-Basic Sci. Reprod. Med.*, vol. 14, no. 2, pp. 127–135, 2008.

[407] A. M. Ruiz-Zapata *et al.*, “Extracellular Matrix Stiffness and Composition Regulate the Myofibroblast Differentiation of Vaginal Fibroblasts,” *Int. J. Mol. Sci.*, vol. 21, no. 13, p. 4762, 2020.

[408] S. B. Orenstein, E. R. Saberski, D. L. Kreutzer, and Y. W. Novitsky, “Comparative analysis of histopathologic effects of synthetic meshes based on material, weight, and pore size in mice,” *J. Surg. Res.*, vol. 176, no. 2, pp. 423–429, 2012.

[409] N. T. H. Farr *et al.*, “A novel characterisation approach to reveal the mechano–chemical effects of oxidation and dynamic distension on polypropylene surgical mesh,” *RSC Adv.*, vol. 11, no. 55, pp. 34710–34723, 2021.

[410] F. J. Rios, R. M. Touyz, and A. C. Montezano, “Isolation and differentiation of human macrophages,” in *Hypertension*, Springer, 2017, pp. 311–320.